Lagunamide family: total synthesis efforts, final structural determination, new family identification, and biological evaluation

by

Kongahapathirage Dona Shashika Sevvandi Perera

B.S., College of Chemical Sciences, Sri Lanka, 2016

AN ABSTRACT OF A DISSERTATION

submitted in partial fulfillment of the requirements for the degree

DOCTOR OF PHILOSOPHY

Department of Chemistry
College of Arts and Sciences

KANSAS STATE UNIVERSITY
Manhattan, Kansas

2024

Abstract

Lagunamide C (LagC) is a cyclic depsipeptide isolated by Tan and co-workers from the cyanobacterium *Lyngbya majsucle* from the western lagoon of Singapore in 2011. It exhibits potent cytotoxicity against a panel of cancer cell lines in low nanomolar concentrations: lymphoma (P388, IC_{50} 24.4 nM), lung (A549, IC_{50} 2.4 nM), prostate (PC3, IC_{50} 2.6 nM), colon (HCT8, IC_{50} 2.1 nM), and ovarian (SK-OV3, IC_{50} 4.5 nM). LagC displays significant antimalarial activity with an IC_{50} of 0.29 μM towards *Plasmodium falciparum* and weak anti-swarming activity towards *Pseudomonas aeruginosa* PA01 at 100 ppm. Numerous stereocenters of LagC are in question, as is some additional structural concerns. As such, our lab has proposed a structure LagC and no total synthesis of this proposed structure of this potent bioactive agent has been reported. While LagC, our proposed structure, has not been synthesized, Lag A & B have been. The extra methylene unit present within the polyketide unit of LagC makes it the only 27 membered macrocycle of the whole aurilide family and limits the utility of the routes to the polyketide units of LagA/B. This dissertation work discloses an improved, scalable, and efficient synthetic route to access the polyketide unit of LagC diastereoselectively, final macrocyclization and ring closing metathesis attempts to access the 27 membered ring of LagC, and efforts in its final structural elucidation. Synthesis of 27 membered aurlide macrocycle analogs, their biological evaluations, and a new proposed mode of action for LagC and its family of natural products is deliberated. Furthermore, based upon the recent discovery of LagD, a methyl truncate variant of LagA, our lab has undergone a synthesis of the proposed natural product LagE based on the same methyl truncation. Synthetic efforts and biological identification of this proposed natural product is also discussed.

Lagunamide family: total synthesis efforts, final structural determination, new family identification, and biological evaluation

by

Kongahapathirage Dona Shashika Sevvandi Perera

B.S., College of Chemical Sciences, Sri Lanka, 2016

A DISSERTATION

submitted in partial fulfillment of the requirements for the degree

DOCTOR OF PHILOSOPHY

Department of Chemistry
College of Arts and Sciences

KANSAS STATE UNIVERSITY
Manhattan, Kansas

2024

Approved by:

Major Professor
Dr. Ryan J. Rafferty

Copyright

© Kongahapathirage Dona Shashika Sevvandi Perera 2024.

Abstract

Lagunamide C (LagC) is a cyclic depsipeptide isolated by Tan and co-workers from the cyanobacterium *Lyngbya majsucle* from the western lagoon of Singapore in 2011. It exhibits potent cytotoxicity against a panel of cancer cell lines in low nanomolar concentrations: lymphoma (P388, IC_{50} 24.4 nM), lung (A549, IC_{50} 2.4 nM), prostate (PC3, IC_{50} 2.6 nM), colon (HCT8, IC_{50} 2.1 nM), and ovarian (SK-OV3, IC_{50} 4.5 nM). LagC displays significant antimalarial activity with an IC_{50} of 0.29 μM towards *Plasmodium falciparum* and weak anti-swarming activity towards *Pseudomonas aeruginosa* PA01 at 100 ppm. Numerous stereocenters of LagC are in question, as is some additional structural concerns. As such, our lab has proposed a structure LagC and no total synthesis of this proposed structure of this potent bioactive agent has been reported. While LagC, our proposed structure, has not been synthesized, Lag A & B have been. The extra methylene unit present within the polyketide unit of LagC makes it the only 27 membered macrocycle of the whole aurilide family and limits the utility of the routes to the polyketide units of LagA/B. This dissertation work discloses an improved, scalable, and efficient synthetic route to access the polyketide unit of LagC diastereoselectively, final macrocyclization and ring closing metathesis attempts to access the 27 membered ring of LagC, and efforts in its final structural elucidation. Synthesis of 27 membered aurlide macrocycle analogs, their biological evaluations, and a new proposed mode of action for LagC and its family of natural products is deliberated. Furthermore, based upon the recent discovery of LagD, a methyl truncate variant of LagA, our lab has undergone a synthesis of the proposed natural product LagE based on the same methyl truncation. Synthetic efforts and biological identification of this proposed natural product is also discussed.

Table of Contents

List of Figures viii
List of Schemes ix
List of Tables xi
Acknowledgements xii
Dedication xiv
Chapter 1 – Natural Products in Medicinal Chemistry 1
1.1 Brief history of natural products and their use as therapeutics 1
1.2 Use of natural products in drug discovery. 4
1.3 Marine natural products 6
1.3.1 Aurilide class of natural products 9
1.3.1.1 Lagunamides 11
1.3.1.2 Biological activity of aurilides 11
Chapter 2 - Previous Synthetic Work 14
2.1 Structure and biological activity relationship of aurilides 14
2.2 Synthesis of the polyketide moieties of the 26 membered depsipetides of the aurilide family 14
2.2.2 Aurilide 14
2.2.3 Kulokekahilide-2 18
2.2.4 Odoamide 20
2.2.5 Lagunamide A 21
2.2.6 Lagunamide B 28
2.2.7 Lagunamide C 29
2.3 Ring closing techniques in aurilides synthesis 30
2.3.1 Macrolactamization 31
2.3.2 Macrolactonization 33
2.3.3 Ring closing metathesis (RCM) 34
2.4 Hypothesis 35
Chapter 3 – Synthetic Efforts Towards Lagunamide C and Proposed Lagunamide E 38
3.1 Retrosynthetic analysis of lagunamide C 38

3.2 Retrosynthetic analysis of the pentapeptide moiety 39
3.2.1 Synthesis of the pentapeptide moiety 39
3.2.1.1 Synthesis of the dipeptide 39
3.2.1.2 Synthesis of the tripeptide 41
3.3 Retrosynthetic analysis of lagunamide C polyketide 42
3.3.2 Exploring a possible new reaction to access 138 installing stereochemistry at C5 43
3.3.3 Synthesis of the lagunamide C polyketide moiety 46
3.4 Cyclization attempts to access lagunamide C 51
3.4.1 Analog macrocycle synthesis 51
3.4.1.1 Route 1 - Macrocyclization 51
3.4.1.2 Route 2 – Ring closing metathesis (RCM) 54
3.4.1.3 Route 3 – Cross metathesis (CM) followed by macrocyclization 57
3.4.2 Lagunamide C macrocycle synthesis 58
3.5 Proposed lagunamide E synthesis 60
3.6 Structure confirmation of the polyketide moiety via crystallization 62
3.7 Studies on the hypothesis of mode of action of aurilides 63
Chapter 4 – Conclusion and Future Work 65
Chapter 5 – References 68
Chapter 6 – Procedures and NMRs 80

List of Figures

Figure 1- New FDA approved drugs from 1981-2019 5
Figure 2- Timeline of FDA approved marine natural product based drugs..... 7
Figure 3 - Marine drug candidates in clinical trials 8
Figure 4 - A) Aurilde family of natural products; B) comparison of aurilide polyketide units.... 10
Figure 5: Proposed and revised structures of kulokekahilide-2..... 19
Figure 6: Proposed and revised structures of lagunamide A 21
Figure 7: Stereoisomers of lagunamide A 23
Figure 8: Isolated and proposed lagunamide B structures 28
Figure 9: Isolated lagunamide D structure and proposed lagunamide E structure 37
Figure 10: (A) Lagunamide C polyketide intermediates and their respective IC_{50} values; 64

List of Schemes

Scheme 1: Attempts to confirm stereochemistry of aurilide polyketide 15
Scheme 2: Synthesis of triols 11a - 11d 16
Scheme 3: Synthesis of aurilide polyketide moiety 17
Scheme 4: Synthesis of triols 22a - 22d 19
Scheme 5: Synthesis of Odoamide polyketide 21
Scheme 6: (A) Synthesis of lagunamide A polyketide;(B) Synthesis of depsipeptides 41 and 42 23
Scheme 7: Lagunamide A polyketide synthesis by Huang et. al 24
Scheme 8: Lagunamide A polyketide synthesis by Chang et.al 25
Scheme 9: Lagunamide A polyketide synthesis by Banasik et. al 26
Scheme 10: Lagunamide A polyketide synthesis by Gorges et.al 27
Scheme 11: Polyketide synthesis of lagunamide B analogue by Chakraborty et. al 29
Scheme 12: (A) Retrosynthetic analysis of probing route to lagunamide C polyketide; (B) Exploration of the set synthetic route to access lagunamide C polyketide analogue 30
Scheme 13: Macrolactamization of (A) kulokekahlide-2 and (B) odoamide 32
Scheme 14: Macrolactonization of (A) kulokekahilide-2 and (B) lagunamide B analog 34
Scheme 15: Ring closing metathesis attempt to access lagunamide A macrocycle 35
Scheme 16: (A) Isolated and revised structure of lagunamide A, Isolated and proposed structure of lagunamide C; (B) hypothesized mechanism of action of aurilides 36
Scheme 17: Ring closing approaches to access lagunamide C 38
Scheme 18: Retrosynthesis analysis of pentapeptide moiety 39
Scheme 19: (A) Synthesis of the model dipeptide; (B) Synthesis of the actual dipeptide; (C) Mechanistic explanation for the retention of stereochemistry at C2 41
Scheme 20: Synthesis of the tripeptide 117 and the pentapeptide 134 42
Scheme 21: Old and new route to access lagunamide C polyketide 43
Scheme 22: Model systems to prove the late-stage epoxidation concept 45
Scheme 23: (A) proposed mechanism for Shi epoxidation; (B) Spiro and planar transition states; (C) Synthesis of the Shi catalyst and epoxidation 46

Scheme 24: Synthesis of the Crimmins auxiliary, Mukaiyama aldol addition and stereochemical explanation using Felkin Anh model 47
Scheme 25: Construction of the synthetic precursor 147 for the late-stage modifications in accessing lagunamide C polyketide 48
Scheme 26:(A) Catalytic mechanism for the Kricshe allylation; (B)Investigation of substrate specificity of Kricshe allylation 50
Scheme 27: Cross metathesis to access lagunamide C polyketide moiety 50
Scheme 28: Model polyketide synthesis 52
Scheme 29: Analog macrocycle synthesis via route 1 53
Scheme 30:(A) RCM retrosynthesis; (B) Synthesis of the analog RCM precursor 55
Scheme 31: RCM catalytic cycle 55
Scheme 32: (A) Retrosynthesis analysis of route 3; (B) Synthetic route 3 58
Scheme 33: Macrocyclization to access lagunamide C 59
Scheme 34: Synthesis of proposed lagunamide E polyketide 60
Scheme 35: Macrocyclization to access proposed lagunamide E 61
Scheme 36: Crystallization attempts on polyketide moiety 62
Scheme 37:Synthetic progress in accessing lagunamide C and proposed lagunamide E 66
Scheme 38: Aurilide analogs for cell penetration and proposed amide analog of aurilides 67

List of Tables

Table 1 - Biological activity of aurilides [IC_{50} in nM (*LC_{50} in nM)] 12
Table 2: Macrolactamization reaction conditions of aurilide 31
Table 3: Macrolactamization reaction conditions of lagunamide A 33
Table 4: Optimization of mono-silylation of 1,8 octanediol 52
Table 5: RCM optimization 57

Acknowledgements

First, I would like to thank Dr. Ryan J. Rafferty, my Ph.D. advisor, for his support and guidance throughout my Ph.D. journey. Your passion for teaching and dedication to work has inspired me in many ways. Thank you for believing in me, encouraging me, and your hard work and time in building me to who I am today.

I would like to acknowledge my committee members: Dr. Daniel Higgins, Dr. Peter Sues, Dr. Jeffrey Comer, Dr. Robert Delong (former member), and Dr. Stefan Bossmann (former member). I am truly grateful for your guidance and support throughout my Ph.D. journey.

I would like to extend my gratitude to all the current and former Rafferty lab members; specially Asantha Fernando, Prathibha Desman, and Anthony Fatino, for all the support you gave me throughout these six years and making the lab environment a place to look forward to attending every day. Thank you to Kameron Wildeman for his support in analyzing the data when writing my dissertation.

My heartfelt gratitude to Kansas State University for this great opportunity to pursue my Ph.D. I would like to extend my sincere thanks to the Department of Chemistry that is full of immensely supportive, welcoming, and caring faculty and staff. Thank you for everything that you did to make my graduate life full of memories to cherish. A special thank you to our department heads Dr. Daniel Higgins (former) and Dr. Christer Aakeroy (current); the organic faculty; NMR directors Dr. Simon Sham (former) and Dr. Tomohiro Kimura (current); Teaching advisors Mr. Michael Hinton (former), Dr. Abhijeet Sinha (former), and Dr. Radhika Nareddy (current); safety officers Dr. Tingting Liu (former) and Dr. Sadish Karunaweera (current). Another big thank you to Mr. Jim Hodgson, Mr. Ron Jackson, Mr. Tobe Eggers, Mr. Bart Bath, and Ms. Kimberly Ross for their immense support and encouragement.

I could not have undertaken this journey without my undergraduate mentors Dr. Dinara Gunasekara, Dr. Dhanushi Welideniya, and Dr. Umayangani Wanninayake who prepared me for graduate school and life; thank you so much for your unwavering support and guidance. My sincere gratitude to the Institute of Chemistry Ceylon (my undergraduate college) and faculty, and Sri Lanka Institute of Nanotechnology (my former workplace) for equipping me and laying the firm foundation for the person who I am today.

I am extremely grateful to the family away from family and true friends I am surrounded here in Manhattan, Kansas. Thank you so much for everything you do. My deep appreciation to my aunts, uncles, cousins, and friends for their tremendous support and abundant love for me.

Words cannot express my gratitude to my beloved parents, Mr. Sarath Perera and Mrs. Kumudinee Perera, for their unfailing love, support, encouragement, and raising me to be the human being who I am today. I am extremely grateful to my loving brother Chathuranga Perera, who always encourages me, uplifts me, and never fails to make me laugh when I feel down. You three have done so many sacrifices for me, and I am forever grateful to you.

Finally, I would like to praise God for the exciting book of life he has written for me. May the glory of this work be to Jesus Christ.

Dedication

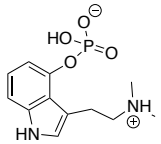
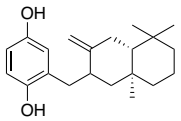
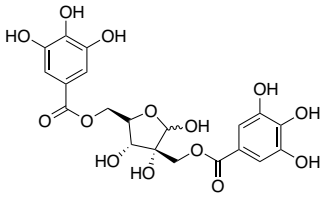
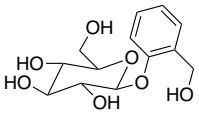
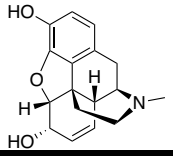
To my loving parents and brother who picked me up when I am down and encouraged me to go on every adventure. Especially this one.

Chapter 1 – Natural Products in Medicinal Chemistry

1.1 Brief history of natural products and their use as therapeutics

Natural products are compounds produced by or found in living organisms[1]. Depending on their function, natural products can be categorized into two main types: primary and secondary metabolites[2]. Primary metabolites are components involved in major metabolic pathways that are required for the survival of living organisms. They play key roles in growth, energy production, development, and reproduction of living organisms[3]. In contrast, secondary metabolites are not absolutely essential for the survival of the organism but help the organism in communication with the same types of species, defense mechanisms, and many others[4]. Secondary metabolites have a diverse range of structures (e.g., alkaloids, polyketides, phenylpropanoids, terpenoids etc.) and provide a wide range of biological activities[5]. While these secondary metabolites have provided an enormous benefit to the host organism, they also have a wide encompassing effects upon other organisms in strikingly different ways. The willow tree provides an abundant source of salicylic acid, which we utilize for the relief of headaches and similar alignments, but the host utilizes it for defense against common pests[6]. This striking difference between what the purpose of the secondary metabolites synthesis verses the potential therapeutic benefit by other organism is what our civilization has rooted most of its therapeutic drug discovery on. Our ancestors utilized different plants and fungi to treat many diseases[7]. Examples include the use of mushrooms belonging to the genus *Psilocybe* to treat anxiety disorders[8], brown algae to treat inflammations/swellings[9], and Witch Hazel stems to treat high blood pressure[10]. It is the secondary metabolites Psilocybin, Zonarol, and Hammamelitanin present in those natural product sources respectively that provide the therapeutic effect (Table 1).

Table 1 - Examples of natural product sources utilized to treat diseases in ancient times.

Natural product source	Active ingredient	Chemical structure	Therapeutic effect
Psilocybe genus of fungi	Psilocybin		Anxiolytic[8]
Brown Algae	Zonarol		Anti-inflammatory[9]
Witch Hazel stem	Hamamelitannin		Diuretic[10]
Willow tree bark	Salicin		Analgesic and antipyretic[6]
Poppy plant	Morphine		Painkiller[11]

Inspired by the ancient therapeutic uses of natural products, scientists have started detailed investigations of natural product sources to identify promising novel therapeutics. One of the first pure natural products to be commercialized as a commercial therapeutic agent was morphine[11], a natural product that was isolated from opium. This natural product was first isolated by German pharmacist Friedrich Serturner in 1805 and introduced to the market by Merck as an analgesic drug in 1826. This natural alkaloid led to a breakthrough in analgesic therapeutics by opening doors to investigate structure based activity of opioids with increased potency and minimized side effects[12,13]. Diacetyl morphine commonly known as heroin was first accessed by the English researcher C.R. Wright in 1874 and commercialized by Bayer company of Germany in 1898, fentanyl by Paul Janssen in 1960, hydromorphone in 1926, methadone in 1947, and buprenorphine

in 1977 are few examples of such synthetic variants of morphine that is currently available in the market[14,15,16,17,18]. The impact of natural products, and their synthetic analogs, is further shown by the discovery and modification of salicin[19]. In 1828, Johann Buchner reported the isolation of the most impactful natural product, salicin, from the bark of willow trees. The purification was further modified in 1838 to access salicylic acid, which was widely used for its analgesic properties. However, salicylic acid caused gastric irritations in patients, which was addressed by Hoffman in 1897 by acetylating the phenol group of acetylic acid, yielding acetylsalicylic acid, which is commonly referred to as aspirin in the pharmaceutical industry. Interestingly, the acetylated phenol has no biological activity. However, once within a human, the acetate group is removed upon absorption into the blood stream to release the bioactive agent salicin. In this, a new drug type was born, that of prodrugs. In this a bioactive agent is masked in a way to prevent either activity or toxic side effects from occurring until a later stage modification. This powerful strategy came about from the studies of natural products and work to enhance their activity. Aspirin, remains today, as the most famous natural-product-based pharmaceutical agent that has been modified available in the market[6]. While ancient drug discovery involved crude extracts from natural product sources as therapeutics, great inventions like above discussed from nature, scientists have started investigating the use of pure natural products as therapeutics.

While natural products throughout human civilization have found numerous therapeutic benefits, one key limitation has yet to be discussed. Access, commonly referred to as isolation of said natural products has many draw backs and concerns. In many cases, the isolation of natural products is extremely difficult and most commonly results in limited material being isolated and the possible elimination of the host organism. To prevent the elimination, destruction of the host organism, synthetic chemists have developed synthetic routes to access the complex structures of

nature-built therapeutic agents, commonly referred to as total synthesis. These synthetic routes were able to decrease the cost of production in large numbers and increase the efficiency of drug manufacturing. Few examples of such natural products that reached the market as a drug are, antibiotics and antifungal agents, erythromycin, and amphotericin B[20]; anticancer agents, paclitaxel, and campothecin[21]; cholesterol-lowering drug lovastatin[22]; immunosuppressant, tacrolimus, and cyclosporin A[23].

1.2 Use of natural products in drug discovery.

In addition to serving as therapeutics themselves and as prodrugs, natural products have paved the foundation for discovering new bioactive agents through efforts in gaining access to them via synthetic means[24,25]. In this, drugs with enhanced activity and improved physicochemical properties have been unlocked[26]. Through this, compounds of natural origin exhibit better biological friendliness and drug likeness, which make them better candidates for drug discovery, have been accessed by the synthetic community[27,28,29]. This can be done mainly via different suitable structure activity guided modifications of the natural product leading to chemical libraries (combinatorial chemistry), and computational drug design (in silico) to support the respective compound selection and optimized experimentation[30]. Between 1981 and 2014 United States Food and Drug Administration (USFDA) has approved 1562 drugs and over one third of them are either pure natural products, herbal mixtures, natural product derivatives, or synthetic drugs derived from natural product pharmacophores[31]. Furthermore, according to the statistical report by Newman et. al about new FDA approved drugs over the past 39 years (1981-2019), approximately 68% of the approved drugs in the market are either natural products or natural product inspired[32] (Figure 1).

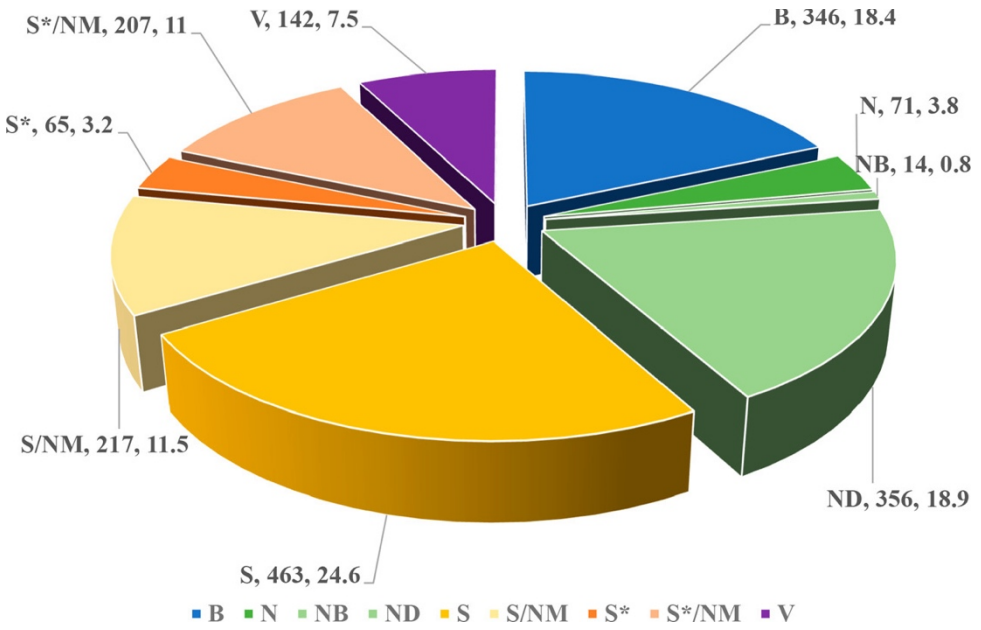


Figure 1- New FDA approved drugs from 1981-2019

B: Biological macromolecules, N: unaltered natural product, NB: Botanical drug (defined mixture), ND: Natural product derivative, S: Synthetic drug, /NM: /Mimic of natural product, S*: Synthetic drug (natural product pharmacophore), V: Vaccine

This highlights the important roles played by natural products, the necessity for medicinal chemists to engage in the total synthesis of natural products and derivatives, and the importance of accessing potential candidates for drug discovery. A few examples of medicinal chemistry areas largely impacted by natural-product-based drug discovery are neuroscience[25], cancer immunotherapy[26], and nanotechnology-assisted personalized drug delivery[33]. Natural products are promising sources for identifying scaffolds with a wide range of structures and bioactivities that can be directly developed or used as a foundation for creating new drugs and carrier vehicles. Among the main natural product sources; plants, animals, microorganisms (fungi and bacteria), and marine; marine sources are the least studied yet a hotspot for innumerous amount of biologically active compounds[34].

1.3 Marine natural products

The ocean covers approximately 70% of the Earth and home for many diverse species[35]. Marine organisms are a source of innumerous amounts of secondary metabolites, which have become a major attraction of many medicinal chemists, and it has only been 60 years since the dawn of their investigation[36,37]. Numerous drugs derived from marine biota are in commercial use and/or under clinical trials; a total of eleven marine-derived natural products are available in the market[38,39]. Among them cytarabine (Cytosar-U®) derived from a natural arabino-nucleoside, trabectedin (ET-743, Yon- delis®) isolated from the tunicate Ecteinascidia turbinata, eribulin mesylate (Halaven®) a synthetic truncated derivative of the polyketide natural product halichondrin B are used as anticancer treatments[40]. Brentuximab vedotin[41] (Adcetris®) and polatuzumab vedotin[42] (Polivy®), are used as antibody drug conjugates to treat cancer. Vedotin acts as a carrier vehicle to transport monoclonal antibodies performing targeted cancer therapy. Lovaza®, Vascepa®, and Epanova® are three fatty acid drugs that are available to treat hypertriglyceridemia[43]. Vidarabine (Vira-A®), a natural arabino-nucleoside, and iota-carrageenan[44] (Carragelose®), a sulfate polysaccharide from marine red algae, are used as antiviral drugs. Ziconotide (Prialt®), a peptide drug derived from cone snails, is used to treat amelioration of severe chronic pain[45] (Figure 2).

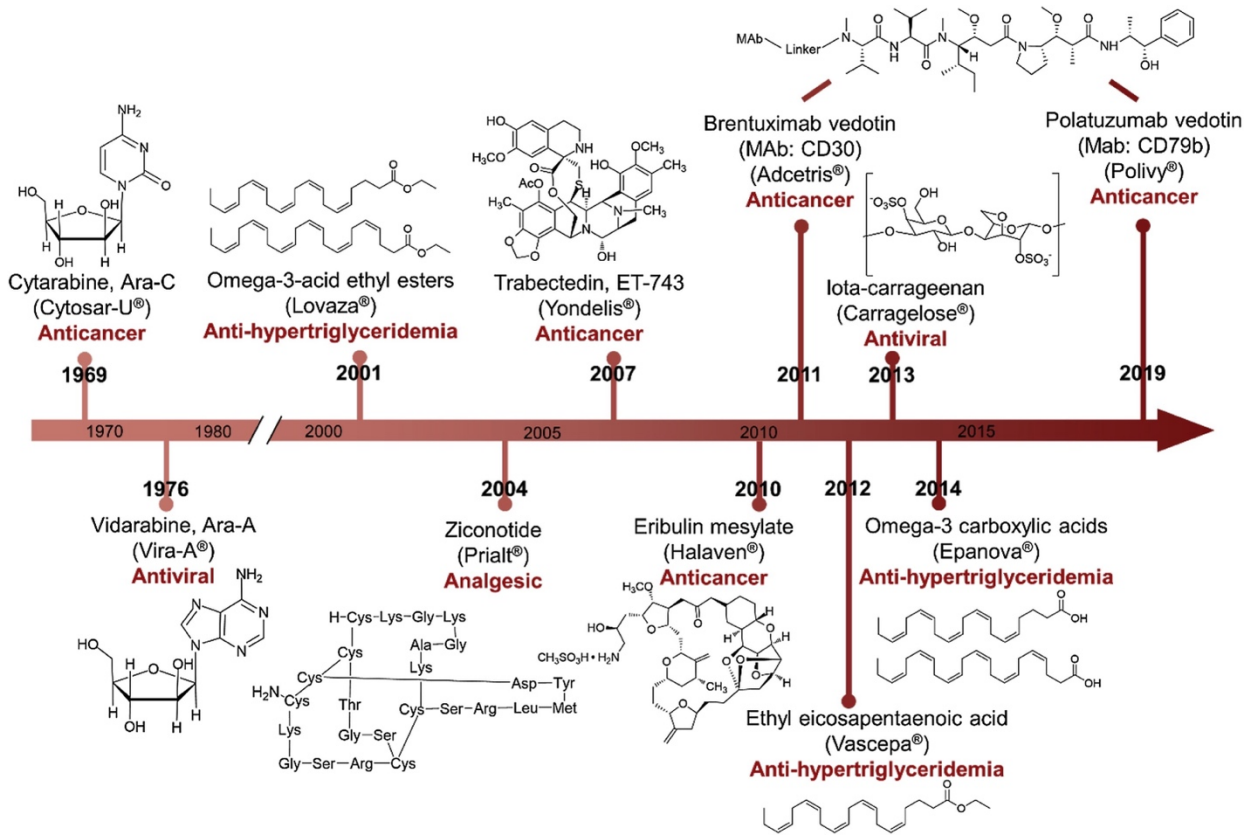


Figure 2- Timeline of FDA approved marine natural product based drugs

To date, more than 20 marine natural product-based drug candidates are currently undergoing different phases of clinical trials in drug development pipeline[38]. Cyclic depsipeptide plitidepsin (isolated from the tunicate *Aplidium albicans*) exhibits limited cytotoxicity in many cancers including melanoma, multiple myeloma, and noncutaneous peripheral T-cell lymphoma and no satisfactory activity in solid tumors when tested as a sole agent[46]. However, the cytotoxicity was increased when tested in combination with other agents like dexamethasone, melphalan, lenalidomide, and bortezomib[47]. The synergism with dexamethasone reported to be more interesting due to its enhanced efficiency at lower dosages that minimizes possible side effects like muscle toxicity, and gastrointestinal were reduced[46]. As a result, plitidepsin is currently in phase III as a drug candidate for the treatment of relapsed/refractory multiple myeloma in combination with dexamethasone[48]. Its mode of action is still under investigation.

Plinabulin, an analog of halimide that was isolated from the marine fungus *Aspergillus* sp., as an antimicrotubular agent[49], and tetrodotoxin (extracted from pufferfish liver) to treat severe pain due to its analgesic effects[50] are two other marine-derived drug candidates in phase III clinical trials (Figure 3). Of these marine natural products, tetrodotoxin is one of the most promising drug candidates given its remarkable performance as a potential replacement for opioids, which are commonly used analgesics for severe pain that causes severe side effects, such as hallucinations, addiction, and dependence. Salinosporamide A, isolated from the marine bacteria *Salinispora tropica,* and ralaniten acetate are in phase II clinical trials for the treatment of multiple myeloma and metastatic castration-resistant prostate cancer (mCRPC), respectively[38]. While chemotherapy is a widely used cancer treatment, some cancers develop resistance to current chemotherapeutics, resulting in increased dosages and the need for novel specific drugs. Hence, the latter mentioned drug candidates can be the hope of many patients with multiple myeloma and mCRPC undergoing chemotherapy or radiotherapy and related adverse side effects.

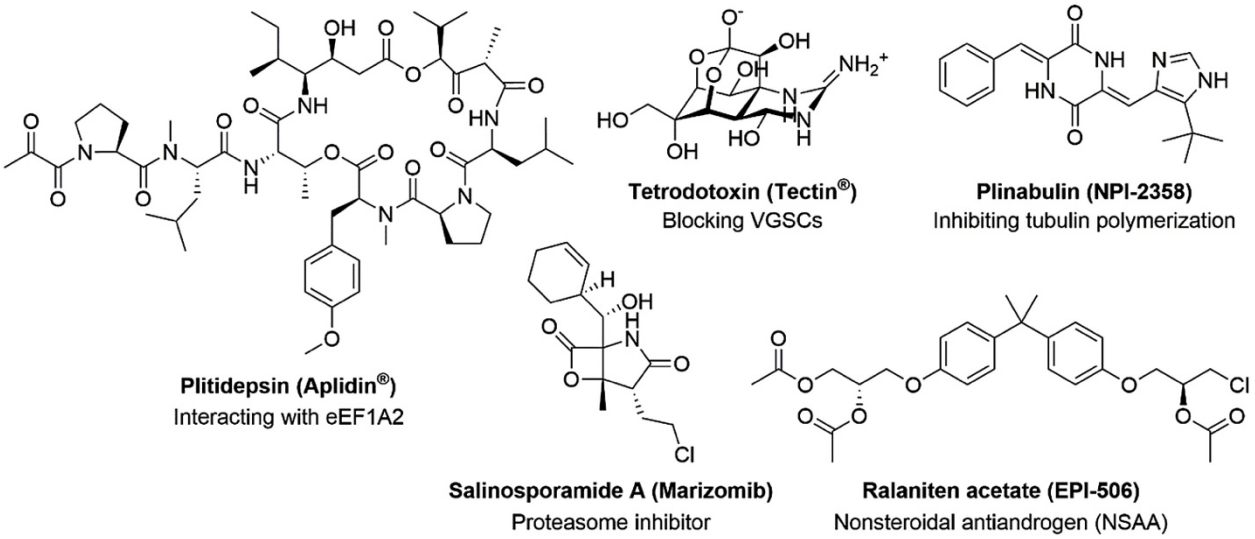


Figure 3 - Marine drug candidates in clinical trials

1.3.1 Aurilide class of natural products

The aurilide family of natural products are cyclic depsipeptides that have been extensively studied by medicinal chemists owing to their promising therapeutic activities[51]. There are ten structurally related aurilides that can be categorized into five main subclasses (Figure 4A). All aurilides are composed of a polyketide moiety, polypeptide moiety, and an alpha hydroxy ester unit. The first aurilide of this family was isolated and characterized by Yamada et.al from the Japanese sea hare *Dolabella Auricularia* in 1996[52]. Following that, in 2000, the discovery and structural elucidation of palau'amide; only 24 membered macrocycle of the family, from the cyanobacterium *Lyngbya* was carried out by Moore et.al[53]. Nakao et.al isolated kulokekahilide-2 in 2004 from cephalaspidean mollusk *Philinopsis speciosa*[54], while aurilide B and aurilide C were isolated from marine cyanobacterium *Lyngbya majuscule* from Papua New Guinea in 2006 by Gerwick et.al[55]. The subclass lagunamides was introduced to the aurilide family by Tan et.al with isolation of lagunamide A and B in 2010[56], followed by lagunamide C; only 27 membered macrocycle of the family, in 2012 from the same cyanobacterium *Lyngbya majuscule*[57]. Teruya et al. reported the isolation of the last subclass of the family, odoamide, in 2016 from the cyanobacterium *Okeania sp.*[58] The latest addition to the aurilide family, lagunamide D, which belongs to the lagunamide subclass, was introduced by Leusch et.al in 2019, and was isolated from a marine cyanobacteria collection in Florida[59]. All aurilides, except for palau'amide and lagunamide C are 26 memebered macrocycles. All the aurilide polyketides include an α, β-unsaturated 5,7-dihydroxy acid containing three adjacent stereocenters, except for odoamide, which contains an extra adjacent stereocenter on the sec pentyl side chain, and lagunamide C, which contains an extra methylene unit in the polyketide chain (Figure 4B). This unique structure

of lagunamide C drew our attention for further investigation of the lagunamide subclass of aurilides.

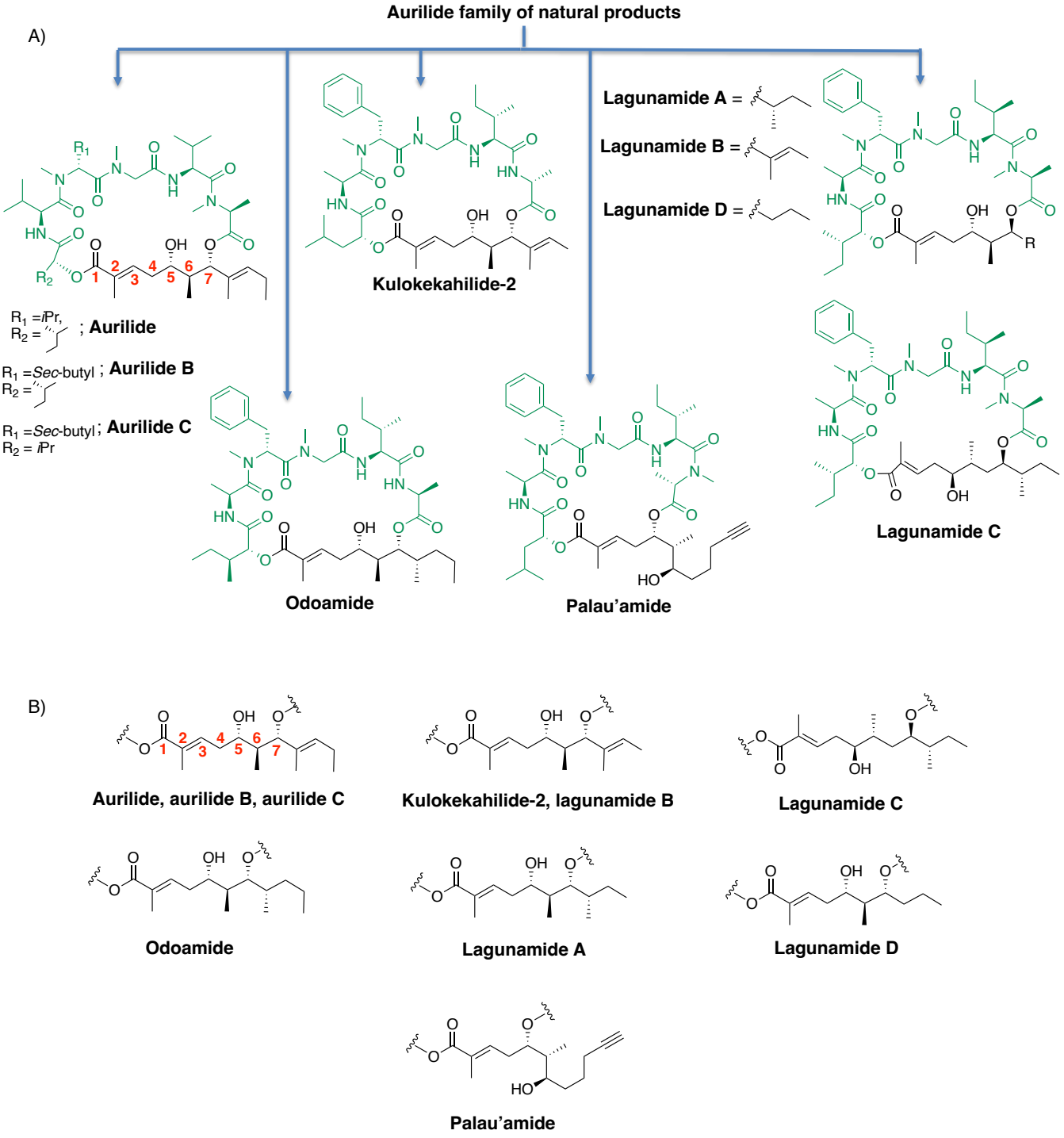


Figure 4 - A) Aurilde family of natural products; B) comparison of aurilide polyketide units

1.3.1.1 Lagunamides

As shown in Figure 4A, lagunamides A, B, and D share the same structure, except for the exocyclic carbon chain of the polyketide moieties (Figure 4B). In contrast, lagunamide C shares the same polypeptide moiety but differs completely from the polyketide moiety bearing an extra methylene unit, making it the only 27 membered aurilide of the entire family and therefore requires a new synthetic route to access this synthetically challenging polyketide. In addition to the need to develop a new synthetic route towards lagunamide C, stereochemical ambiguity about stereocenters at C5, C6, and C8 also needs to be addressed with a synthetic route. Given the aforementioned synthetic challenges, no total synthesis of lagunamide C has been reported to date. With this, our lab is currently undertaking synthetic efforts to gain access to this only 27 membered macrocyclic depsipeptide of the aurilide family.

1.3.1.2 Biological activity of aurilides

All members of the aurilide class are reported to be cytotoxic against many cancer cell lines, including lymphoma, ovarian, colon, and lung, at nanomolar concentrations[60] (Table 2). Aurilides can also act as inducers of apoptosis by interfering with mitochondrial morphogenesis[61,62]. Moreover, lagunamide subclass exhibits antimalarial activity with IC_{50} values of 0.19, 0.91, and 0.29 μM, respectively against *Plasmodium falciparum* strain at 100 ppm and exhibits moderate anti swamping activity against *Pseudomonas aeruginosa* PA01 strain[56,57].

Table 1 - Biological activity of aurilides [IC_{50} in nM (*LC_{50} in nM)]

Aurilides	$HeLaS_3$	P388	BJ	BJ Shp 53	PC3	SK-OV-3	HCT8	NCI-H460	Neuro-2a*	MDA-MB-435	A-10	KB	A549
Aurilide	11												
Aurilide B								10	40				
Aurilide C								50	130				
Kulokekalide-2		4.2				7.5				14.6	59.1		
Palau'amide												13	
Odoamide	26.3												4.2
Lagunamide A		6.4	20.2	58.8	2.5	3.8	1.6						2.9
Lagunamide B		20.5					5.2						
Lagunamide C		24.4			2.6	4.5	2.1						2.4
Lagunamide D													7.1

Upon studying the cytotoxicity values and careful structural analysis of the aurilide family of natural products, we observed a relationship between the two. Aurilide A, B, and C share the same polyketide moiety, but their polypeptide backbones are slightly different, and each exhibit cytotoxicity in different cell lines. On the contrary, the lagunamides share the same polypeptide moiety but differ in their polyketide units. Interestingly, they exhibit different cytotoxic values in common cell lines. Kulokekalide-2, palau'amide, and odoamide, which do not share the polypeptide or polyketide moiety, exhibit different biological activities in different cell lines. This

trend of aurilide cytotoxicity led our group to propose a plausible hypothesis on the mode of action of aurilides as a therapeutic agent, which will be explained further in Chapter 2.

Chapter 2 - Previous Synthetic Work

2.1 Structure and biological activity relationship of aurilides

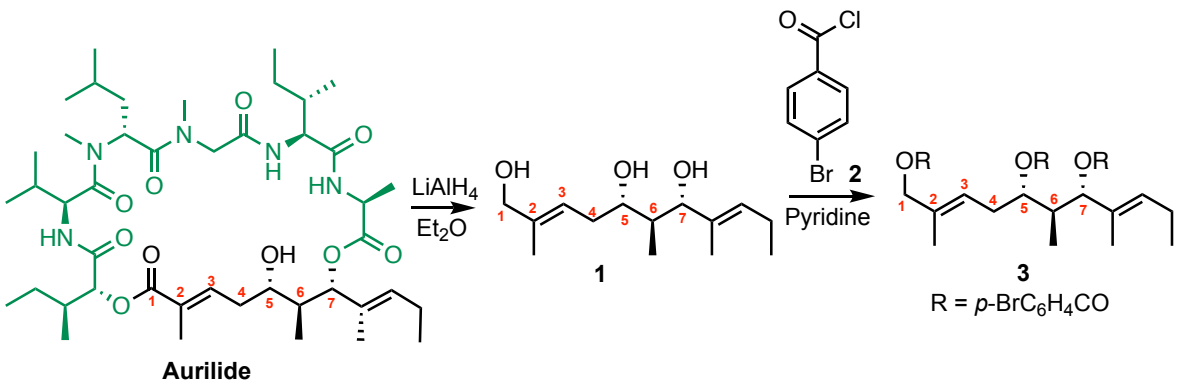
As previously discussed, aurilide, aurilide B, and C possess the same polyketide unit but have differences at the polypeptide units. Interestingly, all of the aurilides exhibit cytotoxicity in similar cell lines at different concentrations. Remarkably, three of the aurilide family members (kulokekahilide-2, palau'amide, and odoamide), exhibit cytotoxicity in different cell lines, but still with low nanomolar (nM) IC_{50} values. Similarly, in the lagunamide subfamily, all members share the same polypeptide moiety but bear different polyketide moieties, exhibiting different values of cytotoxicity in similar cell lines (See Figure 4, chapter 1). This unique pattern of same polypeptides aurilide having similar cell line selectivity and differences in the polyketide afford difference in IC_{50} activity.

Assembly of the polypeptide units of each of the aurilide family members is well established via standard amidation chemistry. This report discusses the key steps of the different synthetic routes established to build the architecture of the respective polyketide moieties of the aurilides isolated to date.

2.2 Synthesis of the polyketide moieties of the 26 membered depsipetides of the aurilide family

2.2.2 Aurilide

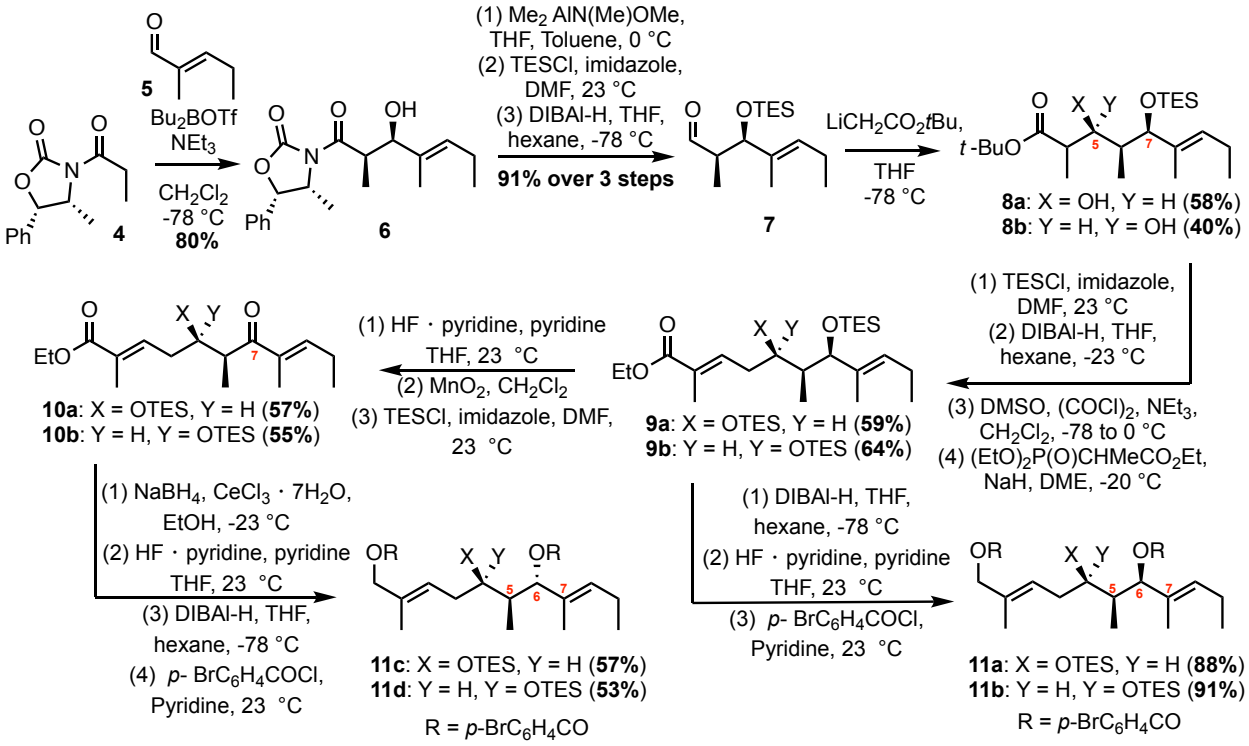
After the isolation of the first aurilide in 1996 by Suenaga et.al, the first reported synthetic efforts on its polyketide were performed by the same group in the same year to confirm the absolute stereochemistry of the three adjacent stereocenters (C5, C6, and C7)[63]. For this purpose, isolated natural product was first treated with $LiAlH_4$ resulting the triol **1** followed by acylation with *p*-bromobenzoyl chloride (**2**) to yield the tris(*p*-bromobenzoate) (**3**) (Scheme 1).



Scheme 1: Attempts to confirm stereochemistry of aurilide polyketide

To elucidate the stereochemistry of **3**, synthetic efforts were directed towards synthesis of each diastereomer (**11a** - **11d**) (Scheme 2). The synthesis commenced with the Evans type auxiliary **4** undergoing a boron mediated aldol reaction with trans-2-methyl-2-pentenal (**5**), resulting in Evans syn aldol **6** with a dr >95:5 in 80% yield. Transamidation using Weinreb amide followed by hydroxy group protection, and reduction of the amide group using DIBAl-H resulted in aldehyde **7.** The aldehyde was reacted with the organolithium ester $LiCH_2COOtBu$ to afford the two diastereomers about C5 **8a** (58% yield) and **8b** (40% yield). Resulted alcohols **8a** and **8b** were then converted to allylic esters **9a** (59% yield) and **9b** (64% yield) via silyl ether formation, complete reduction of the tert-butyl ester to an alcohol followed by Swern oxidation, and subsequent Horner-Emmons reaction with $(EtO)_2P(O)CH(Me)COOEt$. Esters **9a** and **9b** were subjected to reduction, desilylation, and acylation with *p*-BrC_6H_4COCl to obtain the expected tris(*p*-bromobenzoate) **11a** (88% yield) and **11b** (91% yield), respectively. Diols obtained via the desilylation of **9a** and **9b** were oxidized to access enones **10a** and **10b** (at C7) in 57% and 55% yield respectively. Obtained enones were then subjected to stereoselective ketone reduction in the presence of $CeCl_3$, desilylation, DIBAl-H reduction, and *p*-bromobenzoylation to afford the expected tris(*p*-bromobenzoate) **11c** (57% yield) and **11d** (53% yield), respectively (Scheme 2).

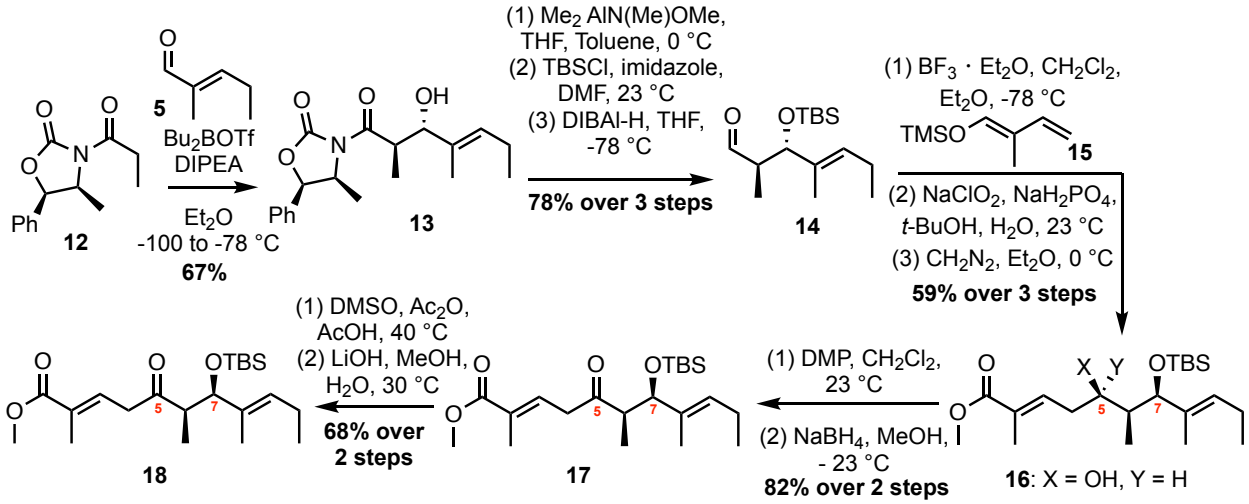
Detailed analysis of the 1H NMR spectra and circular dichroism (CD) spectra of the synthetic polyketide analogs **11a**, **11b**, **11c**, and **11d** was carried out and proved that the data for **11d** were identical to those for **3**. Hence, the absolute stereochemistry at C5, C6, and C7 was proven to be sinister, confirming the stereo structure of the polyketide of aurilide.



Scheme 2: Synthesis of triols 11a - 11d

Suenaga et.al achieved the first total synthesis of aurilide in 1997 relying upon their instrumental work in establishing stereochemistry at C5-C7[64]. Their optimized route of the polyketide started with the enantiomerically pure auxiliary **12** by employing an anti-aldol addition with the aldehyde **5** rather than the syn addition previously used. In this they accessed the anti-aldol product **13** as a single diastereomer in 67% yield. Elaboration of **13** onto **14** was performed with similar chemistry employed in Scheme 2 above in accessing the aldehyde **7** from alcohol **6**. Obtained aldehyde 14 was subjected to vinylogous Mukaiyama aldol reaction with 2-methyl-1-

trimethylsiloxy-1,3-butadiene (**15**), followed by diazomethane to deliver allylic ester **16**. Polyketide framework was now accessed in **16**, all that was required next was inversion of the free alcohol, which was accomplished by Des Martin acid and stereo selective reduction with $NaBH_4$ to afford **17** in 82% yield over two steps. The resulting alcohol was protected with a methylthiomethyl group and subjected to ester hydrolysis to afford the polyketide moiety **18** over 11 synthetic steps in 17% overall yield (Scheme 3).



Scheme 3: Synthesis of aurilide polyketide moiety

In 2003, Takahashi et.al attempted the total synthesis of aurilide and synthesized a 24 membered library of aurilide analogs that differed in polypeptide moiety to explore the importance of the peptide subunit[65]. However, data related to this study have not yet been reported. All analogs were composed of the same polyketide moiety, which was accessed using the same reaction conditions as in Scheme 3 above by Suenaga.

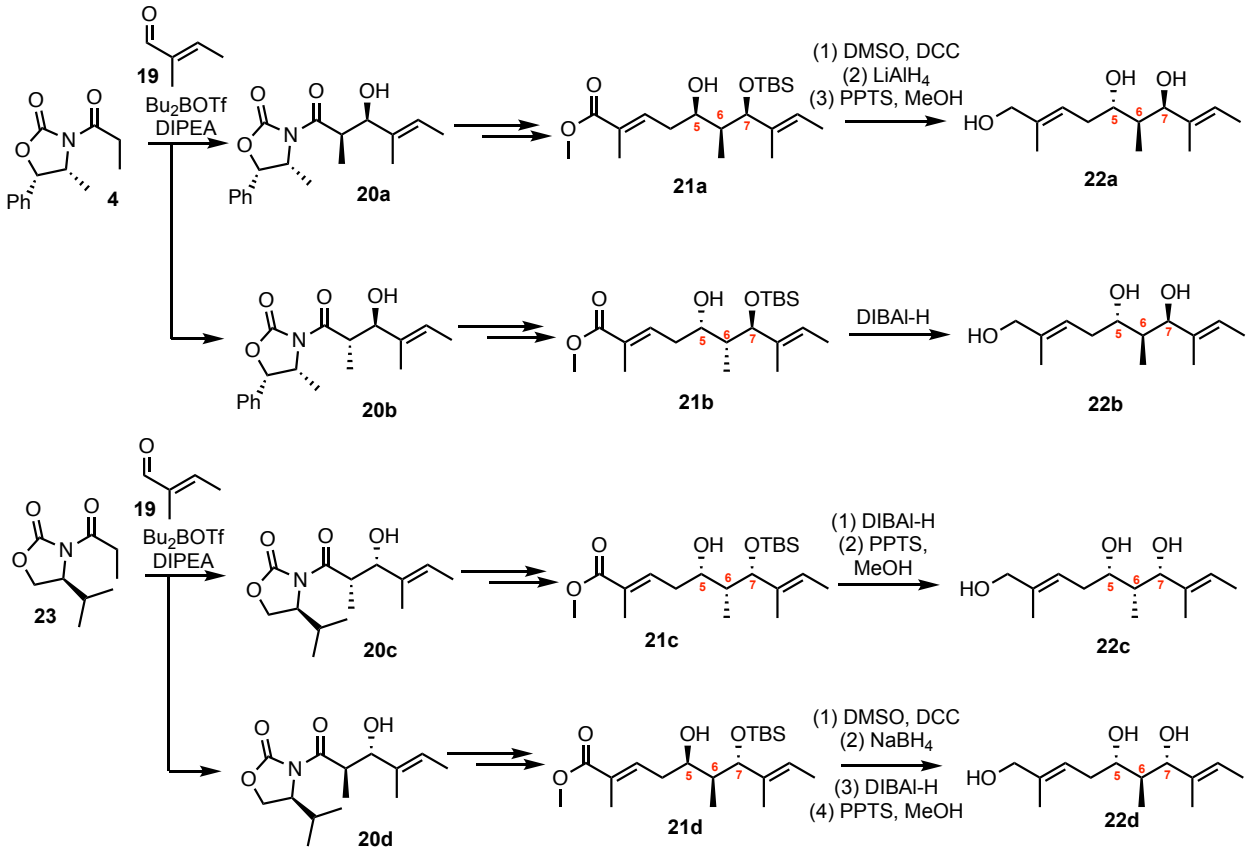
2.2.2 Aurilide B and C

Since the isolation of aurilides B and aurilide C in 2006 by Han et.al, no total synthesis/ attempts have been reported. One main reason is that both aurilides B and C share the same

polyketide moiety as aurilide, which has already been synthetically accessed. However, the absolute stereo structures of aurilides B and C were confirmed by NMR spectroscopy, chiral HPLC, and high-resolution fast atom bombardment mass spectrometry (HR-FABMS)[66].

2.2.3 Kulokekahilide-2

Nakao et.al were the first to access the polyketide moiety of kulokekahilide-2 in 2004, in an effort to confirm the stereochemistry at C5, C6, and C7[67]. The only difference between the aurilide and kulokekahilide-2 polyketide moieties is the ethyl substituent on the exocyclic olefine in aurilide while kulokekahilide-2 has a methyl substituent (See Figure 4, chapter 1). Hence, Nakao had implemented the same strategy as Suenaga and coworkers where they diastereoselectively synthesized triols **22a**, **22b**, **22c**, and **22d** and compared them with the triol obtained by the degradation of the isolated natural product. Starting from Evans auxiliaries **4** and **23**, the same synthetic route reported by Suenaga was utilized to access methyl esters **21a**, **21b**, **21c**, and **21d** via aldol products **20a** (syn), **20b** (trans), **20c**(syn), and **20d**(trans), respectively. **21a** was treated under Pfitzner–Moffatt oxidation conditions, followed by reduction with $LiAlH_4$ and desilylation to access triol **22a** with (*S*) stereochemistry at C5. Similarly, **21d** was transformed to **22d** over four steps. Compounds **21b** and **21c** were treated with DIBAl-H to reduce the methyl ester to access triols **22b** and **22c** in one and two steps, respectively (Scheme 4). Detailed analysis of the diastereomers proved that the data for **22d** were identical to those for the triol obtained by degradation of the isolated kulokekahilide-2, and the absolute stereochemistry at C5, C6, and C7 were proven to be of sinister configuration. Based on the established synthetic route to the polyketide, Nakao group achieved the first total synthesis of kulokekahilide-2 in 2007, which underwent a stereochemical revision at carbons 10, 19, and 22 on the polypeptide moiety, proving that the actual structure was **24** (Figure 5)[68].



Scheme 4: Synthesis of triols 22a - 22d

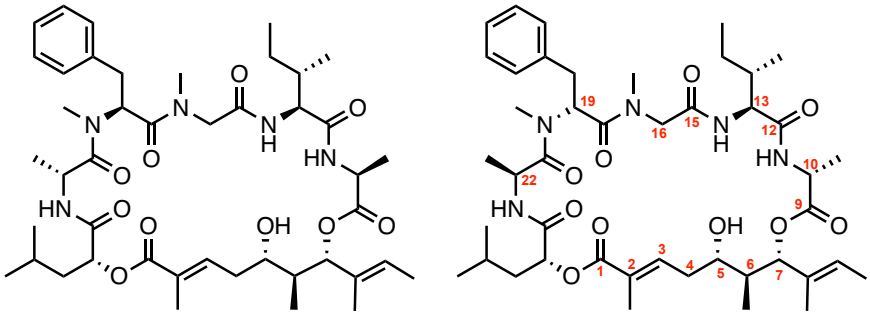


Figure 5: Proposed and revised structures of kulokekahilide-2

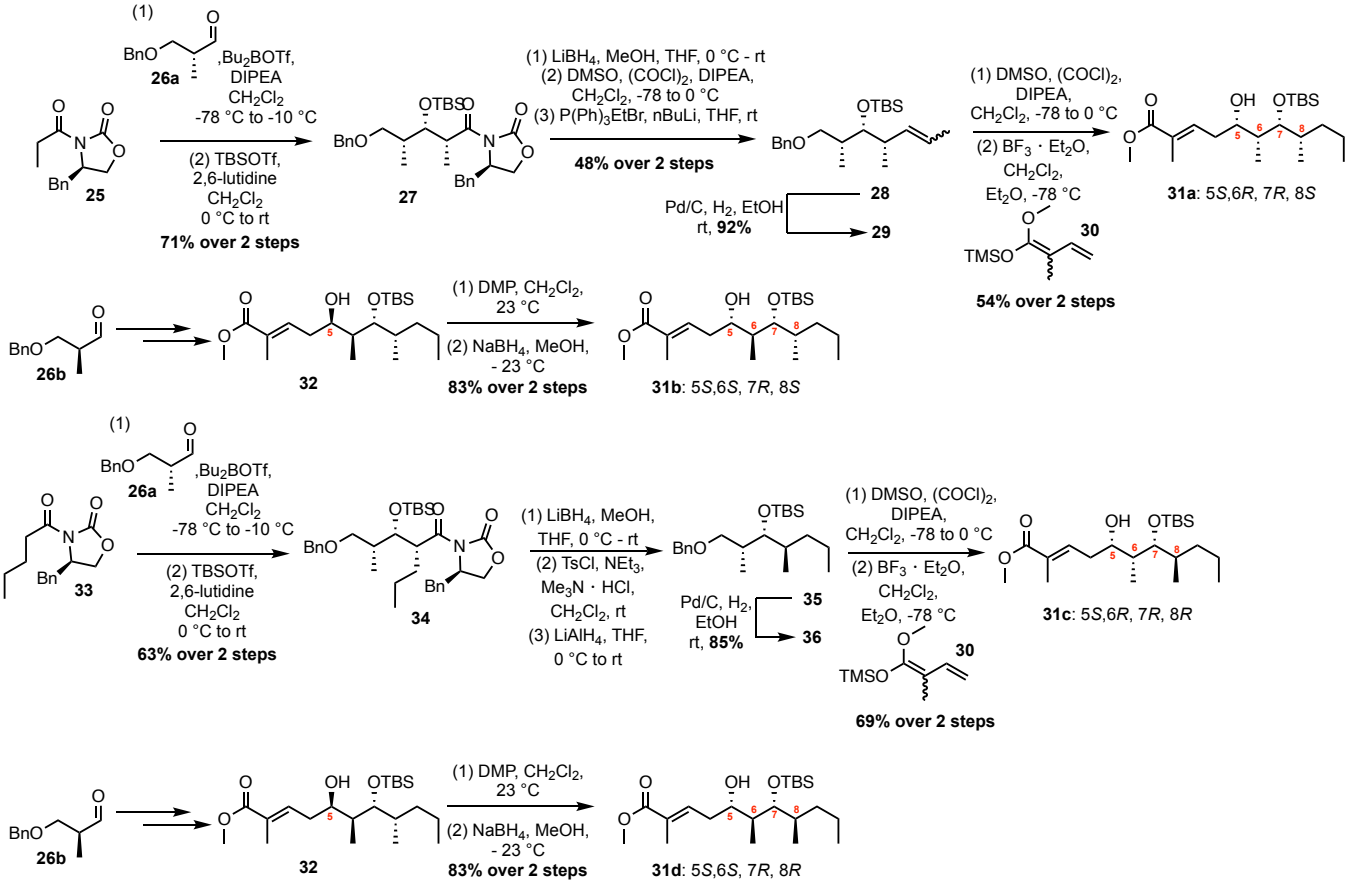
Utilizing the synthetic route established by Nakao et. al, in 2014, Han et. al synthesized a ^{11}C labelled radioactive polyketide of kulokekahilide-2 for positron emission tomography (PET) analysis[69]. It was intended to investigate the mode of action of kulokekahilide-2 using the

synthesized positron emitting radionucleotide which will be included in future reports by Han group.

2.2.4 Odoamide

So far, each polyketide has possessed three stereocenters, but the aurilide family of the odoamides have four contiguous stereocenters, C5, C6, C7, and C8, that need to be set. In 2016, Sueyoshi et. al confirmed the absolute stereochemistry around these carbon centers as 5*S*, 6*S*, 7*R*, and 8*S*, using a similar strategy reported by Suenaga and coworkers[70]. This marks the first synthetic study on the polyketide moiety of odoamide (Scheme 5). The synthetic route commenced with an Evans type chiral auxiliary **25**, undergoing a boron mediated aldol reaction with aldehyde **26a**, followed by silylation of the resulting alcohol to yield **27** in 71% yield over 2 steps. Reductive cleavage of the auxiliary, followed by Swern oxidation and Wittig olefination with ethyl triphenylphosphonium bromide, resulted in **28** as a mixture of stereoisomers around the newly formed olefin (Z:E = 7:1). Both benzyl group deprotection and alkene reduction were achieved via a Pd catalyzed hydrogenation to give **29** in 92% yield, which was again treated with Swern oxidation conditions to obtain the respective aldehyde. The obtained aldehyde was transformed into allylic ester **31a** (51% yield) via a vinylogous Mukaiyama aldol reaction with **30**. Dihydroxy ester **31b** was prepared following the same procedure as described above, starting from aldehyde **26b**, except for the stereochemical inversion (via DMP oxidation followed by stereoselective reduction with $NaBH_4$) at C5 of **32**. Starting with Evans chiral auxiliary **33**, aldehydes **26a,** and **26b**, the synthesis of **31c** and **31d** was carried out by devising the same key synthetic transformations respectively (Scheme 5). After confirming that the polyketide fragment **31b** was analogous to the isolated natural product polyketide moiety (14% overall yield in 10 synthetic

steps), the established synthetic route was utilized by the same group to achieve the first total synthesis of odoamide.



Scheme 5: Synthesis of Odoamide polyketide

2.2.5 Lagunamide A

The first reported synthetic work on the lagunamide A polyketide was done by Dai et.al in 2012, which also led to the revision of the stereochemistry at C7 and C30 in the isolated structure[71] (Figure 3).

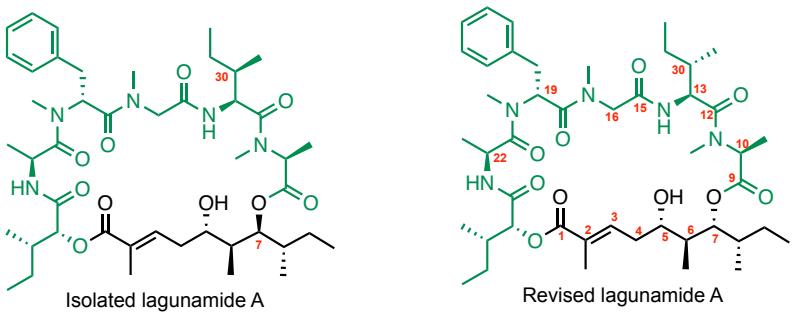
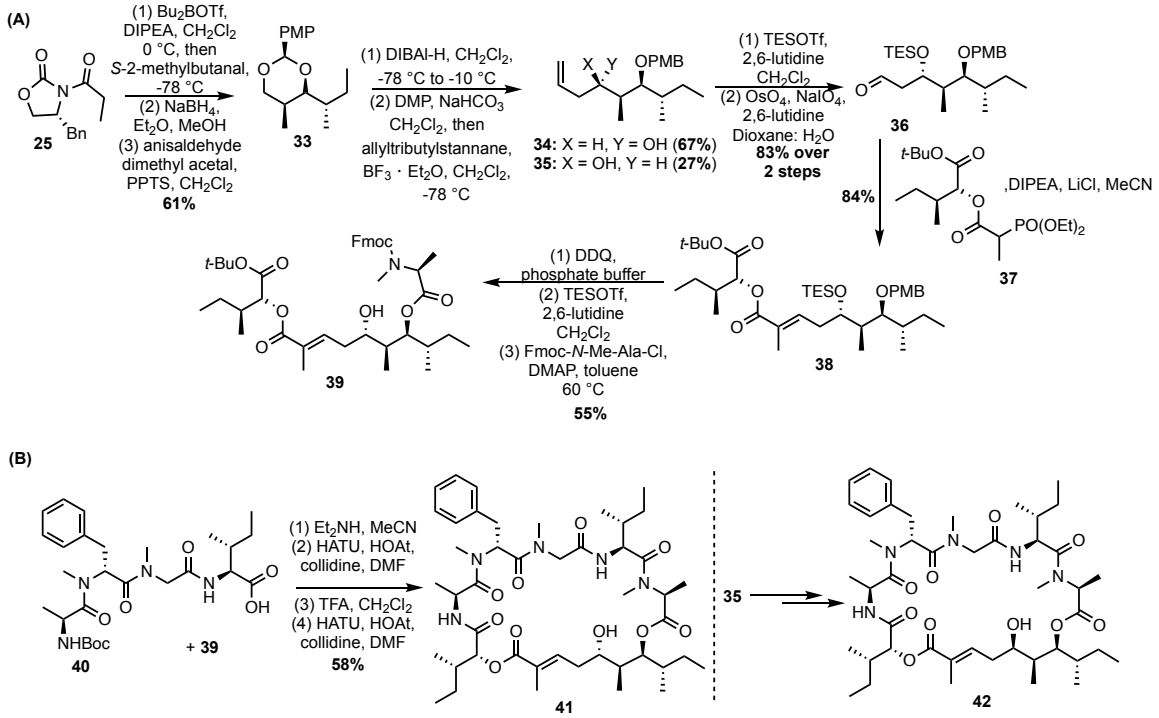


Figure 6: Proposed and revised structures of lagunamide A

Synthesis of the polyketide moiety was initiated with a boron mediated syn aldolization between Evans auxiliary **25** and *S*-2-methylbutanal, followed by reductive cleavage of the auxiliary and acetylation of the resulting diol with anisaldehyde dimethyl acetate to access acetal **33** in 61% yield (Scheme 6A). Next, the anisalidine acetal was reductively cleaved using DIBAl-H and subjected to DMP oxidation. The respective aldehyde was treated with allyltributylstannane, under Keck's conditions, to achieve diastereoselective allylation to yield homoallylic alcohols **34** and **35** in 67% and 27% yield respectively. Proceeding with **34**, silylation of the free alcohol followed by Lemieux–Johnson oxidation gave aldehyde **36** in 83% yield over 2 steps, which was then subjected to Horner Wadsworth Emmons (HWE) condensation with the synthesized phosphonate **37** furnishing **38** in 84% yield. Deprotection of the PMB group also led to partial desilylation of the TES group, which was reprotected with TESOTf to give polyketide moiety **39** (Scheme 24). Over a sequence of five steps, **39** was transformed into depsipeptide **41** to achieve the first total synthesis of the reported structure of lagunamide A. Simultaneously, depsipeptide **42** (epimer of **41**) was accessed starting from **35** using the same chemistry (Scheme 6B). Unfortunately, the spectroscopic data of either of the structures did not match the originally reported structure of lagunamide A. This led the authors to access four different stereoisomers of lagunamide A, where **43** and **44** were synthesized by focusing on the polyketide moiety and **45** and **46** by focusing on the polypeptide moiety (Figure 7). To their delight, the spectroscopic data of **46** matched the reported data for lagunamide A.



Scheme 6: (A) Synthesis of lagunamide A polyketide;(B) Synthesis of depsipeptides 41 and 42

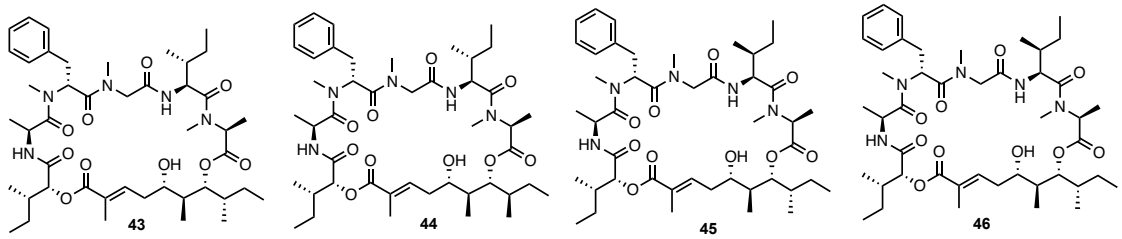
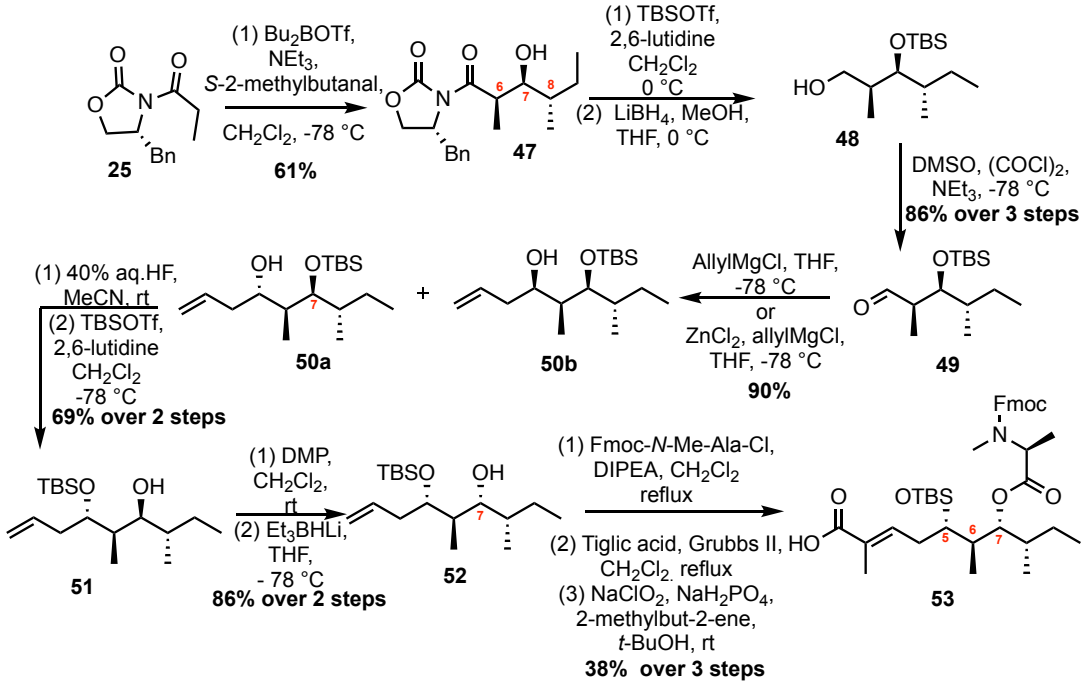


Figure 7: Stereoisomers of lagunamide A

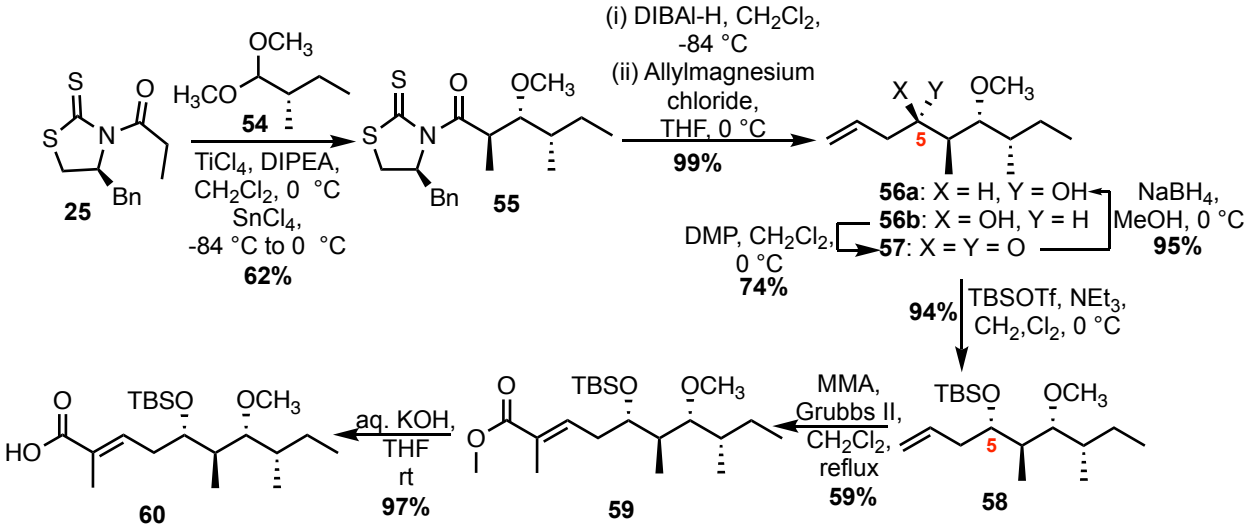
In 2013, Huang et. al reported an asymmetric total synthesis of lagunamide A, in which C6, C7, and C8 stereocenters of the polyketide were installed in a single step[72] (syn aldol **47**, Scheme 7). This transformation involves a boron mediated syn aldol reaction between Evans auxiliary **25** and *S*-2-methylbutanal to access syn aldol product **47** in 61% yield. Silylation followed by reductive cleavage of the chiral auxiliary resulted in alcohol **48** in 95% yield, which was elaborated onto the aldehyde **49** via Swern oxidation. Subjecting 49 to allyl Grignard afforded the two diastereomers **50a** and **50b** in 11% and 81% yield respectively. Unfortunately, the desired diastereomer was **50a**. To favor the diastereomer, reaction was performed in the presence of the

Lewis acid $ZnCl_2$ to afford **50a** and **50b**, but now in a 90% and 10% yield respectively. While **50a** was used in the synthetic route to access the first proposed structure of lagunamide A, it was necessary to invert the stereochemistry around C7 of alcohol **50a** to access the polyketide moiety of the revised structure of lagunamide A. Hence, alcohol **50a** was first desilylated, followed by selective silylation with TBSOTf to access **51** in 69% yield over 2 steps with high regioselectivity. Silylation was done at a very temperature (-78 °C) allowing the less sterically hindered alcohol at C4 (kinetically favored) to undergo selective protection. It was then subjected to DMP oxidation followed by reduction with lithium triethylborohydride to yield the desired alcohol **52** with dr >99:1 and coupled with Fmoc-N-Me-L-Ala-Cl to form the respective ester. Resulted ester was then subjected to cross metathesis conditions with tiglic acid in the presence of Grubbs II catalyst and subsequent Pinnick oxidation to yield the polyketide moiety **53** of lagunamide A in 10% overall yield over 12 synthetic steps (Scheme 7).



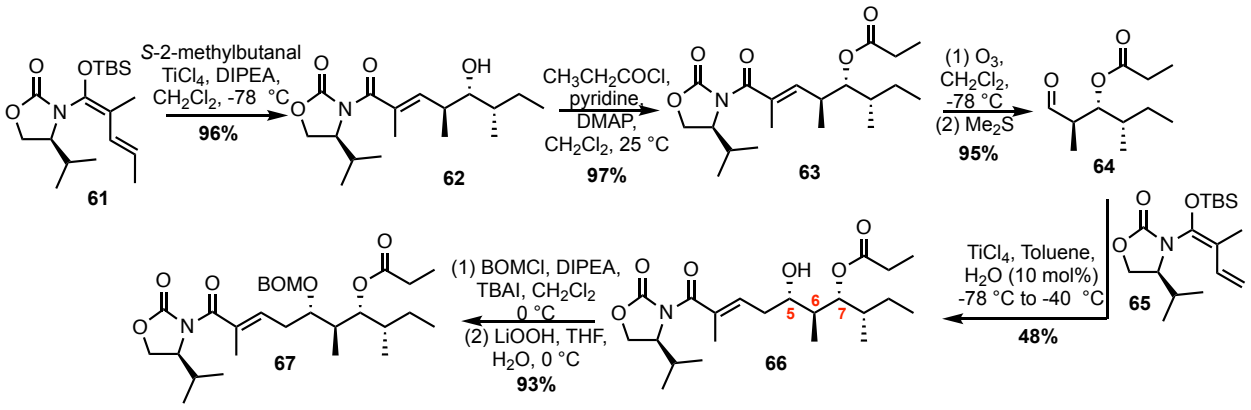
Scheme 7: Lagunamide A polyketide synthesis by Huang et. al

In 2014, Chang et.al reported a more robust stereoselective and efficient synthetic route to access the lagunamide A polyketide fragment[73] (Scheme 8). Chang group was the first to report the utility of a Crimmins auxiliary in the synthesis of aurilide polyketides. Chiral acetal **54** was accessed by treating commercially available *S*-2-methylbutanol with methanol and catalytic *p*-toluenesulfonic acid. It then undergoes an acetal aldol reaction with Crimmins chiral auxiliary **25**, yielding aldol adduct **55** in 62% yield with a dr of 82:18. Reductive cleavage of the auxiliary with DIBAl-H resulted in the respective aldehyde, which underwent a subsequent Grignard reaction with allyl magnesium chloride to give homoallylic alcohols **56a** and **56b** in a dr of 2:3 with an overall yield of 99%. The stereochemistry at C5 in alcohol **56b** was inverted to obtain the desired alcohol **56a** by performing DMP oxidation (**57**), followed by stereoselective reduction with $NaBH_4$. This yielded the desired alcohol, **56a**, with an improved dr of 8:1. The obtained alcohol **56a** was then silylated to yield **58** in 94% and subjected to cross metathesis condition with methyl methacrylate in the presence of Grubbs II to yield the methyl ester **59**. Obtained ester was saponified to access the desired polyketide moiety **60** of lagunamide A with an overall yield of 23% in 7 steps.



Scheme 8: Lagunamide A polyketide synthesis by Chang et.al

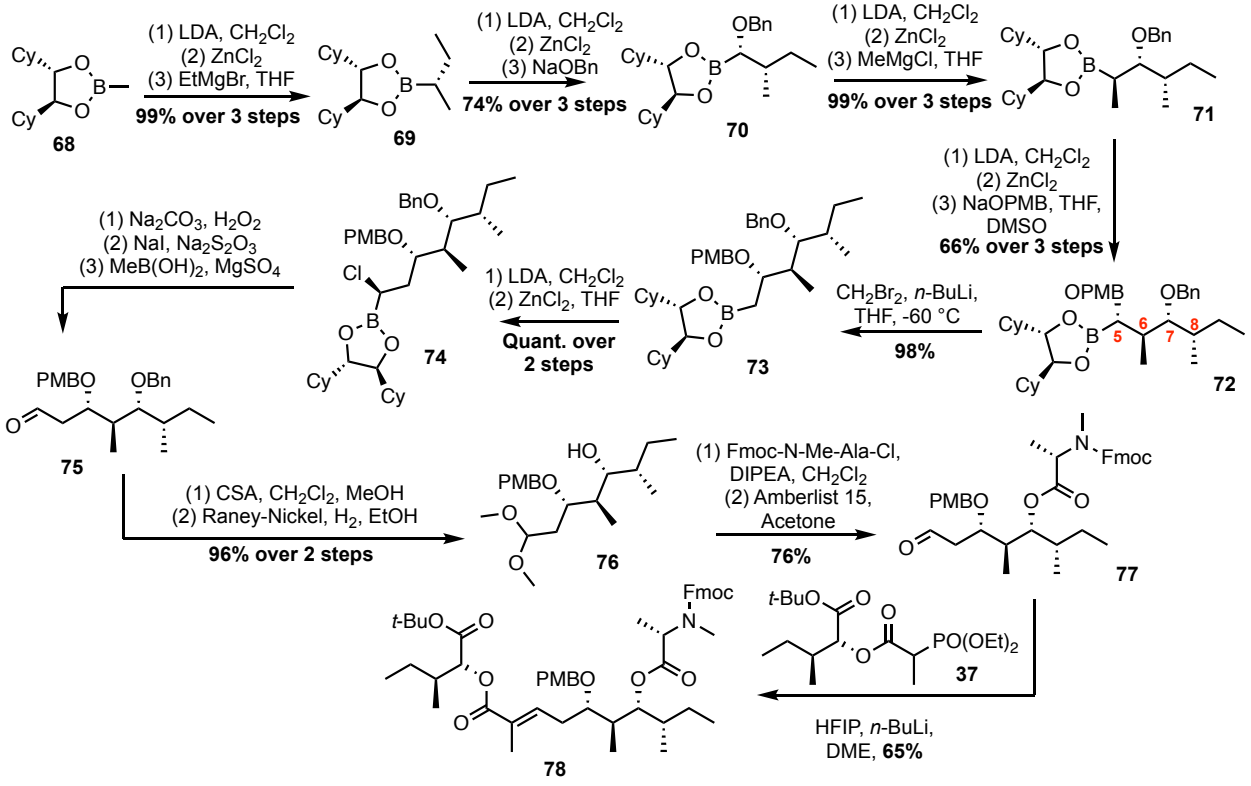
In 2016 Banasik et. al reports another improved synthetic route to access the lagunamide A polyketide moiety utilizing two repetitive vinylogous Mukaiyama aldol reactions (VMAR) to install three of the four adjacent stereocenters (C5, C6, and C7)[74] (Scheme 9). The synthetic route starts with the first VMAR between commercially available *S*-2-methylbutanal and chiral vinylketene silyl N,O-acetal **61** in the presence of the Lewis acid $TiCl_4$ to give the anti-aldol product **62** in 96% yield with a dr >98:2. The obtained alcohol was protected as the propionate ester (**63**), which yielded aldehyde **64** upon ozonolysis in 95% yield over 2 steps. Aldehyde **64** undergoes the second VMAR with chiral vinylketene silyl N,O-acetal **65**, resulting in anti-aldol product **66** in 48% yield, which was then protected as a benzyloxymethyl acetal (BOM). The selective oxidative cleavage of the chiral auxiliary with lithium hydroperoxide resulted in the expected polyketide moiety **67** with an overall yield of 39% in 7 synthetic steps. (Scheme 9).



Scheme 9: Lagunamide A polyketide synthesis by Banasik et. al

The latest improved synthetic strategy for the polyketide moiety of lagunamide A has been reported by Gorges et. al in 2018[75]. Reported strategy is based on Matteson Homologation, in which stereoselectivity is achieved via a chiral boronic ester (Scheme 10). Synthesis starts with methyl boronic ester **68** undergoing the first Matteson homologation with ethyl magnesium bromide to result the second boronic ester **69** as a single diastereomer in quantitative yield. Three

similar homologations with benzyl alcoholate, methyl Grignard reagent, and *p*-methoxybenzylate yielded boronic esters **70**, **71**, and **72**, with 74%, 99%, and 66% respectively. With all four contiguous stereocenters (C5-C8) being installed, a fifth homologation was performed to introduce a methylene unit, which was accomplished by an in-situ generated bromoethyl lithium at -60 °C, resulting in boronic ester **73** in 98% yield. The final homologation generated α-chloroboronic ester **74** in quantitative yield, which was oxidized to aldehyde **75**. Acetal formation, debenzylation (acetal **76**), and condensation with Fmoc-N-Me-L-Ala-Cl, followed by acetal hydrolysis, yielded aldehyde **77** in 73% yield over 4 steps. A HWE reaction was performed between aldehyde **77** and phosphonate **37** to assemble lagunamide A polyketide containing molecule **78** with an overall yield of 22% in 20 syntehtic steps (Scheme 10).



Scheme 10: Lagunamide A polyketide synthesis by Gorges et.al

2.2.6 Lagunamide B

To date, only synthetic work on the lagunamide B polyketide moiety was reported by Chakraborty et.al in 2014[76]. With the stereochemical revision of lagunamide A by Dai et.al in 2012, Chakraborty group suggest the stereochemistry at C7 and C30 of lagunamide B to be inverted as well (Figure 8). However, the authors first attempted to access the structure reported by isolation chemists, which is an analog of the actual natural product. The synthetic route of the polyketide starts with a $TiCl_4$ catalyzed Evans syn aldolization between the auxiliary **25** and aldehyde **19**, followed by silylation to yield **79** in 82% yield over 2 steps (Scheme 11). Reductive cleavage of the auxiliary followed by oxidation with a pyridine-sulfur trioxide complex yielded aldehyde **80** (75% over 2 steps), which underwent a boron mediated aldol reaction with chiral auxiliary **81**, providing a mixture of diastereomers **82a** and **82b** with a dr of 2:1 and overall yield of 63%. Protection of the free alcohol of the desired aldol product **82a** as a MOM ether, reductive cleavage of the auxiliary followed by oxidation with pyridine-sulfur trioxide complex generated aldehyde **83** in 64% yield over 2 steps. α-hydroxy ester **84** was coupled with 2-(diethoxyphosphoryl) propanoic acid (**85**) and the resulting propionate was condensed with the aldehyde **83** followed by debenzylation to afford the analogue polyketide moiety **86** of isolated lagunamide B with 12% overall yield in 11 synthetic steps (Scheme 11).

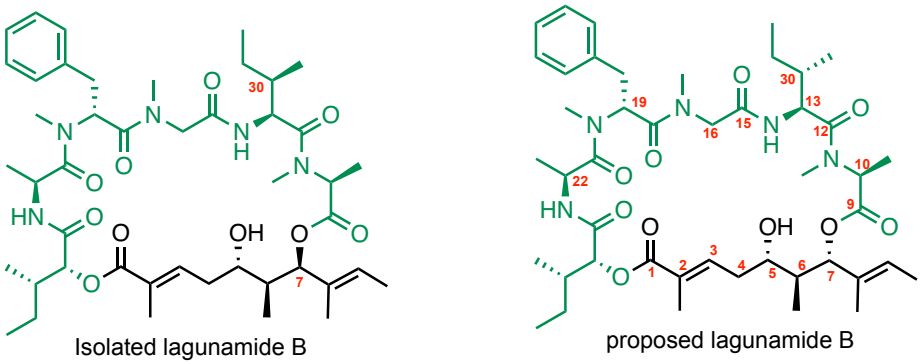
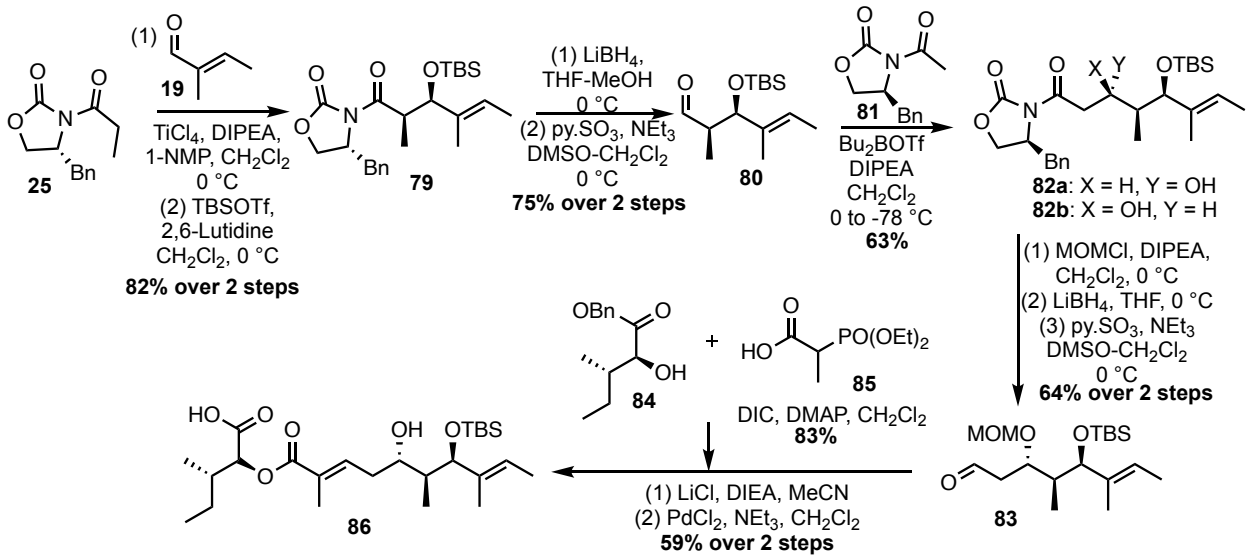


Figure 8: Isolated and proposed lagunamide B structures

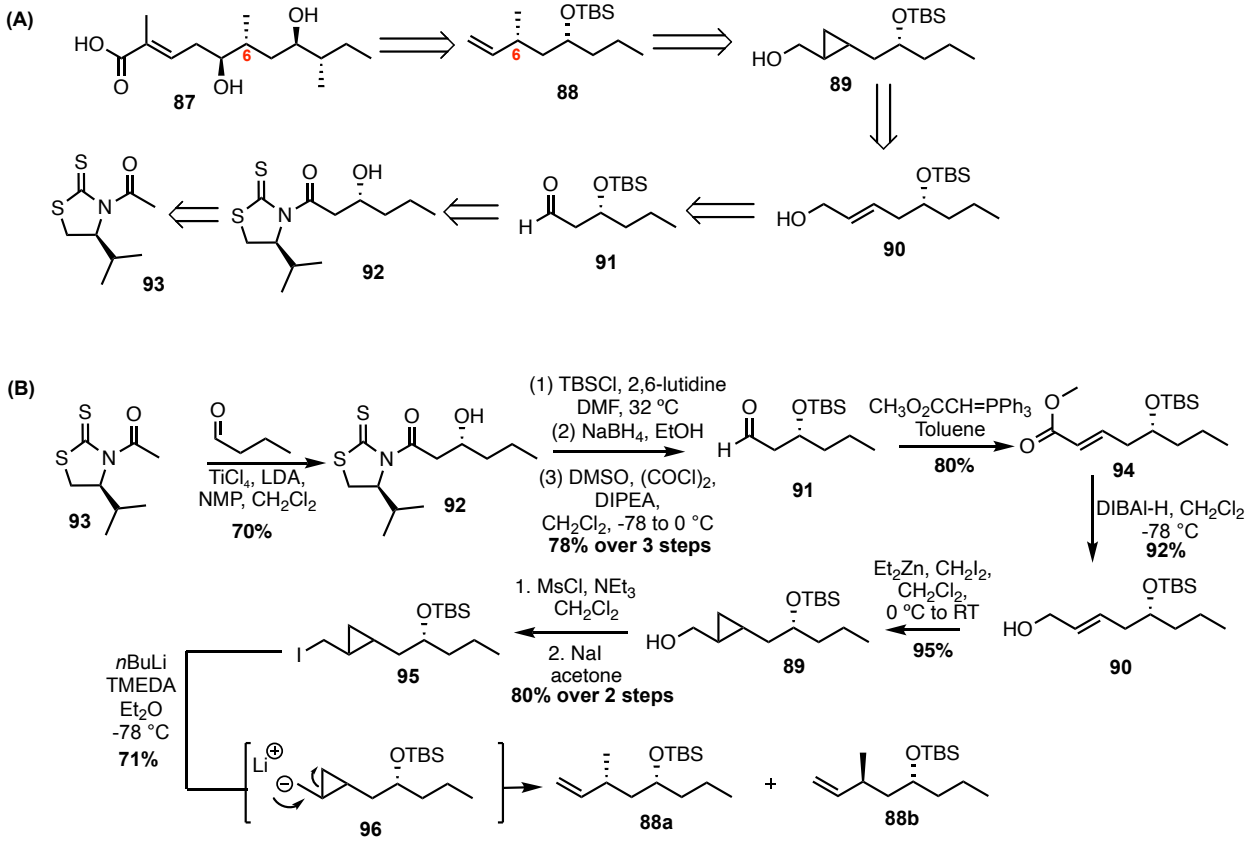


Scheme 11: Polyketide synthesis of lagunamide B analogue by Chakraborty et. al

2.2.7 Lagunamide C

Aurilides discussed so far are either 26 membered or 24 membered macrocycles whereas lagunamide C contain and extra methylene unit in its polyketide moiety making it the only 27-member cyclic depsipeptide in the aurilide family. This unique feature makes accessing the lagunamide C structure synthetically challenging and hence no total synthesis has been reported to date. Insertion of the extra methylene unit in the polyketide moiety and the final macrocyclization intrigue synthetic chemists to achieve the first total synthesis of lagunamide C. Our lab in 2018 undertook a probing project into the synthesis of the lagunamide C polyketide **87**. Fatino et al. reported an efficient synthetic route that can be utilized to install this extra methylene unit onto the polyketide moiety[77]. More importantly, feasibility in incorporating a cyclopropanation followed by subsequent ring opening to install the C6 methyl unit, the linchpin step of this probing project was established (Scheme 12A). The forward synthesis starts with a Crimmins type auxiliary **93** undergoing a $TiCl_4$ mediated aldol reaction with a commercially available aldehyde, butanal, providing **92** in 70% yield with a dr of 20:1 (Scheme 12B). Silylation and reductive cleavage of the chiral auxiliary followed by Swern oxidation resulted aldehyde **91**

in 78% yield over 3 steps, which was then subjected to Wittig olefination to yield methyl ester **94**. Reduction of the ester with DIBAl-H yielded the precursor for the linchpin cyclopropanation, allylic alcohol **90** in 95% yield. Cyclopropanation (compound **89**) followed by subsequent ring opening via the transition state **96** provided the expected polyketide intermediate as a mixture of diastereomers, **88a** and **88b** in 71% yield. Utilization of this established linchpin step in the diastereoselective synthesis of the lagunamide C polyketide will be discussed in Chapter 3.



Scheme 12: (A) Retrosynthetic analysis of probing route to lagunamide C polyketide; (B) Exploration of the set synthetic route to access lagunamide C polyketide analogue

2.3 Ring closing techniques in aurilides synthesis

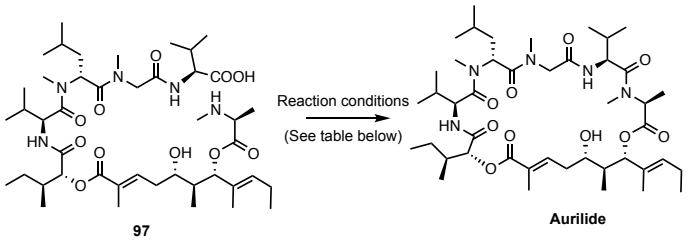
The final cyclization step in all synthetic routes for accessing the 26-member cyclic depsipeptides of the aurilide family can be summarized under three main categories as follows.

Macrolactamization: final ring closing was performed via cyclic amide (lactam) bond formation, Macrolactonization: final ring closing through a cyclic ester (lactone) bond, and ring closing metathesis (RCM): ring closing via an intramolecular metathesis of two terminal alkenes. Each synthetic attempt will be described below.

2.3.1 Macrolactamization

Final ring closing step of aurilide in all the reported synthetic routes were achieved via macrolactamization by condensing the N terminal of N-Me-*L*-Ala onto the C-terminal of L-valine (precursor **97**). Suenaga et. al was the first to access the cyclodepsipeptide, aurilide via macrolactamization in 1997[64]. They were able to access aurilide in 32% yield using Bop-Cl mediated peptide coupling conditions. Same reaction was attempted by Takashi et. al in 2003 with EDCI mediated solid phase peptide coupling conditions to access the macrocycle with a purity of 48% via HPLC analysis[65]. Suenaga et.al in 2004 reported an optimized macrolactamization step to access aurilide with EDCI·HCl mediated peptide coupling conditions[78]. The latter gave the highest yield reported so far in macrolactamization of aurilide synthesis which is 66%. Table 2 below summarizes the reaction conditions used for each synthesis.

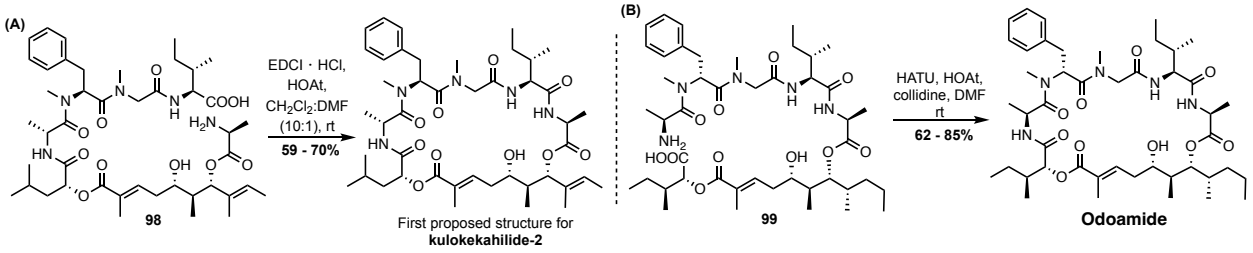
Table 2: Macrolactamization reaction conditions of aurilide



97 Aurilide

Research group, year	Reaction conditions
Suenaga et. al, 1997	Bop-Cl, Et_3N, CH_2Cl_2, 23 °C, 32%
Takahashi et. al, 2003	EDCI, HOAt, 10% DMF/CH_2Cl_2 (1mM), rt, 24 h
Suenaga et. al, 2004	EDCI·HCl, HOAt, CH_2Cl_2:DMF (10:1), rt, 66%

In the first total synthesis of the proposed kulokekahilide-2 structure and its analogs by Takada et.al in 2007 and 2008 respectively, ring closure was performed via macrolactamization of the precursor **98** using the latest conditions reported by Suenaga and coworkers in 2004[68,79] (Scheme 13A). The yields obtained for the target macrocycles were ranging from 59 – 70%. In 2016, Kaneda et. al also utilize a macrolactamization strategy in their first total synthesis of odoamide. They report accessing the macrocycle via a different disconnection approach compared to aurilide and kulokekahilide-2; condensation of N terminal of alanine with the C terminal of *D-allo*-isoleucine moiety[80](Scheme 13B) . Macrolactamization of the precursor **99** was achieved using HATU mediated peptide coupling conditions and the yield range from 62% to 85%.

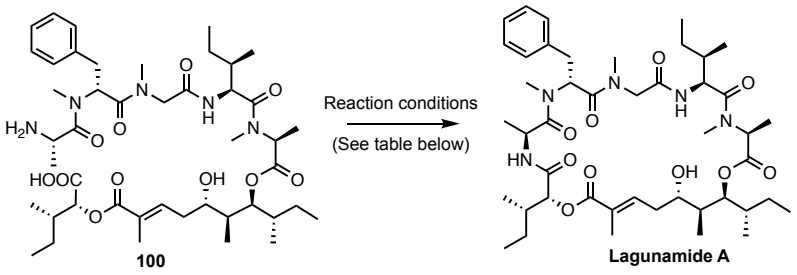


Scheme 13: Macrolactamization of (A) kulokekahlide-2 and (B) odoamide

Ring closure to access lagunamide A and its derivatives were completed via macrolactamization by and Gorges et. al, Dai et. al, and Huang et. al, in 2004, 2012, and 2013 respectively[71,72,75]. All three groups were following the same disconnection approach (precursor **100**) used by Kaneda et. al in total synthesis of odoamide to close 26 membered ring. All three groups also use the same peptide coupling reagent, HATU but with different reaction conditions

and additives. However, Dai et. al reports the highest yield obtained in a macrolactamization of an aurilide member so far. Table 3 below summarizes the reaction conditions used for each synthesis.

Table 3: Macrolactamization reaction conditions of lagunamide A

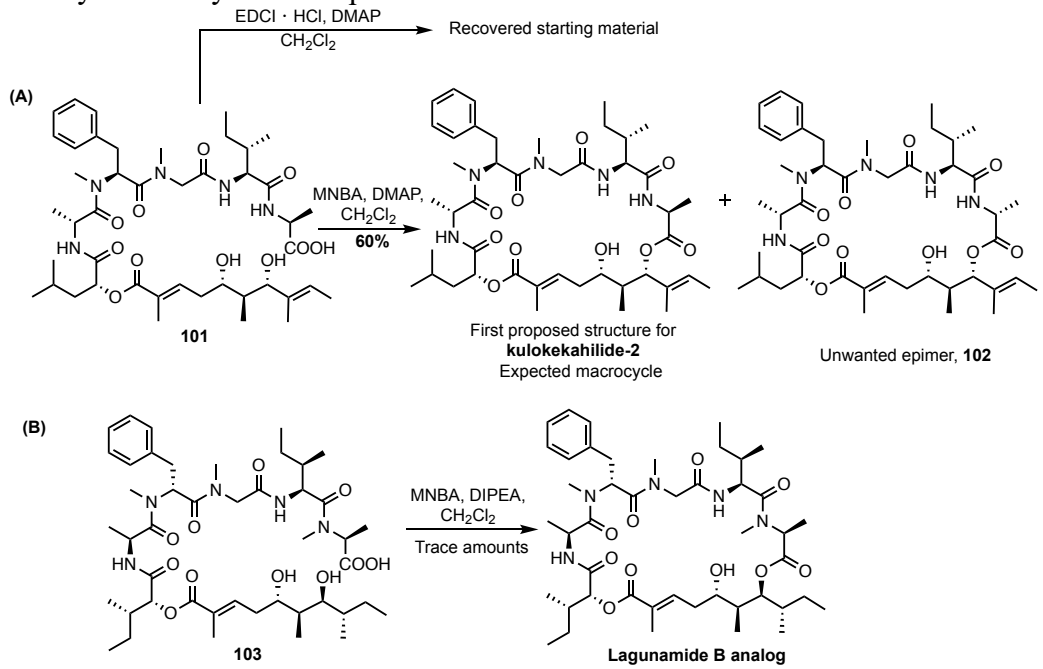


Research group, year	Reaction conditions
Dai et.al, 2012	HATU, HOAt, collidine, DMF, 71%
Huang et.al, 2013	HATU, DIPEA, CH_2Cl_2 (1 mM), rt,
Gorges et.al, 2004	HATU, HOAt, collidine, DMF (1 mM), rt, 45%

2.3.2 Macrolactonization

First reported macrolactonization attempted to access an aurilide member was in 2007 by Nakao et. al in the synthesis of the first proposed structure of kulokekahilide-2[81]. This first attempt was performed using EDCI·HCl and DMAP where the starting material **101** was recovered in quantitative yield. The second attempt was carried out under Shiina lactonization conditions using 2-methyl-6-nitrobenzoic anhydride (MNBA) and DMAP, which yielded the expected cyclic product in 60% yield (Scheme 14A). However, they observed that macrolactonization resulted in epimerization around the α-C of the N-methyl-L-alanine moiety, leading to the epimer **102**. This led Nakao group choose macrolactamization over macrolactonization in the ring closure efforts enroute to the revised structure of Kulokekahilide-2. In 2014, synthetic work done by Chakraborty et. al towards the synthesis of lagunamide B analog **103**, the final cyclization was performed by establishing an ester bond using Shiina lactonization conditions with MNBA[76] (Scheme 14B).

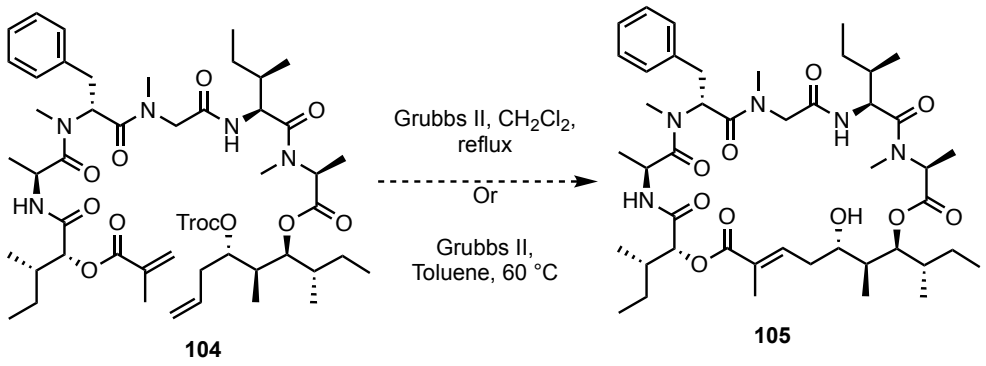
Unfortunately, the yield was poor for further analysis and optimizations on the final cyclization step is currently underway and is expected in the future.



Scheme 14: Macrolactonization of (A) kulokekahilide-2 and (B) lagunamide B analog

2.3.3 Ring closing metathesis (RCM)

Only reported work on utilizing a RCM strategy in accessing an aurilide is by Huang et. al in 2013 in diverse synthesis of lagunamide A. Envisioning to access the depsipeptide **105** as the E isomer of the alkene, they attempted RCM of the diene **104** with Grubbs 2nd generation catalyst. Unfortunately, the expected macrocycle **105** was not obtained (Scheme 15). Huang group has screened only two solvents at two different tempetatures with Grubbs II. Hence, further investigation into this method of ring closure is required.

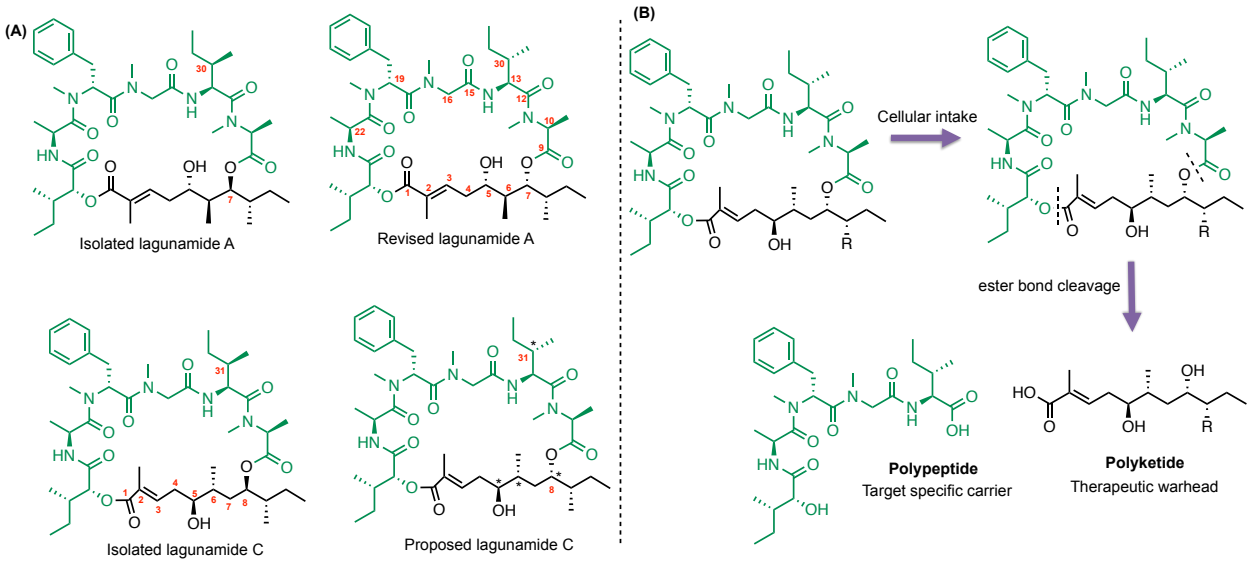


Scheme 15: Ring closing metathesis attempt to access lagunamide A macrocycle

2.4 Hypothesis

Among all aurilides reported to date, lagunamide C is the only 27 membered cyclodepsipeptide of the entire aurilide family, limiting the direct application of previously reported synthetic routes to aurilide polyketide moieties, making it more synthetically challenging. This synthetic challenge, along with the ambiguous stereocenters in the reported lagunamide C structure and interesting biological activity drew attention of our Rafferty lab. Based upon the total synthesis and structure revision of Lag A by Dai et. al, our lab proposes the structure of lagunamide C to be inverted at C8 and C31 (Scheme 16A). With the great work done by Fatino et. al on the polyketide moiety synthesis of proposed lagunamide C as the foundation, this work discusses an improved diastereoselective synthetic route to achieve the first total synthesis of the proposed only 27-member cyclodepsipeptide in aurilide family, lagunamide C followed by stereochemical assignment of the ambiguous stereocenters highlighted in blue stars (C5, C6, C8, C31). Moreover, after a detailed analysis of the cytotoxicity of aurilide members, our lab hypothesize that the polypeptide moiety assists the delivery of the natural product into the cell, which, upon internalization, is cleaved at the ester bonds by esterase to release the therapeutic polyketide moiety (Scheme 16B). This hypothesis will be tested using synthetic proposed lagunamide C, polyketide

moiety, and polypeptide moiety. synthesis of the amide analog of prooosed lagunamide C by replacing the ester linkages to further support this hypothesis will be carried out. Furthermore, the total synthesis of this only 27 membered aurilide will open doors to explore a new gene cluster in the marine cyanobacterium *Lyngbya majuscule*, leading to the discovery of many promising marine drugs. With versatile synthetic handles on lagunamide C, its application as a natural drug carrier vehicle is also discussed.



Scheme 16: (A) Isolated and revised structure of lagunamide A, Isolated and proposed structure of lagunamide C; (B) hypothesized mechanism of action of aurilides

With the introduction of the latest member, lagunamide D, to the aurilide family in 2019 and its structural similarity to lagunamide A, we propose a possible new natural product for the aurilide family, lagunamide E (Figure 9). This will be the 27 membered ring analog of lagunamide D. Synthetic efforts to access the polyketide moiety of the proposed natural product lagunamide E were initiated by Fatino et al. during the feasibility study in incorporating a cyclopropanation followed by subsequent ring opening to install the C6 methyl unit on the polyketide moiety of

lagunamide C. Further modifications and developments of the established route to complete the synthesis of the proposed lagunamide E are also discussed in this report.

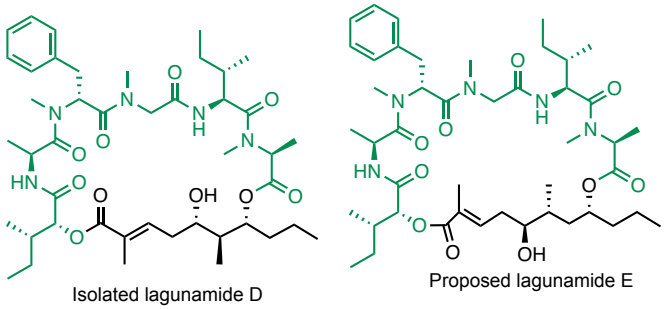
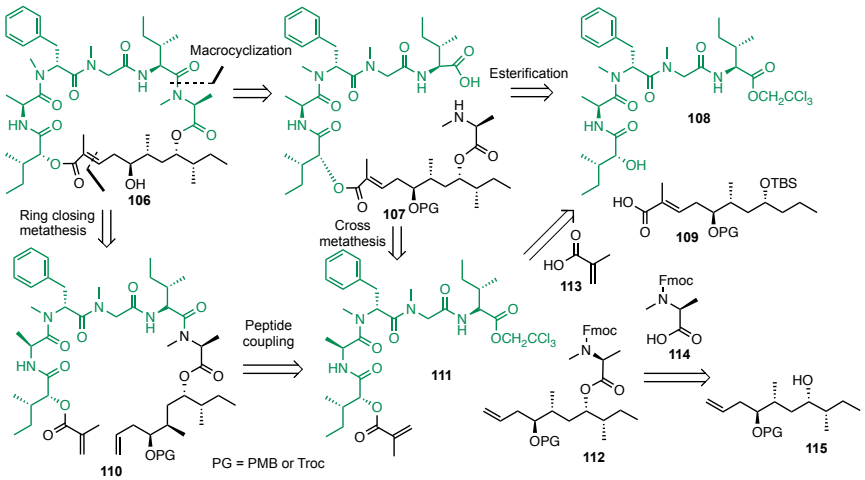


Figure 9: Isolated lagunamide D structure and proposed lagunamide E structure

Chapter 3 – Synthetic Efforts Towards Lagunamide C and Proposed Lagunamide E

3.1 Retrosynthetic analysis of lagunamide C

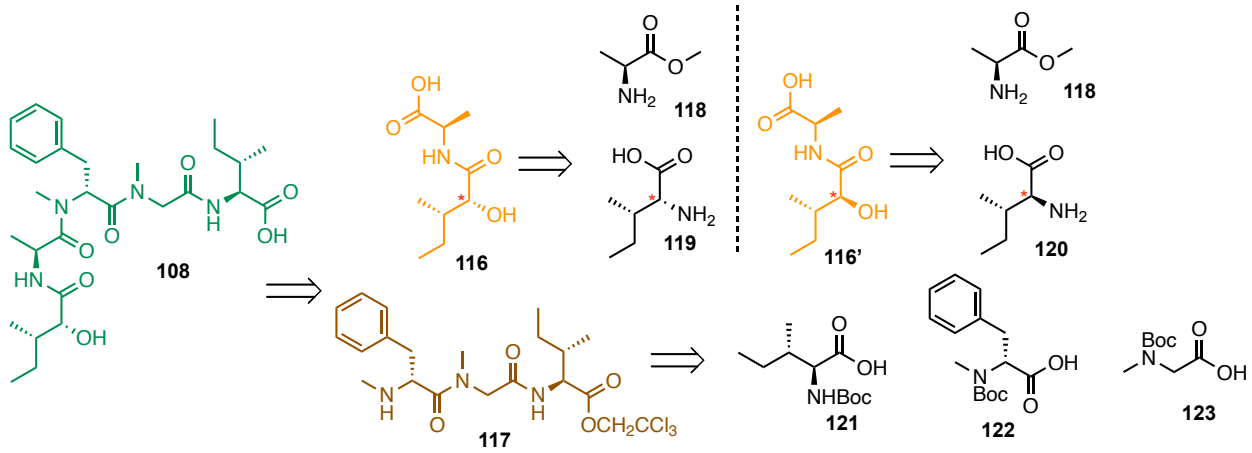
Inspired by the previous synthetic work done on aurilides explained in chapter two, three different approaches were explored in accessing the final 27 membered macrocycle of lagunamide C: 1) macrocyclization, 2) cross metathesis followed by macrocyclization, and 3) ring closing metathesis. The first suggested route involves condensation of the polyketide moiety (**109**) on to the pentapeptide backbone (**108**) to access ester **107**, which will undergo macrocyclization to give **106**. In the second route, macrocyclization precursor **107** can be accessed via cross metathesis of the olefins **111** and **112**, via Grubbs second generation catalyst, followed by macrocyclization as in route 1 above. The third cyclization approach involves a ring closing metathesis (RCM) of the diene **110** that can be accessed by coupling of the free amine of **112** with free carboxylic acid of **111**. Compound **111** is envisioned to access by condensing methacrylic acid (MAA, **113**) onto the pentapeptide moiety (**108**). *N*-Fmoc-methyl-L-alaninol (**114**) will be coupled with the alcohol **115** (an intermediate of the lagunamide C polyketide synthetic route) to access alkene **112** (Scheme 17).



Scheme 17: Ring closing approaches to access lagunamide C

3.2 Retrosynthetic analysis of the pentapeptide moiety

The pentapeptide moiety common for all three ring closing approaches was envisioned to access by coupling the dipeptide **116** and tripeptide **117** (Scheme 18). Dipeptide is composed of two commercially available amino acids *L*-alanine methyl ester (**118**) and *D*-alloisoleucine (**119**) whereas tripeptide will be assembled using commercially available Boc-*L*-isoleucine (**121**), Boc sarcosine (**123**), and *D*-phenylalanine (**122**). However, *D*-alloisoleucine (~ $1800/ 1g) is an expensive amino acid to purchase in the market. Hence, synthesis of the dipeptide was first attempted on a model amino acid, *L*-isoleucine (**120**, ~ $16/ 1g) which is comparatively very cheap resulting the model dipeptide, **116'**.



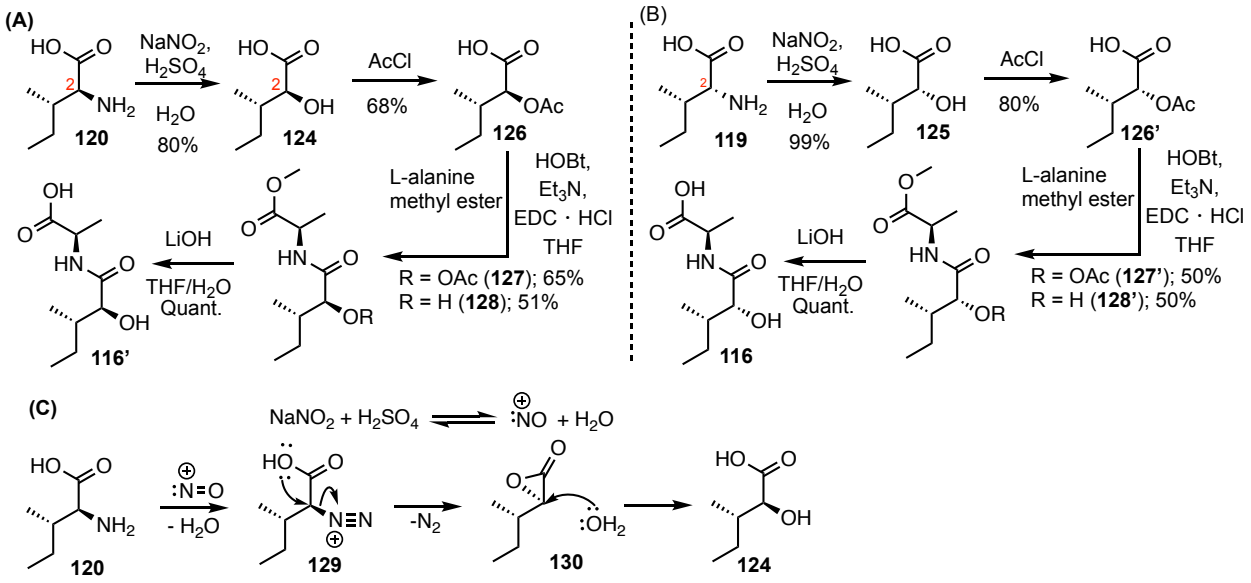
Scheme 18: Retrosynthesis analysis of pentapeptide moiety

3.2.1 Synthesis of the pentapeptide moiety

3.2.1.1 Synthesis of the dipeptide

First step of the synthesis involves diazotization of *L*-isoleucine to access the secondary alcohol **124** with the retention of stereochemistry around C2, as outlined in Scheme 19[82]. Once the diazonium salt (**129**) of the amine is formed, anchiomeric participation of the neighboring carboxylic acid forms an alpha-lactone (**130**) from the back face. This facilitates release of nitrogen gas. Next, the ring is hydrolyzed by a water molecule approaching from the same face as N_2 gas

was released yielding the alcohol **124**, shown in Scheme 3-C. Acetylation of the obtained alcohol (**126**) was performed to suppress any competing side reactions that can occur. Coupling the second amino acid *L*-alanine methyl ester followed by saponification led to the model dipeptide (**116'**) in 35% overall yield in 4-steps. However, to increase the efficiency of the route, coupling of *L*-alanine methyl ester to the unmasked alcohol **124** was attempted. To our surprise, the coupling afforded the same dipeptide in 41% yield in 3-steps. Having accessed the desired model system dipeptide, efforts were directed towards the actual dipeptide **116** commencing from **119**, Scheme 2-B. Unexpectedly, diazotization reaction of the amine afforded the alcohol, albeit at shockingly low yielded of 15%. After exploring different reaction times and equivalents, it was found that using 3 equivalents of $NaNO_2$ and 10 equivalents of H_2SO_4, along with an increased reaction time of 40 hours gave access to alcohol **125** in 99% yield. Acetylation (**126'**), coupling with *L*-alanine methyl ester, and subsequent saponification yielded the dipeptide **116** in 39% overall yield. In an effort to increase this yield of **116** the free alcohol **125** was coupled with *L*-alanine methyl ester. Shockingly, the yields obtained for the acetylated system (**127'**) and free alcohol (**128'**) were the same. Moreover, latter route upon saponification yielded the expected dipeptide **116** in 3 steps with an increased overall yield of 50%.

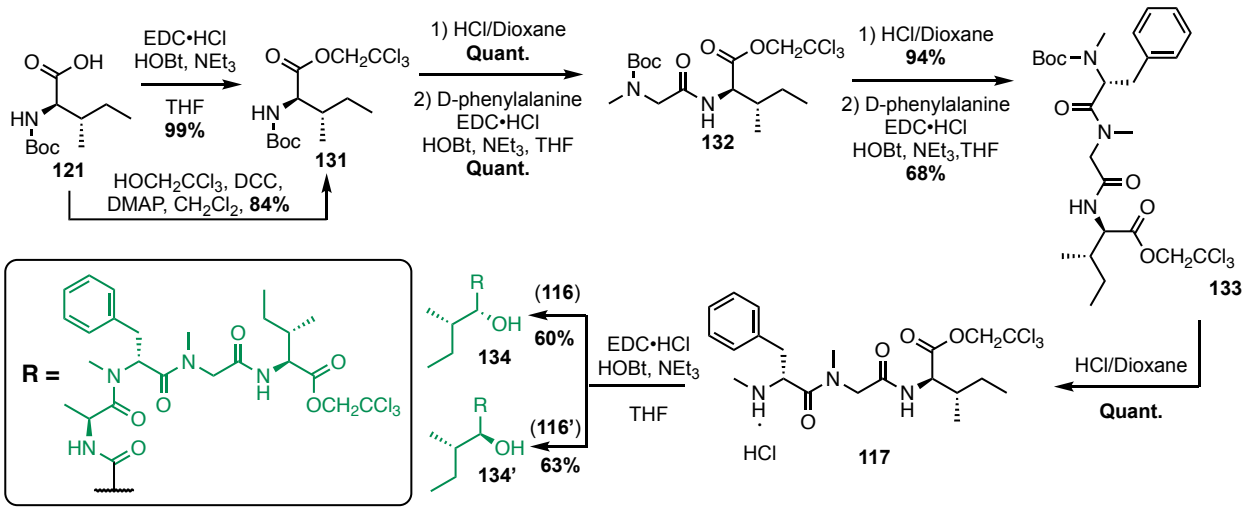


Scheme 19: (A) Synthesis of the model dipeptide; (B) Synthesis of the actual dipeptide; (C) Mechanistic explanation for the retention of stereochemistry at C2

3.2.1.2 Synthesis of the tripeptide

Tripeptide **117** was accessed starting from commercially available Boc-*L*-Isoleucine and coupling to trichloro ethanol to install the synthetically robust troc "like" handle (Scheme 20). Compound **131** was first attempted using DCC coupling conditions, however, purification of the target compound was hindered due to the urea byproduct being inseparable by column chromatography. Next, coupling under EDC·HCl conditions obtained compound **131** in 90% yield, with no purification issues. Deprotection of the Boc group upon **131** was accomplished with 4M HCl/Dioxane to afford the free amine, which was then coupled to Boc sarcosine with EDC·HCl to access dipeptide **132**. Accessing tripeptide **117** was performed in an analogous fashion (that of accessing dipeptide **116**), from **132**, 4M HCl/Dioxane, and *D*-phenyl alanine to furnishing **133** in 68% yield. Tripeptide **117** was treated with 4M HCl/Dioxane to obtain the amine hydrochloride salt and coupled with model dipeptide to test the reaction conditions with EDC·HCl. It was able to

access **134'** in good yields and the same reaction conditions were devised to access the pentapeptide masked with trichloro ethanol **134** in good yield.

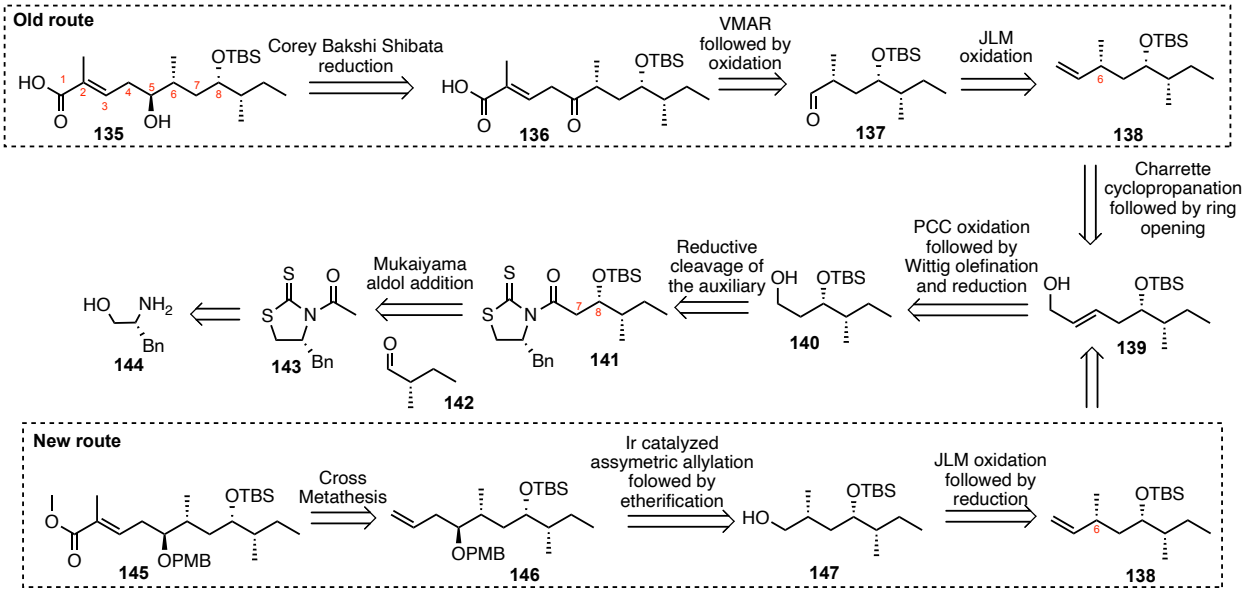


Scheme 20: Synthesis of the tripeptide 117 and the pentapeptide 134

3.3 Retrosynthetic analysis of lagunamide C polyketide

Our first retrosynthetic analysis to access the polyketide of lagunamide C (**135**) involved late-stage installation of the alcohol at C5 via Corey Bakshi Shibata reduction of the homoallylic ketone, **136**, Scheme 21. Access of the homoallylic ketone **136** was envisioned to arise from a vinylogous Mukaiyama aldol reaction (VMAR) upon aldehyde **137**, with the E-olefin as the desired geometry. Performing a Malaprade–Lemieux–Johnson (JLM) oxidation upon **138** is envisioned to access aldehyde **137**. Charrette cyclopropanation of the allylic alcohol **139** followed by subsequent ring opening is expected to yield **138** with expected stereochemistry at C6. Secondary alcohol **140** can be oxidized with subsequent Wittig olefination and reduction to access **139**. Reductive cleavage of the Crimmin's auxiliary of aldol product **141** will lead to the alcohol **140**. Aldol product **141** will be accessed via a Mukaiyama aldol addition reaction onto the acetylated Crimmins auxiliary **143**, that will be accessed starting from the commercially available amino acid *D*-phenyl alaninol, **144**. This Mukaiyama aldol reaction will set the stereochemistry at

C8 and install the extra methylene unit C7. Elaboration of **138** onto **135**, as illustrated in Scheme 21 was an older approach developed in the lab by a previous researcher[77]. However, this previous route from **138** to **135** was plagued with scale issues, numerous side products, and also did not afford the needed stereoselectivity. The current proposed route for accessing the polyketide of lagunamide C diverges from **138**. In this, the methyl ester form of the polyketide (**145**) was envisioned to be accessed via a Grubbs II mediated cross metathesis between olefin **146** and methyl,methacrylate. Grubbs II is expected to provide the E-olefin geometry about C2-C3 of **145**. Cross metathesis precursor, alkene **146** is expected to be accessed via a Krische allylation to install the *S* alcohol at C5 from **147**. In an analogous approach to the "old route", **147** can be accessed from **138** via a JLM oxidation, but here with a subsequent reduction to give **147**.



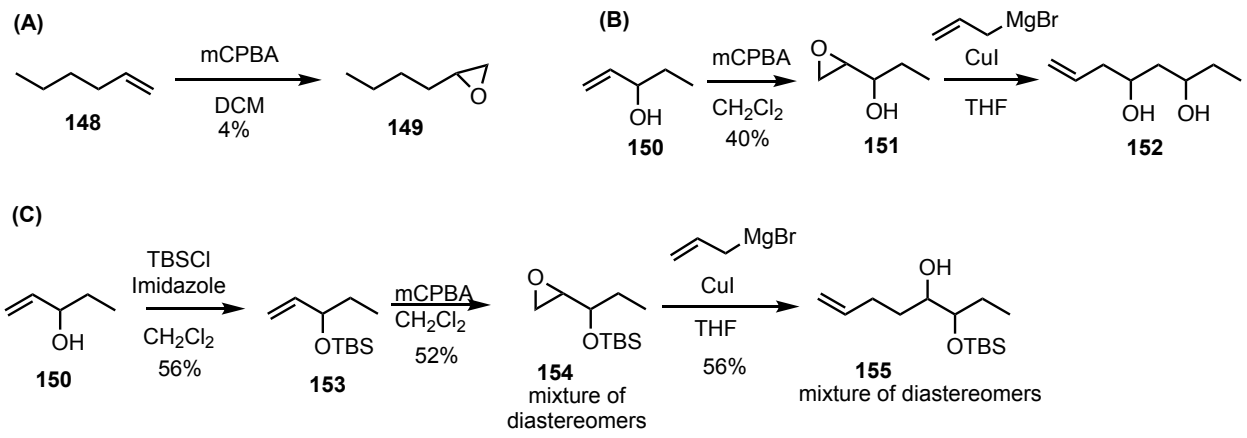
Scheme 21: Old and new route to access lagunamide C polyketide

3.3.2 Exploring a possible new reaction to access 138 installing stereochemistry at C5

Prior to the "current" route, outlined in Scheme 21, was undertaken an alternative approach was explored based upon olefin **138**. The general concept was to epoxide the terminal olefin and

then ring open it with vinyl Grignard to furnish **146**, as the free alcohol. The key step of this approach for the access of the single enantiomer **145** is for the facially selective epoxidation of the olefin. Before exploring this epoxidation strategy upon **138**, some model systems were explored to test the feasibility of the approach. Prior to exploring facially selective epoxidation conditions, *m*CPBA was used. The first model alkene explored was 1-hexene (**148**), treating it with *m*CPBA afforded the desired epoxide **149**, albeit in only a 4% yield (Scheme 22-A). The volatility of the alkene used also played a major role in this low yield. Next, 1-penten-3-ol (**150**) was selected to be explored given that it has a higher boiling point and could provide more of the epoxide with less lost due to evaporation. Treating **150** to *m*CPBA afforded the corresponding epoxide **151** in 40% yield (Scheme 22-B). When the resulted epoxide was subjected to ring opening with allyl magnesium bromide in the presence of copper expecting diol **152**, but it resulted in many side reactions that made it impossible to investigate the reaction further. Hypothesizing that the free alcohol of **151** is interfering with the addition, due to proton abstraction by the Grignard, a new strategy with the same starting material was devised.

Protection of the allylic alcohol with TBSCl, imidazole in CH_2Cl_2 gave access to the TBS protected system, **153** in 56% yield (Scheme 22-C). Epoxidation was performed with *m*CPBA to afford **154** as a mixture of diastereomers in 52% yield. Subjecting the epoxide mixture to allyl magnesium bromide, copper (I) iodine in THF afforded a mixture of diastereomers of the alkyl addition product, **155**, in 56% yield.

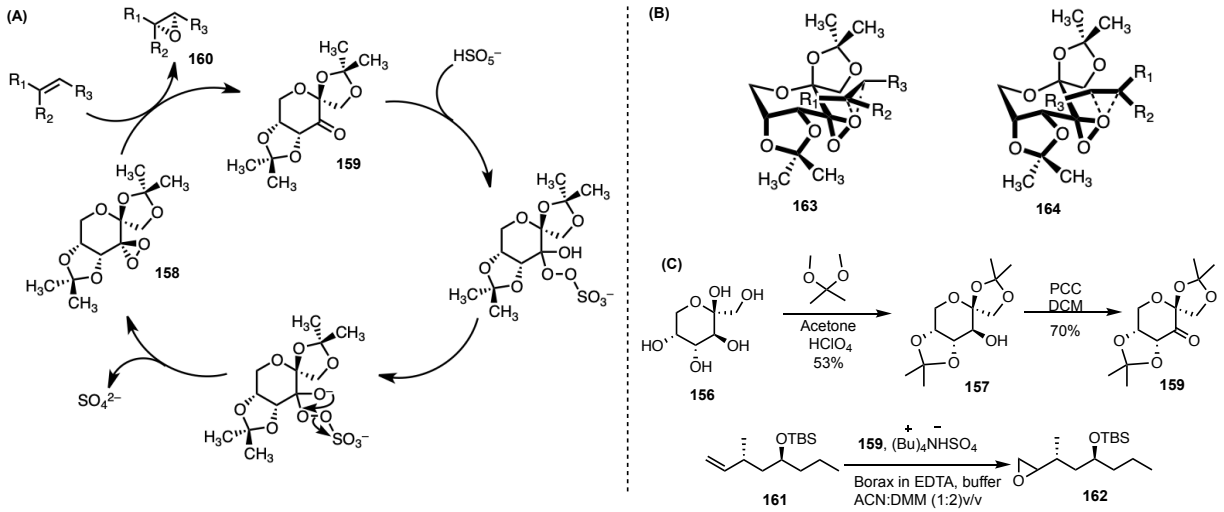


Scheme 22: Model systems to prove the late-stage epoxidation concept

With the success of the alkyl addition upon the model system epoxide shown in Scheme 22, efforts were directed towards facial select epoxidation conditions. While other facially selective epoxidation reagents have been reported in the literature[83], their selectivity upon terminal olefins are poor. With that, the Shi asymmetric epoxidation conditions were investigated, due to their strong and robust ability to work with terminal and internal olefins based upon small difference within the fructose catalyst[84].

The Shi epoxidation has been proven to be a powerful facially selective epoxidation reagent, that is based and built from the commercially available D or L fructose. The fructose configuration is what provides the facial selectivity. While cyclic fructose (**156**) possesses the needed ketone for dioxirane formation, for epoxidation, the free hydroxyl groups interfere with the reaction. As such, they are protected as the ketal counterparts (**157**) to suppress their direct nucleophilic participation but keeping their steric effects, Scheme 23-A. Upon ketal protection, subjecting the system to oxone affords the desired dioxirane **158**. This intermediate performs epoxidation (**161**) via two transition states, a spiro (**163**) and planar (**164**). Where spiro state which is favored electronically due to the stabilized electron delocalization between the antibonding pi orbital of the olefine and lone pair in the non-bonding orbital of dioxirane oxygen (Scheme 23-B). In our hands, fructose

156 was elaborated onto the **157** in 53% yield and subsequently oxidized to its ketone variant (**159**) in 70% yield, and then elaborated onto the dioxirane species **158** with DMDO. With the Shi catalyst (**159**) in hand, epoxidation of a model polyketide intermediate **161** was undertaken (Scheme 23-C). Subjecting **161** to Shi epoxidation in a solvent mixture of Dimethoxymethane (DMM) and CH_3CN (2:1 v/v), and the reaction was buffered to maintain the pH around 10.5 to avoid competing Baeyer-Villiger reaction that will lead to decompositions, afforded **162** a mixture of diastereomers. This can be due to the reduced steric hindrance of the alkene substrate employed. In this transition state, smaller R1 and larger R3 groups supports higher enantioselectivity. But in the case of our alkene, both R1 and R2 are hydrogens. With this justification, we decided to continue with the proposed Iridium catalyzed synthetic steps to install the alcohol at C5 via Kirshe allylation.

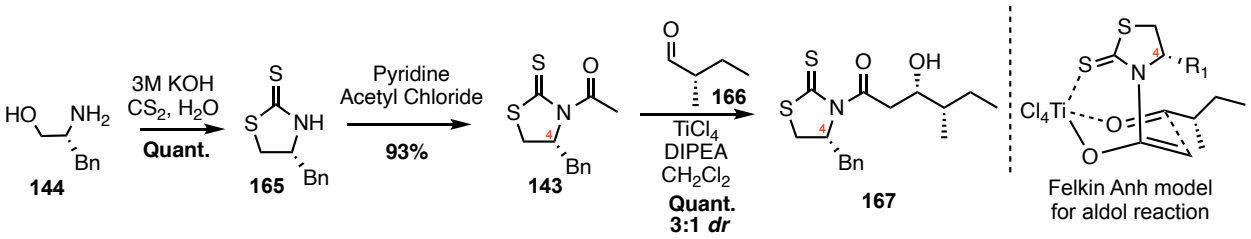


Scheme 23: (A) proposed mechanism for Shi epoxidation; (B) Spiro and planar transition states; (C) Synthesis of the Shi catalyst and epoxidation

3.3.3 Synthesis of the lagunamide C polyketide moiety

Latest synthetic campaign started with the Crimmins auxiliary **165** that was obtained by condensing carbon disulfide, 2 equivalences to ensure the full thio Crimmins auxiliary formation,

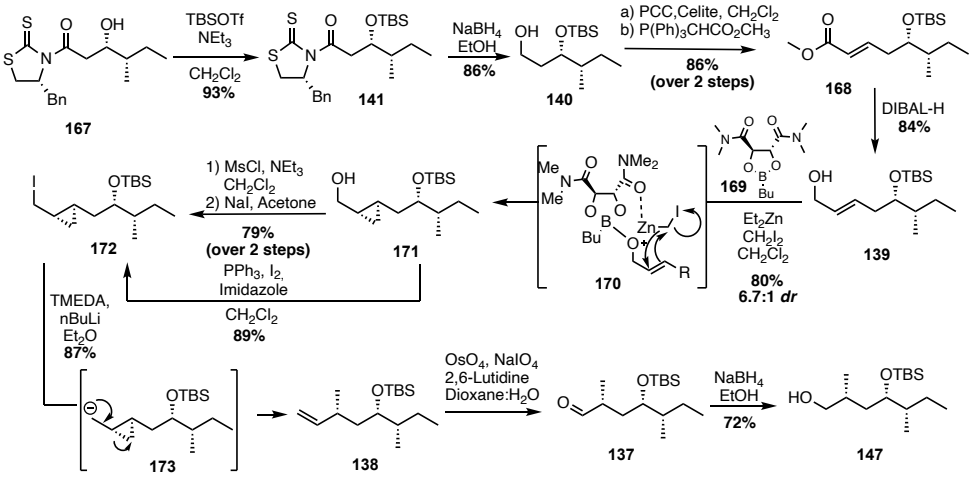
onto commercially available amino acid D-phenyl alaninol (**144**). N-acetylation of the obtained auxiliary **165** was performed with acetyl chloride and pyridine to access **143** in 93% yield, the system required to install the methylene unit (C7) after Mukaiyama aldol addition. Use of a bulkier handle (R1) on the C4 of the chiral auxiliary was required to improve the diastereoselectivity of the aldol reaction. This can be explained via the Felkin Anh model shown in Scheme 24. To perform the aldol addition, commercially available (*S*)-methyl butanol was oxidized using PCC to give (*S*)-methyl butanal (**166**), not shown, and added onto the Crimmins auxiliary **143** in the presence of titanium tetrachloride, DIPEA in CH_2Cl_2 that yielded the product as a mixture of diastereomers in quantitative yield. Separation of the two diastereomers to isolate the expected aldol product **167**, while challenging, was achieved after optimizations of column chromatography procedures. The reaction gave a diastereomeric ratio of 3:1, which was obtained with a quantitative yield for this reaction.



Scheme 24: Synthesis of the Crimmins auxiliary, Mukaiyama aldol addition and stereochemical explanation using Felkin Anh model

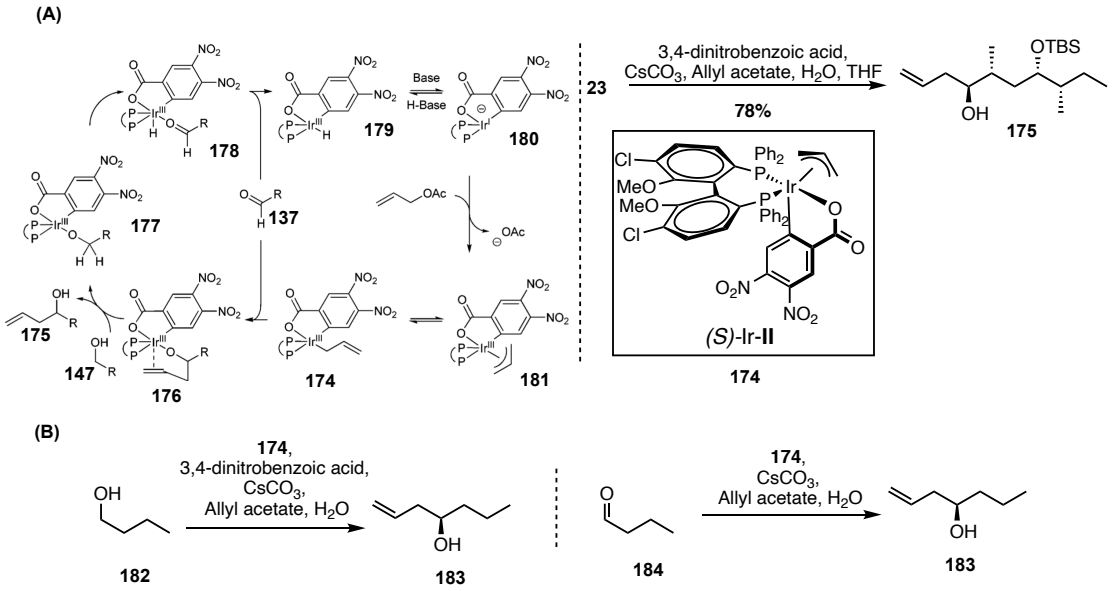
Silylation of the alcohol **167** furnished **141** in 93% yield, which was subsequently reduced with $NaBH_4$ in ethanol to furnish alcohol **140** (Scheme 25). Subjecting **140** to PCC oxidation followed by Wittig olefination in one pot approach gave enoate **168** in 86% over two-steps. Allylic alcohol **139** is the precursor for linchpin reaction of this route, as in our previously delineated work. Charrete cyclopropanation was accomplished by treating **168** with DIBAL-H with a 84% yield of **139**. The obtained allylic alcohol **139** was subjected to the facially selective cyclopropanation,

using the chiral boronic catalyst butylboronic acid N,N,N,N-tetramethyl-L-tartaric acid diamide ester (**169**), that allowed for the setting of the cyclopropane ring **171** in **80%** yield, with a dr of 6.7:1. Deoxo iodination of **171** was accomplished by transforming the alcohol into a mesylate that will readily cleave during the SN2 attack by the sodium iodide to access **172** in 79% yield over two-steps. This step reaction was later replaced by a single step conversion with triphenylphosphine, iodine, and imidazole. Latter conditions enhanced the efficiency of the synthetic route by reducing number of synthetic steps and improved yields, 89% over one-steps compared to the previous yield of 79% over two-steps. With **172** in hand, the ring opening of the cyclopropane ring was undertaken with *n*-BuLi and TMEDA -78 °C to promote the lithium-halogen exchange and subsequent ring opening to install the desired stereochemistry at C6 through the transition state **173** (Scheme 25). An enhanced diastereomeric ratio of 6.7:1 was obtained after complete separation of the challenging diastereomeric mixture via optimized column chromatography in 87% yield of the desired olefin **138**. Olefin **138** was treated with OsO_4 and $NaIO_4$ to undergo a JLM oxidation yielding aldehyde **137** that was reduced subsequently to access **147**, the precursor for Kirsche allylation (Scheme 25).



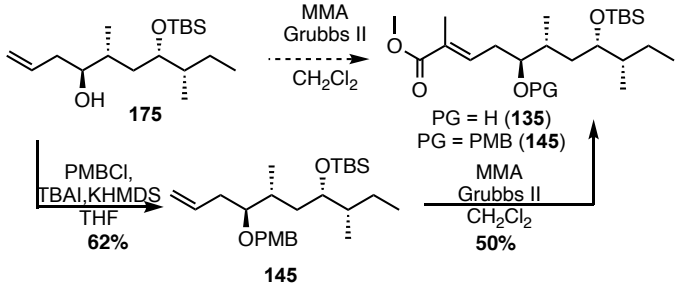
Scheme 25: Construction of the synthetic precursor 147 for the late-stage modifications in accessing lagunamide C polyketide

Inspired by the work of Franco et. al, iridium catalyst **174** was used to access **175** via an asymmetric alcohol-mediated carbonyl reductive coupling[85]. Per the procedure outlined by Krische et.al, the catalytic mechanism initiates when the alcohol adds onto the Ir (III) complex (Scheme 26A). High inductive effect of the 4-nitro group on the phenyl ring causes increase in the Lewis acidic property of Ir center (**177**) promoting the alcohol dehydrogenation leading to the Ir(III)-H (**179**) and an alpha stereogenic aldehyde (**137**). The same inductive effect of the 4-nitro group also facilitate the deprotonation of the obtained Ir(III)-H (**179**) with $CsCO_3$ resulting in the Ir(I) complex (**180**). Allyl acetate will undergo an oxidative addition onto the Ir(I) complex forming a π-allyl Ir(III) complex (**181**). The alpha stereogenic aldehyde (**137**) formed earlier in the cycle will then add on via the carbonyl to form the alkoxide-Ir(III) complex (**176**) that will undergo a product-to-reactant alkoxide exchange will furnish the expected homoallylic alcohol (Scheme 26A). After careful study of the catalytic mechanism, with the intention of increasing the atom economy by reducing a synthetic step, investigations were done to explore if the direct introduction of the alpha stereogenic aldehyde (**137**) will result in the homoallylic alcohol **175**. This was studied on a model primary alcohol, 1-butanol (**182**) and its corresponding aldehyde, butanal (**184**) (Scheme 26B) under same conditions. However, introduction of the aldehyde directly into the catalyst did not yield the expected allylic alcohol **183**, but many side reactions were observed whereas the reaction with the alcohol introduction proceeded to yield the expected allyl alcohol. This proves that in situ generation of the aldehyde was necessary for the reaction to proceed.



Scheme 26:(A) Catalytic mechanism for the Kricshe allylation; (B)Investigation of substrate specificity of Kricshe allylation

Grubbs second generation catalyst was explored to mediated cross metathesis of free alcohol **175** with methyl methacrylate. Unfortunately, the return of **175** was observed under these conditions. Further investigation into the literature showed the precedence that free alcohol competes to incorporate into the Ru complex and eventually shuts down the cross metathesis by deactivating the catalyst. Hence masking the free alcohol with a robust protecting group was necessary. This was achieved by transforming the alcohol into a PMB ether **145** in 62% yield, which is envisioned to be deprotected with DDQ. Treating PMB ether **145** with methyl methacrylate under cross metathesis conditions afforded the target polyketide methyl ester of lagunamide C (**145**) (Scheme 27).



Scheme 27: Cross metathesis to access lagunamide C polyketide moiety

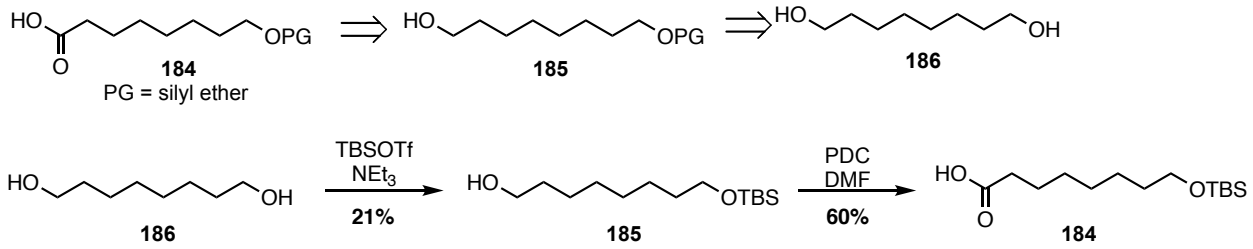
3.4 Cyclization attempts to access lagunamide C

3.4.1 Analog macrocycle synthesis

3.4.1.1 Route 1 - Macrocyclization

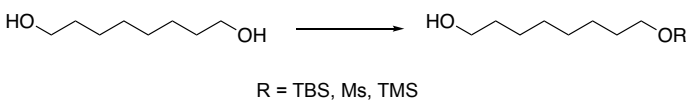
Having accessed the key synthetic handles **145** (polyketide) and **134** (polypeptide), ring closing attempts to achieve the first total synthesis of lagunamide C was implemented. Rather than exploring the most viable synthetic route using the precious material, a model polyketide moiety **184** analogous to **135** was used, also that a carbon tethered system could be used to help explore the polypeptide penetration hypothesis. It was envisioned to access **184** by a mono-silylation followed by a functional group conversion of commercially available 1,8-octanediol (**186**) (Scheme 28). Even though there are literature precedence for mono silylation of linear terminal diols, with carbon chain lengths of 7 through 12, no references were available for a mono silylation of a 1,8 diol. With this in mind, a series of reaction conditions were investigated to access mono silyl protected 1,8 octane diol **185** (Table 4). Reaction was first attempted with reported conditions for mono silylation of 1,7 heptane diol with TBSCl and Imidazole in dichloromethane. Reaction yielded only 5% of the mono substituted diol and the rest 95% was diprotected diol and the starting material. Assuming the extra 0.5 equivalent of TBSCl used is favoring the di silylated alcohol, another reaction was done with same conditions but with 1.1 equivalents of TBSCl. This led to an increase in yield (15%) of expected product but major yield being the deprotected diol and the starting material. Further reduction of the TBSCl equivalents to 0.9 yielded the expected product in 25% yield while the other 75% diprotected diol and the starting material. Different addition rates and order of additions couldn't enhance the product yield beyond 25%. When the addition of the base was done at 0 C and gradually brought to room temperature the yields were not affected. Hence different bases in different ratios (NEt_3 and NaH) were tested yet the yield did not improve

(entry 4, 5, and 6). Next, different silyl reagents were employed. Yields did not change drastically except with MsCl which was 53%. However, when a more stronger silylating agent was used, yield of the desired product dropped again to 21%. Envisioning to make use of the disylilated diol, it was subjected to an equivalent controlled desilylation with TBAF. Except for 14%, rest was completely deprotected to the starting material 1,8-octandiol. Since the actual system contain a TBS handle, the model polyketide with TBS group was pushed forward.



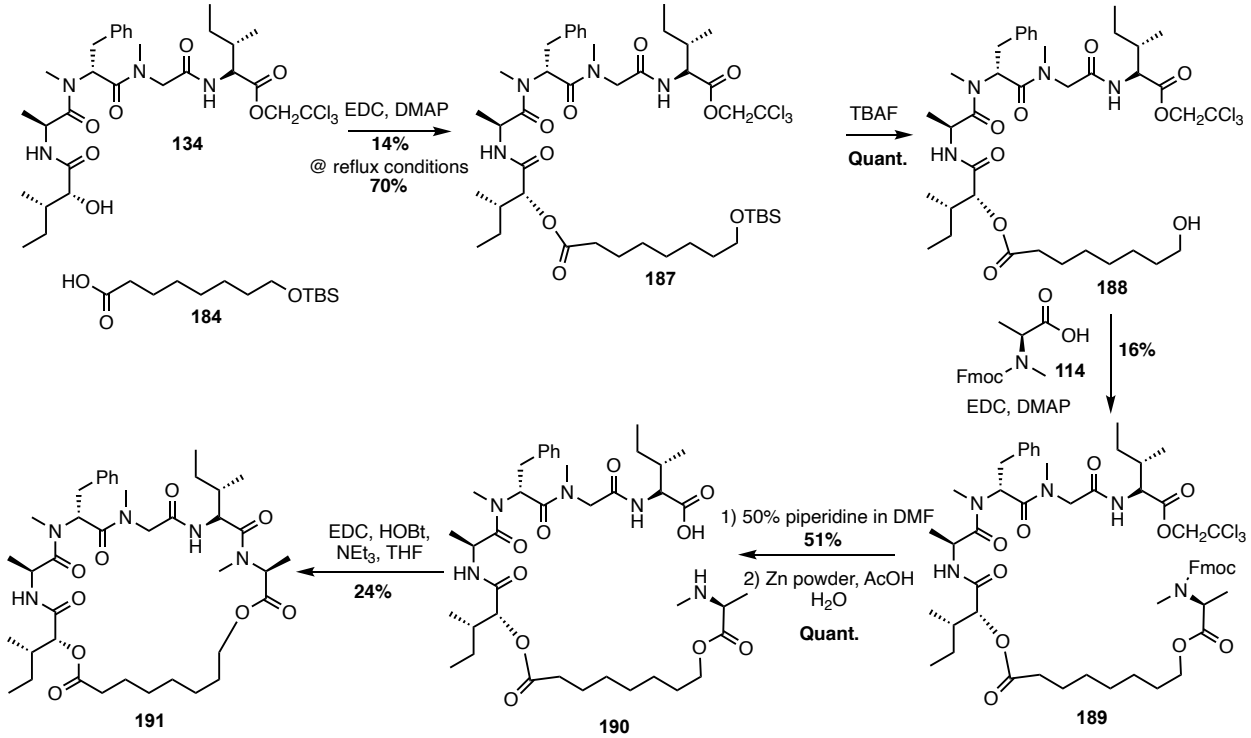
Scheme 28: Model polyketide synthesis

Table 4: Optimization of mono-silylation of 1,8 octanediol



Trial	Reagents	Equivalents used	%Y and Comments
1	**186**: Imidazole:TBSCl	1: 1.09: 1.5	5% Product + diprotected diol + SM
2	**186**: Imidazole:TBSCl	1: 1.1: 1	11% Product + diprotected diol + SM
3	**186**: Imidazole:TBSCl	1: 1.1: 0.9	25% Product + diprotected diol + SM
4	**186**: NEt_3:TBSCl		
5	**186**: NaH:TBSCl	1: 1: 0.9	Trace amount of Product + diprotected diol + SM
6	**186**: NaH:TBSCl	1: 0.9: 0.9	Trace amount of Product + SM
7	**186**: NaH:TBSCl	1: 1.1: 0.9	28% Product + diprotected diol + SM
8	**186**:NaH:TMSCl	1: 1.1: 1	7% Product + diprotected diol + SM
9	**186**: NEt_3:TMSCl	1: 2.5: 1	37% Product + diprotected diol + SM
10	**186**: NaH:MsCl	1: 1.1: 1	53% Product + diprotected diol + SM
11	**186**: NEt_3:TBSOTf	1: 2: 1	21% Product + diprotected diol + SM

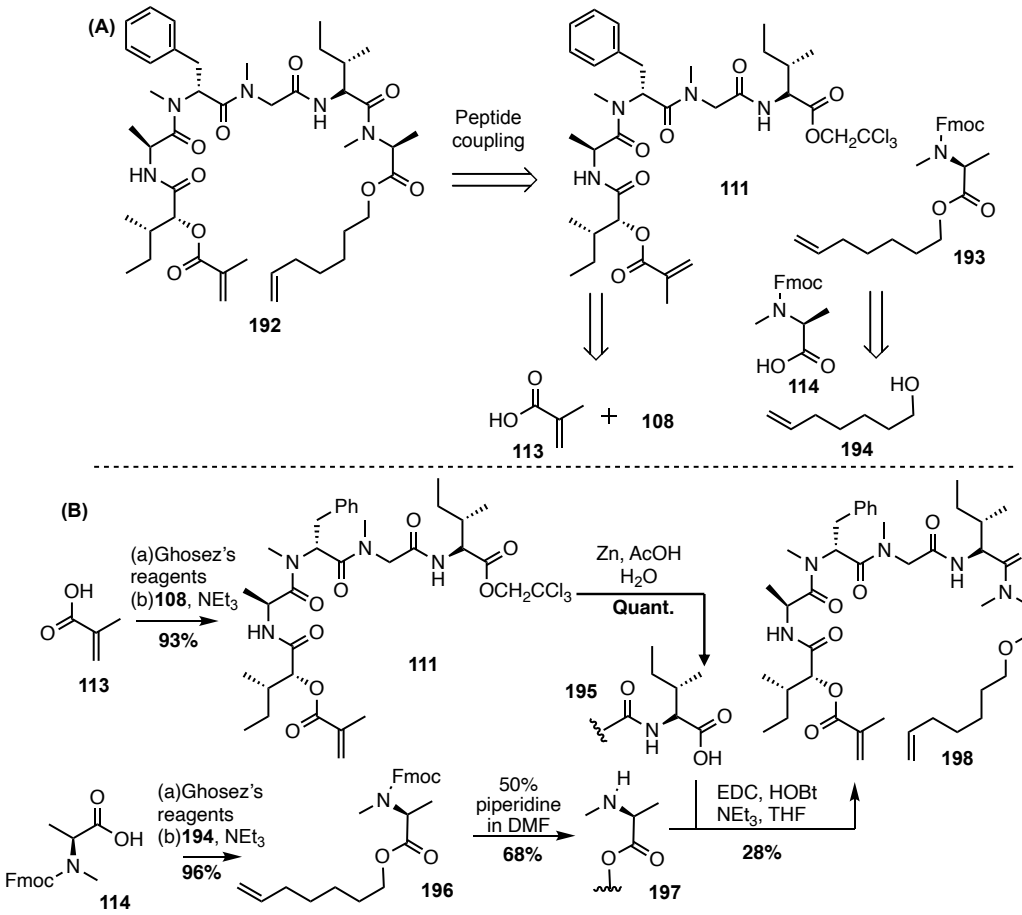
With compound **184** in hand, conditions to couple to the pentapeptide moiety via various peptide coupling conditions were explored (Scheme 29). First, EDC·HCl coupling conditions were attempted. However, the HCl generated insitu from the reagent resulted in cleavage of the formed ester bond returning starting material. Next, rather than using the HCl salt employing EDC provided the ester **187** in a 14% yield, which was further increased to 70% when refluxed. Desilylation (**188**) followed by a second acid chloride coupling with Fmoc -N methyl-*L*-alaninol resulted the substrate **189**. Screening various concentrations of piperdine in DMF, along with reaction times, allowed for Fmoc deprotection in 51% yield. The trichloro ester was removed via troc like deprotection conditions with Zn to afford the synthetic precursor **190** in quantitative yields. With **190** in hand the proposed first ring closing macrocyclization attempt was performed. Subjecting **190** to EDC, HOBt and NEt_3 in THF afforded macrocycle **191** in 24% yield after 7 days of stirring.



Scheme 29: Analog macrocycle synthesis via route 1

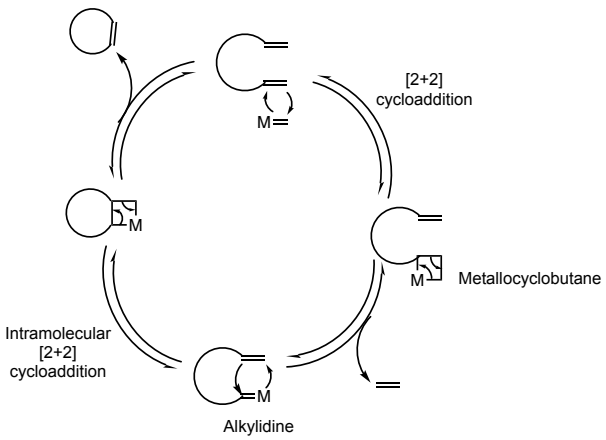
3.4.1.2 Route 2 – Ring closing metathesis (RCM)

Concurrent to the macrocyclization conditions disclosed above, ring closing metathesis conditions were also being explored. It was envisioned that precursor **192** could be cyclized via RCM (Scheme 30-A). Compound **192** could be accessed from the coupling of the pentapeptide/methacrylic acid unit **111** and the Fmoc-N-methyl-*L*-alanine/1- hexenol ester **193**. The formation of **111** is thought to arise from the coupling of the pentapeptide (**108**) to methacrylic acid (**113**) via acid chloride formation with Ghosez's reagent. Alkene **193** is expected to be accessed by condensing Fmoc-N-methyl-*L*-alanine (**114**) onto commercially available 1- hexenol (**194**). Formation of the MAA acid chloride via Ghosez reagent followed by the addition of pentapeptide **108** furnished **111** in excellent yields (Scheme 30-B). Concurrently, Fmoc-N-methyl-*L*-alanine (**114**) was transformed to its acid chloride utilizing Ghosez's reagent, and then had added commercially available 1- hexenol (**194**) to furnish **193** in 96% yield. Employing NEt_3 was essential to quench any in situ HCl that was formed during the acid chloride formation in the access of both **111** and **193**. Alkene **111** was subjected to troc like deprotection with Zn and acetic acid in H_2O to access the free carboxylic acid **195** in quantitative yields while the free amine **197** was accessed by Fmoc deprotection of **196** in 68% yield, via the methodology established in route 1 above. The two precursors **195** and **197** were coupled together via EDC peptide coupling conditions to access the diene **198** in 28% yield (Scheme 30-B).



Scheme 30:(A) RCM retrosynthesis; (B) Synthesis of the analog RCM precursor

To form the macrocycle via ring closing metathesis, first key step is formation of the metallocyclobutane intermediate by a [2+2] cycloaddition between the diene and the catalyst. Resulted metallocyclobutane then cycloeliminates via a productive pathway losing ethylene gas and forming a new species alkylidine or a non-productive pathway which result in the starting diene shutting down the catalytic cycle. If it undertakes the productive pathway, alkylidine undergoes an intramolecular [2+2] cycloaddition resulting another metallocyclobutane intermediate that undergo cycloelimination resulting the expected cyclized

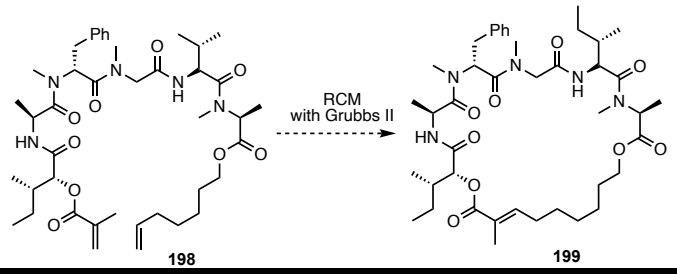


Scheme 31: RCM catalytic cycle

product. One key competing reaction that takes place in this step is alkylidine undergoing 2+2 cycloaddition with a second diene in the reaction mixture instead of the second terminal alkene in the same molecule. This can lead to polymerization giving poor yields of the RCM product.

With the mechanism in mind, screening of various conditions to promote the RCM was explored, outlined in Table 5 below. Attempted first were conditions reported by Grubbs et. al (Table 5, entry 1), however only starting material **198** was recovered which can be due to the alkylidine undergoing the unproductive pathway or ethylene formed insitu is hindering the reaction by deactivating the Ru catalyst. Hence attempting to explore equivalence effects of Grubbs II was then performed using an extra 0.1 equivalent of Grubbs II added after the reaction was running. Unfortunately, this resulted in the complete recovery of starting material once again. To further explore and study the effects of additional catalyst, the procedure was altered where 0.05 equivalents of the Grubbs II catalyst was added in every 8 h for 3 times, which added up the total catalyst loading to be 0.15 equivalents, yet complete recovery of starting material was observed. Intending to elevate the temperature of the system, a solvent with a higher boiling point was used. Reaction was first attempted at rt with THF. Since no product spot was observed when monitoring with thin layer chromatography, reaction temperature was gradually elevated to reflux. However, these attempts also ended recovering the diene **198**. Use of a robust novel Ru catalyst (RuI) generated in house was attempted following the reported procedure, but it did not yield the expected macrocycle even when the catalyst loading was increased up to 20% mol and under reflux conditions. Hypothesizing formation of the metallocycle that allows the condensation of the two dienes to form the ring is hindered due to possible steric effects by the ligands on the catalysts used, use of Stewards Grubbs catalyst that has less bulky groups on the ligands is currently in progress to access the 27 membered ring **199**.

Table 5: RCM optimization



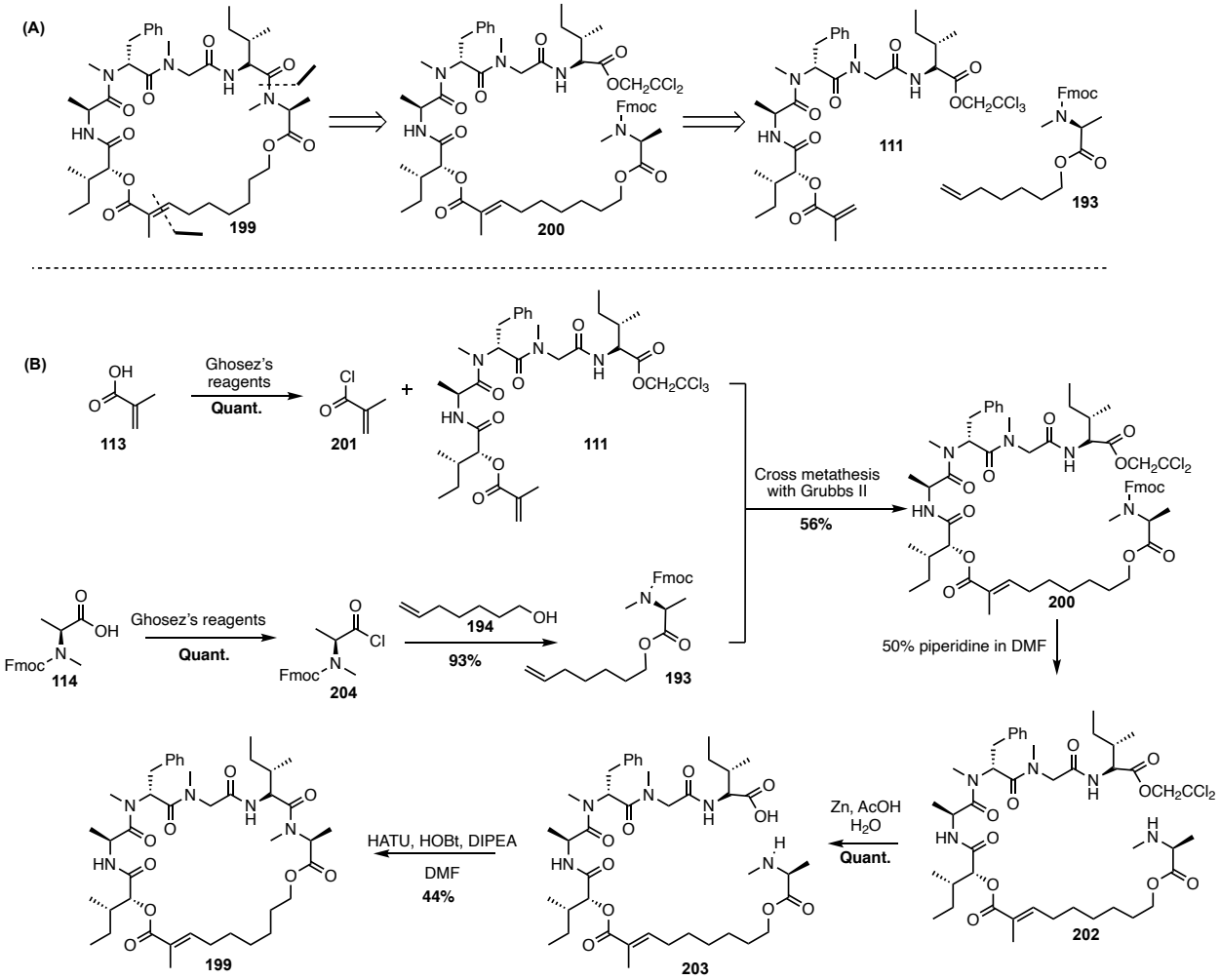
198 199

Trial	Catalyst, loading mol%	Solvent	Reaction time	Temperature	Comments
1	**Grubbs II**, 10%	DCM	24 h	Reflux	Recovered **198**
2	**Grubbs II**, 10%x2	DCM	24 h x 2	Reflux	Recovered **198**
3	**Grubbs II**, 5%x3	THF	24 h	RT - Reflux	Recovered **198**
4	**RuI**, 10%x2	$CHCl_3$	24 h	RT - Reflux	Recovered **198**
5	**Stewart Grubbs,** 10%x2	THF		Reflux	Recovered **198**

3.4.1.3 Route 3 – Cross metathesis (CM) followed by macrocyclization

In the attempts to explore further macrocyclization routes, while RCM conditions were under investigation an alternative cross metathesis followed by macrocyclization was explored. In this, the desired macrocycle **199** was thought to be accessed via the alanine residue and the polypeptide chain. Accessing **200** was envisioned to arise from a peptide coupling via the functionalized polypeptide **111** and alanine/hexene unit **193** (Scheme 32-A). Accessing **111** via the esterification of methyl acrylate and the polypeptide could be performed as described previously. Concurrently, the Fmoc-N-methyl-alanine was transformed into its acid chloride (**204**) reacted with hept-1-en-7-ol (**194**) to afford **193**. Subjecting **111** and **193** to cross metathesis conditions with Grubbs II afforded **200** in 56% yield. Fmoc deprotection was accomplished with 50% piperidine in DMF to access the free amine **202**. Deprotection of the trichloroethanol, via troc like deprotection conditions with Zn, acetic acid in water gave access to the free carboxylic acid **203** in quantitative yields. Inspired by the macrocyclization attempts done by Dai et. al in synthesis of the 26 membered macrocycle lagunamide A, precursor **203** was treated with HATU mediated peptide

coupling conditions. After careful monitoring of the reaction for 7 days with TLC, the second 27 membered macrocycle was accessed in 44% yield (Scheme 32-B).

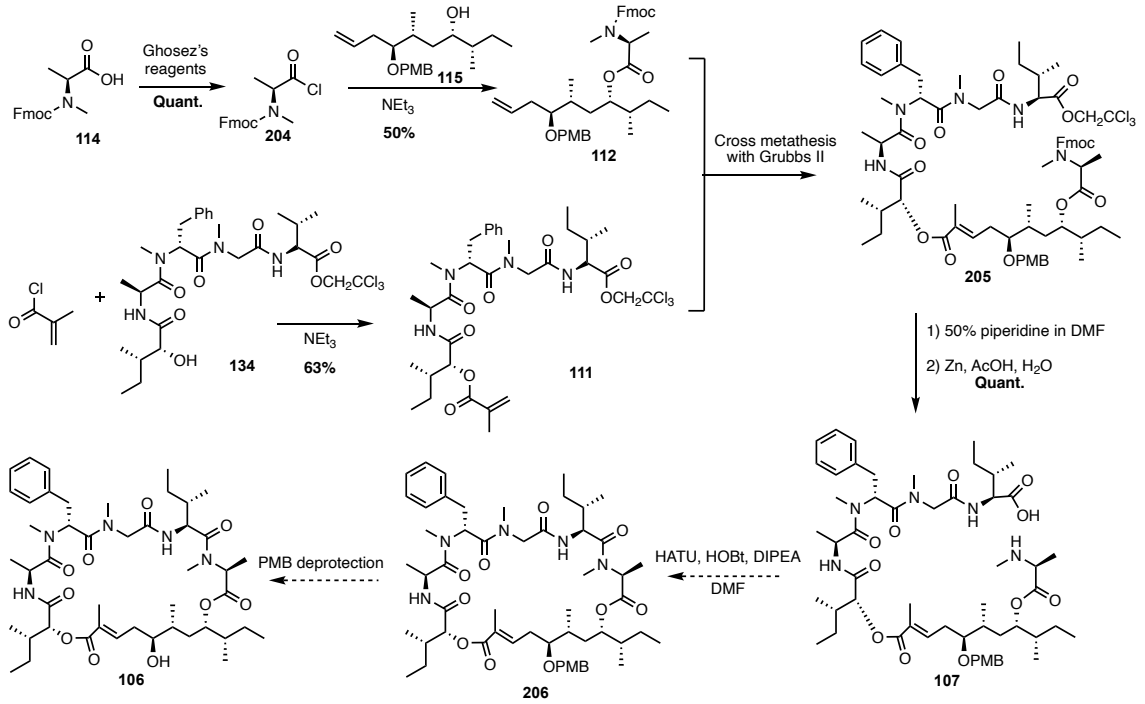


Scheme 32: (A) Retrosynthesis analysis of route 3; (B) Synthetic route 3

3.4.2 Lagunamide C macrocycle synthesis

Having established two possible routes to access a 27 membered macrocycle (carbon tethered analog), and a third route being under investigation, accessing the macrocyclic depsipeptide lagunamide C was implemented. For this, route 3 which exhibited highest overall yield involving an early-stage cross metathesis followed by macrocyclization was executed. In this step, any starting material that does not react can be easily isolated via column chromatography and subject to the reaction again. Fmoc-N-methyl-*L*-alaninol (**114**) was transformed into its acid chloride **204**

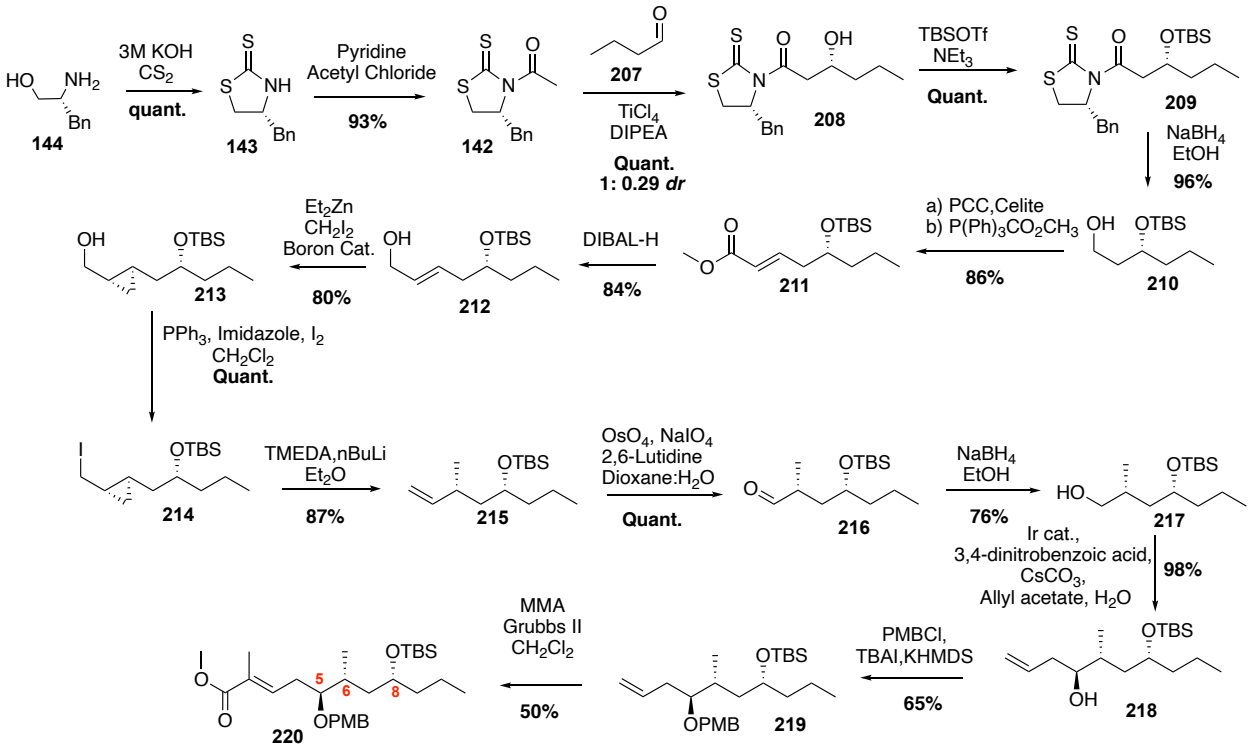
using Ghosez's reagent and coupled with the free alcohol **115** accessed by desilylation of the lagunamide C polyketide intermediate **146** with TBAF, not shown here. Obtained alkene **115** was then subjected to Grubbs II mediated cross metathesis conditions to access the alkene **205**. Continuous flush of Argon through the system with an extra equivalent of the catalyst was required to push the reaction forward by removing trapped ethylene byproduct that can deactivate the Grubbs catalyst by coordinating to Ruthenium. Alkene **205** was then subjected to Fmoc deprotection followed by troc like deprotection to access the free amine and free carboxylic respectively (**107**). Precursor **107** was treated with HATU mediated peptide coupling conditions established in route 3 above to access the macrocycle **206** over 7 days (Scheme 33). However, the reaction was performed in a very small scale of 4 mg and with literature precedence of low yields obtained in macrocyclizations, enough material was not obtained to confirm the product by NMR spectroscopy. Bringing up more material to perform the final macrocyclization in a larger scale to access **206** is currently underway.



Scheme 33: Macrocyclization to access lagunamide C

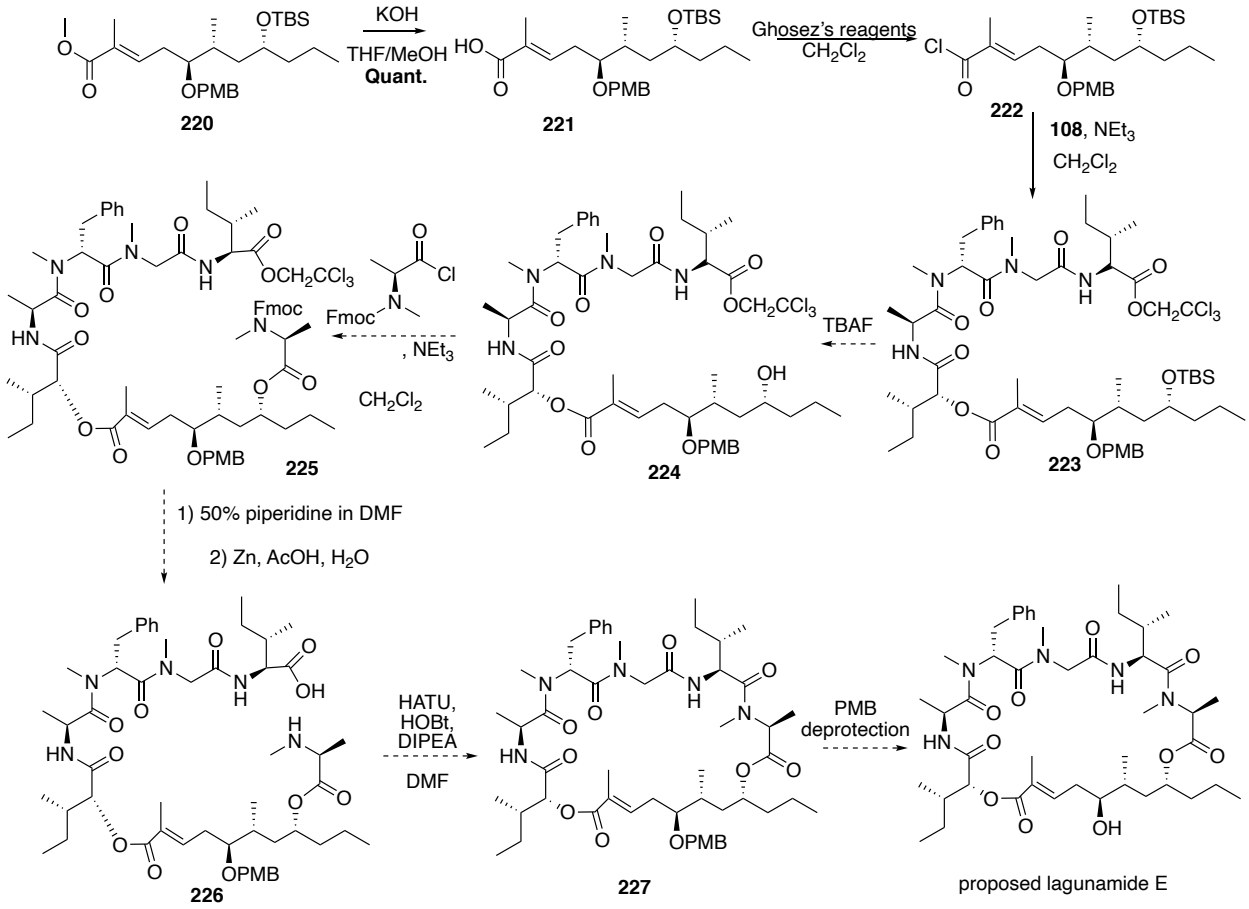
3.5 Proposed lagunamide E synthesis

Isolation of lagunamide D in 2019 made us draw our attention to look back at the model polyketide approach our lab established to explore the linchpin reaction in the synthetic route. Based off that reported route further modifications and developments were done to establish a scalable and efficient synthetic route to access the proposed lagunamide E structure which is an analog macrocycle that has 27 members in the ring just like lagunamide C, but with absence of that exocyclic methyl unit at C9 (Figure 4, Chapter 1). The synthetic route starts with a commercially available aldehyde, 1-butanal (**207**) which is more like the methyl deleted version of the starting aldehyde of lagunamide C polyketide route. Same diastereoselective strategies as in lagunamide C polyketide synthetic route was used to install the stereocenters at C8, C6, and C5 (Scheme 34).



Scheme 34: Synthesis of proposed lagunamide E polyketide

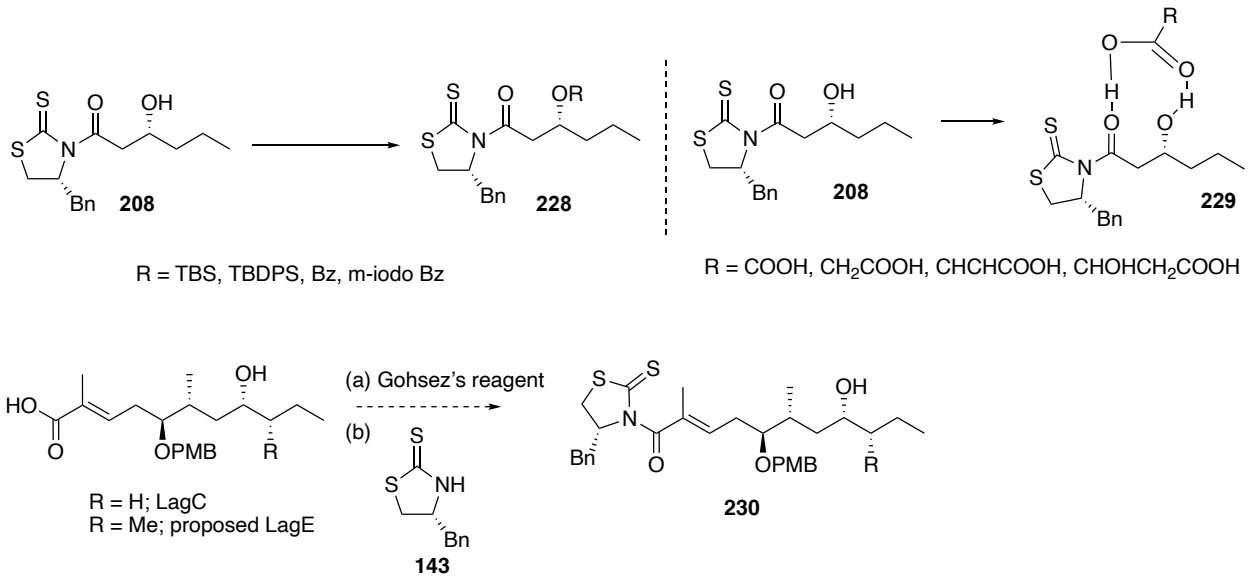
Obtained proposed lagunamide E polyketide **220** was saponified (**221**) and treated with Ghosez's reagent to form the acid chloride (**222**) that undergo a nucleophilic attack from the free alcohol of pentapeptide to form the ester **223** (Scheme 35). Obtained silyl ether will then be desilylated to access compound **224**. Free alcohol will be coupled with the acid chloride of Fmoc-N-methyl-*L*-alaninol to access compound **225**. Lastly, functional group deprotections to yield the precursor **226** followed by HATU mediated peptide coupling to access the proposed 27 membered analog (**227**) of lagunamide D is currently underway.



Scheme 35: Macrocyclization to access proposed lagunamide E

3.6 Structure confirmation of the polyketide moiety via crystallization

However, attempts on obtaining a crystal structure on aldol product of proposed lagunamide E (**208**) was not successful. Firstly, the most classical approach of protecting the alcohol group with bulky groups were attempted (**228**). When none of them was successful, a different approach with co-crystallization was tried. Four different carboxylic acids that can form H-bonding with the ketone and alcohol of the aldol product were used as conformers. Unfortunately, the crystals analyzed belonged only to the coformers themselves. Moreover, halogenation of the phenyl group of the chiral auxiliary was attempted but was not able to obtain crystals. With all the attempts in mind a new crystallization attempt is currently underway to access the compound **230** (Scheme 36). We envision that the chiral auxiliary will lead the polyketide moiety to form crystals which can be utilized to confirm all the ambiguous stereocenters of the lagunamide C polyketide and establish the stereocenters of proposed lagunamide E to support the spectroscopic data we have gathered.



Scheme 36: Crystallization attempts on polyketide moiety

3.7 Studies on the hypothesis of mode of action of aurilides

Studies on the proposed hypothesis of aurilides where we propose the polyketide moiety is the therapeutic warhead while the polypeptide moiety assist in selectivity/ penetration was first tested with lagunamide C polyketide intermediates shown below (Figure 37-A). The cytotoxicity (IC_{50}) of the mentioned intermediates were tested in cancer cell lines A549 (lung) and HCT8 (colon) using Alamar blue by incubating for 72h. When the advance enone intermediate **231** was tested it exhibited significant cytotoxicity in the said cell lines. In contrast, the allylic alcohol (**232**) had increased IC_{50} value referring to decreased cytotoxicity while the reintroduced enone system (**233**) exhibited increased cytotoxicity. Diol **234** when tested exhibited very poor to no cytotoxicity emphasizing the importance of the enone for the therapeutic effect. However, when its aldehyde counterpart **235** was tested, cytotoxicity increased. These values obtained were expected for **235** due to known activity of aldehydes inside a biological system. The diastereomeric mixture of lagunamide C polyketide (**237**) exhibited cytotoxicity in nanomolar concentrations while the oxidized ketone counterpart **238** showed cytotoxicity in similar nanomolar range. When the respective methyl truncate analogs **236**, **239**, and **240** were tested, their cytotoxicity values did not deviate much compared to **233**, **237**, and **238** respectively, suggesting that the methyl unit at C42 has a minimal impact to the activity of lagunamide C. Thus, cytotoxicity study confirms that the enone functionality is key to the therapeutic effect and supports our hypothesis on the polyketide arm role and suggests the role of polypeptide in targeting/penetration. Furthermore, accumulation studies of the polypeptide moiety (**108**) and the two carbon tethered analogs (**191** and **199**) were explored in A549 cancer cell line (Figure 37-B). To our delight, according to single experiment data, we were able to observe accumulation of the two carbon tethered analogs inside the cell. However, no accumulation of **108** was observed. This can be due to the more polar nature of the

polypeptide moiety that limits penetration through the cell membrane. This further supports our proposed hypothesis on the polypeptide moiety being involved in targeting/ penetration. However, duplicate, and triplicate experiments on the cell penetration studies are currently underway to further conclude the proposed hypothesis.

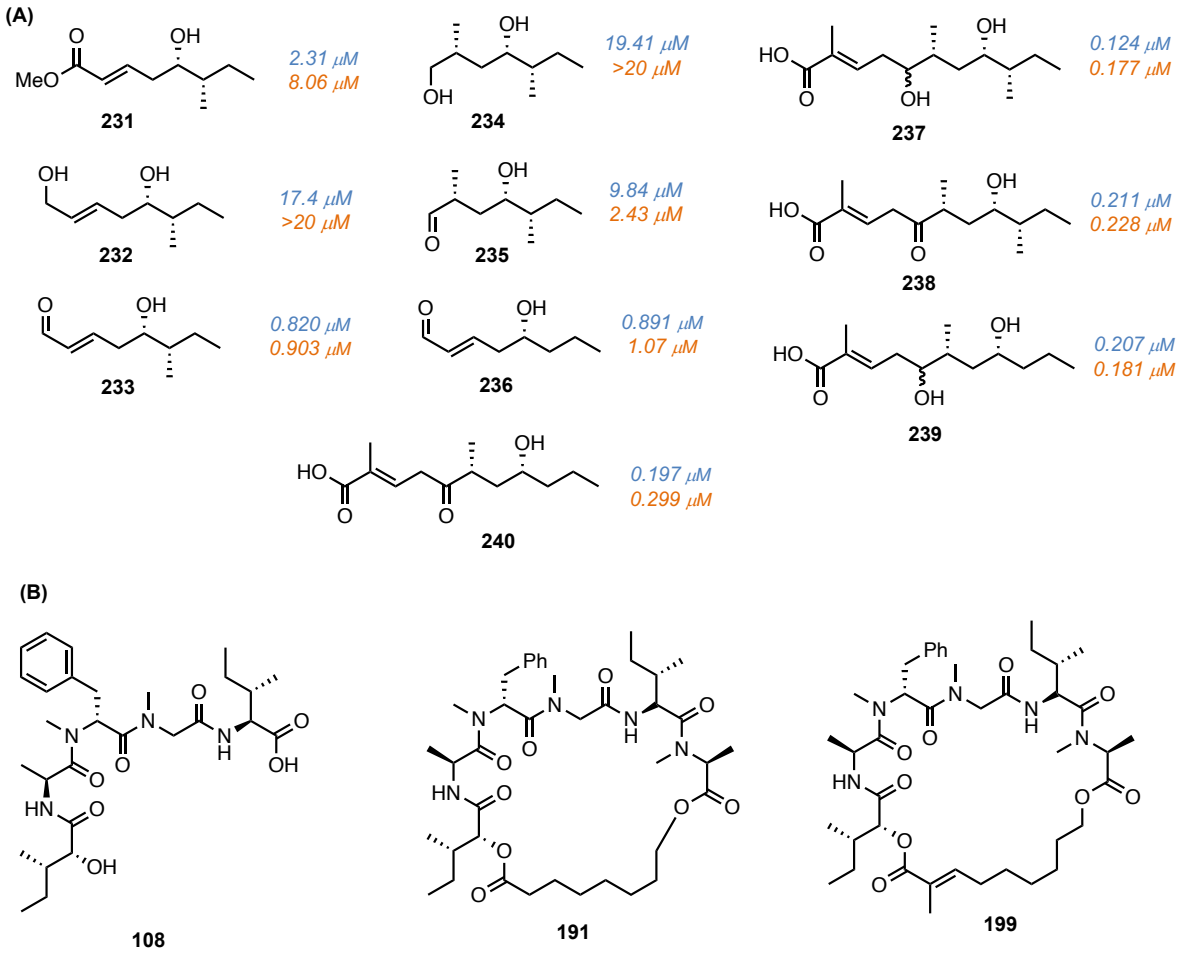
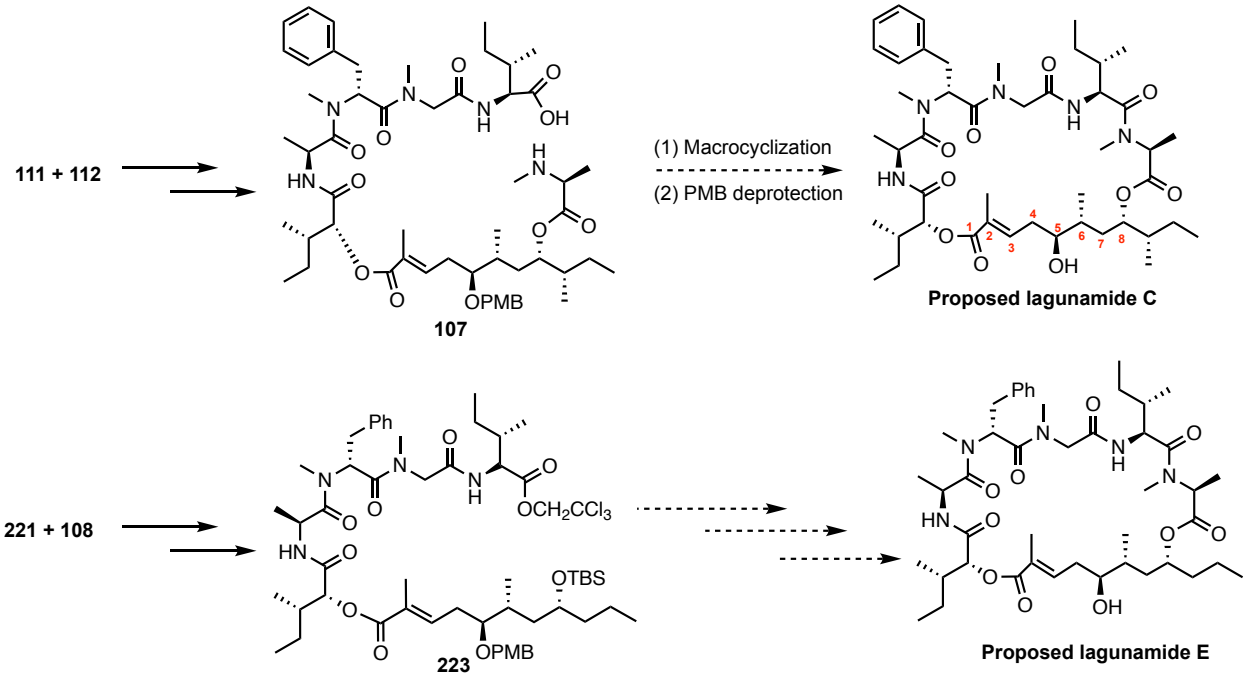


Figure 10: (A) Lagunamide C polyketide intermediates and their respective IC_{50} values; (B) Compounds used to explore cell penetration

Chapter 4 – Conclusion and Future Work

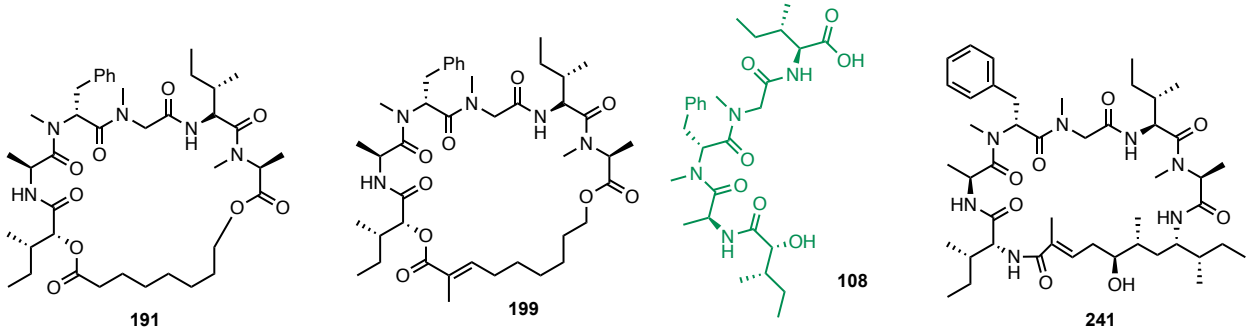
A scalable, efficient, and diastereoselective synthetic route has been developed to access the polyketide of the only 27 membered depsipeptide of the aurilide family, lagunamide C and its C42 methyl truncate analog proposed lagunamide E. Improved, efficient, and a scalable synthetic route was designed to access the pentapeptide moiety of the lagunamide family in gram scale. Three different routes; 1) macrocyclization, 2) cross metathesis followed by macrocyclization, and 3) ring closing metathesis were explored to achieve a 27-membered macrocycle. First two routes were successfully established accessing two 27 membered aurilide analogs while the latter route will be further investigated in the future. Once accomplished, that will be the first successful ring closing metathesis employed in accessing an aurilide to be reported. Efforts are currently underway in setting the final macrocyclization in larger scale to access the first total synthesis of proposed lagunamide C which is only two steps away. Furthermore, efforts in accessing a crystal structure of the compound **230** to resolve the stereochemistry at ambiguous stereocenters C5 and C6 of the lagunamide C polyketide moiety is currently underway. Accessing the 27 membered macrocycle of the proposed natural product lagunamide E is also currently underway and only 5 steps away (Scheme 37). We envision to suggest isolation of our proposed natural product lagunamide E in the cyanobacterium, *Lyngbya majsucle.* This will open doors to explore a new gene cluster within the marine source that will result in many other potential therapeutics.



Scheme 37:Synthetic progress in accessing lagunamide C and proposed lagunamide E

Once accessed, lagunamide C can be further investigated for its promising anticancer properties and its potential as a drug delivery system. The carbonyl groups present in lagunamide C can chelate currently used metal-based cancer therapeutics in the market, like cis platin in its ring and transport into the cell which will allow the drug to be used at very low doses and in turn reduce side effects. Furthermore, the polyketide chain of the macrocycle can be functionalized to yield prodrug conjugates that will serve as carrier vehicles to many therapeutics (e.g.: with 6-thiopurine). This potential carrier vehicle character of lagunamide C is further confirmed by the cell penetration studies discussed in chapter 3 above, which reports the accumulation of the 27 membered analog macrocycles inside A549 cells. Proposed lagunamide E is also expected to exhibit surprising cytotoxicity and similar potentials, given the structural similarities to lagunamide C.

Cytotoxicity studies done on polyketide intermediates and the results obtained by single experiment penetration studies explored with the synthesized 27-member aurilide analogs and the polypeptide moiety together provide proof to our proposed hypothesis of therapeutic warhead nature of the polyketide moiety and the targeted delivery properties of the polypeptide moiety. However, the duplicate and triplicate penetration experiments are in progress to confirm our proposed hypothesis. To further evaluate the mode of action of aurilides inside the cell we envision to access the amide analog (**241**) of the aurilides (Scheme 38). The synthetic route established to access proposed lagunamide C will be utilized in accessing **241**. As per our hypothesis, if esterase inside the cell cleaves the aurilide macrocycle at ester bonds releasing the polyketide moiety to give the therapeutic activity as a sole agent, the amide analog upon biological evaluation should exhibit very little to no activity and should stay intact inside the cell.



Scheme 38: Aurilide analogs for cell penetration and proposed amide analog of aurilides

Chapter 5 – References

(1) Samuelsson, G. *Drugs of Natural Origin : A Textbook of Pharmacognosy*, 4th rev. ed.; Apotekarsocieteten: Sweden, 1999.

(2) Mushtaq, S.; Abbasi, B. H.; Uzair, B.; Abbasi, R. Natural Products as Reservoirs of Novel Therapeutic Agents. *EXCLI J. 17Doc420 ISSN 1611-2156* **2018**. https://doi.org/10.17179/EXCLI2018-1174.

(3) Tariq, A.; Zeng, F.; Graciano, C.; Ullah, A.; Sadia, S.; Ahmed, Z.; Murtaza, G.; Ismoilov, K.; Zhang, Z. Regulation of Metabolites by Nutrients in Plants. In *Plant Ionomics*; John Wiley & Sons, Ltd, 2023; pp 1–18. https://doi.org/10.1002/9781119803041.ch1.

(4) Jeyasri, R.; Muthuramalingam, P.; Karthick, K.; Shin, H.; Choi, S. H.; Ramesh, M. Methyl Jasmonate and Salicylic Acid as Powerful Elicitors for Enhancing the Production of Secondary Metabolites in Medicinal Plants: An Updated Review. *Plant Cell Tissue Organ Cult. PCTOC* **2023**, *153* (3), 447–458. https://doi.org/10.1007/s11240-023-02485-8.

(5) Seigler, D. S. *Plant Secondary Metabolism*; Springer US, 1998.

(6) Desborough, M. J. R.; Keeling, D. M. The Aspirin Story – from Willow to Wonder Drug. *Br. J. Haematol.* **2017**, *177* (5), 674–683. https://doi.org/10.1111/bjh.14520.

(7) Dias, D. A.; Urban, S.; Roessner, U. A Historical Overview of Natural Products in Drug Discovery. *Metabolites* **2012**, *2* (2), 303–336. https://doi.org/10.3390/metabo2020303.

(8) MacCallum, C. A.; Lo, L. A.; Pistawka, C. A.; Deol, J. K. Therapeutic Use of Psilocybin: Practical Considerations for Dosing and Administration. *Front. Psychiatry* **2022**, *13*, 1040217. https://doi.org/10.3389/fpsyt.2022.1040217.

(9) Li, Y.; Zheng, Y.; Zhang, Y.; Yang, Y.; Wang, P.; Imre, B.; Wong, A. C. Y.; Hsieh, Y. S. Y.; Wang, D. Brown Algae Carbohydrates: Structures, Pharmaceutical Properties, and Research Challenges. *Mar. Drugs* **2021**, *19* (11), 620. https://doi.org/10.3390/md19110620.

(10) Moerman, D. E. *Medicinal Plants of Native America, Vols. 1 and 2*; Technical Reports; University of Michigan Press, 1987.

(11) Ji, H.; Li, X.; Zhang, H. Natural Products and Drug Discovery: Can Thousands of Years of Ancient Medical Knowledge Lead Us to New and Powerful Drug Combinations in the Fight against Cancer and Dementia? *EMBO Rep.* **2009**, *10* (3), 194–200. https://doi.org/10.1038/embor.2009.12.

(12) 4. Morphine-Like Drugs and Synthetic Derivatives ATrain Education.Pdf.

(13) Turnaturi, R.; Piana, S.; Spoto, S.; Costanzo, G.; Reina, L.; Pasquinucci, L.; Parenti, C. From Plant to Chemistry: Sources of Active Opioid Antinociceptive Principles for Medicinal Chemistry and Drug Design. *Molecules* **2023**, *28* (20), 7089. https://doi.org/10.3390/molecules28207089.

(14) Sneader, W. The Discovery of Heroin. *The Lancet* **1998**, *352* (9141), 1697–1699. https://doi.org/10.1016/S0140-6736(98)07115-3.

(15) Fentanyl.Pdf.

(16) Clark, T. P. The History and Pharmacology of Buprenorphine: New Advances in Cats. *J. Vet. Pharmacol. Ther.* **2022**, *45* (S1). https://doi.org/10.1111/jvp.13073.

(17) Murray, A.; Hagen, N. A. Hydromorphone. *J. Pain Symptom Manage.* **2005**, *29* (5), 57–66. https://doi.org/10.1016/j.jpainsymman.2005.01.007.

(18) Methadone-2020.Pdf.

(19) Kumar, S.; Paul, S.; Walia, Y. K.; Kumar, A.; Singhal, P. Therapeutic Potential of Medicinal Plants: A Review. **2015**.

(20) Tevyashova, A. N.; Olsufyeva, E. N.; Solovieva, S. E.; Printsevskaya, S. S.; Reznikova, M. I.; Trenin, A. S.; Galatenko, O. A.; Treshalin, I. D.; Pereverzeva, E. R.; Mirchink, E. P.; Isakova, E. B.; Zotchev, S. B.; Preobrazhenskaya, M. N. Structure-Antifungal Activity Relationships of Polyene Antibiotics of the Amphotericin B Group. *Antimicrob. Agents Chemother.* **2013**, *57* (8), 3815–3822. https://doi.org/10.1128/AAC.00270-13.

(21) Gordaliza, M. Natural Products as Leads to Anticancer Drugs. *Clin. Transl. Oncol.* **2007**, *9* (12), 767–776. https://doi.org/10.1007/s12094-007-0138-9.

(22) Newman, D. J.; Cragg, G. M. Natural Product Scaffolds as Leads to Drugs. *Future Med. Chem.* **2009**, *1* (8), 1415–1427. https://doi.org/10.4155/fmc.09.113.

(23) Li, J. W.-H.; Vederas, J. C. Drug Discovery and Natural Products: End of an Era or an Endless Frontier? *Science* **2009**, *325* (5937), 161–165. https://doi.org/10.1126/science.1168243.

(24) Newman, D. J.; Cragg, G. M. Natural Product Scaffolds as Leads to Drugs. *Future Med. Chem.* **2009**, *1* (8), 1415–1427. https://doi.org/10.4155/fmc.09.113.

(25) Martin, S. F. Bridging Known and Unknown Unknowns: From Natural Products and Their Mimics to Unmet Needs in Neuroscience. *Acc. Chem. Res.* **2022**, *55* (17), 2397–2408. https://doi.org/10.1021/acs.accounts.1c00773.

(26) Dong, S.; Guo, X.; Han, F.; He, Z.; Wang, Y. Emerging Role of Natural Products in Cancer Immunotherapy. *Acta Pharm. Sin. B* **2022**, *12* (3), 1163–1185. https://doi.org/10.1016/j.apsb.2021.08.020.

(27) Balunas, M. J.; Kinghorn, A. D. Drug Discovery from Medicinal Plants. *Life Sci.* **2005**, *78* (5), 431–441. https://doi.org/10.1016/j.lfs.2005.09.012.

(28) Drahl, C.; Cravatt, B. F.; Sorensen, E. J. Protein-Reactive Natural Products. *Angew. Chem. Int. Ed.* **2005**, *44* (36), 5788–5809. https://doi.org/10.1002/anie.200500900.

(29) Li, Z.; Zhao, T.; Li, J.; Yu, Q.; Feng, Y.; Xie, Y.; Sun, P. Nanomedicine Based on Natural Products: Improving Clinical Application Potential. *J. Nanomater.* **2022**, *2022*, 1–11. https://doi.org/10.1155/2022/3066613.

(30) Schmidt, B.; Ribnicky, D. M.; Poulev, A.; Logendra, S.; Cefalu, W. T.; Raskin, I. A Natural History of Botanical Therapeutics. *Metabolism* **2008**, *57*, S3–S9. https://doi.org/10.1016/j.metabol.2008.03.001.

(31) Newman, D. J.; Cragg, G. M. Natural Products as Sources of New Drugs from 1981 to 2014. *J. Nat. Prod.* **2016**, *79* (3), 629–661. https://doi.org/10.1021/acs.jnatprod.5b01055.

(32) Newman, D. J.; Cragg, G. M. Natural Products as Sources of New Drugs over the Nearly Four Decades from 01/1981 to 09/2019. *J. Nat. Prod.* **2020**, *83* (3), 770–803. https://doi.org/10.1021/acs.jnatprod.9b01285.

(33) Peng, S.; Wang, Y.; Sun, Z.; Zhao, L.; Huang, Y.; Fu, X.; Luo, R.; Xue, J.; Yang, S.; Ling, L.; Zhang, Z. Nanoparticles Loaded with Pharmacologically Active Plant-Derived Natural Products: Biomedical Applications and Toxicity. *Colloids Surf. B Biointerfaces* **2023**, *225*, 113214. https://doi.org/10.1016/j.colsurfb.2023.113214.

(34) Jiménez, C. Marine Natural Products in Medicinal Chemistry. *ACS Med. Chem. Lett.* **2018**, *9* (10), 959–961. https://doi.org/10.1021/acsmedchemlett.8b00368.

(35) Altmann, K.-H. Drugs from the Oceans: Marine Natural Products as Leads for Drug Discovery. *CHIMIA* **2017**, *71* (10), 646. https://doi.org/10.2533/chimia.2017.646.

(36) Romano, G.; Costantini, M.; Sansone, C.; Lauritano, C.; Ruocco, N.; Ianora, A. Marine Microorganisms as a Promising and Sustainable Source of Bioactive Molecules. *Mar. Environ. Res.* **2017**, *128*.

(37) Newman, D.; Cragg, G. Drugs and Drug Candidates from Marine Sources: An Assessment of the Current "State of Play." *Planta Med.* **2016**, *82* (09/10), 775–789. https://doi.org/10.1055/s-0042-101353.

(38) Jiménez, C. Marine Natural Products in Medicinal Chemistry. *ACS Med. Chem. Lett.* **2018**, *9* (10), 959–961. https://doi.org/10.1021/acsmedchemlett.8b00368.

(39) Banerjee, P.; Mandhare, A.; Bagalkote, V. Marine Natural Products as Source of New Drugs: An Updated Patent Review (July 2018-July 2021). *Expert Opin. Ther. Pat.* **2022**, *32* (3), 317–363. https://doi.org/10.1080/13543776.2022.2012150.

(40) Liang, X.; Luo, D.; Luesch, H. Advances in Exploring the Therapeutic Potential of Marine Natural Products. *Pharmacol. Res.* **2019**, *147*, 104373. https://doi.org/10.1016/j.phrs.2019.104373.

(41) Deng, C.; Pan, B.; O'Connor, O. A. Brentuximab Vedotin. *Clin. Cancer Res.* **2013**, *19* (1), 22–27. https://doi.org/10.1158/1078-0432.CCR-12-0290.

(42) Sehn, L. H.; Herrera, A. F.; Flowers, C. R.; Kamdar, M. K.; McMillan, A.; Hertzberg, M.; Assouline, S.; Kim, T. M.; Kim, W. S.; Ozcan, M.; Hirata, J.; Penuel, E.; Paulson, J. N.; Cheng, J.; Ku, G.; Matasar, M. J. Polatuzumab Vedotin in Relapsed or Refractory Diffuse Large B-Cell Lymphoma. *J. Clin. Oncol.* **2020**, *38* (2), 155–165. https://doi.org/10.1200/JCO.19.00172.

(43) Ito, M. K. A Comparative Overview of Prescription Omega-3 Fatty Acid Products.

(44) Leibbrandt, A.; Meier, C.; König-Schuster, M.; Weinmüllner, R.; Kalthoff, D.; Pflugfelder, B.; Graf, P.; Frank-Gehrke, B.; Beer, M.; Fazekas, T.; Unger, H.; Prieschl-Grassauer, E.; Grassauer, A. Iota-Carrageenan Is a Potent Inhibitor of Influenza A Virus Infection. *PLoS ONE* **2010**, *5* (12), e14320. https://doi.org/10.1371/journal.pone.0014320.

(45) Shilpi, J. A.; Uddin, S. J. Analgesic and Antipyretic Natural Products. In *Annual Reports in Medicinal Chemistry*; Elsevier, 2020; Vol. 55, pp 435–458. https://doi.org/10.1016/bs.armc.2020.03.003.

(46) Alonso-Álvarez, S.; Pardal, E.; Sánchez-Nieto, D.; Navarro, M.; Caballero, M. D.; Mateos, M. V.; Martin, A. Plitidepsin: Design, Development, and Potential Place in Therapy. *Drug Des. Devel. Ther.* **2017**, *Volume11*, 253–264. https://doi.org/10.2147/DDDT.S94165.

(47) Depenbrock, H.; Peter, R.; Faircloth, G.; Manzanares, I.; Jimeno, J.; Hanauske, A. In Vitro Activity of Aplidine, a New Marine-Derived Anti-Cancer Compound, on Freshly Explanted Clonogenic Human Tumour Cells and Haematopoietic Precursor Cells. *Br. J. Cancer* **1998**, *78* (6), 739–744. https://doi.org/10.1038/bjc.1998.570.

(48) Spicka, I.; Ocio, E. M.; Oakervee, H. E.; Greil, R.; Banh, R. H.; Huang, S.-Y.; D'Rozario, J. M.; Dimopoulos, M. A.; Martínez, S.; Extremera, S.; Kahatt, C.; Alfaro, V.; Carella, A. M.; Meuleman, N.; Hájek, R.; Symeonidis, A.; Min, C.-K.; Cannell, P.; Ludwig, H.; Sonneveld, P.; Mateos, M. V. Randomized Phase III Study (ADMYRE) of Plitidepsin in Combination with Dexamethasone vs. Dexamethasone Alone in Patients with Relapsed/Refractory Multiple Myeloma. *Ann. Hematol.* **2019**, *98* (9), 2139–2150. https://doi.org/10.1007/s00277-019-03739-2.

(49) Cimino, P.; Huang, L.; Du, L.; Wu, Y.; Bishop, J.; Dalsing-Hernandez, J.; Kotlarczyk, K.; Gonzales, P.; Carew, J.; Nawrocki, S.; Jordan, M.; Wilson, L.; Lloyd, G.; Wirsching, H.-G.

Plinabulin, an Inhibitor of Tubulin Polymerization, Targets KRAS Signaling through Disruption of Endosomal Recycling. *Biomed. Rep.* **2019**. https://doi.org/10.3892/br.2019.1196.

(50) Lago, J.; Rodríguez, L.; Blanco, L.; Vieites, J.; Cabado, A. Tetrodotoxin, an Extremely Potent Marine Neurotoxin: Distribution, Toxicity, Origin and Therapeutical Uses. *Mar. Drugs* **2015**, *13* (10), 6384–6406. https://doi.org/10.3390/md13106384.

(51) Michon, S.; Cavelier, F.; Salom-Roig, X. J. Synthesis and Biological Activities of Cyclodepsipeptides of Aurilide Family from Marine Origin. *Mar. Drugs* **2021**, *19* (2), 55. https://doi.org/10.3390/md19020055.

(52) Suenaga, K.; Mutou, T.; Shibata, T.; Itoh, T.; Kigoshi, H.; Yamada, K. Isolation and Stereostructure of Aurilide, a Novel Cyclodepsipeptide from the Japanese Sea Hare Dolabella Auricularia. *Tetrahedron Lett. Int. J. Rapid Publ. Prelim. Commun. Org. Chem.* **1996**, *37* (37).

(53) Williams, P. G.; Yoshida, W. Y.; Quon, M. K.; Moore, R. E.; Paul, V. J. The Structure of Palau'amide, a Potent Cytotoxin from a Species of the Marine Cyanobacterium *Lyngbya*. *J. Nat. Prod.* **2003**, *66* (12), 1545–1549. https://doi.org/10.1021/np034001r.

(54) Nakao, Y.; Yoshida, W. Y.; Takada, Y.; Kimura, J.; Yang, L.; Mooberry, S. L.; Scheuer, P. J. Kulokekahilide-2, a Cytotoxic Depsipeptide from a Cephalaspidean Mollusk *Philinopsis Speciosa*. *J. Nat. Prod.* **2004**, *67* (8), 1332–1340. https://doi.org/10.1021/np049949f.

(55) Han, B.; Gross, H.; Goeger, D. E.; Mooberry, S. L.; Gerwick, W. H. Aurilides B and C, Cancer Cell Toxins from a Papua New Guinea Collection of the Marine Cyanobacterium *Lyngbya m Ajuscula*. *J. Nat. Prod.* **2006**, *69* (4), 572–575. https://doi.org/10.1021/np0503911.

(56) Tripathi, A.; Puddick, J.; Prinsep, M. R.; Rottmann, M.; Tan, L. T. Lagunamides A and B: Cytotoxic and Antimalarial Cyclodepsipeptides from the Marine Cyanobacterium *Lyngbya Majuscula*. *J. Nat. Prod.* **2010**, *73* (11), 1810–1814. https://doi.org/10.1021/np100442x.

(57) Tripathi, A.; Puddick, J.; Prinsep, M. R.; Rottmann, M.; Chan, K. P.; Chen, D. Y.-K.; Tan, L. T. Lagunamide C, a Cytotoxic Cyclodepsipeptide from the Marine Cyanobacterium Lyngbya Majuscula. *Phytochemistry* **2011**, *72* (18), 2369–2375. https://doi.org/10.1016/j.phytochem.2011.08.019.

(58) Sueyoshi, K.; Kaneda, M.; Sumimoto, S.; Oishi, S.; Fujii, N.; Suenaga, K.; Teruya, T. Odoamide, a Cytotoxic Cyclodepsipeptide from the Marine Cyanobacterium Okeania Sp. *Tetrahedron* **2016**, *72* (35), 5472–5478. https://doi.org/10.1016/j.tet.2016.07.031.

(59) Luo, D.; Putra, M.; Ye, T.; Paul, V.; Luesch, H. Isolation, Structure Elucidation and Biological Evaluation of Lagunamide D: A New Cytotoxic Macrocyclic Depsipeptide from Marine Cyanobacteria. *Mar. Drugs* **2019**, *17* (2), 83. https://doi.org/10.3390/md17020083.

(60) Tripathi, A.; Fang, W.; Leong, D. T.; Tan, L. T. Biochemical Studies of the Lagunamides, Potent Cytotoxic Cyclic Depsipeptides from the Marine Cyanobacterium Lyngbya Majuscula. *Mar. Drugs* **2012**, *10* (12), 1126–1137. https://doi.org/10.3390/md10051126.

(61) Huang, X.; Huang, W.; Li, L.; Sun, X.; Song, S.; Xu, Q.; Zhang, L.; Wei, B.-G.; Deng, X. Structure Determinants of Lagunamide A for Anticancer Activity and Its Molecular Mechanism of Mitochondrial Apoptosis. *Mol. Pharm.* **2016**, *13* (11), 3756–3763. https://doi.org/10.1021/acs.molpharmaceut.6b00564.

(62) Semenzato, M.; Cogliati, S.; Scorrano, L. Prohibitin(g) Cancer: Aurilide and Killing by Opa1-Dependent Cristae Remodeling. *Chem. Biol.* **2011**, *18* (1), 8–9. https://doi.org/10.1016/j.chembiol.2011.01.001.

(63) Suenaga, K.; Mutou, T.; Shibata, T.; Itoh, T.; Kigoshi, H.; Yamada, K. Isolation and Stereostructure of Aurilide, a Novel Cyclodepsipeptide from the Japanese Sea Hare Dolabella Auricularia. *Tetrahedron Lett.* **1996**, *37* (37), 6771–6774. https://doi.org/10.1016/S0040-4039(96)01464-5.

(64) Aurilide 1997 Synthesis.Pdf.

(65) Takahashi, T.; Nagamiya, H.; Doi, T.; Griffiths, P. G.; Bray, A. M. Solid Phase Library Synthesis of Cyclic Depsipeptides: Aurilide and Aurilide Analogues. *J. Comb. Chem.* **2003**, *5* (4), 414–428. https://doi.org/10.1021/cc020091r.

(66) Han, B.; Gross, H.; Goeger, D. E.; Mooberry, S. L.; Gerwick, W. H. Aurilides B and C, Cancer Cell Toxins from a Papua New Guinea Collection of the Marine Cyanobacterium *Lyngbya m Ajuscula*. *J. Nat. Prod.* **2006**, *69* (4), 572–575. https://doi.org/10.1021/np0503911.

(67) Nakao, Y.; Yoshida, W. Y.; Takada, Y.; Kimura, J.; Yang, L.; Mooberry, S. L.; Scheuer, P. J. Kulokekahilide-2, a Cytotoxic Depsipeptide from a Cephalaspidean Mollusk *Philinopsis Speciosa*. *J. Nat. Prod.* **2004**, *67* (8), 1332–1340. https://doi.org/10.1021/np049949f.

(68) Takada, Y.; Mori, E.; Umehara, M.; Nakao, Y.; Kimura, J. Reinvestigation of the Stereochemistry of Kulokekahilide-2. *Tetrahedron Lett.* **2007**, *48* (43), 7653–7656. https://doi.org/10.1016/j.tetlet.2007.08.093.

(69) Han, C.; Doi, H.; Kimura, J.; Nakao, Y.; Suzuki, M. ¹¹C-Labeling of the C(1)-C(10) Dihydroxy Acid Moiety for the Study on the Synthesis of Kulokekahilide-2 PET Tracer. *Int. J. Org. Chem.* **2014**, *04* (04), 269–277. https://doi.org/10.4236/ijoc.2014.44029.

(70) Sueyoshi, K.; Kaneda, M.; Sumimoto, S.; Oishi, S.; Fujii, N.; Suenaga, K.; Teruya, T. Odoamide, a Cytotoxic Cyclodepsipeptide from the Marine Cyanobacterium Okeania Sp. *Tetrahedron* **2016**, *72* (35), 5472–5478. https://doi.org/10.1016/j.tet.2016.07.031.

(71) Dai, L.; Chen, B.; Lei, H.; Wang, Z.; Liu, Y.; Xu, Z.; Ye, T. Total Synthesis and Stereochemical Revision of Lagunamide A. *Chem. Commun.* **2012**, *48* (69), 8697. https://doi.org/10.1039/c2cc34187e.

(72) Huang, W.; Ren, R.-G.; Dong, H.-Q.; Wei, B.-G.; Lin, G.-Q. Diverse Synthesis of Marine Cyclic Depsipeptide Lagunamide A and Its Analogues. *J. Org. Chem.* **2013**, *78* (21), 10747–10762. https://doi.org/10.1021/jo401687s.

(73) Liu, H.-M.; Chang, C.-Y.; Lai, Y.-C.; Yang, M.-D.; Chang, C.-Y. An Efficient Synthesis of the C27–C45 Fragment of Lagunamide A, a Cyclodepsipeptide with Potent Cytotoxic and Antimalarial Properties. *Tetrahedron Asymmetry* **2014**, *25* (2), 187–192. https://doi.org/10.1016/j.tetasy.2013.11.020.

(74) Banasik, B. A.; Wang, L.; Kanner, A.; Bergdahl, B. M. Further Insight into the Asymmetric Vinylogous Mukaiyama Aldol Reaction (VMAR); Application to the Synthesis of the C27–C45 Segment of Lagunamide A. *Tetrahedron* **2016**, *72* (19), 2481–2490. https://doi.org/10.1016/j.tet.2016.03.079.

(75) Gorges, J.; Kazmaier, U. Matteson Homologation-Based Total Synthesis of Lagunamide A. *Org. Lett.* **2018**, *20* (7), 2033–2036. https://doi.org/10.1021/acs.orglett.8b00576.

(76) Pal, S.; Chakraborty, T. K. Toward the Total Synthesis of a Lagunamide B Analogue. *Tetrahedron Lett.* **2014**, *55* (24), 3469–3472. https://doi.org/10.1016/j.tetlet.2014.04.079.

(77) Fatino, A.; Weese, C.; Valdez, S.; Jiménez-Somarribas, A.; Rafferty, R. J. Synthetic Studies towards Lagunamide C: Polyketide Assembly Investigations. *Tetrahedron Lett.* **2018**, *59* (7), 624–627. https://doi.org/10.1016/j.tetlet.2017.12.083.

(78) Suenaga, K.; Mutou, T.; Shibata, T.; Itoh, T.; Fujita, T.; Takada, N.; Hayamizu, K.; Takagi, M.; Irifune, T.; Kigoshi, H.; Yamada, K. Aurilide, a Cytotoxic Depsipeptide from the Sea Hare Dolabella Auricularia: Isolation, Structure Determination, Synthesis, and Biological Activity. *Tetrahedron* **2004**, *60* (38), 8509–8527. https://doi.org/10.1016/j.tet.2004.06.125.

(79) Takada, Y.; Umehara, M.; Nakao, Y.; Kimura, J. Revised Absolute Stereochemistry of Natural Kulokekahilide-2. *Tetrahedron Lett.* **2008**, *49* (7), 1163–1165. https://doi.org/10.1016/j.tetlet.2007.12.050.

(80) Kaneda, M.; Sueyoshi, K.; Teruya, T.; Ohno, H.; Fujii, N.; Oishi, S. Total Synthesis of Odoamide, a Novel Cyclic Depsipeptide, from an Okinawan Marine Cyanobacterium. *Org. Biomol. Chem.* **2016**, *14* (38), 9093–9104. https://doi.org/10.1039/C6OB01583B.

(81) Takada et al. - 2007 - Reinvestigation of the Stereochemistry of Kulokeka.Pdf.

(82) Mamer, O. A.; Reimer, M. L. On the Mechanisms of the Formation of L-Alloisoleucine and the 2-Hydroxy-3-Methylvaleric Acid Stereoisomers from L-Isoleucine in Maple Syrup Urine Disease Patients and in Normal Humans. *J. Biol. Chem.* **1992**, *267* (31), 22141–22147. https://doi.org/10.1016/S0021-9258(18)41646-8.

(83) De Faveri, G.; Ilyashenko, G.; Watkinson, M. Recent Advances in Catalytic Asymmetric Epoxidation Using the Environmentally Benign Oxidant Hydrogen Peroxide and Its Derivatives. *Chem Soc Rev* **2011**, *40* (3), 1722–1760. https://doi.org/10.1039/C0CS00077A.

(84) Shi_asymmetric_epoxidation_reaction.Pdf.

(85) Schmitt, D. C.; Dechert-Schmitt, A.-M. R.; Krische, M. J. Iridium-Catalyzed Allylation of Chiral β-Stereogenic Alcohols: Bypassing Discrete Formation of Epimerizable Aldehydes. *Org. Lett.* **2012**, *14* (24), 6302–6305. https://doi.org/10.1021/ol3030692.

Chapter 6 – Procedures and NMRs

General Methods

All reactions were performed in an inert Argon (Ar) atmosphere with flame dried or oven dried glassware and stir bars with anhydrous solvents or open atmosphere, unless otherwise noted. All commercially available regents were used as received unless otherwise mentioned. Reactions were monitored by thin layer chromatography (TLC) developed on 0.25 mm E. Merck silica gel plates (60F-254) and the visualized using UV light followed by PMA/heat or $KMnO_4$/heat. Silica gel column chromatography was performed with silica gel grade 60 (230-400 mesh). Anhydrous diethyl ether (Et_2O), toluene (PhMe), *N,N*-dimethylsulforamide (DMF), tetrahydrofuran (THF), and dichloromethane (CH_2Cl_2) were all degassed with Ar and passed through a dual column solvent purification system (Pure Process Technology) before introducing to the reactions. Acetone, ethanol (EtOH), and methanol (MeOH) were used after drying over activated molecular sieves. Nuclear magnetic resonance (NMR) spectra were recorded on a Bruker spectrometer for ^1H (400 MHz or 600 MHz) and ^{13}C (101 MHz or 151MHz) in deuterated chloroform ($CDCl_3$), unless otherwise indicated. The chemical shifts are given in parts per million (ppm) relative to residual $CHCl_3$ δ 7.26 ppm for proton spectra and relative to $CDCl_3$ at δ 77.22 ppm for carbon spectra, unless otherwise noted. Signal patterns are indicated as br, broad peak; s, singlet; d, doublet; t, triplet; q, quartet; m, multiplet.

Standard protocol for peptide coupling reactions using EDC·HCl

Unless otherwise specified, free carboxylic acid (1 eq.), free amine (1 eq.), and HOBt (1.05 eq.) were dissolved in anhydrous THF (1M to the free acid). Round bottom flask (RBF) was cooled to 0 °C and stirred for 10 minutes. Next, NEt_3 (3.5 eq.) was added and stirred for 15 minutes. Then EDC·HCl (1.05 eq.) was added to the reaction at 0 °C and the reaction was allowed to stir at room temperature (rt) overnight. It was quenched with 2 eq. of deionized (DI) H_2O by volume, extracted with CH_2Cl_2 (x3), the combined organic layers were washed with a saturated (sat'd) aqueous (aq) solution of $NaHCO_3$ followed by a brine solution, dried over anhydrous sodium sulfate (Na_2SO_4) and concentrated under reduced pressure. The crude material was purified via flash silica chromatography.

Standard protocol for Boc deprotections

Substrate (1 eq.) was dissolved in 4 M HCl in dioxane solution (starting material concentration was 0.25 M in solution) at rt under ambient atmosphere and constantly monitored via TLC until the starting material disappeared. Reaction mixture was concentrated under reduced pressure to obtain a pure white solid that was carried forward to next step with no further purification.

Standard protocol for saponification (base-mediated ester hydrolysis)

Unless otherwise specified, methyl ester (1 eq.) was dissolved in THF (0.25M) in a RBF (flask A) and cooled to 0 °C. In. a separate RBF (flask B), LiOH (2.5 eq.) was dissolved in DI H_2O (1.16 M) and cooled to 0 °C. The content in RBF B was added dropwise to RBF A at 0 °C and stirred at rt until starting material disappeared on TLC. Reaction was quenched carefully with a 1M HCl allowing the reaction pH to reach ~2, extracted with EtOAc (x3), the combined organic layers

were dried with anhydrous Na_2SO_4 and concentrated under reduced pressure. Crude material was carried forward to next step with no further purification.

Standard protocol for trichloro ethanol deprotection

Unless otherwise specified, substrate (1eq.) was dissolved in glacial acetic acid (0.02M) and zinc powder (20 mg/0.01 mmol) was added. Resulting mixture was stirred for 30 minutes at rt and DI H_2O (0.1M) was added. Stirring was continued for 16 h and reaction mixture was filtered through a short plug of celite. Obtained filtrate was evaporated under reduced pressure to yield a pure white solid that was carried forward with no further purification.

Standard protocol for fluorenylmethyloxycarbonyl (Fmoc) deprotection

Unless otherwise specified, to the substrate (1eq.) was dissolved in DMF and piperidine (100 eq.) was added slowly dropwise. Final concentration of piperidine was achieved to be 50% in DMF. Reaction was stirred at rt overnight, quenched with a sat'd $NH_4Cl_{(aq)}$ solution, extracted with CH_2Cl_2 (x3), the combined organic layers were dried over anhydrous Na_2SO_4 and concentrated under reduced pressure. The obtained crude material was purified via silica gel column chromatography.

Standard protocol for silyl ether deprotection

Unless otherwise specified, in a flame dried RBF, silyl ether (1eq.) was dissolved anhydrous THF (0.066M). RBF was cooled to 0 °C and TBAF (1M in THF) (0.031 mL, 0.031 mmol, 1 eq.) was added dropwise. Temperature of the reaction was allowed to come to rt gradually while it was monitored via TLC until the starting disappeared. Reaction was quenched with a sat'd $NH_4Cl_{(aq)}$ solution, extracted with CH_2Cl_2 (x3), the combined organic layers were dried over anhydrous

Na_2SO_4 and concentrated under reduced pressure. The obtained crude material was purified via silica gel column chromatography.

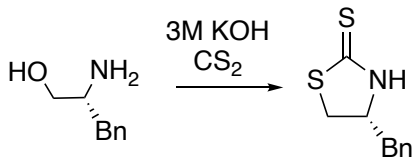
Standard protocol for acid chloride mediated coupling reactions

Unless otherwise specified, in a flame dried RBF (A), the free carboxylic acid (1 eq.) was dissolved in anhydrous CH_2Cl_2 (0.6M) under an Ar atmosphere and cooled to 0 °C. Next, 1-Chloro-N,N,2-trimethyl-1-propenylamine (Ghosez's reagent, 1 eq.) was added under an Ar atmosphere and stirred the reaction at rt for 1 h. In a separate flame dried RBF (B), respective amine or alcohol (1 eq.) and NEt_3 (dried over molecular sieves (MS), 1.1 eq.) were dissolved in anhydrous CH_2Cl_2 (0.1M). After 1 h, content in RBF B was transferred to the crude mixture in RBF A slowly dropwise under an Ar atmosphere at rt. Reaction was continued to stir at rt under an Ar atmosphere overnight, concentrated under reduced pressure at rt, and purified via silica gel column chromatography.

Standard protocol for cross metathesis reactions

Unless otherwise specified, in a flame dried RBF, less substituted olefine (1 eq.) was dissolved in anhydrous CH_2Cl_2 (0.04M) under an Ar atmosphere. Next, more substituted olefine (3 eq.) and Grubbs second generation catalyst (0.1 eq. or 10 mol%) was added under an Ar atmosphere and refluxed overnight while maintaining a positive Ar pressure in the system. Reaction was brought to rt temperature gradually and resulted crude reaction mixture was purified via silica gel column chromatography.

(*R*)-4-benzylthiazolidine-2-thione (165)



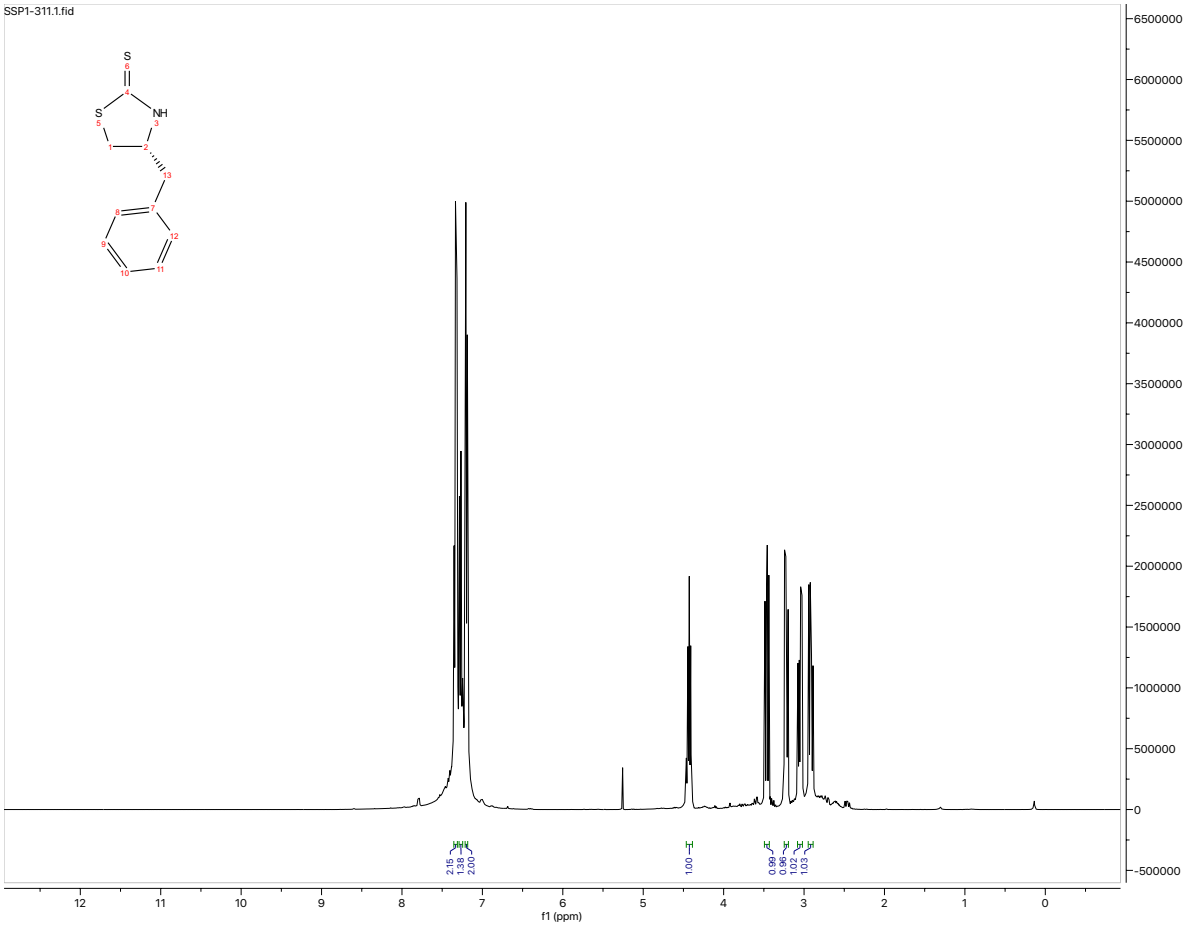
165

To a freshly prepared 3M aqueous solution of KOH (40 mL), was added *D*-phenyl alaninol (3 g, 19.84 mmol, 1 eq.) followed by CS_2 (6.00 mL, 99.2 mmol, 5 eq.). The reaction mixture was refluxed at 102 °C while purging a stream of Ar gas though the system for 2 h, the solution turned color from pale yellow to orange to dark red. Purging of Ar was stopped after 2 h and reaction was continued to reflux at 114 °C overnight. Over the course of reflux time stirring solution has turned color from dark red to pale yellow. Next, the reaction was gradually brought to rt and diluted with of DI H_2O (2eq. by volume), extracted with CH_2Cl_2 (x3), the combined organic layers were dried over anhydrous sodium sulfate (Na_2SO_4) and concentrated under reduced pressure. The resulting pale yellow solid (4.15g, quantitative yield) was carried forward to the next step without further purification. ^{1}H NMR (400 MHz, $CDCl_3$) δ 7.35 – 7.31 (m, 2H), 7.29 – 7.25 (m, 1H), 7.22 – 7.18 (m, 2H), 4.43 (p, *J* = 7.1 Hz, 1H), 3.46 (dd, *J* = 11.3, 7.8 Hz, 1H), 3.22 (dd, *J* = 11.3, 6.4 Hz, 1H), 3.05 (dd, *J* = 13.6, 6.7 Hz, 1H), 2.92 (dd, *J* = 13.6, 7.4 Hz, 1H).

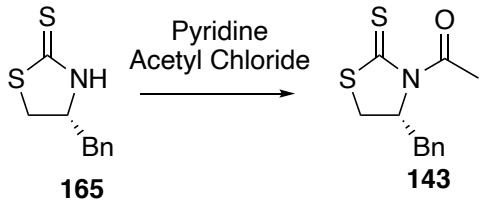
Notebook entries:

Procedure: SSP1-311

^{1}H NMR: SSP1-311 (Crude)


SSP1-311.1.fid
S
NH
f1 (ppm)
2.15
1.38
2.00
1.00
0.99
0.96
1.02
1.03

(*R*)-1-(4-benzyl-2-thioxothiazolidin-3-yl)ethan-1-one (143)



165 **143**

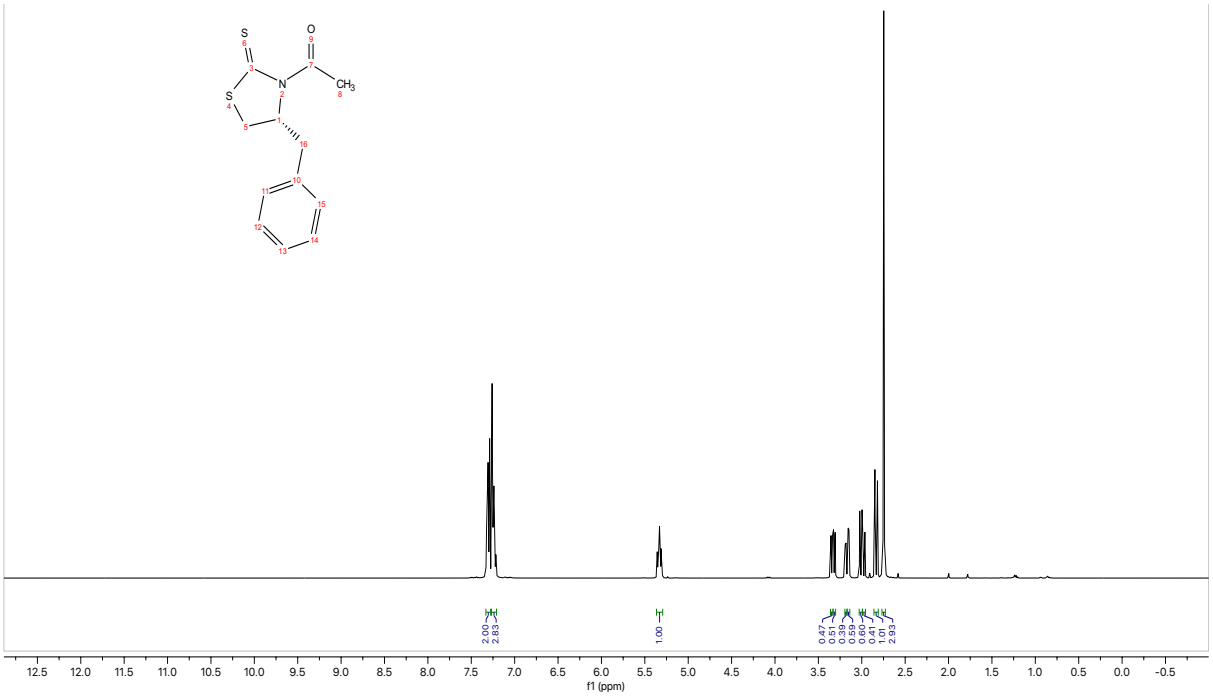
Crude **165** (4.02 g, 19.2 mmol, 1 eq.) was dissolved in anhydrous CH_2Cl_2 (20.89 mL, 0.92M) under an Ar atmosphere and cooled to 0 °C. Pyridine (2.07 mL, 25.54 mmol, 1.33 eq.) was added rapidly while stirring the solution vigorously. Next, acetyl chloride (1.64 mL, 23.04 mmol, 1.2 eq.) was added slowly dropwise over 15 minutes. Once the addition was complete, reaction flask was gradually brought to rt and continued stirring for 1 h. Then, MeOH (0.13 mL) was added rapidly under an Ar atmosphere at rt and stirred the reaction for further 20 minutes. Reaction mixture was then transferred to a separatory funnel and washed with DI H_2O (x2), the combined aqueous layers were back extracted with CH_2Cl_2. The combined organic layers were washed with 1N HCl solution (x2) and combined aqueous layers were back extracted with CH_2Cl_2. The combined organic layers were dried over anhydrous Na_2SO_4 and concentrated under reduced pressure. The crude material was purified via flash silica gel chromatography (1:3 EtOAc: hexane) to afford **143** as bright yellow crystals (3.2 g, 93% yield).

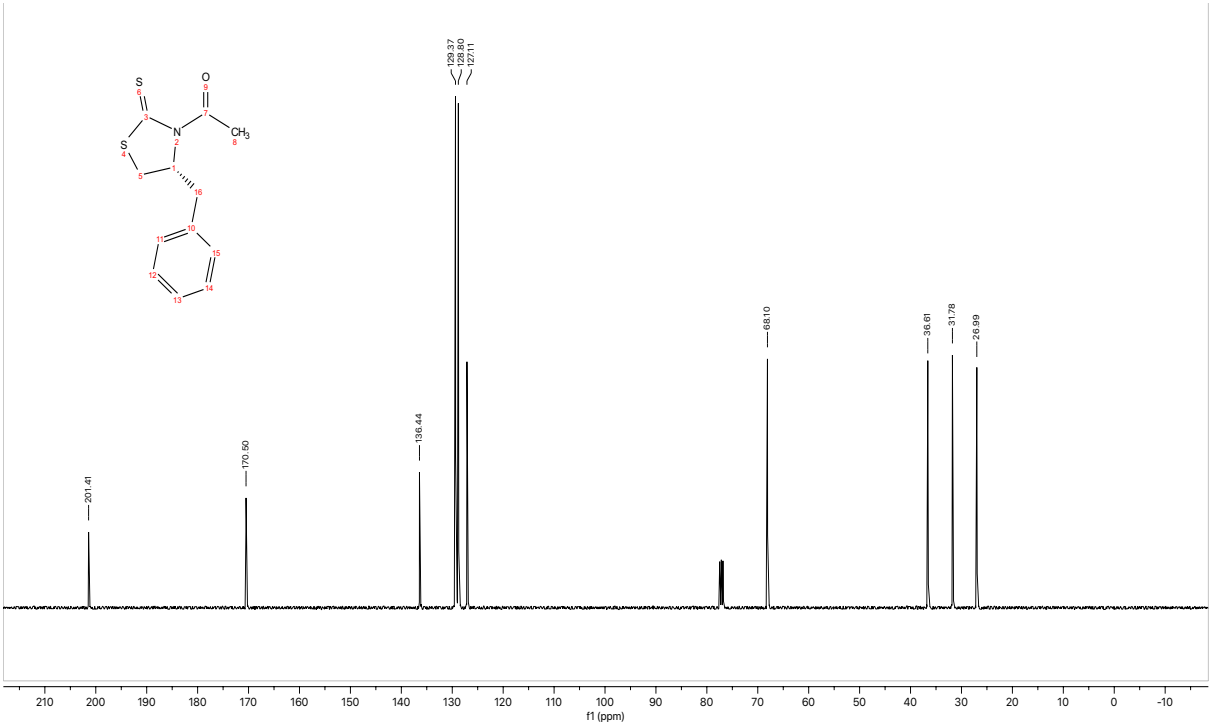
^{1}H NMR (400 MHz, $CDCl_3$) δ 7.33 – 7.28 (m, 2H), 7.27 – 7.21 (m, 3H), 5.33 (ddd, *J* = 10.8, 7.1, 3.8 Hz, 1H), 3.33 (dd, *J* = 7.3, 1.1 Hz, 1H), 3.17 (dd, *J* = 13.2, 3.9 Hz, 1H), 2.99 (dd, *J* = 13.2, 10.5 Hz, 1H), 2.83 (d, *J* = 11.6 Hz, 1H), 2.75 (s, 3H). ^{13}C NMR (101 MHz, $CDCl_3$) δ 201.41, 170.49, 136.44, 129.36, 128.80, 127.11, 68.10, 36.61, 31.78, 26.99.

Notebook entries:

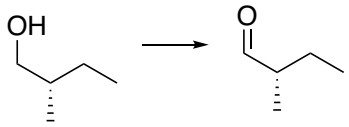
Procedure: SSP2-072 and SSP2-334

^{1}H NMR and ^{13}C NMR: SSP2-072





Synthesis of (*S*)-2-methylbutanal (166)



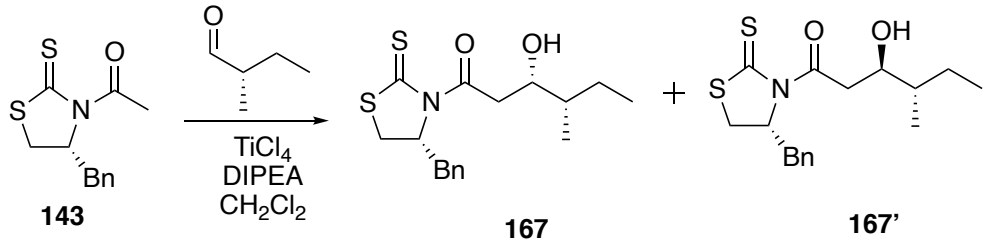
166

A flame dried RBF was charged with PCC (0.598 g, 2.78 mmol, 1.5 eq.), celite (0.598 g, 1:1 mass ratio with PCC), and anhydrous CH_2Cl_2 (3.7 mL, 0.5M) under an Ar atmosphere. Next, (*S*)-2-methylbutanol (0.2 mL, 1.85 mmol, 1 eq.) was added dropwise to the stirring mixture and continued stirring for 1 h. Then the reaction mixture was filtered through a fritted Buchner filter funnel under vacuum. Collected filtrate was directly transferred to the next reaction via a syringe.

Notebook entries:

Procedure: SSP2-132

(3*S*,4*S*)-1-((*R*)-4-benzyl-2-thioxothiazolidin-3-yl)-3-hydroxy-4-methylhexan-1-one (167)

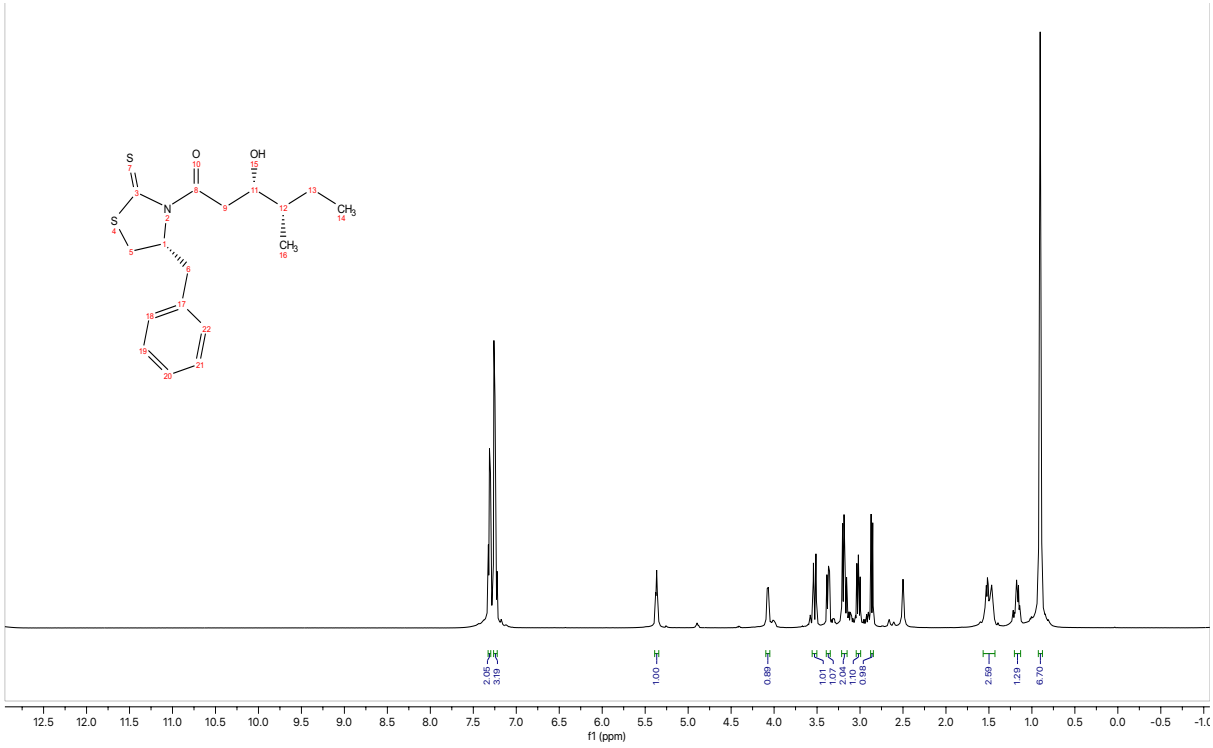


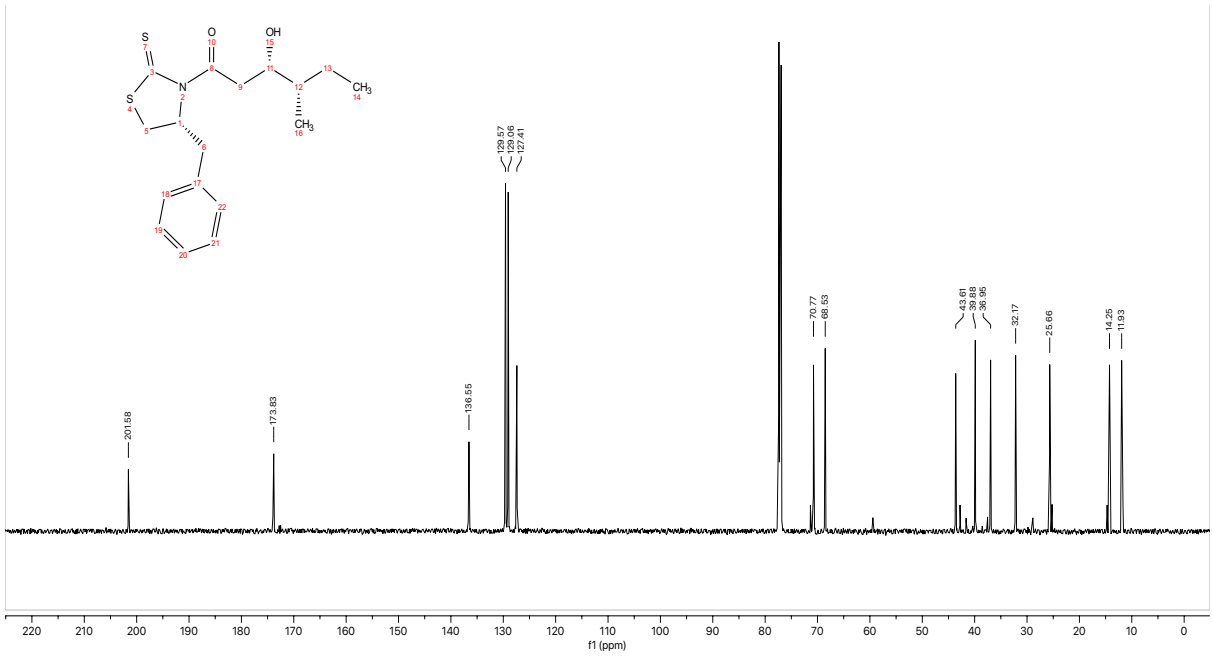
In a flame dried RBF, compound **143** (0.5 g, 1.99 mmol, 1 eq.), was dissolved in anhydrous CH_2Cl_2 (11.7 mL, 0.17M) under an Ar atmosphere and then cooled to -78 °C. Next, 1M solution of $TiCl_4$ in CH_2Cl_2 (~2 mL, 1.99 mmol, 1 eq.) was added slowly dropwise. After stirring the reaction for 5 minutes, DIPEA (0.69 mL, 3.98 mmol, 2 eq.) was added slowly dropwise and continued stirring at -78 °C for 30 minutes. Then, crude solution of compound **166** (0.64 mL, 5.97 mmol, 3 eq.) was added and stirred the reaction for further 30 minutes at -78 °C. The reaction was quenched with a half saturated (sat'd) $NH_4Cl_{(aq)}$ solution at -78 °C, gradually brought to rt, and extracted with CH_2Cl_2 (x3), the combined organic layers were dried over anhydrous Na_2SO_4 and concentrated under reduced pressure. Obtained crude compound was subjected to flash silica column chromatography (gradient elution; 100% hexane, 1:4 EtOAc: hexane, 1:3 EtOAc: hexane) to access **167** as a bright yellow viscous oil and **167'** as bright yellow crystals (0.4909 g, 73% yield, *dr* 3.45:1). ^{1}H NMR (600 MHz, $CDCl_3$) δ 7.31 (t, *J* = 7.6 Hz, 2H), 7.24 (dd, *J* = 14.8, 6.9 Hz, 3H), 5.37 (ddd, *J* = 10.9, 7.2, 4.0 Hz, 1H), 4.07 (d, *J* = 4.2 Hz, 1H), 3.53 (dd, *J* = 17.7, 2.0 Hz, 1H), 3.37 (dd, *J* = 11.5, 7.2 Hz, 1H), 3.21 – 3.15 (m, 2H), 3.02 (dd, *J* = 13.2, 10.5 Hz, 1H), 2.86 (d, *J* = 11.5 Hz, 1H), 1.55 – 1.43 (m, 3H), 1.17 (dt, *J* = 12.8, 7.5 Hz, 1H), 0.90 (t, *J* = 7.0 Hz, 6H). ^{13}C NMR (151 MHz, $CDCl_3$) δ 201.58, 173.83, 136.55, 129.57, 129.06, 127.41, 70.77, 68.53, 43.61, 39.88, 36.95, 32.17, 25.66, 14.25, 11.93.

Notebook entries: Procedure: SSP2-338

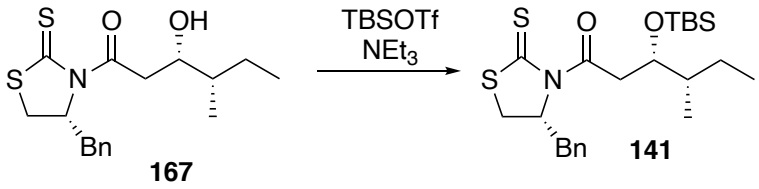
Procedure: SSP2-338

^{1}H NMR and ^{13}C NMR: SSP2-218





Synthesis of (3*S*,4*S*)-1-((*R*)-4-benzyl-2-thioxothiazolidin-3-yl)-3-((*tert*-butyldimethylsilyl)oxy)-4-methylhexan-1-one (141)



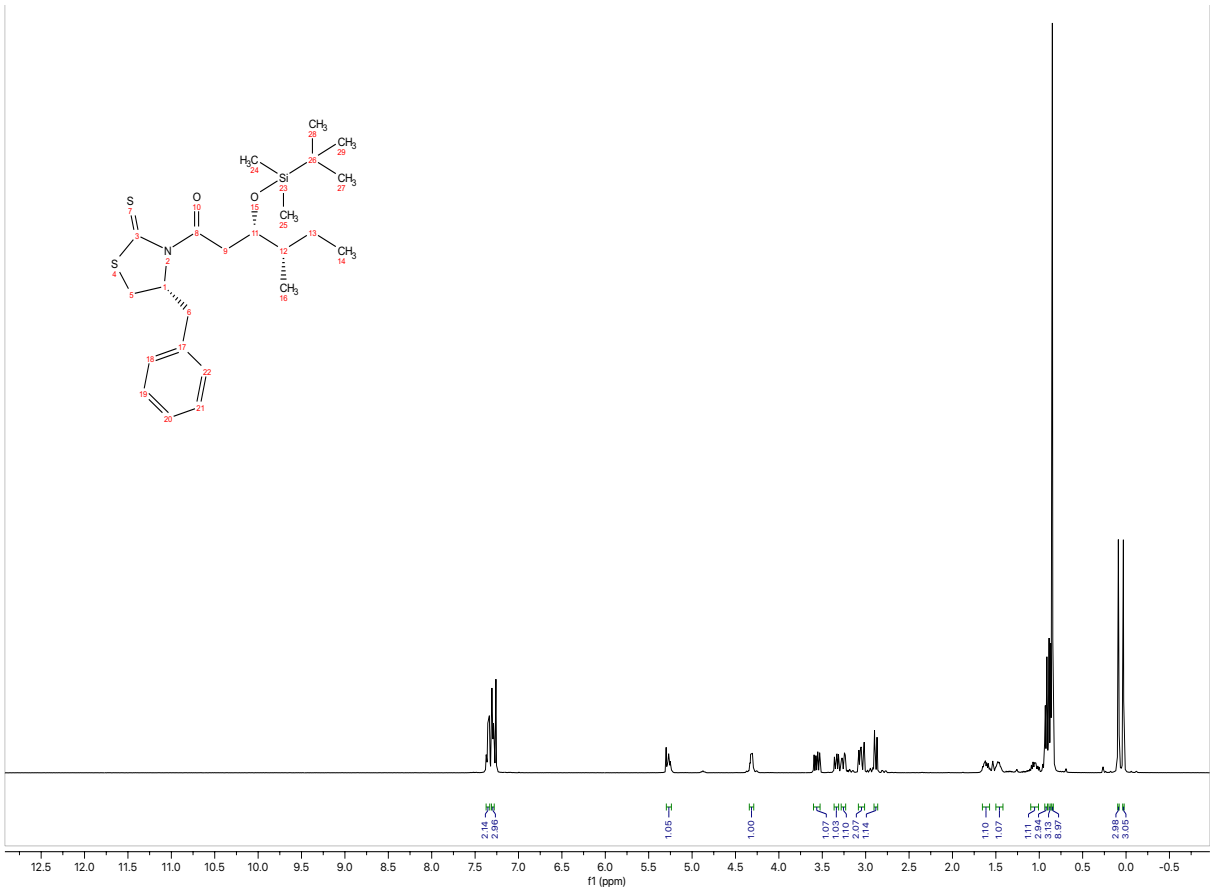
167 **141**

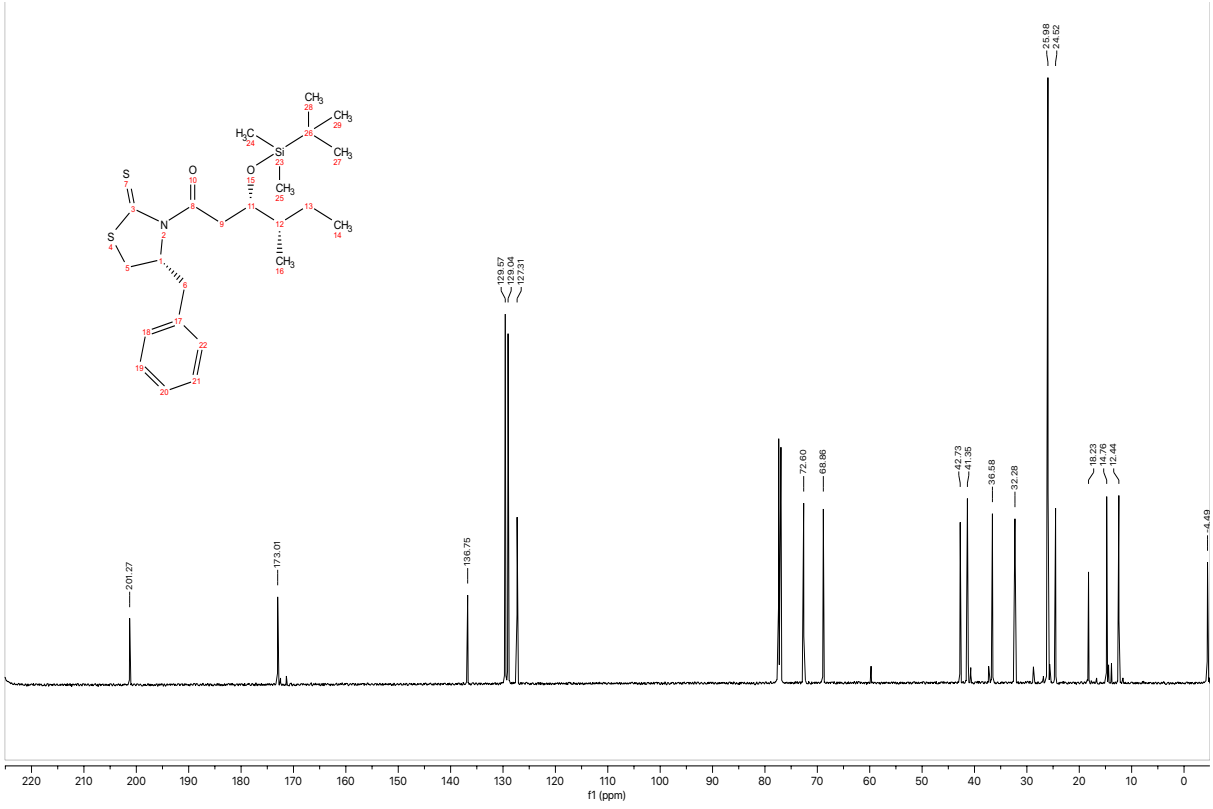
In a flame dried RBF, compound **167** (0.0688 g, 0.204 mmol, 1 eq.), was dissolved in anhydrous CH_2Cl_2 (2.04 mL, 0.1M) under an Ar atmosphere and cooled to 0 °C. Next, TBSOTf (0.094 mL, 0.408 mmol, 2 eq.) followed by NEt_3 (0.114 mL, 0.815 mmol, 4 eq.) was added and left to stir overnight while the temperature was brought to rt gradually. The reaction was quenched with a sat'd $NH_4Cl_{(aq)}$ solution, extracted with CH_2Cl_2 (x3), the combined organic layers were dried over anhydrous Na_2SO_4 and concentrated under reduced pressure. The crude material was subjected to flash silica column chromatography (1:9 EtOAc: hexane) to afford **141** as bright yellow crystals (0.0921 g, quantitative yield). ^{1}H NMR (400 MHz, $CDCl_3$) δ 7.37 – 7.33 (m, 2H), 7.31 – 7.28 (m, 3H), 5.27 (qd, *J* = 7.0, 3.5 Hz, 1H), 4.32 (dt, *J* = 8.6, 3.1 Hz, 1H), 3.56 (dd, *J* = 17.0, 8.6 Hz, 1H), 3.34 (dd, *J* = 11.5, 7.1 Hz, 1H), 3.26 (dd, *J* = 13.0, 3.9 Hz, 1H), 3.08 – 3.01 (m, 2H), 2.88 (d, *J* = 11.5 Hz, 1H), 1.62 (ddd, *J* = 12.6, 7.4, 4.5 Hz, 1H), 1.50 – 1.42 (m, 1H), 1.10 – 1.01 (m, 1H), 0.92 (d, *J* = 7.4 Hz, 3H), 0.88 (d, *J* = 6.9 Hz, 3H), 0.85 (s, 9H), 0.09 (s, 3H), 0.03 (s, 3H). ^{13}C NMR (151 MHz, $CDCl_3$) δ 201.27, 173.01, 136.75, 129.57, 129.04, 127.31, 72.60, 68.86, 42.73, 41.35, 36.58, 32.28, 25.98, 24.52, 18.23, 14.76, 12.44, -4.49.

Notebook entries:

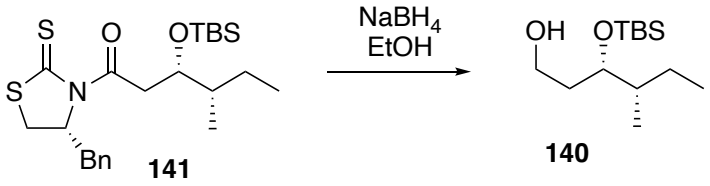
Procedure: SSP2-136

^{1}H NMR and ^{13}C NMR: SSP2-221


f1 (ppm)


201.27
173.01
136.75
129.67
129.04
127.31
72.60
68.86
42.73
41.35
36.58
32.28
25.98
24.52
18.23
14.76
12.44
4.49
f1 (ppm)

(3*S*,4*S*)-3-((*tert*-butyldimethylsilyl)oxy)-4-methylhexan-1-ol (140)

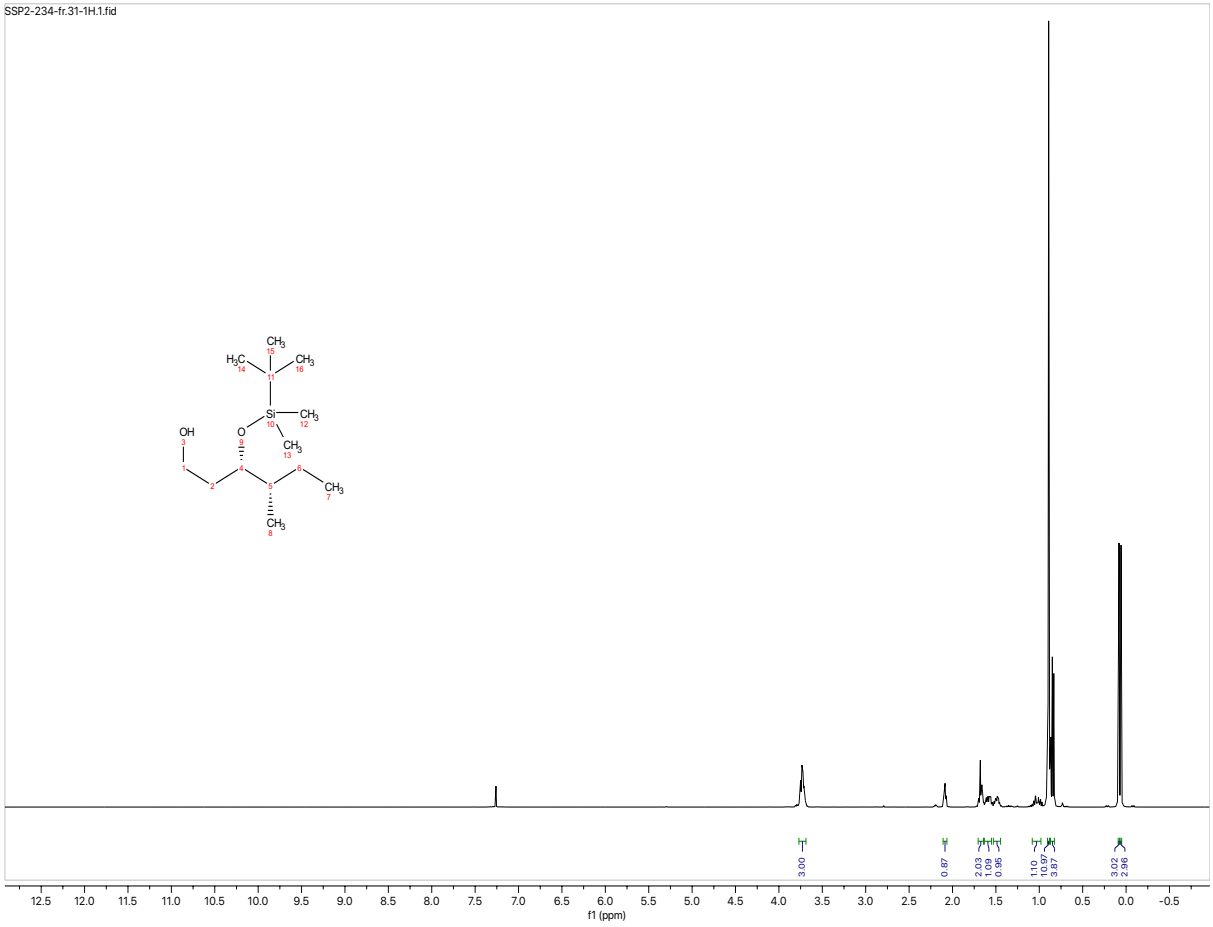


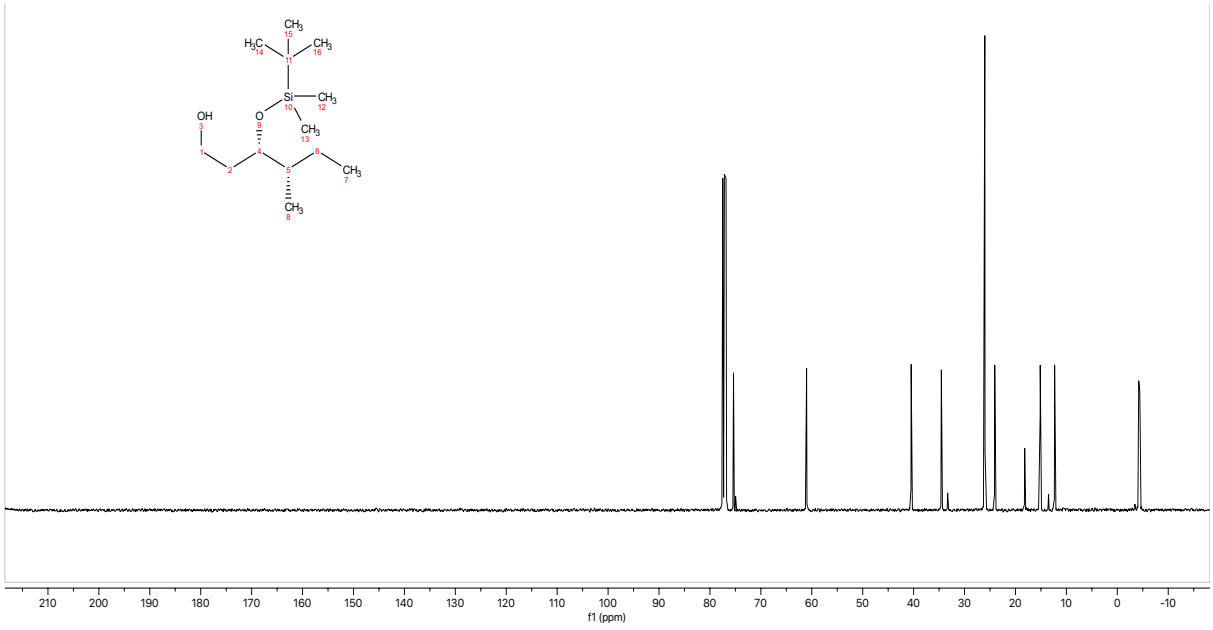
In a flame dried RBF, compound **141** (0.578 g, 1.28 mmol, 1 eq.) was dissolved in anhydrous EtOH (dried over MS) (7.5 mL, 0.17M) under an Ar atmosphere and cooled to 0 °C. Next, $NaBH_4$ (0.0968 g, 2.56 mmol, 2 eq.) was added portion wise and stirred the reaction at rt until yellow color of the reaction disappear. The RBF was cooled to 0 °C and quenched with a sat'd $NH_4Cl_{(aq)}$ solution (addition was done dropwise) and extracted with CH_2Cl_2 (x3). The combined organic layers were dried over anhydrous Na_2SO_4 and concentrated under reduced pressure at rt. The crude compound was purified via flash silica column chromatography (1:6 EtOAc: hexane) to afford **140** as a colorless oil (0.302 g, 96% yield). ^{1}H NMR (400 MHz, $CDCl_3$) δ 3.78 – 3.68 (m, 3H), 2.09 (t, J = 5.1 Hz, 1H), 1.67 (q, 2H), 1.63 – 1.55 (m, 1H), 1.53 – 1.44 (m, 1H), 1.08 – 0.95 (m, 1H), 0.91 – 0.88 (m, 11H), 0.85 (t, J = 7.1 Hz, 4H), 0.08 (s, 3H), 0.06 (s, 3H). ^{13}C NMR (101 MHz, $CDCl_3$) δ 75.37, 61.02, 40.48, 34.56, 26.02, 24.07, 18.19, 15.14, 12.31, -4.20, -4.42.

Notebook entries:

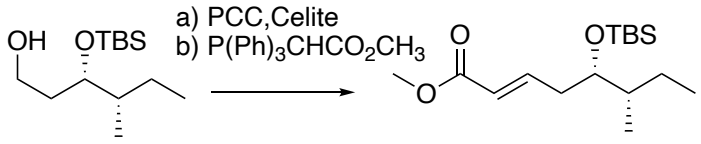
Procedure: SSP2-234

^{1}H NMR and ^{13}C NMR: SSP2-234


SSP2-234-fr.31-1H.1.fid
3.00
0.87
2.03
1.09
0.95
1.10
10.97
3.87
3.02
2.96
f1 (ppm)


f1 (ppm)

Methyl (5*S*,6*S*,*E*)-5-((*tert*-butyldimethylsilyl)oxy)-6-methyloct-2-enoate (168)



140 **168**

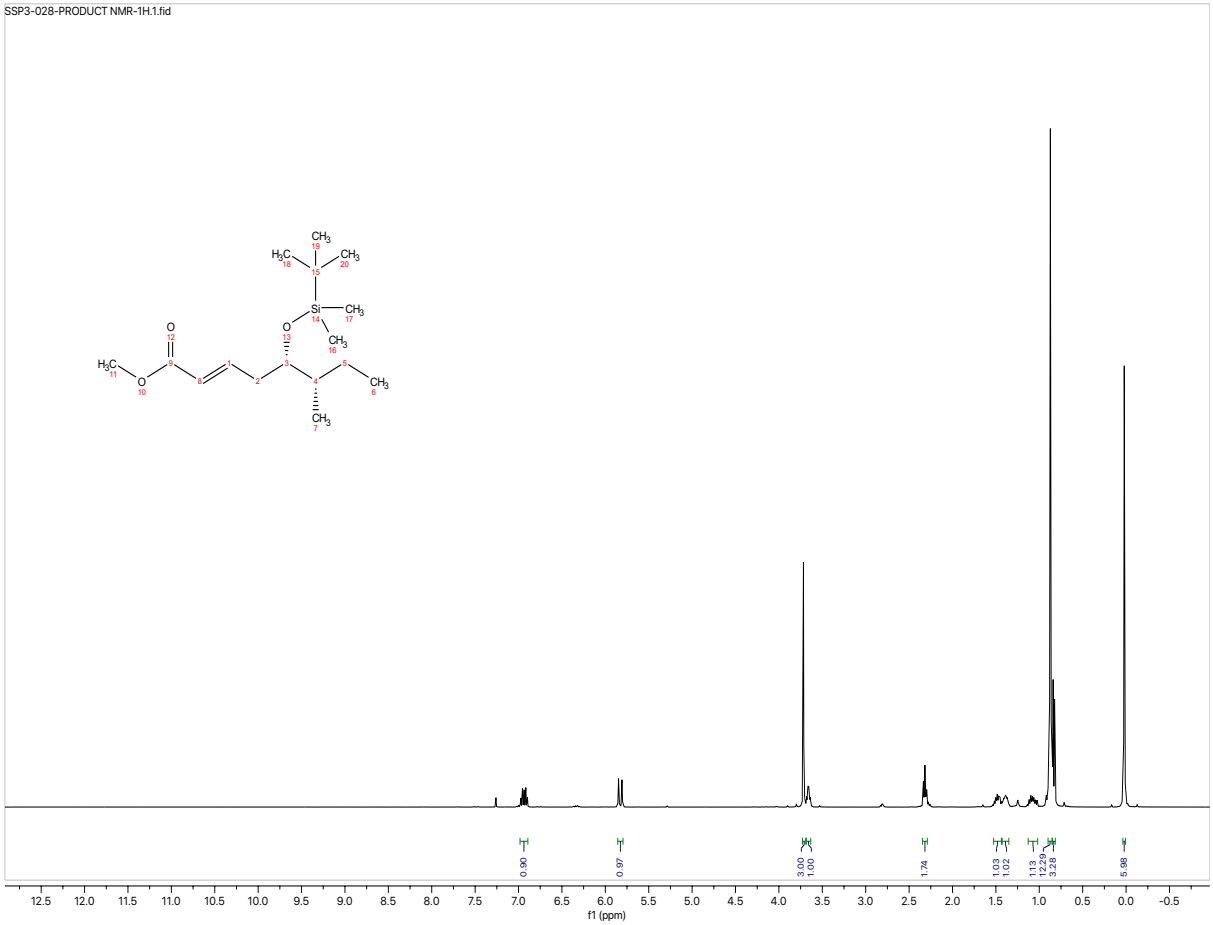
A flame dried RBF was charged with PCC (0.6826 g, 3.17 mmol, 1.5 eq.), celite (0.6826 g, 1:1 mass ratio with PCC), and anhydrous CH_2Cl_2 (5.86 mL, 0.36M) under an Ar atmosphere. Next, alcohol **140** (0.5203 g, 2.11 mmol, 1 eq.) was added dropwise to the stirring mixture and continued stirring for 2 h. Methyl (triphenylphosphoranylidene)acetate (1.2 g, 3.59 mmol, 1.7 eq.) was introduced to the reaction and allowed to stir overnight. The reaction was filtered through a fritted Buchner filter funnel under vacuum. The collected filtrate was concentrated under reduced pressure at rt and subjected to flash silica column chromatography (gradient elution; 100% hexane, 1:9 EtOAc: hexane, 1:6 EtOAc: hexane; 1:4 EtOAc: hexane) to afford **168** as a colorless oil over 2 steps (0.548 g, 86% yield). ^{1}H NMR (400 MHz, $CDCl_3$) δ 6.94 (dt, *J* = 15.4, 7.6 Hz, 1H), 5.83 (d, *J* = 1.5 Hz, 1H), 3.72 (s, 3H), 3.66 (td, *J* = 6.2, 3.6 Hz, 1H), 2.31 (t, *J* = 3.2 Hz, 2H), 1.48 (dq, *J* = 12.7, 4.7 Hz, 1H), 1.43 – 1.35 (m, 1H), 1.13 – 1.02 (m, 1H), 0.87 (s, 12H), 0.83 (d, *J* = 6.8 Hz, 3H), 0.02 (s, 6H). ^{13}C NMR (101 MHz, $CDCl_3$) δ 167.01, 147.10, 122.66, 74.84, 51.51, 40.20, 37.29, 25.97, 25.36, 18.23, 13.92, 12.20, -4.19, -4.45.

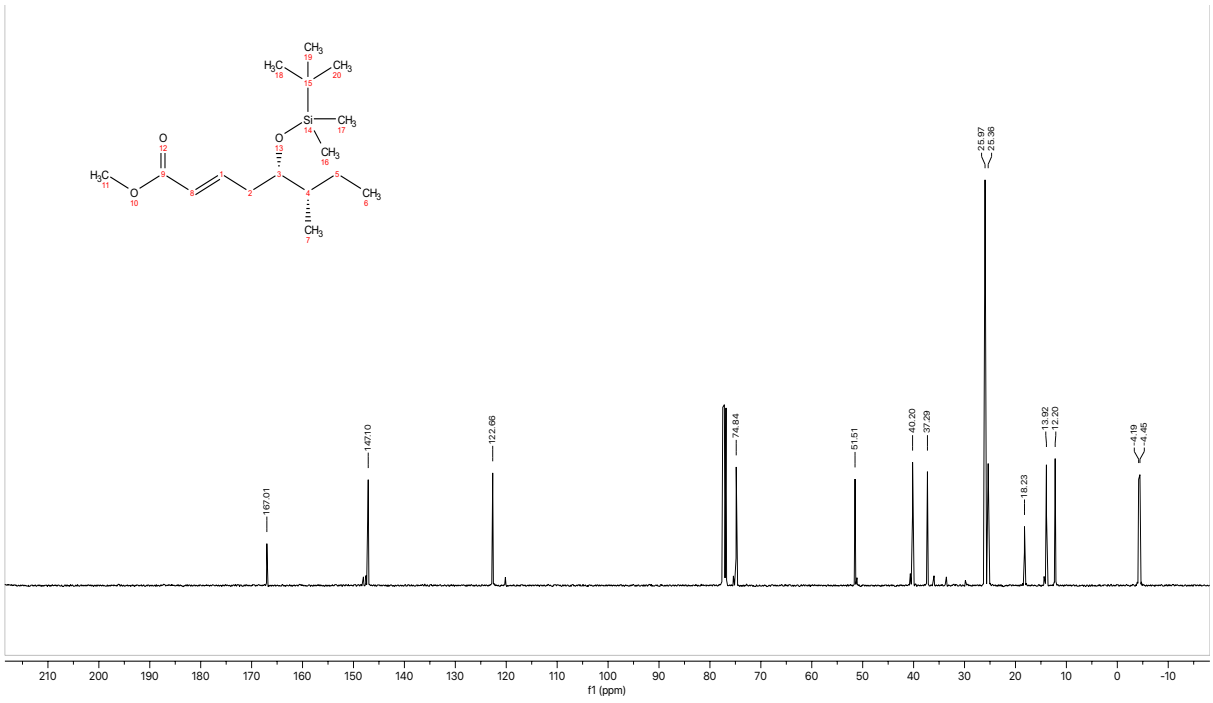
Notebook entries:

Procedure: SSP2-327

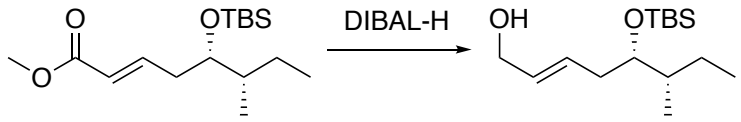
^{1}H NMR and ^{13}C NMR: SSP3-028

SSP3-028-PRODUCT NMR-1H.1.fid





(5*S*,6*S*,*E*)-5-((*tert*-butyldimethylsilyl)oxy)-6-methyloct-2-en-1-ol (139)



168 **139**

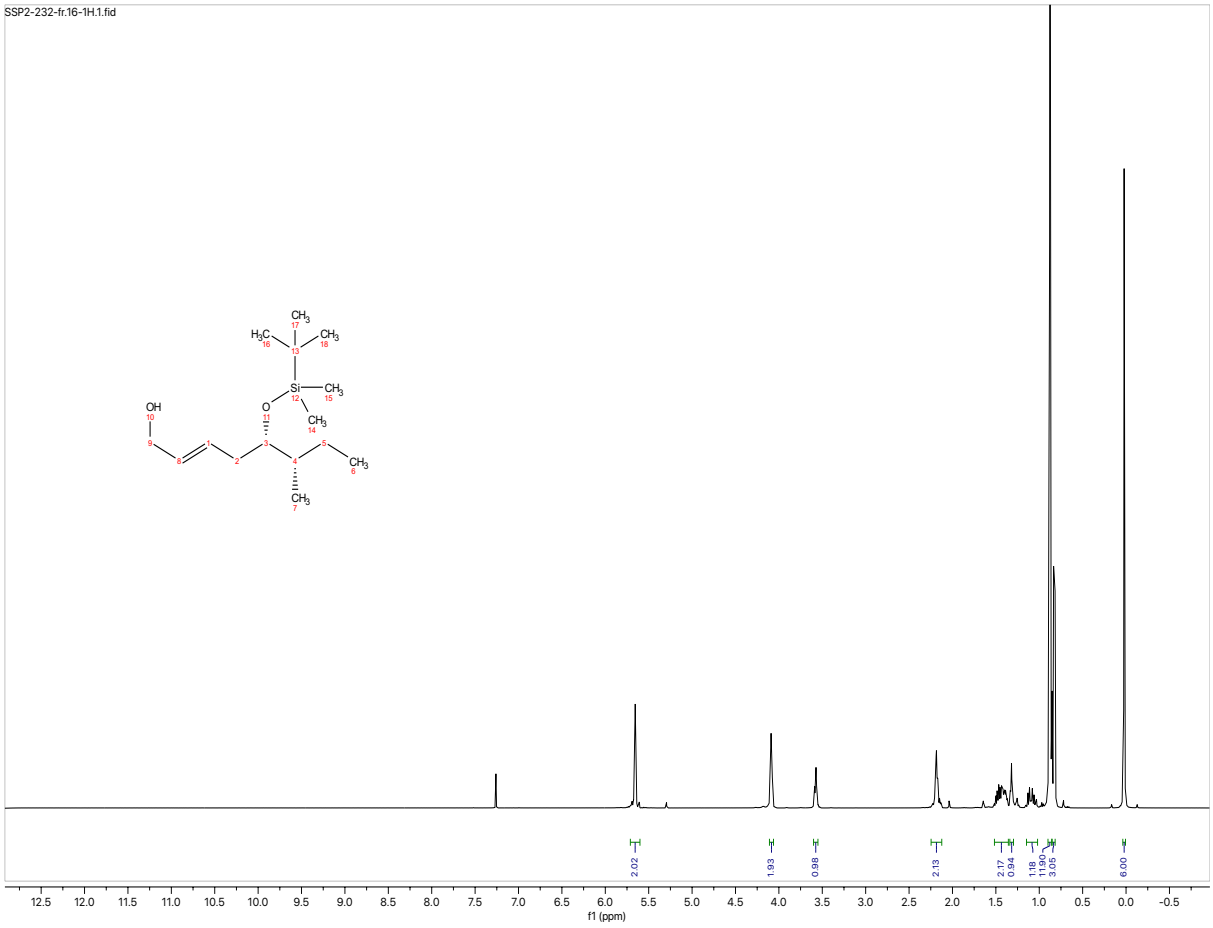
In a flame dried RBF, compound **168** (0.3433 g, 1.14 mmol, 1 eq.), was dissolved in anhydrous THF (5.7 mL, 0.2M) and cooled to -78 °C. A freshly prepared solution of DIBAL-H (1M in THF, 2.9 mL, 2.86 mmol, 2.5 eq.) was added under an Ar atmosphere and stirred overnight while temperature was allowed to reach to rt gradually. The reaction was then cooled to 0 °C, quenched with a dropwise addition of sat'd aqueous solution of Rochelle's salt, stirred at rt overnight, and extracted with CH_2Cl_2 (x3). The ombined organic layers were dried over anhydrous Na_2SO_4 and concentrated under reduced pressure at rt. The crude material was subjected to flash silica column chromatography (1:6 EtOAc: hexane) to access **139** as a colorless oil (0.262 g, 84% yield).

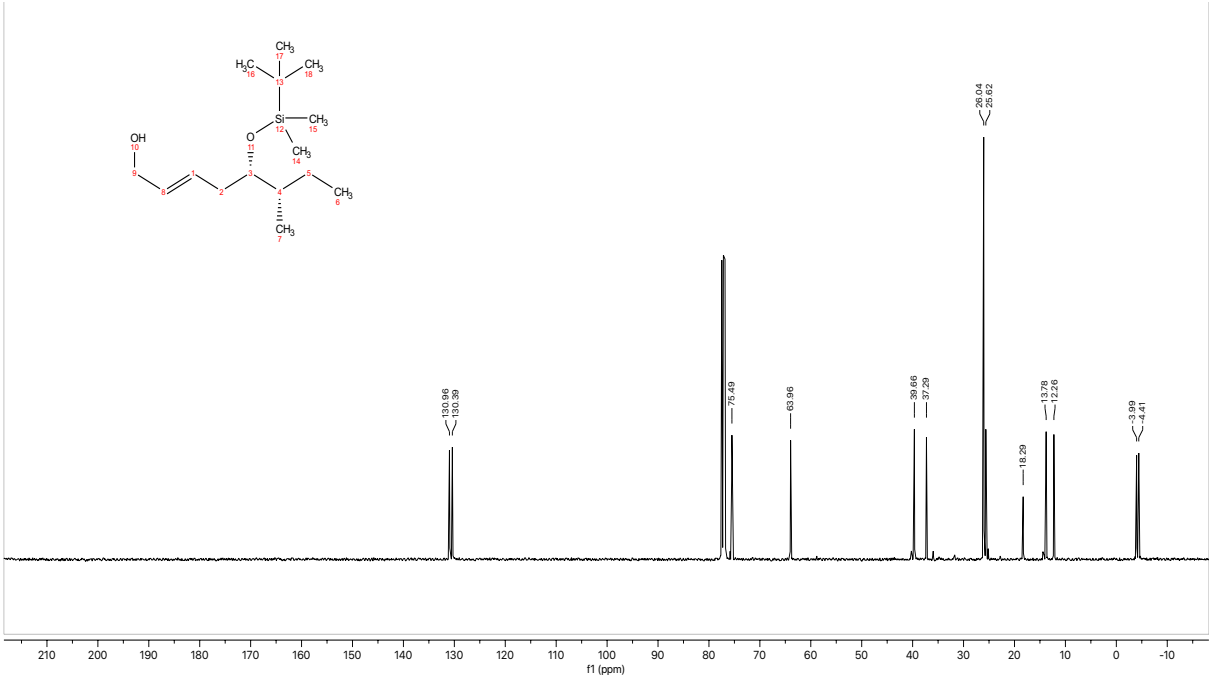
^{1}H NMR (400 MHz, $CDCl_3$) δ 5.71 – 5.60 (m, 2H), 4.08 (d, *J* = 4.5 Hz, 2H), 3.58 (td, *J* = 6.2, 3.5 Hz, 1H), 2.25 – 2.12 (m, 2H), 1.52 – 1.36 (m, 2H), 1.34 – 1.30 (m, 1H), 1.16 – 1.02 (m, 1H), 0.87 (d, *J* = 3.5 Hz, 12H), 0.85 – 0.82 (m, 3H), 0.02 (d, *J* = 1.1 Hz, 6H). ^{13}C NMR (101 MHz, $CDCl_3$) δ 130.96, 130.39, 75.49, 63.96, 39.66, 37.29, 26.04, 25.62, 18.29, 13.78, 12.26, -3.99, -4.41.

Notebook entries:

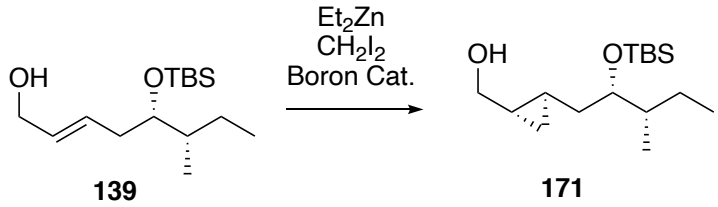
Procedure: SSP2-352

^{1}H NMR and ^{13}C NMR: SSP2-232


SSP2-232-fr.16-1H.1.fid
2.02
1.93
0.98
2.13
2.17
0.94
1.18
1.90
3.05
6.00
f1 (ppm)


130.96
130.39
75.49
63.96
39.66
37.29
26.04
25.62
18.29
13.78
12.26
-3.99
-4.41
f1 (ppm)

((1*S*,2*R*)-2-((2*S*,3*S*)-2-((*tert*-butyldimethylsilyl)oxy)-3-methylpentyl)cyclopropyl)methanol (171)



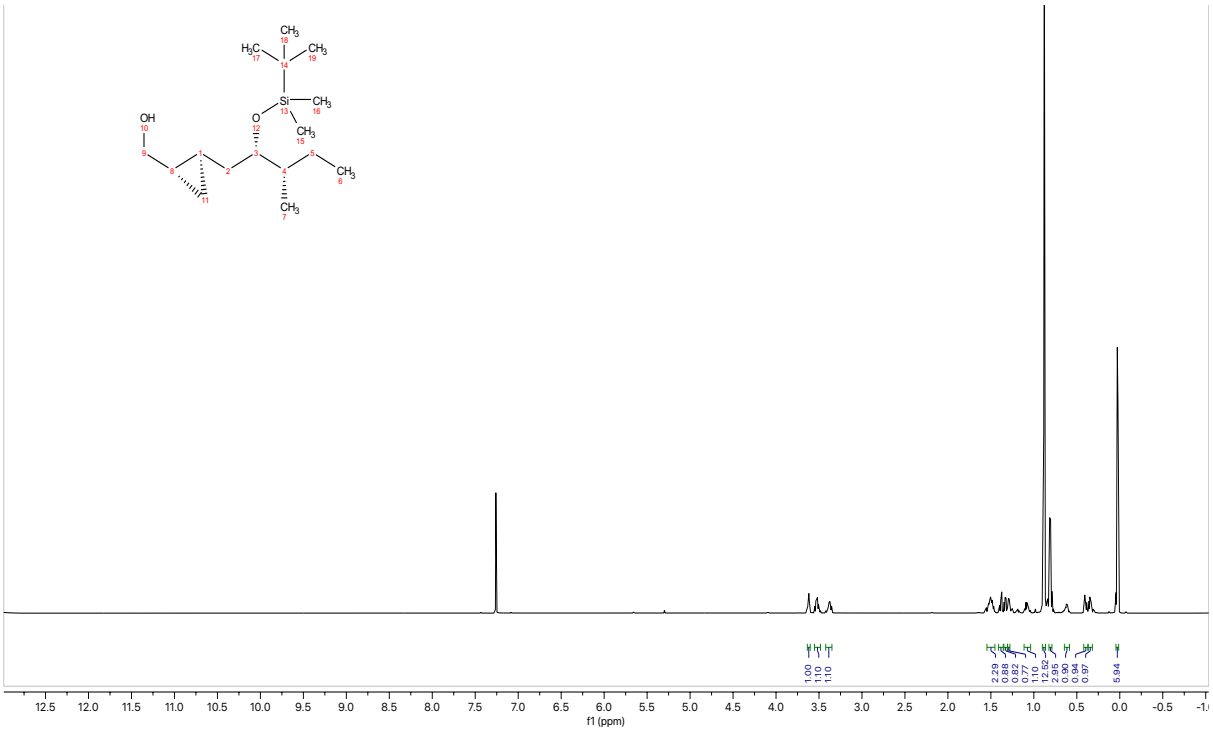
139 **171**

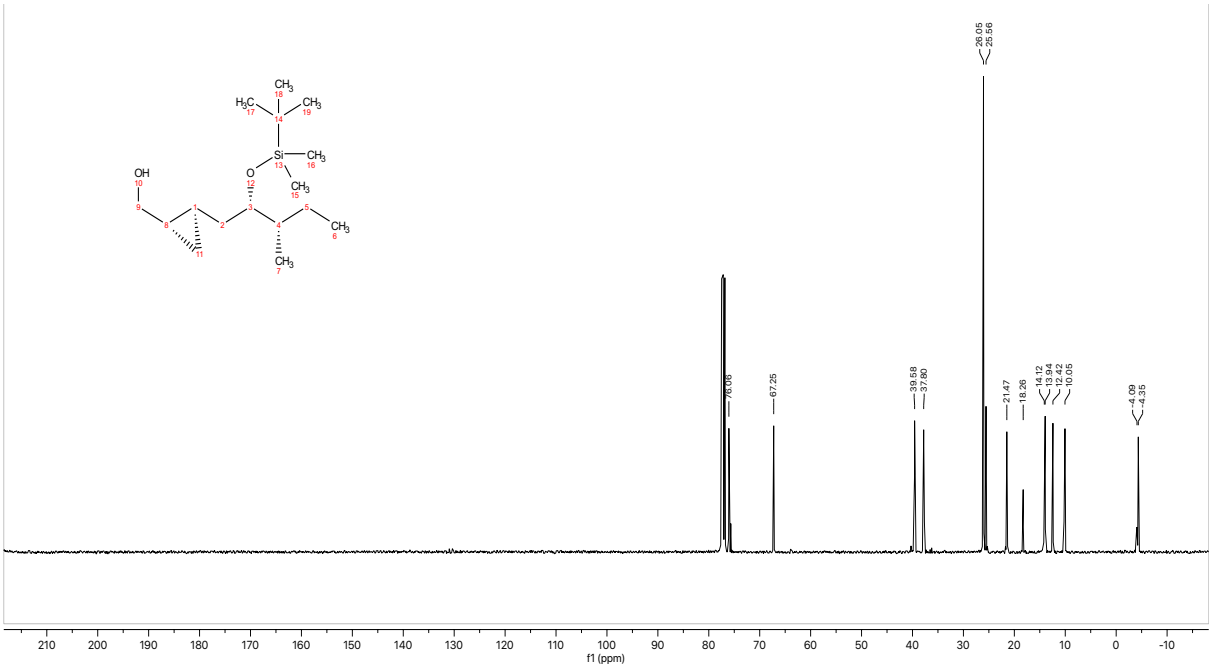
A flame dried RBF (A) was charged with anhydrous CH_2Cl_2 (2.84 mL, 0.1M), MS, freshly prepared 1M solution of Et_2Zn in THF (2.84 mL, 2.84 mmol, 10 eq.) under an Ar atmosphere, and cooled to 0 °C, CH_2I_2 (0.46 mL, 5.69 mmol, 20 eq.) was added dropwise, and stirred for 15 minutes. A second flame dried RBF (B) was charged with compound **139** (77.5 mg, 0.284 mmol, 1 eq.), anhydrous CH_2Cl_2 (2.84 mL, 0.1M), and MS. Next (4*R*,5*R*)-2-butyl-N^4,N^4,N^5,N^5-tetramethyl-1,3,2-dioxaborolane-4,5- dicarboxamide (0.086 mL, 0.341 mmol, 1.2 eq.) was added and stirred the solution for 15 minutes under an Ar atmosphere at rt. Then the flask B was cooled to 0 °C, transferred to flask A at 0 °C, and stirred while allowing to warm to rt overnight. The resulting mixture was quenched with a sat'd aqueous solution of NH_4Cl (until the emulsion were broken), extracted with CH_2Cl_2 (x3), the combined organic layers were dried with Na_2SO_4, and concentrated under reduced pressure at rt. The crude material was then purified via flash column chromatography (1:6 EtOAc:hexane) to produce a colorless oil, **171** (0.076 g, 93% yield, *dr* 6.7:1). ^{1}H NMR (600 MHz, $CDCl_3$) δ 3.62 (td, *J* = 6.2, 3.1 Hz, 1H), 3.52 (m, *J* = 14.2, 6.3 Hz, 1H), 3.42 – 3.35 (m, 1H), 1.55 – 1.45 (m, 2H), 1.41 – 1.25 (m, 3H), 1.12 – 1.04 (m, 1H), 0.88 (d, *J* = 3.3 Hz, 12H), 0.86 – 0.79 (m, 4H), 0.64 – 0.59 (m, 1H), 0.40 (dt, *J* = 8.8, 4.7 Hz, 1H), 0.34 (dt, *J* = 8.2, 4.8 Hz, 1H), 0.03 (d, *J* = 4.9 Hz, 6H). ^{13}C NMR (101 MHz, $CDCl_3$) δ 76.06, 67.25, 39.58, 37.80, 26.05, 25.56, 21.47, 18.26, 14.12, 13.94, 12.42, 10.05, -4.09, -4.35.

Notebook entries:

Procedure: SSP2-206

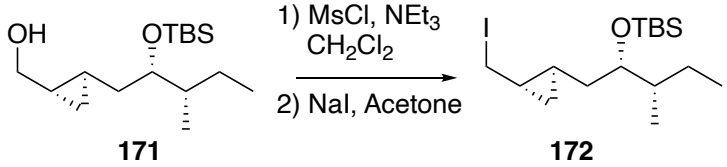
^{1}H NMR and ^{13}C NMR: SSP3-029





***Tert*-butyl(((2*S*,3*S*)-1-((1*R*,2*S*)-2-(iodomethyl)cyclopropyl)-3-methylpentan-2-yl)oxy)dimethylsilane (172)**

Method A



171 **172**

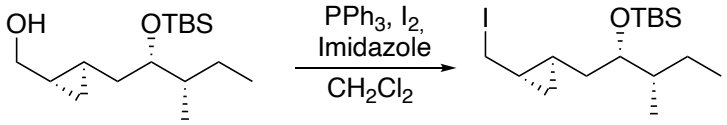
In a FDRBF alcohol **171** (0.1068 g, 0.373 mmol, 1 eq.) was dissolved in anhydrous CH_2Cl_2 (2.48 mL, 0.15M) under an Ar atmosphere, and MS were added. The mixture was cooled the RBF to 0 °C, MsCl (0.05 mL, 0.634 mmol, 1.7 eq.) followed NEt_3 (0.16 mL, 1.12 mmol, 3 eq.) were added and stirred at 0 °C for 15 minutes followed by at rt for 15 minutes. The reaction mixture was concentrated under reduced pressure at rt. The resulting crude mixture was dissolved in anhydrous acetone (dried over MS, 2.48 mL, 0.15 M) and $NaI_{(S)}$ (0.503 g, 3.35 mmol, 9 eq.) was added under an Ar atmosphere at rt. Stirred the reaction for 1 h and quenched with a sat'd solution mixture of $NaHCO_3$: $Na_2S_2O_3$(1:1). Quenched reaction was extracted with CH_2Cl_2 (x3), dried with anhydrous Na_2SO_4, and concentrated under reduced pressure at rt. The crude material was then purified via flash column chromatography (1:9 CH_2Cl_2:hexane) to obtain **172** as a colorless oil (0.132 g, 89% yield). ^{1}H NMR (600 MHz, $CDCl_3$) δ 3.63 (td, *J* = 6.3, 3.1 Hz, 1H), 3.24 (dd, *J* = 9.7, 7.3 Hz, 1H), 3.15 (d, *J* = 7.8 Hz, 0H), 3.06 (dd, *J* = 9.7, 8.3 Hz, 1H), 1.55 – 1.45 (m, 2H), 1.42 – 1.25 (m, 2H), 1.12 – 1.01 (m, 2H), 0.88 (d, *J* = 3.3 Hz, 12H), 0.80 (t, *J* = 7.5 Hz, 3H), 0.75 – 0.68 (m, 1H), 0.65 – 0.60 (m, 1H), 0.45 (dt, *J* = 9.1, 4.6 Hz, 1H), 0.03 (s, 6H). ^{13}C NMR (151 MHz, $CDCl_3$) δ 75.82, 39.73, 38.02, 26.06, 25.38, 23.51, 22.78, 18.25, 17.94, 13.95, 13.92, 12.45, -3.96, -4.30.

Notebook entries:

Procedure: SSP2-211

^{1}H NMR and ^{13}C NMR: SSP3-032

Method B



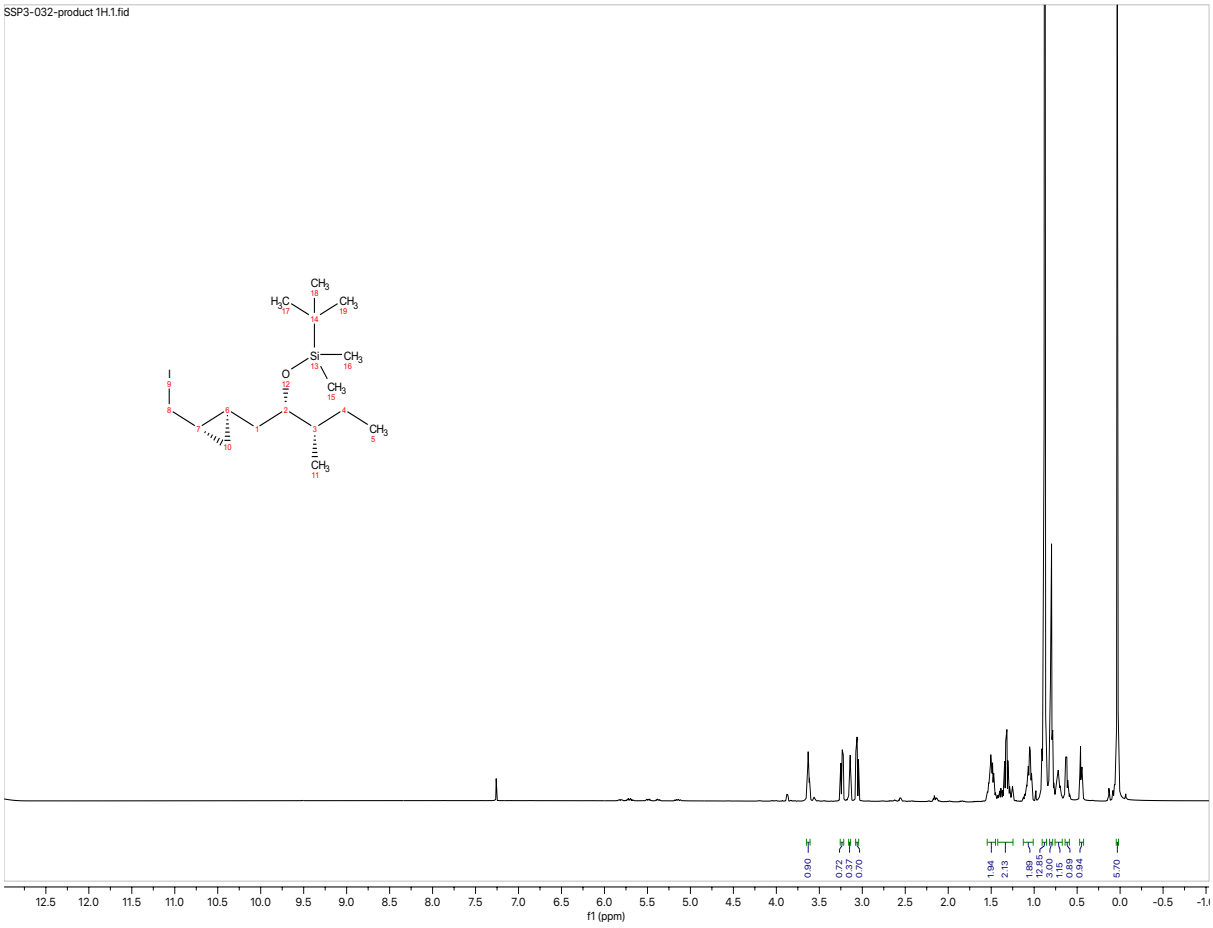
171 **172**

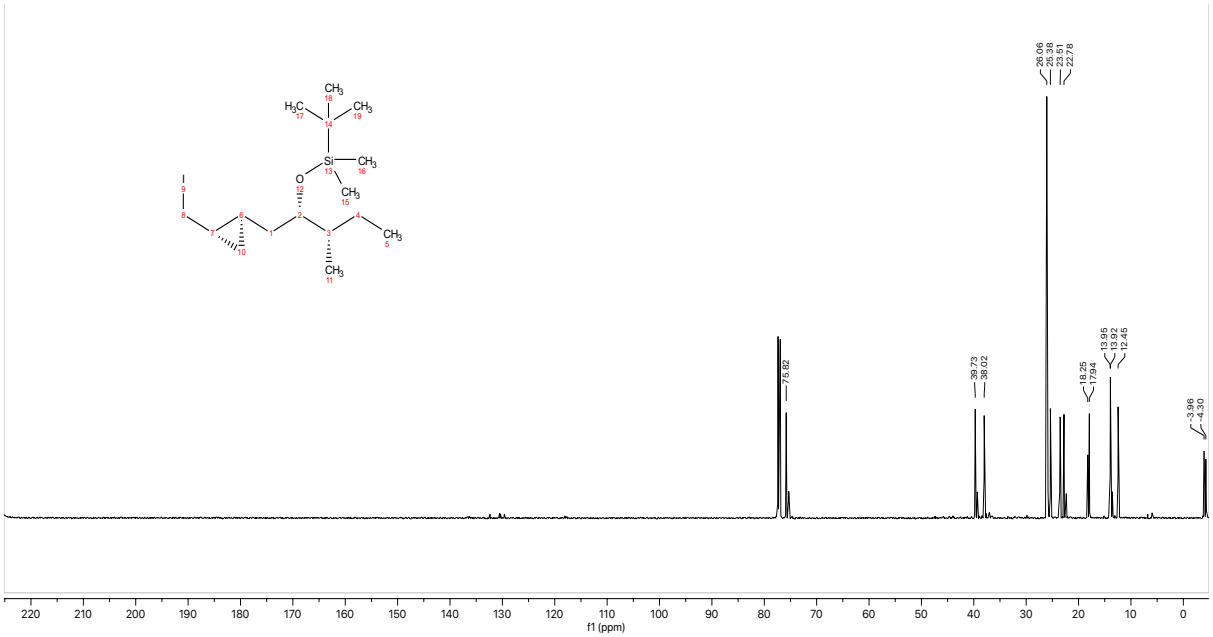
In a flame dried RBF, PPh_3 (0.107 g, 0.408 mmol, 2 eq.) was dissolved in anhydrous CH_2Cl_2 (4.1 mL, 0.05M) under Ar and cooled to 0 °C followed by addition of I_2 (0.104 g, 0.408 mmol, 2 eq.) and Imidazole (0.042 g, 0.613 mmol, 3 eq.). The reaction was stirred for 15 minutes at rt, added the alcohol **171** (0.0585 g, 0.204 mmol, 1 eq.), and stirred for 1 h. Quenched the reaction with a sat'd solution of $Na_2S_2O_{3(aq)}$, resulting mixture was stirred until yellow color disappeared, extracted with CH_2Cl_2 (x3), combined organic layers were dried over anhydrous Na_2SO_4 and concentrated under reduced pressure at rt. The crude compound was purified by flash silica column chromatography (gradient elution: 1:30 EtOAc: hexane, 1:20 EtOAc: hexane, 1:9 EtOAc: hexane) to access **172** as a colorless oil (0.0723 g, 89% yield).

Notebook entries:

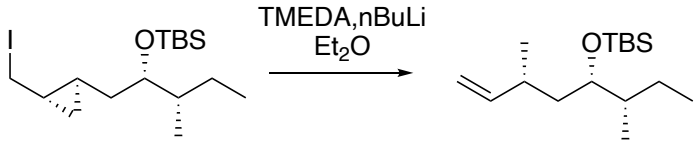
Procedure: SSP3-039

^{1}H NMR: SSP3-039


SSP3-032-product 1H.1.fid
0.90
0.72
0.37
0.70
1.94
2.13
1.89
12.85
3.00
1.15
0.89
0.94
5.70
f1 (ppm)


26.06
25.38
25.15
22.78
75.62
39.73
38.02
18.25
17.94
13.95
13.92
12.45
-3.96
-4.80
f1 (ppm)

***Tert*-butyl(((3*S*,4*S*,6*R*)-3,6-dimethyloct-7-en-4-yl)oxy)dimethylsilane (138)**



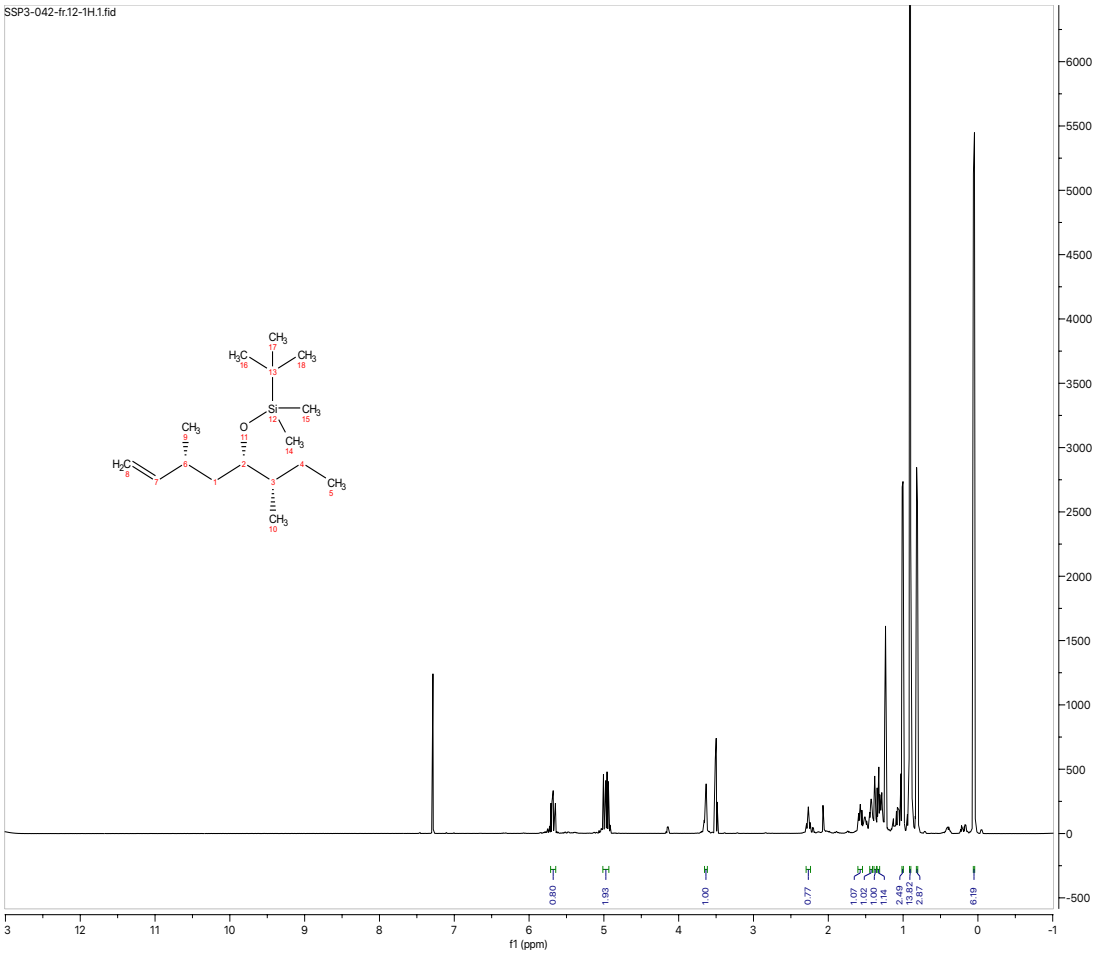
172 **138**

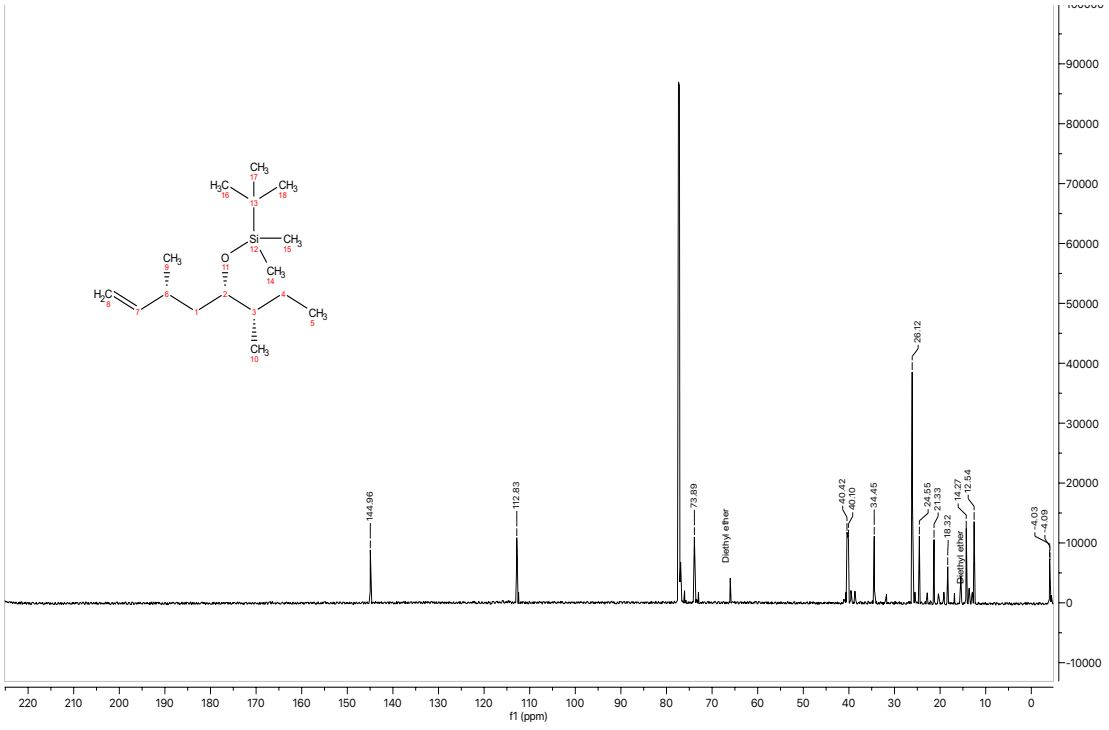
A flame dried RBF was charged with compound **172** (0.4999 g, 1.26 mmol, 1 eq.), anhydrous Et_2O (12.6 mL, 0.1M) followed by MS under an Ar atmosphere, cooled the RBF to -78 °C, and TMEDA (0.38 mL, 2.52 mmol, 2 eq.) followed by 1.15M nBuLi in hexanes (2.2 mL, 2.52 mmol, 2 eq.) was added dropwise. The reaction was stirred for 1 h at -78 °C and quenched with DI H_2O (1 eq. by volume). The reaction was gradually brought to rt, extracted with Et_2O (x3), the combined organic layers were dried over anhydrous Na_2SO_4 and concentrated under reduced pressure at rt. The crude material was subjected to flash silica column chromatography (1:3 heptane: hexane or 100% hexane) to access **138** as a colorless oil (0.3027 g, 89% yield). ^{1}H NMR (600 MHz, $CDCl_3$) δ 5.65 (ddd, *J* = 17.3, 10.3, 7.7 Hz, 1H), 4.99 – 4.91 (m, 2H), 3.61 (ddd, *J* = 7.7, 4.7, 3.0 Hz, 1H), 2.27 – 2.21 (m, 1H), 1.58 – 1.52 (m, 1H), 1.42 – 1.38 (m, 1H), 1.36 – 1.33 (m, 1H), 1.32 – 1.29 (m, 1H), 0.98 (d, *J* = 6.9 Hz, 2H), 0.88 (d, *J* = 3.0 Hz, 14H), 0.79 (d, *J* = 6.9 Hz, 3H), 0.03 (d, *J* = 8.5 Hz, 6H). ^{13}C NMR (151 MHz, $CDCl_3$) δ 144.96, 112.83, 73.89, 40.42, 40.10, 34.45, 26.12, 24.55, 21.33, 18.32, 14.27, 12.54, -4.03, -4.09.

Notebook entries:

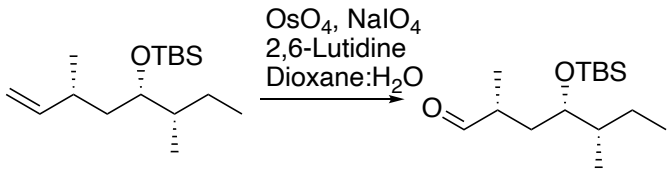
Procedure: SSP2-252

^{1}H NMR and ^{13}C NMR: SSP3-042


SSP3-042-fr.12-1H.1.fid
f1 (ppm)


144.96
112.83
73.89
Diethyl ether
40.42
40.10
34.45
26.12
24.55
21.33
18.32
Diethyl ether
14.27
12.54
-4.03
-4.09
f1 (ppm)

(2*R*,4*S*,5*S*)-4-((*tert*-butyldimethylsilyl)oxy)-2,5-dimethylheptanal (S1)



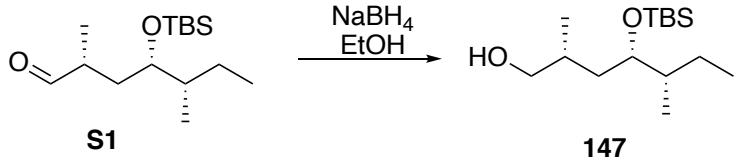
138 **S1**

Alkene **138** (0.161 g, 0.595 mmol, 1 eq.) was dissolved in a 3:1 mixture of Dioxane: DI H_2O (0.13M, 4.6 mL). Next 2,6-lutidine (0.09 mL, 0.774 mmol, 1.3 eq.) followed by OsO_4 4 wt.% in H_2O (0.756 mL, 0.12 mmol, 0.2 eq.) was added and stirred the reaction for 20 minutes (reaction turned black). Then $NaIO_4$ (0.293 g, 1.4 mmol, 2.3 eq.) was added and continued stirring overnight. The reaction that has turned into an off-white slurry was quenched with a sat'd aqueous solution of $Na_2S_2O_3$, extracted with Et_2O (x3), the combined organic layers were dried over anhydrous Na_2SO_4 and concentrated under reduced pressure at rt. The crude material was carried forward to the next step without further purification.

Notebook entries:

Procedure: SSP2-264

(2*R*,4*S*,5*S*)-4-((*tert*-butyldimethylsilyl)oxy)-2,5-dimethylheptan-1-ol (147)



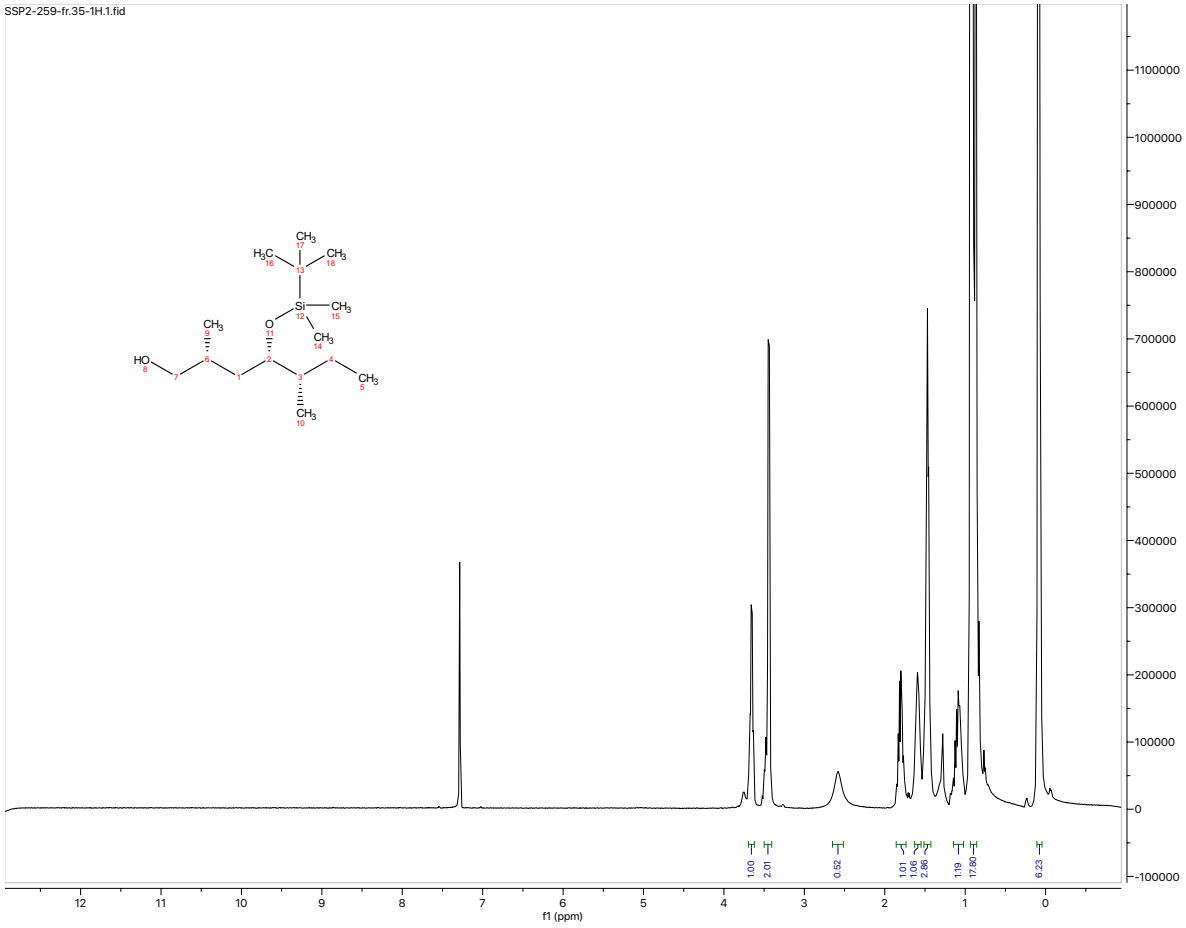
S1 **147**

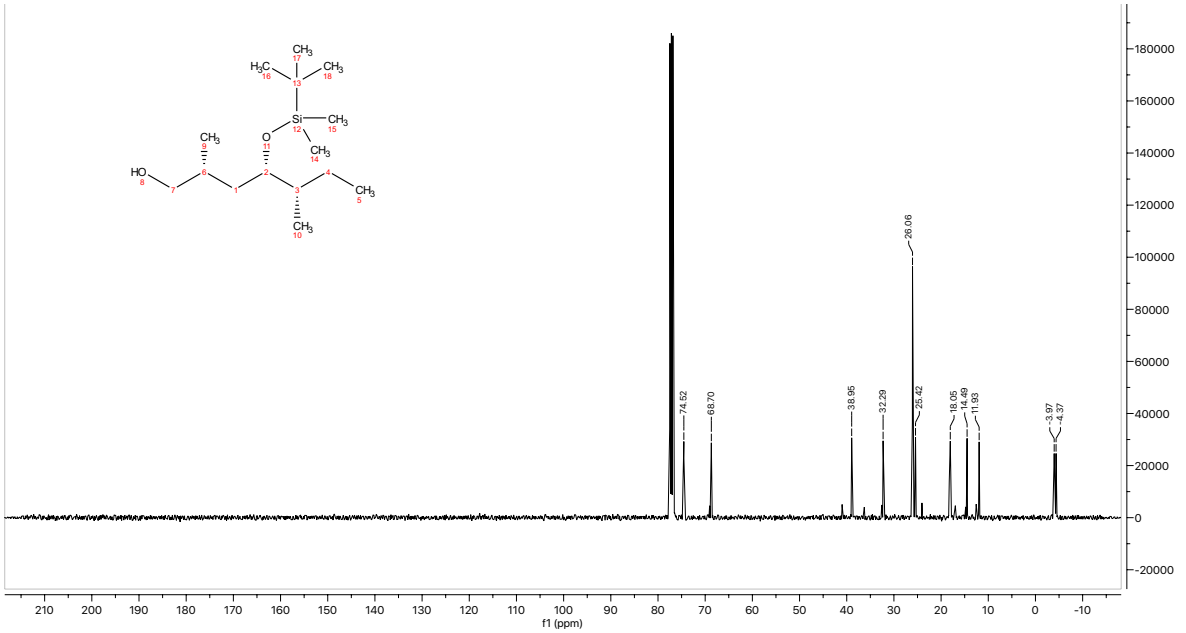
Aldehyde **S1** (0.256 g, 0.94 mmol, 1 eq..), was dissolved in anhydrous EtOH (dried over MS) (5.53 mL, 0.17M) under an Ar atmosphere and cooled to 0 °C. Next, $NaBH_4$ (0.088 g, 2.35 mmol, 2.5 eq.) was added portion wise and stirred the reaction for 2 h at rt. The RBF was cooled to 0 °C, quenched with a sat'd $NH_4Cl_{(aq)}$ solution (addition was done dropwise), extracted with CH_2Cl_2 (x3), the combined organic layers were dried over anhydrous Na_2SO_4 and concentrated under reduced pressure at rt. The crude material was purified via flash silica column chromatography (1:9 EtOAc: hexane) to afford **147** as a colorless oil (0.1022g, 40% yield over two steps). ^{1}H NMR (400 MHz, $CDCl_3$) δ 3.63 (qd, *J* = 5.6, 2.0 Hz, 1H), 3.47 – 3.38 (m, 2H), 1.79 (dt, *J* = 14.2, 7.1 Hz, 1H), 1.60 – 1.52 (m, 1H), 1.49 – 1.40 (m, 3H), 1.06 (tt, *J* = 14.7, 7.9 Hz, 1H), 0.91 – 0.83 (m, 18H), 0.06 (dd, *J* = 4.9, 1.9 Hz, 6H). ^{13}C NMR (101 MHz, $CDCl_3$) δ 74.52, 68.70, 38.95, 32.29, 26.06, 25.42, 18.05, 14.49, 11.93, -3.97, -4.37.

Notebook entries:

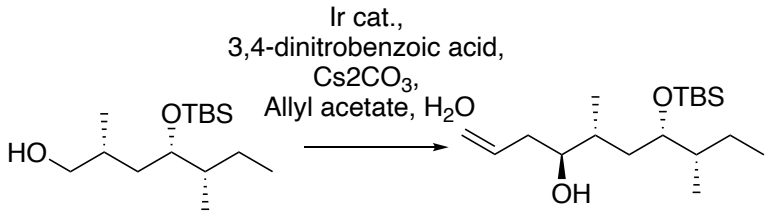
Procedure: SSP2-259

^{1}H NMR and ^{13}C NMR: SSP2- 259


SSP2-259-fr.35-1H.1.fid
1.00
2.01
0.62
1.01
1.06
2.66
1.19
17.80
6.23
f1 (ppm)


74.52
68.70
38.95
32.29
26.06
25.42
18.05
14.49
11.93
-3.97
-4.37
f1 (ppm)

(4*S*,5*R*,7*S*,8*S*)-7-((*tert*-butyldimethylsilyl)oxy)-5,8-dimethyldec-1-en-4-ol (175)



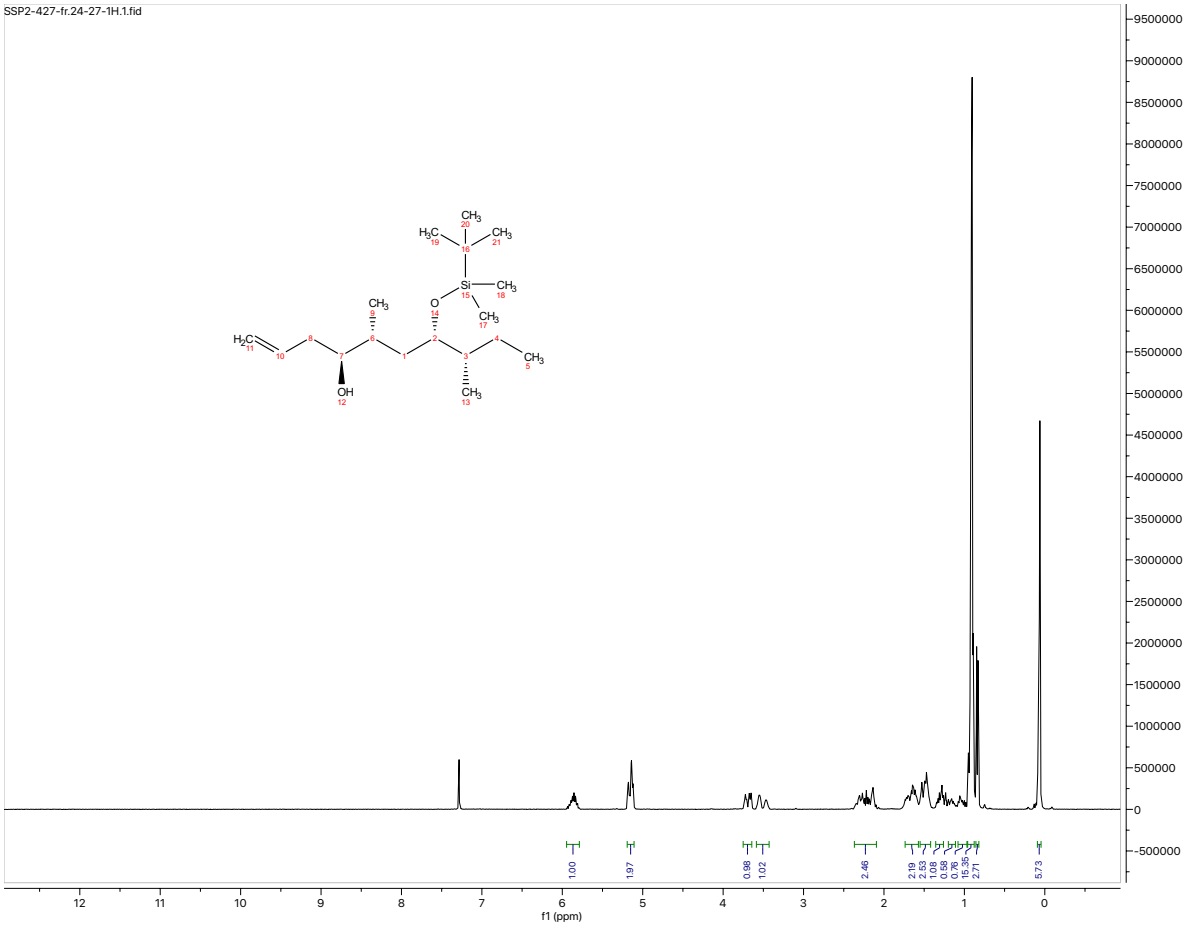
147 **175**

Alcohol **147** (0.117 g, 0.426 mmol, 1 eq.) was dissolved in anhydrous THF (~1.1 mL, 0.4M) and transferred to a pressure tube under an Ar atmosphere. Next Iridium catalyst (0.047 g, 0.0426 mmol, 0.1 eq.), 3,4 – dinitrobenzoic acid (0.009 g, 0.0426 mmol, 0.1 eq.), $CsCO_3$ (0.14 g, 0.0426 mmol, 1 eq.), allyl acetate (0.09 mL, 0.852 mmol, 2 eq.) and DI H_2O (0.08 mL, 4.26 mmol, 10 eq.) was added respectively. Cap of the pressure tube was closed tightly and stirred the reaction at 100 °C overnight. The crude reaction mixture was subjected to flash silica column chromatography (1:9 EtOAc: hexane) to access **175** as a colorless oil (0.1321 g, 98% yield). ^{1}H NMR (400 MHz, $CDCl_3$) δ 5.85 (ddt, *J* = 24.2, 9.6, 7.2 Hz, 1H), 5.19 – 5.11 (m, 2H), 3.69 (ddt, *J* = 22.4, 9.2, 3.1 Hz, 1H), 3.59 – 3.43 (m, 1H), 2.37 – 2.09 (m, 2H), 1.74 – 1.57 (m, 2H), 1.49 (ddd, *J* = 19.1, 8.4, 4.7 Hz, 3H), 1.30 (dt, *J* = 18.7, 6.9 Hz, 1H), 1.20 – 1.11 (m, 1H), 1.08 – 0.97 (m, 1H), 0.90 (dt, *J* = 5.0, 2.4 Hz, 16H), 0.84 (d, *J* = 6.7 Hz, 3H), 0.09 – 0.05 (m, 6H).

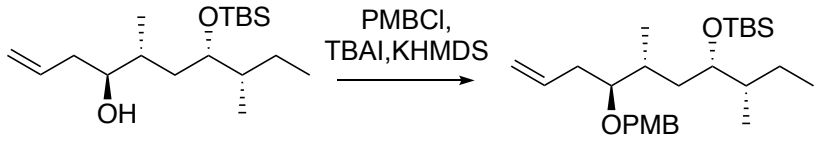
Notebook entries:

Procedure: SSP2- 377

^{1}H NMR and ^{13}C NMR: SSP2-263 or SSP2-427


SSP2-427-fr.24-27-1H.1.fid
f1 (ppm)
1.00
1.97
0.98
1.02
2.46
2.19
2.53
1.08
0.88
0.78
15.35
2.71
5.73

***Tert*-butyl(((3*S*,4*S*,6*R*,7*S*)-7-((4-methoxybenzyl)oxy)-3,6-dimethyldec-9-en-4-yl)oxy)dimethylsilane (146)**



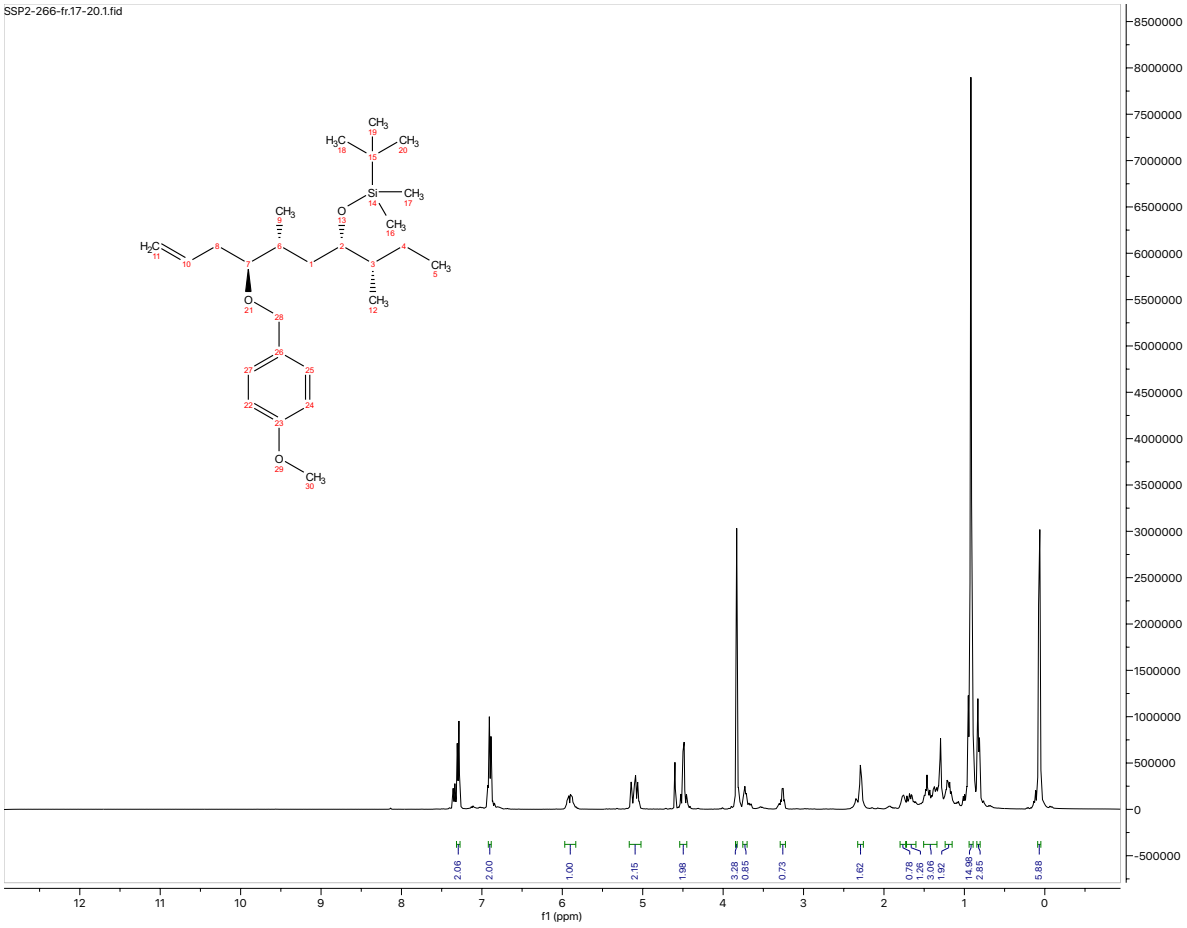
175 **146**

Alcohol **175** (0.0673 g, 0.214 mmol, 1 eq.) was dissolved in anhydrous THF (~1.1 mL, 0.2M) in a flame dried RBF under an Ar atmosphere. Next TBAI (0.004 g, 0.011 mmol, 0.05 eq.), 0.5M KHMDS solution in toluene (0.86 mL, 0.043 mmol, 2 eq.) followed PMBCl (0.05 mL, 0.342 mmol, 1.6 eq.). The reaction was stirred overnight, quenched with a sat'd $NH_4Cl_{(aq)}$ solution, extracted with CH_2Cl_2 (x3), the combined organic layers were dried over anhydrous Na_2SO_4 and concentrated under reduced pressure at rt. The crude material was subjected to flash silica column chromatography (1:9 EtOAc: hexane) to afford the PMB ether **146** as a colorless oil (0.0591 g, 64%). ^{1}H NMR (400 MHz, $CDCl_3$) δ 7.30 (d, *J* = 8.3 Hz, 2H), 6.90 (d, *J* = 8.0 Hz, 2H), 5.91 (ddt, *J* = 18.0, 11.5, 7.4 Hz, 1H), 5.17 – 5.02 (m, 2H), 4.54 – 4.45 (m, 2H), 3.84 (d, *J* = 4.1 Hz, 3H), 3.73 (t, *J* = 6.9 Hz, 1H), 3.26 (q, *J* = 5.7 Hz, 1H), 2.29 (t, *J* = 6.6 Hz, 2H), 1.76 (dq, *J* = 9.7, 4.7 Hz, 1H), 1.72 – 1.60 (m, 1H), 1.51 – 1.34 (m, 3H), 1.24 – 1.15 (m, 2H), 0.93 (d, *J* = 6.4 Hz, 15H), 0.82 (d, *J* = 6.5 Hz, 3H), 0.07 (d, *J* = 6.4 Hz, 6H).

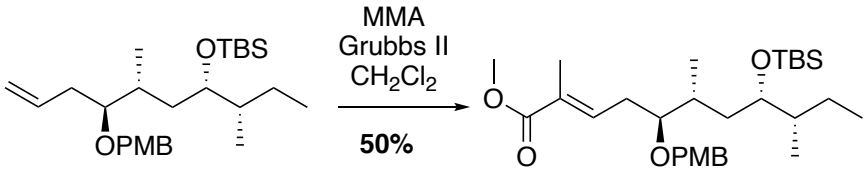
Notebook entries:

Procedure: SSP2-268

^{1}H NMR: SSP2-266


SSP2-266-fr.17-20.1.fid
f1 (ppm)
2.06
2.00
1.00
2.15
1.98
3.28
0.85
0.73
1.62
0.78
1.26
3.06
1.92
14.98
2.65
5.88

Methyl (5*S*,6*R*,8*S*,9*S*,*E*)-8-((*tert*-butyldimethylsilyl)oxy)-5-((4-methoxybenzyl)oxy)-2,6,9-trimethylundec-2-enoate (145)



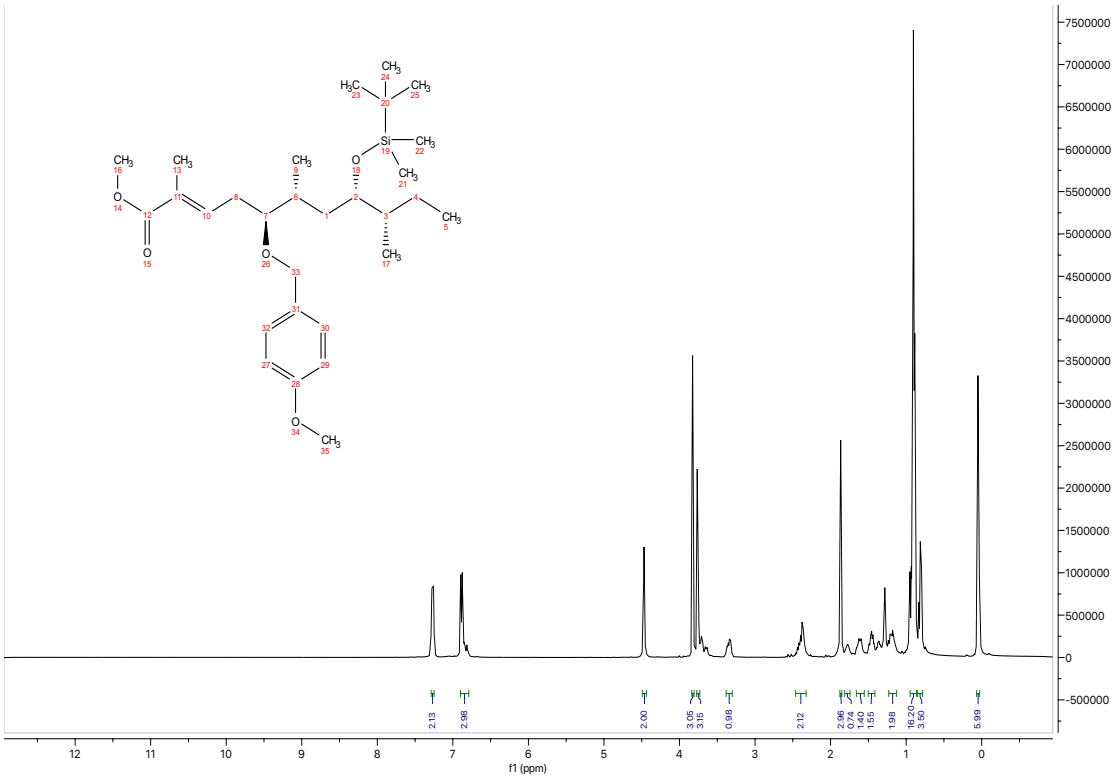
146 **145**

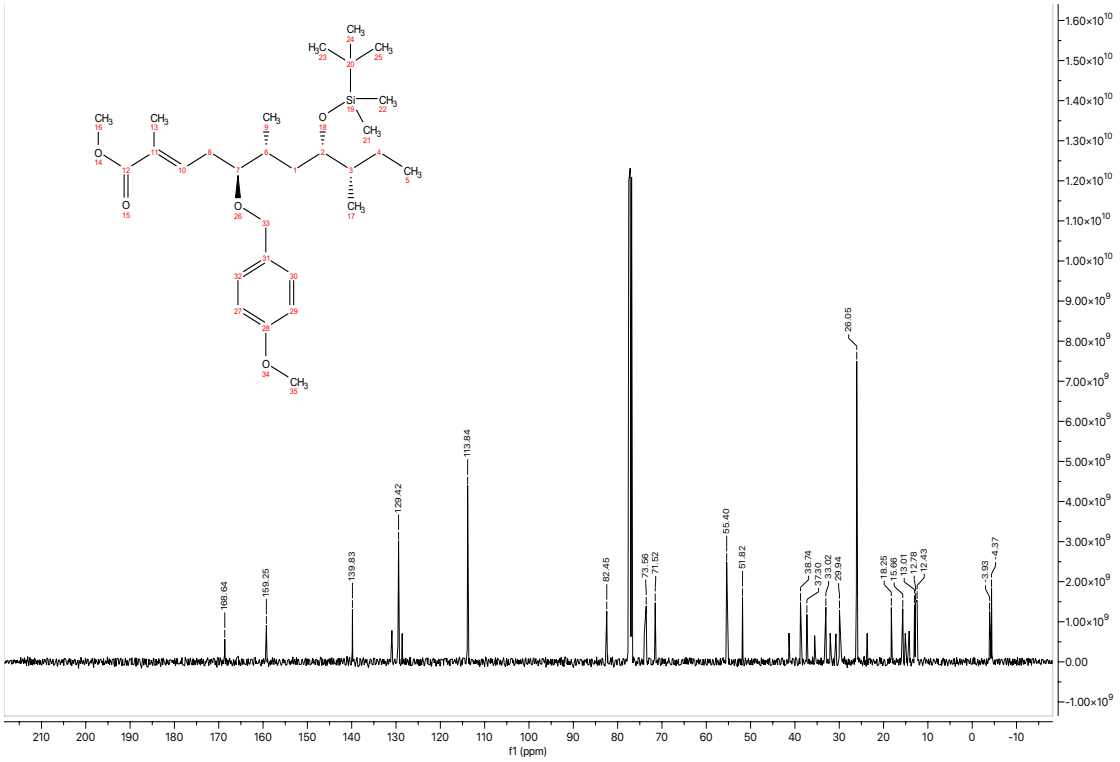
Reaction was performed using standard protocol for cross metathesis except that 10 equivalents of the more substituted olefine, MMA was added. The crude material was subjected to flash column chromatography (1:9 EtOAc: hexane) to afford methyl ester **145** as a viscous oil in 50% yield. ^{1}H NMR (400 MHz, $CDCl_3$) δ 7.29 – 7.25 (m, 2H), 6.90 – 6.79 (m, 3H), 4.47 (d, *J* = 3.4 Hz, 2H), 3.83 (s, 3H), 3.76 (d, *J* = 5.6 Hz, 3H), 3.38 – 3.30 (m, 1H), 2.39 (dq, *J* = 11.6, 6.3, 4.9 Hz, 2H), 1.87 (s, 3H), 1.81 – 1.74 (m, 1H), 1.61 (dtd, *J* = 15.1, 11.2, 9.9, 5.1 Hz, 1H), 1.46 (dq, *J* = 13.0, 6.2 Hz, 2H), 1.18 (ddt, *J* = 15.2, 7.7, 4.6 Hz, 2H), 0.90 (d, *J* = 6.1 Hz, 16H), 0.81 (t, *J* = 7.6 Hz, 4H), 0.06 (s, 6H). ^{13}C NMR (101 MHz, $CDCl_3$) δ 168.64, 159.25, 139.83, 129.42, 113.84, 82.45, 73.56, 71.52, 55.40, 51.82, 38.74, 37.30, 33.02, 29.94, 26.05, 18.25, 15.66, 13.01, 12.78, 12.43, -3.93, -4.37.

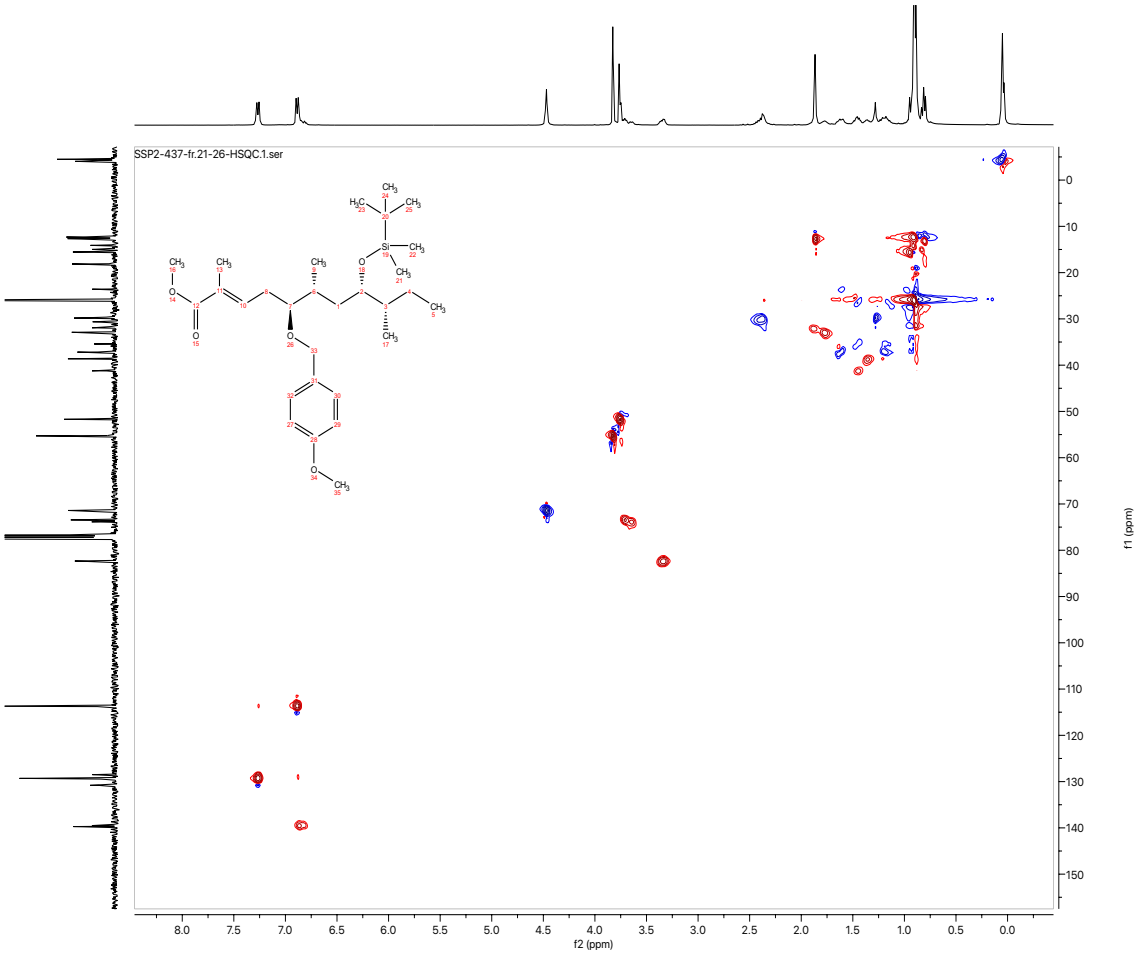
Notebook entries:

Procedure: SSP2-437

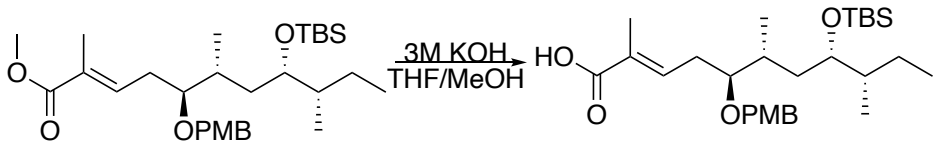
^{1}H NMR, ^{13}C NMR, and HSQC: SSP2-437


2.13
2.98
2.00
3.05
3.15
0.98
2.12
2.96
0.74
1.40
1.55
1.98
16.20
3.50
5.99
f1 (ppm)


168.64
159.25
139.83
129.42
113.84
82.45
73.56
71.62
55.40
51.82
38.74
37.30
37.02
29.94
26.05
18.25
15.66
13.01
12.78
12.43
-3.93
-4.37
f1 (ppm)


SSP2-437-fr.21-26-HSQC.1.ser
f2 (ppm)
f1 (ppm)

(5*S*,6*R*,8*S*,9*S*,*E*)-8-((*tert*-butyldimethylsilyl)oxy)-5-((4-methoxybenzyl)oxy)-2,6,9-trimethylundec-2-enoic acid (S3)

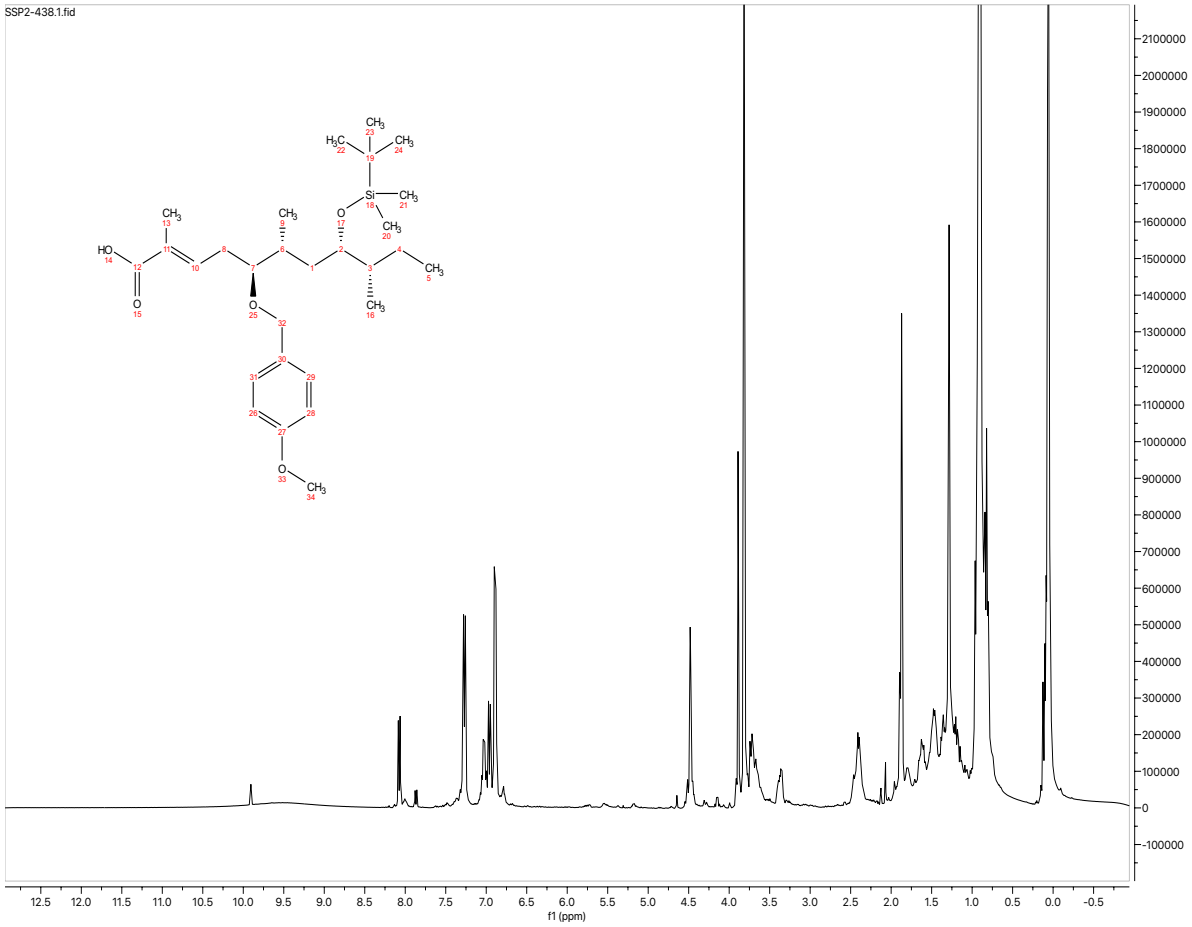


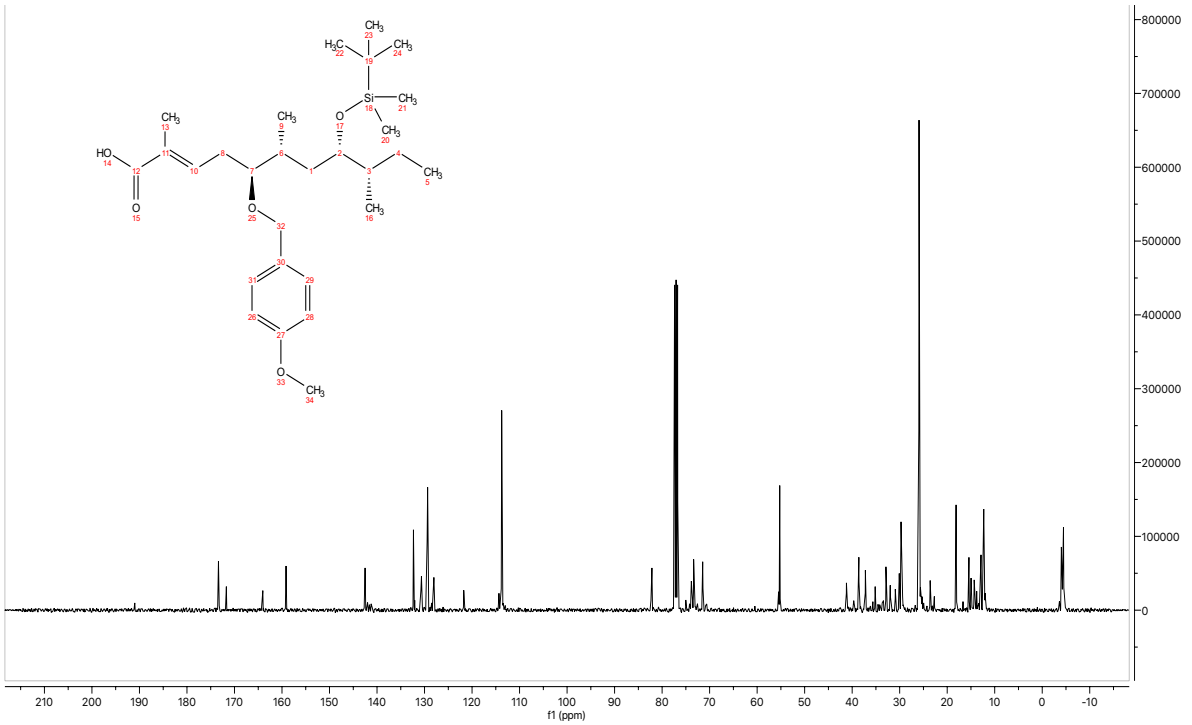
Methyl ester **145** (0.0933 g, 0.184 mmol, 1 eq.) was dissolved in 1:1 mixture of THF:MeOH (1.84 mL, 0.1M). Next, a. freshly prepared solution of aq. 3M KOH (1.23mL, 0.15M) was added and refluxed at boiling point of MeOH for 5 h. Reaction mixture was gradually brought to rt and quenched with a 1M HCl ($_{aq}$) solution until the reaction pH ~1. The resulting crude mixture was extracted with CH_2Cl_2 (x3), combined organic layers were dried over anhydrous Na_2SO_4 and concentrated under reduced pressure at rt to access the carboxylic acid **S3** as a white solid.

Notebook entries:

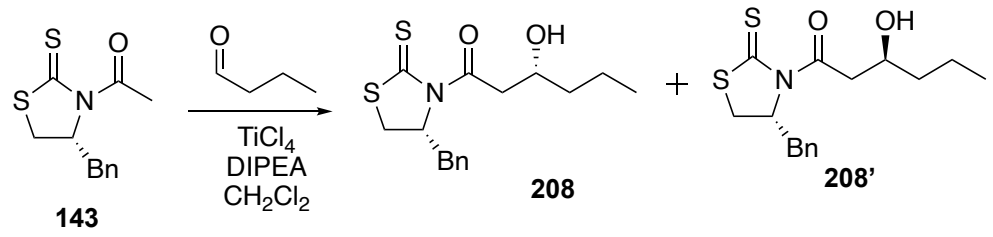
Procedure: SSP2-438

^{1}H NMR and ^{13}C NMR: SSP2-438 (Crude)


SSP2-438.1.fid
f1 (ppm)


f1 (ppm)

(*R*)-1-((*R*)-4-benzyl-2-thioxothiazolidin-3-yl)-3-hydroxyhexan-1-one (208)

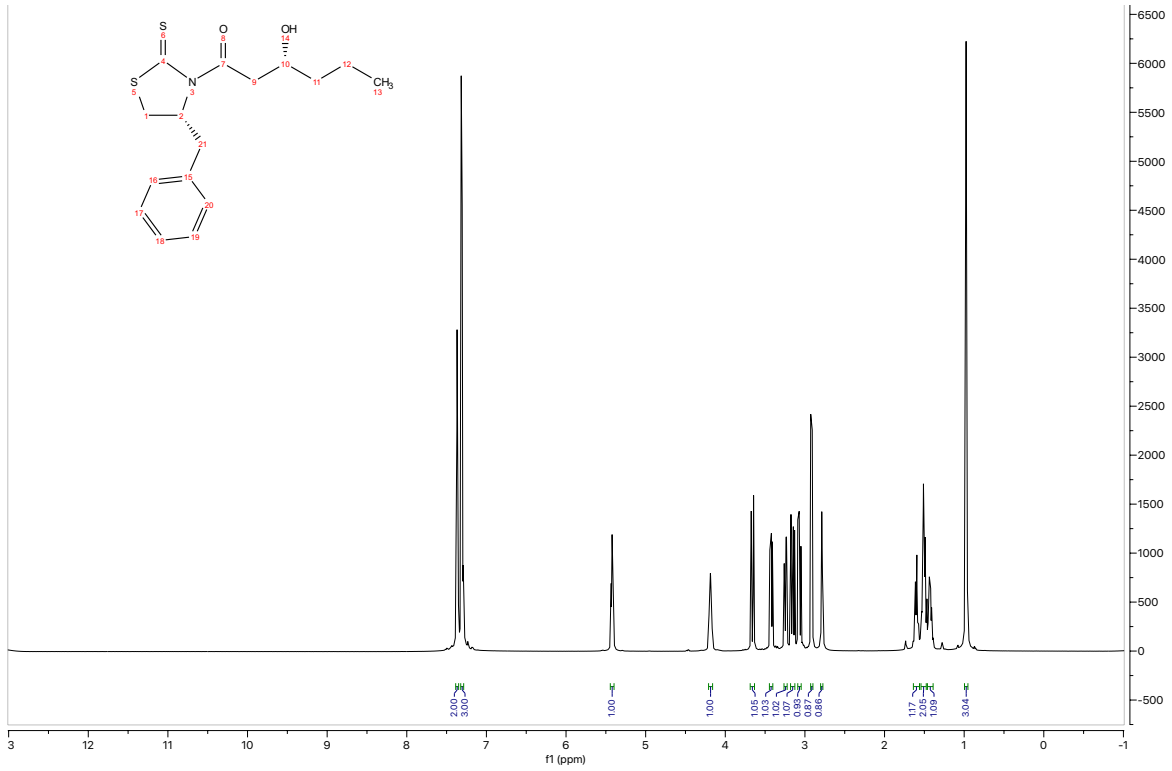


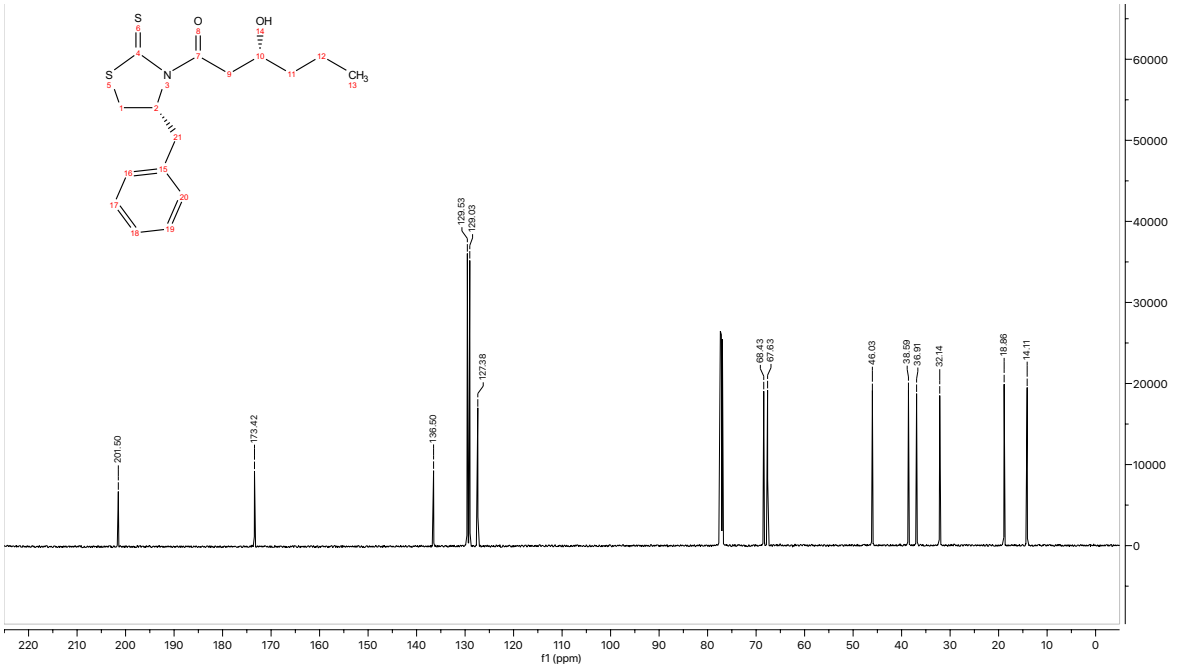
In a flame dried RBF, compound **143** (0.5 g, 1.99 mmol, 1 eq.) was dissolved in anhydrous CH_2Cl_2 (11.7 mL, 0.17M) under an Ar atmosphere and cooled to -78 °C. Next, 1M solution of $TiCl_4$ in CH_2Cl_2 (~2 mL, 1.99 mmol, 1 eq.) was added slowly dropwise. After stirring the reaction for 5 minutes, DIPEA (0.69 mL, 3.98 mmol, 2 eq.) was added slowly dropwise and continued stirring at -78 °C for 30 minutes. Then, butyraldehyde (0.64 mL, 5.97 mmol, 3 eq.) was added and stirred the reaction for further 30 minutes at -78 °C. The reaction was quenched with a half saturated (sat'd) $NH_4Cl_{(aq)}$ solution at -78 °C, gradually brought to rt, extracted with CH_2Cl_2 (x3), the combined organic layers were dried over anhydrous Na_2SO_4 and concentrated under reduced pressure. The crude compound was subjected to flash column chromatography (1:3 EtOAc: hexane) to access **208** as a bright yellow viscous oil and **208'** as bright yellow crystals (0.3625 g, 56% yield, overall quant.). ^{1}H NMR (600 MHz, $CDCl_3$) δ 7.37 (t, *J* = 7.5 Hz, 2H), 7.31 (d, *J* = 7.4 Hz, 3H), 5.42 (ddd, *J* = 10.8, 7.1, 4.0 Hz, 1H), 4.18 (ddt, *J* = 10.1, 6.9, 3.5 Hz, 1H), 3.66 (dd, *J* = 17.8, 2.4 Hz, 1H), 3.42 (dd, *J* = 11.5, 7.2 Hz, 1H), 3.25 (dd, *J* = 13.2, 4.0 Hz, 1H), 3.15 (dd, *J* = 17.7, 9.4 Hz, 1H), 3.07 (dd, *J* = 13.2, 10.5 Hz, 1H), 2.92 (d, *J* = 11.5 Hz, 1H), 2.79 (d, *J* = 3.7 Hz, 1H), 1.64 – 1.56 (m, 1H), 1.54 – 1.48 (m, 2H), 1.46 – 1.39 (m, 1H), 0.98 (t, *J* = 7.0 Hz, 3H).

Notebook entries:

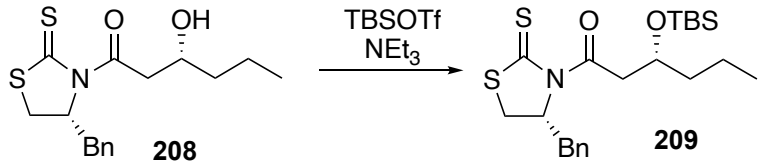
Procedure: SSP2-160

^{1}H NMR and ^{13}C NMR: SSP2-080


f1 (ppm)


201.50
173.42
136.50
129.53
129.03
127.38
68.43
67.63
46.03
38.59
36.91
32.14
18.86
14.11
f1 (ppm)

(R)-1-(R)-4-benzyl-2-thioxothiazolidin-3-yl)-3-((*tert*-butyldimethylsilyl)oxy)hexan-1-one (209)

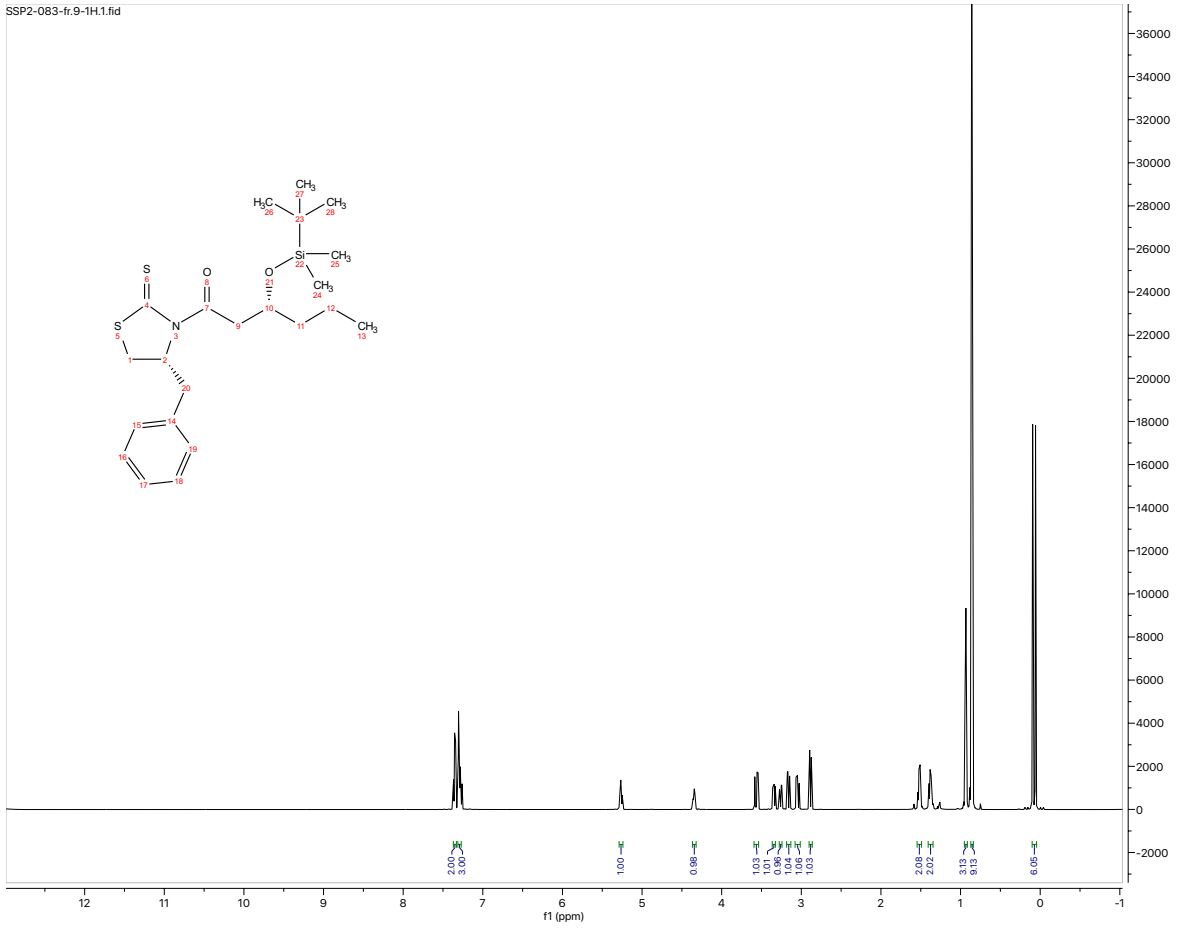


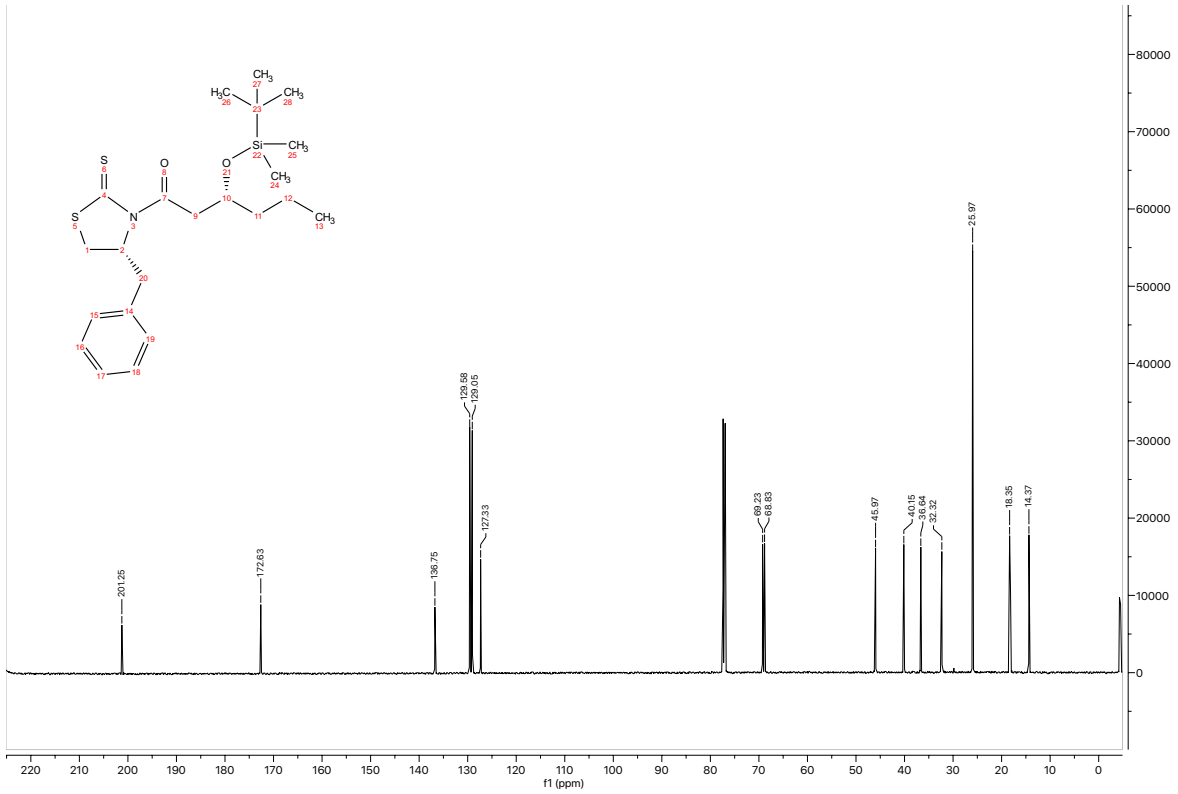
In a flame dried RBF, compound **208** (0.3763 g, 1.16 mmol, 1 eq.), was dissolved in anhydrous CH_2Cl_2 (11.6 mL, 0.1M) under an Ar atmosphere and cooled to 0 °C. Next, TBSOTf (0.53 mL, 2.33 mmol, 2 eq.) followed by NEt_3 (0.65 mL, 4.65 mmol, 4 eq.) was added and left to stir overnight while the temperature was brought to rt gradually. The reaction was quenched with a sat'd $NH_4Cl_{(aq)}$ solution, extracted with CH_2Cl_2 (x3), the combined organic layers were dried over anhydrous Na_2SO_4 and concentrated under reduced pressure. The crude material was subjected to flash silica column chromatography (1:9 EtOAc: hexane) to afford **209** as bright yellow crystals (0.507 g, quantitative yield). ^{1}H NMR (600 MHz, $CDCl_3$) δ 7.37 – 7.33 (m, 2H), 7.31 – 7.27 (m, 3H), 5.27 (ddd, *J* = 10.7, 7.0, 3.7 Hz, 1H), 4.35 (dtd, *J* = 8.1, 5.7, 3.7 Hz, 1H), 3.56 (dd, *J* = 16.7, 8.2 Hz, 1H), 3.34 (ddd, *J* = 11.5, 7.1, 1.1 Hz, 1H), 3.26 (dd, *J* = 13.2, 3.7 Hz, 1H), 3.16 (dd, *J* = 16.8, 3.8 Hz, 1H), 3.05 (dd, *J* = 13.2, 10.7 Hz, 1H), 2.88 (d, *J* = 11.5 Hz, 1H), 1.55 – 1.49 (m, 2H), 1.41 – 1.35 (m, 2H), 0.93 (t, *J* = 7.4 Hz, 3H), 0.86 (s, 9H), 0.08 (d, *J* = 21.7 Hz, 6H). ^{13}C NMR (151 MHz, $CDCl_3$) δ 201.25, 172.63, 136.75, 129.58, 129.05, 127.33, 69.23, 68.83, 45.97, 40.15, 36.64, 32.32, 25.97, 18.35, 14.37.

Notebook entries:

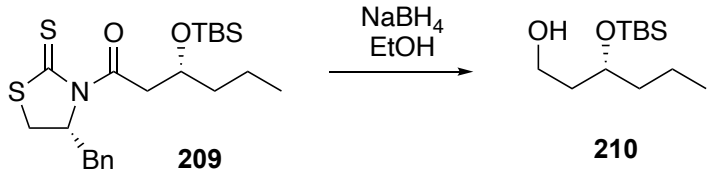
Procedure: SSP2-166

^{1}H NMR and ^{13}C NMR: SSP2-083


SSP2-083-fr.9-1H.1.fid
f1 (ppm)


201.25
172.63
136.75
129.58
129.05
127.33
69.23
68.83
45.97
40.15
36.64
32.32
25.97
18.35
14.37
f1 (ppm)

(*R*)-3-((*tert*-butyldimethylsilyl)oxy)hexan-1-ol (210)

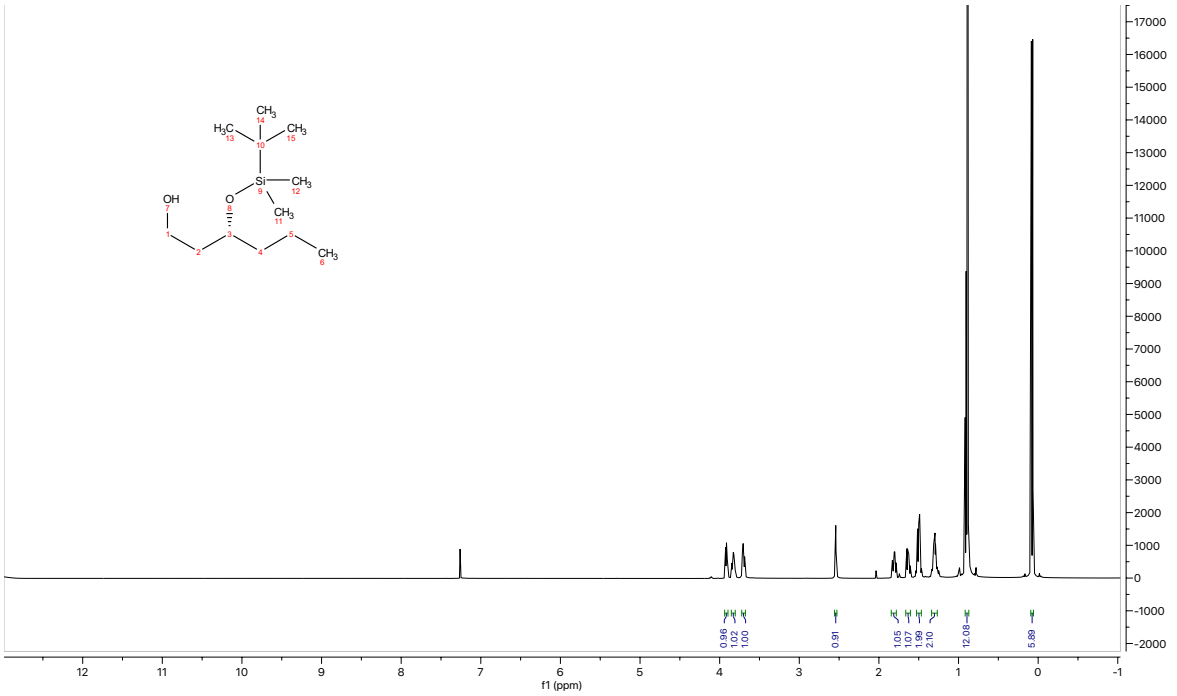


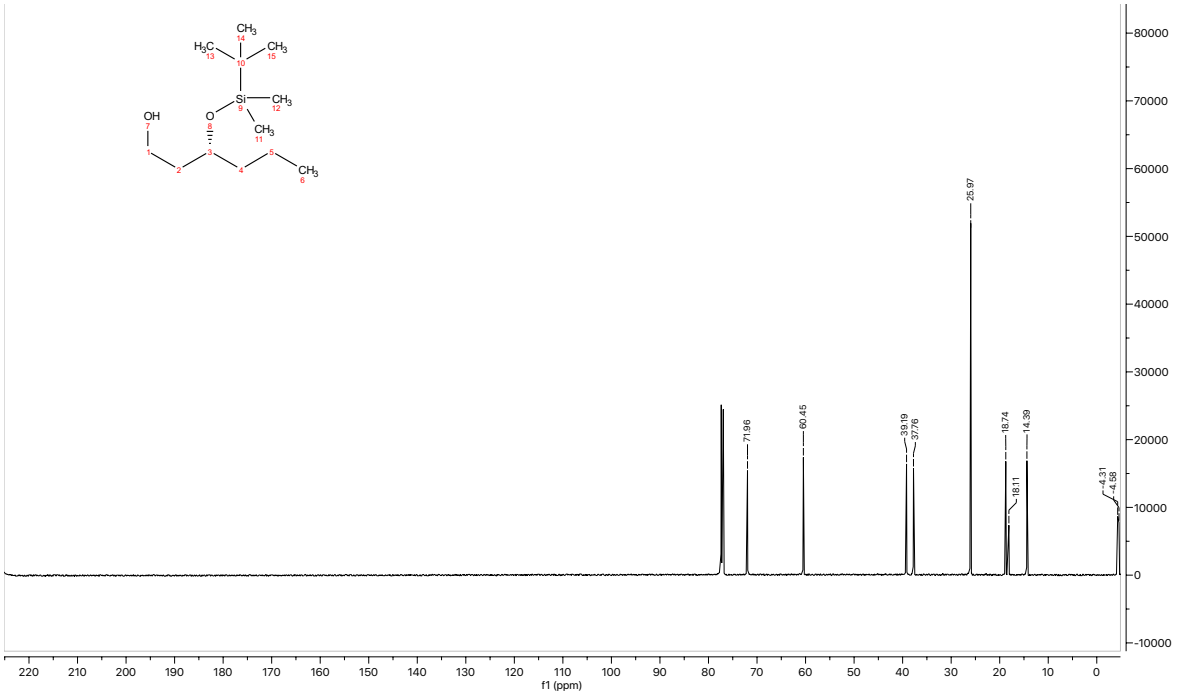
In a flame dried RBF, compound **209** (0.315 g, 0.718 mmol, 1 eq.), was dissolved in anhydrous EtOH (dried over MS) (4.23 mL, 0.17M) under an Ar atmosphere and cooled to 0 °C. Next, $NaBH_4$ (0.0968 g, 2.56 mmol, 2 eq.) was added portion wise and stirred the reaction at rt until yellow color of disappear. Cooled the RBF to 0 °C, quenched with a sat'd $NH_4Cl_{(aq)}$ solution (addition was done dropwise), extracted with CH_2Cl_2 (x3), the combined organic layers were dried over anhydrous Na_2SO_4 and concentrated under reduced pressure at rt. The crude compound was purified via flash silica column chromatography (1:6 EtOAc: hexane) to afford **210** as a colorless oil (0.154g, 93% yield). ^{1}H NMR (600 MHz, $CDCl_3$) δ 3.92 (qd, *J* = 6.3, 4.1 Hz, 1H), 3.83 (ddt, *J* = 12.5, 8.6, 4.2 Hz, 1H), 3.70 (dq, *J* = 10.8, 5.4 Hz, 1H), 2.54 (t, *J* = 5.1 Hz, 1H), 1.84 – 1.78 (m, 1H), 1.63 (dtd, *J* = 14.4, 6.0, 4.3 Hz, 1H), 1.50 (dq, *J* = 8.5, 6.3 Hz, 2H), 1.30 (dddd, *J* = 14.0, 10.2, 5.1, 2.9 Hz, 2H), 0.89 (d, *J* = 11.2 Hz, 12H), 0.08 (d, *J* = 10.2 Hz, 6H). ^{13}C NMR (151 MHz, $CDCl_3$) δ 71.96, 60.45, 39.19, 37.76, 25.97, 18.74, 18.11, 14.39, -4.31, -4.58.

Notebook entries:

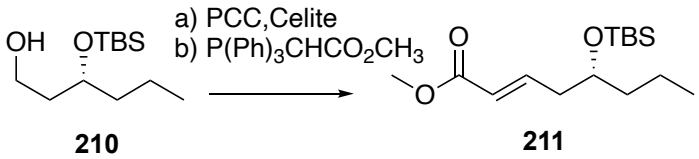
Procedure: SSP2-029

^{1}H NMR and ^{13}C NMR: SSP2-085


f1 (ppm)
0.96
1.02
1.00
0.91
1.05
1.07
1.99
2.10
12.08
5.89


f1 (ppm)
71.96
60.45
39.19
37.76
25.97
18.74
18.11
14.39
14.31
14.58

Methyl (*R*,*E*)-5-((*tert*-butyldimethylsilyl)oxy)oct-2-enoate (211)



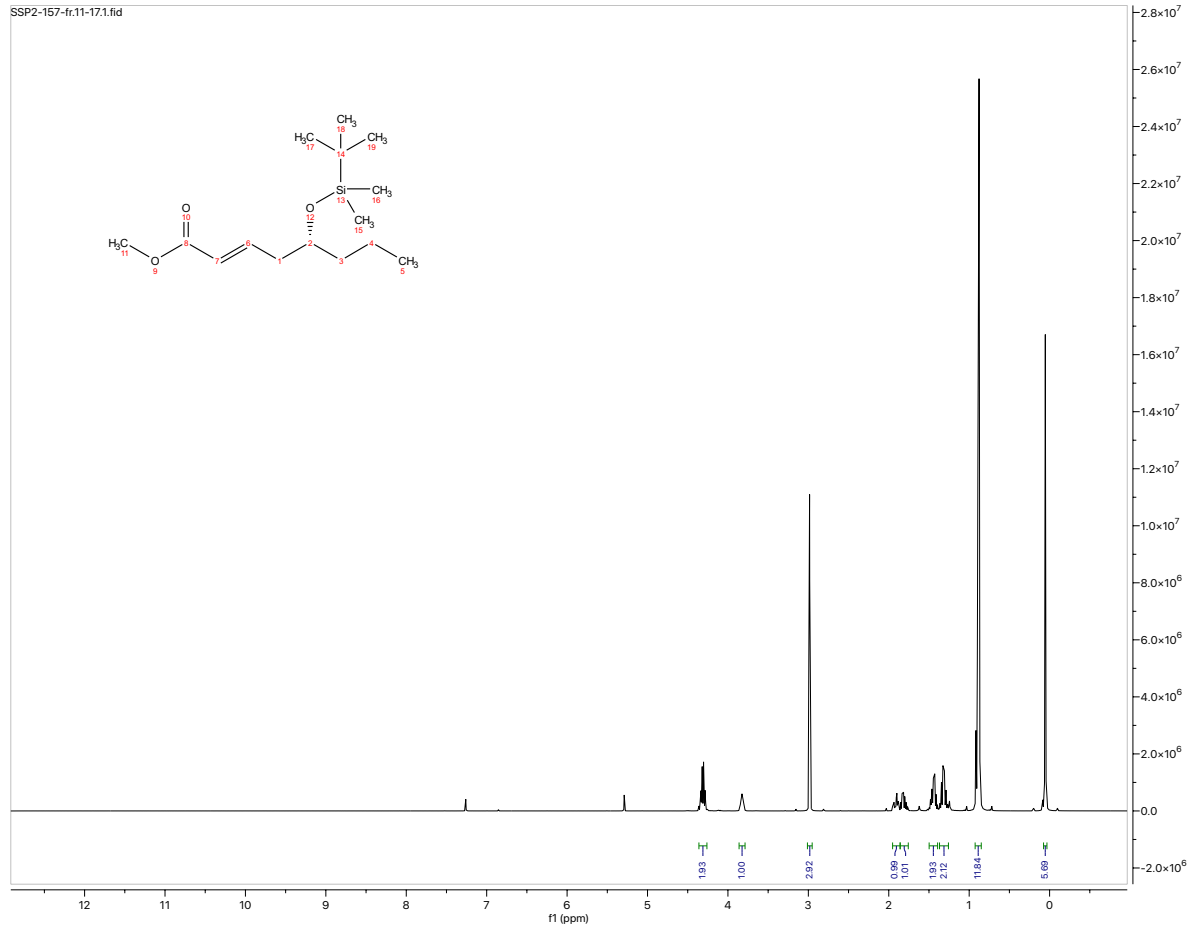
210 **211**

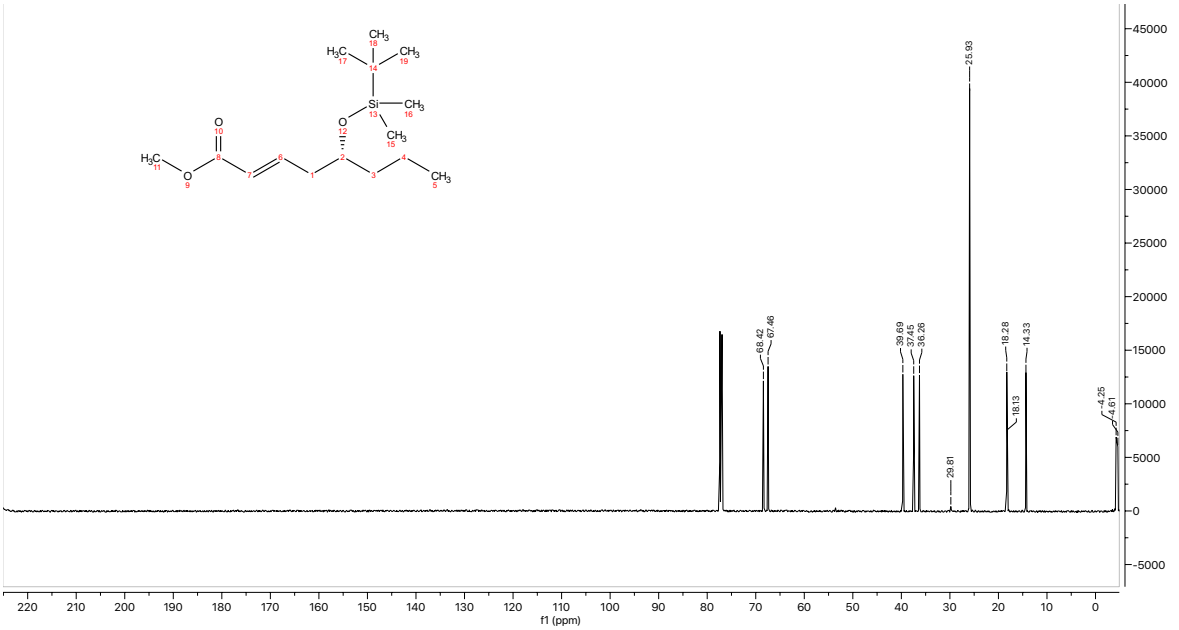
A flame dried RBF was charged with PCC (0.1888 g, 0.876 mmol, 1.5 eq.), celite (0.1888 g, 1:1 mass ratio with PCC), and anhydrous CH_2Cl_2 (1.6 mL, 0.36M) under an Ar atmosphere. Next, **210** (0.136 g, 0.584 mmol, 1 eq.) was added dropwise to the stirring mixture and continued stirring for 2 h. Then methyl(triphenylphosphoranylidene)acetate (0.332 g, 0.992 mmol, 1.7 eq.) was introduced to the reaction under an Ar atmosphere and left to stir overnight. Reaction was filtered through a fritted Buchner filter funnel under vacuum, collected filtrate was concentrated under reduced pressure at rt, and subjected to flash silica column chromatography (gradient elution; 100% hexane, 1:9 EtOAc: hexane, 1:6 EtOAc: hexane; 1:4 EtOAc: hexane) to afford **211** as a colorless oil over 2 steps (0.1318 g, 79% yield).^{1}H NMR (400 MHz, $CDCl_3$) δ 4.36 – 4.26 (m, 2H), 3.86 – 3.79 (m, 1H), 2.98 (s, 3H), 1.91 (ddt, *J* = 14.4, 7.3, 3.7 Hz, 1H), 1.86 – 1.76 (m, 1H), 1.50 – 1.39 (m, 2H), 1.37 – 1.26 (m, 2H), 0.89 (d, *J* = 8.6 Hz, 12H), 0.05 (s, 6H). ^{13}C NMR (151 MHz, $CDCl_3$) δ 68.42, 67.46, 39.69, 37.45, 36.26, 29.81, 25.93, 18.28, 18.13, 14.33, -4.25, -4.61.

Notebook entries:

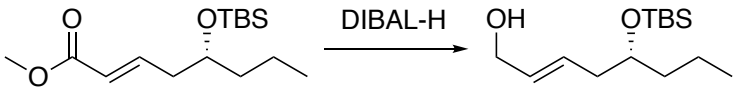
Procedure: SSP1-319

^{1}H NMR and ^{13}C NMR: SSP2-157


SSP2-157-fr.11-17.1.fid
f1 (ppm)


68.42
67.46
39.69
37.45
36.26
29.81
25.93
18.28
18.13
14.33
4.25
4.61
f1 (ppm)

(*R*,*E*)-5-((*tert*-butyldimethylsilyl)oxy)oct-2-en-1-ol (212)



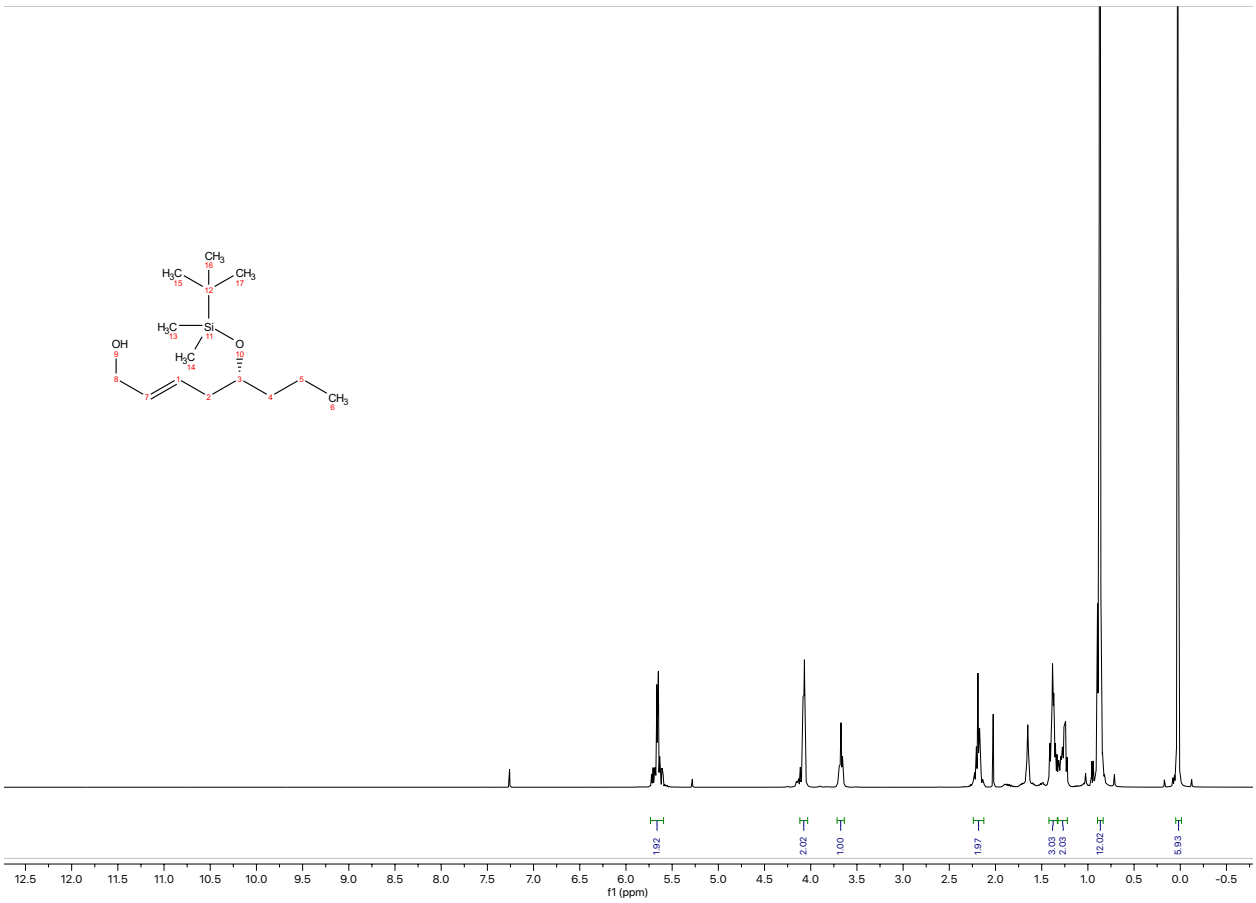
211 **212**

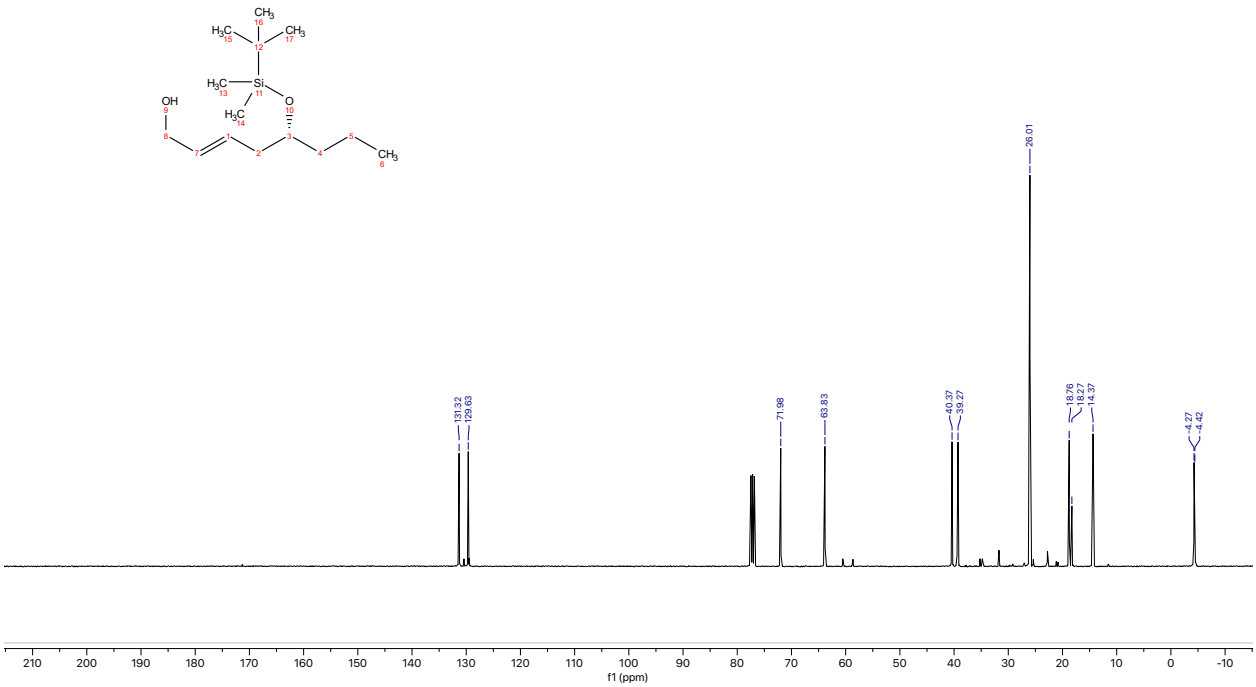
In a flame dried RBF, compound **211** (1.073 g, 3.75 mmol, 1 eq.), was dissolved in anhydrous THF (18.7 mL, 0.2M) under an Ar atmosphere and cooled to -78 °C. A freshly prepared solution of DIBAL-H (1M in THF, 9.4 mL, 9.36 mmol, 2.5 eq.) was added and left the reaction to stir overnight while temperature was allowed to reach to rt gradually. The reaction was then cooled to 0 °C, quenched with a dropwise addition of sat'd aq. solution of Rochelle's salt, stirred at rt overnight, and extracted with CH_2Cl_2 (x3). The combined organic layers were dried over anhydrous Na_2SO_4 and concentrated under reduced pressure at rt. The crude compound was subjected to flash silica column chromatography (1:6 EtOAc: hexane) to access **212** as a colorless oil (0.824 g, 85% yield). ^{1}H NMR (400 MHz, $CDCl_3$) δ 5.73 – 5.59 (m, 2H), 4.07 (d, J = 4.7 Hz, 2H), 3.67 (p, J = 5.7 Hz, 1H), 2.24 – 2.12 (m, 2H), 1.65 (s, 1H), 1.43 – 1.33 (m, 3H), 1.32 – 1.22 (m, 2H), 0.87 (s, 10H), 0.03 (s, 6H). ^{13}C NMR (101 MHz, $CDCl_3$) δ 131.32, 129.63, 71.98, 63.83, 40.37, 39.27, 26.01, 18.76, 18.27, 14.37, -4.27, -4.42.

Notebook entries:

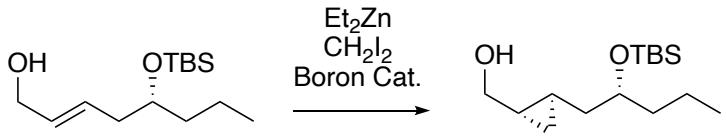
Procedure: SSP2-191

^{1}H NMR and ^{13}C NMR: SSP2-105


1.92
2.02
1.00
1.97
3.03
2.03
12.02
5.93
f1 (ppm)


131.32
129.68
71.98
63.83
40.37
39.27
26.01
18.76
18.27
14.37
-4.27
-4.42
f1 (ppm)

((1*S*,2*R*)-2-((*R*)-2-((*tert*-butyldimethylsilyl)oxy)pentyl)cyclopropyl)methanol (213)



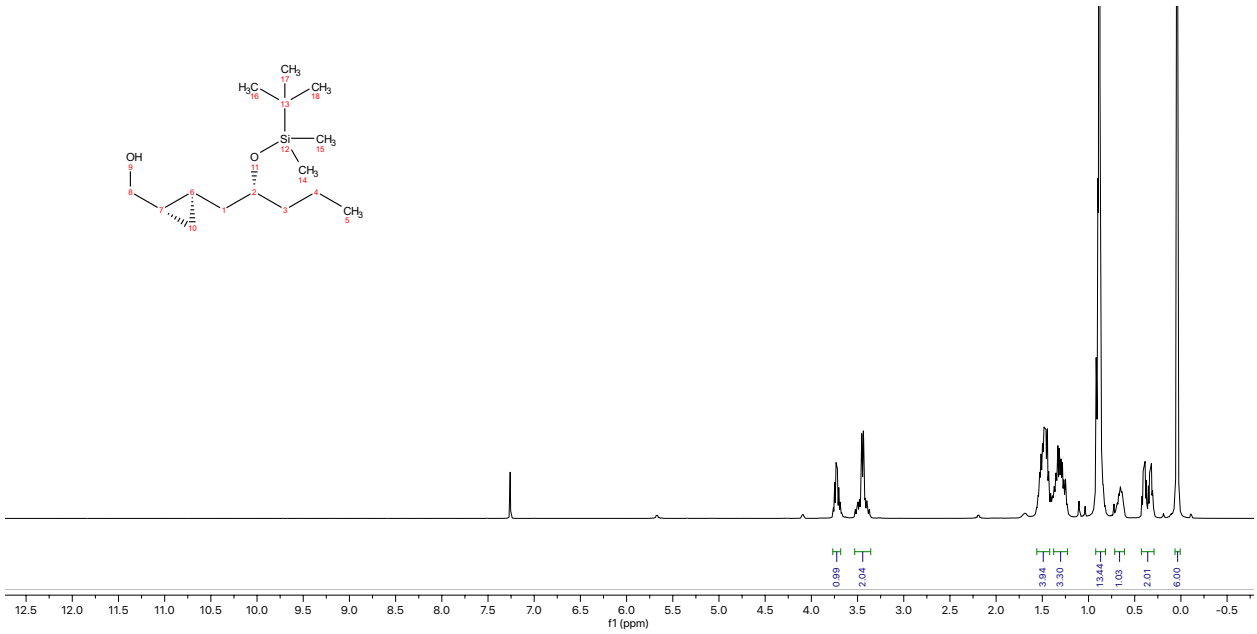
212 **213**

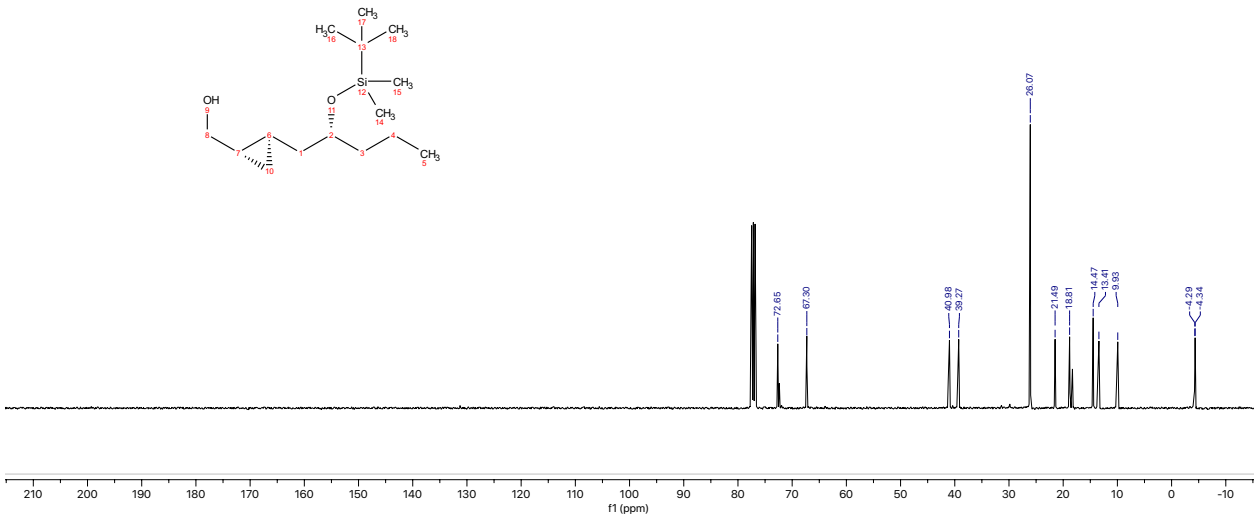
A flame dried RBF (A) was charged with anhydrous CH_2Cl_2 (28.4 mL, 0.1M), MS, and a freshly prepared 1M solution of Et_2Zn in THF (28.4 mL, 28.4 mmol, 10 eq.) under an Ar atmosphereand cooled to 0 °C. Next, CH_2I_2 (4.6 mL, 56.84 mmol, 20 eq.) was added dropwise, and stirred for 15 minutes. A second flame dried RBF (B) was charged with compound **212** (0.8198 g, 2.84 mmol, 1 eq.), anhydrous CH_2Cl_2 (28.4 mL, 0.1M), and MS. Next (4*R*,5*R*)-2-butyl-N_4,N_4,N_5,N_5-tetramethyl-1,3,2-dioxaborolane-4,5- dicarboxamide (0.86 mL, 3.41 mmol, 1.2 eq.) was added and stirred the solution for 15 minutes under an Ar atmosphere at rt. Then the flask B was cooled to 0 °C, transferred to flask A at 0 °C and stirred overnight while allowing to warm to rt overnight. The resulting mixture was quenched with a sat'd aqueous solution of NH_4Cl (until the emulsion were broken), extracted with CH_2Cl_2 (x3), the combined organic layers were dried with Na_2SO_4, and concentrated under reduced pressure at rt. The crude material was then purified via flash silica column chromatography (1:6 EtOAc:hexane) to produce a colorless oil, **213** (0.773 g, quantitative yield).

Notebook entries:

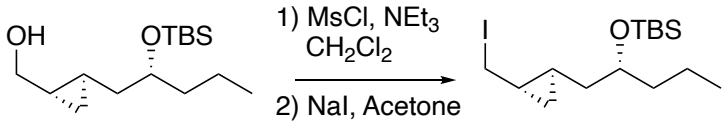
Procedure: SSP2-196

^{1}H NMR and ^{13}C NMR: SSP2-196


0.99
2.04
3.94
3.30
13.44
1.03
2.01
6.00
f1 (ppm)


72.65
67.30
40.98
39.27
26.07
21.49
18.81
14.47
13.41
9.93
-4.29
-4.34
f1 (ppm)

***Tert*-butyl(((*R*)-1-((1*R*,2*S*)-2-(iodomethyl)cyclopropyl)pentan-2-yl)oxy)dimethylsilane (214)**



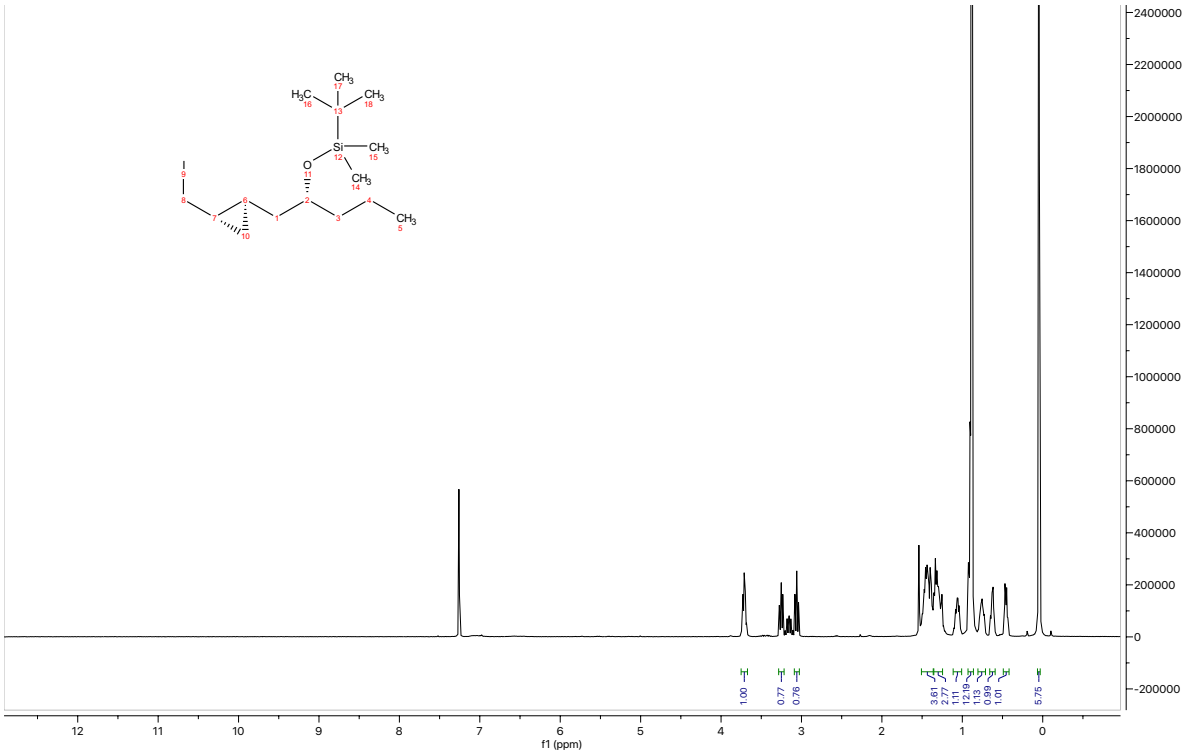
213 **214**

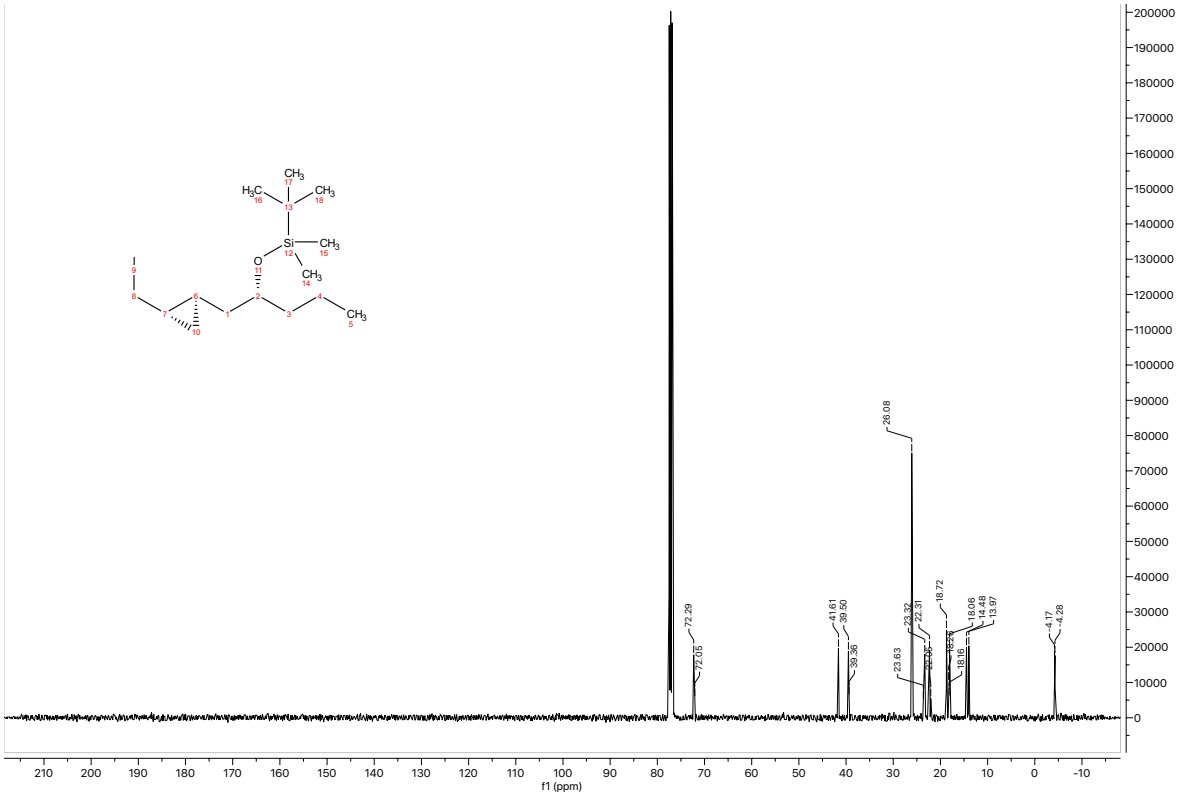
In a flame dried RBF, alcohol **213** (0.8174 g, 2,.99 mmol, 1 eq.) was dissolved in anhydrous CH_2Cl_2 (20 mL, 0.15M) under an Ar atmosphere, and MS were added. The mixture was cooled to 0 °C, MsCl (0.4 mL, 5.1 mmol, 1.7 eq.) followed NEt_3 (1.25 mL, 8.99 mmol, 3 eq.) were added and stirred at 0 °C for 15 minutes followed by at rt for 15 minutes. The reaction was concentrated under reduced pressure at rt. Resulting crude mixture was dissolved in anhydrous acetone (dried over MS, 20 mL, 0.15 M) and $NaI_{(S)}$ (4 g, 26.99 mmol, 9 eq.) was added at rt. Stirred the reaction for 1 h, quenched with a sat'd solution mixture of $NaHCO_3$: $Na_2S_2O_3$ (1:1), extracted with CH_2Cl_2 (x3), dried with anhydrous Na_2SO_4, and concentrated under reduced pressure at rt. The crude material was then purified via flash column chromatography (1:30 CH_2Cl_2:hexane) to obtain **214** as a colorless oil (0.1318 g, 88% yield). ^{1}H NMR (400 MHz, $CDCl_3$) δ 3.71 (p, *J* = 5.8 Hz, 1H), 3.25 (dd, *J* = 9.8, 7.2 Hz, 1H), 3.06 (t, *J* = 9.0 Hz, 1H), 1.51 – 1.36 (m, 4H), 1.35 – 1.25 (m, 3H), 1.07 (ddt, *J* = 11.8, 7.9, 3.6 Hz, 1H), 0.93 – 0.86 (m, 12H), 0.75 (dd, *J* = 11.4, 5.7 Hz, 1H), 0.62 (dq, *J* = 11.2, 3.9, 3.0 Hz, 1H), 0.46 (dt, *J* = 9.2, 4.7 Hz, 1H). ^{13}C NMR (101 MHz, $CDCl_3$) δ 72.29, 72.05, 41.61, 39.50, 39.36, 26.08, 23.63, 23.32, 22.31, 22.05, 18.72, 18.26, 18.16, 18.06, 14.48, 13.97, -4.17, -4.28.

Notebook entries:

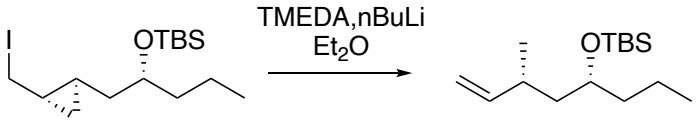
Procedure: SSP2-203

^{1}H NMR and ^{13}C NMR: SSP3-112


1.00
0.77
0.76
3.61
2.77
1.11
1.19
1.13
0.99
1.01
5.75
f1 (ppm)


72.29
72.05
41.61
39.50
39.36
26.08
23.32
22.91
23.63
22.30
18.72
18.26
18.16
18.06
14.48
13.97
-4.17
-4.28
f1 (ppm)

Tert-butyldimethyl(((4R,6R)-6-methyloct-7-en-4-yl)oxy)silane (215)



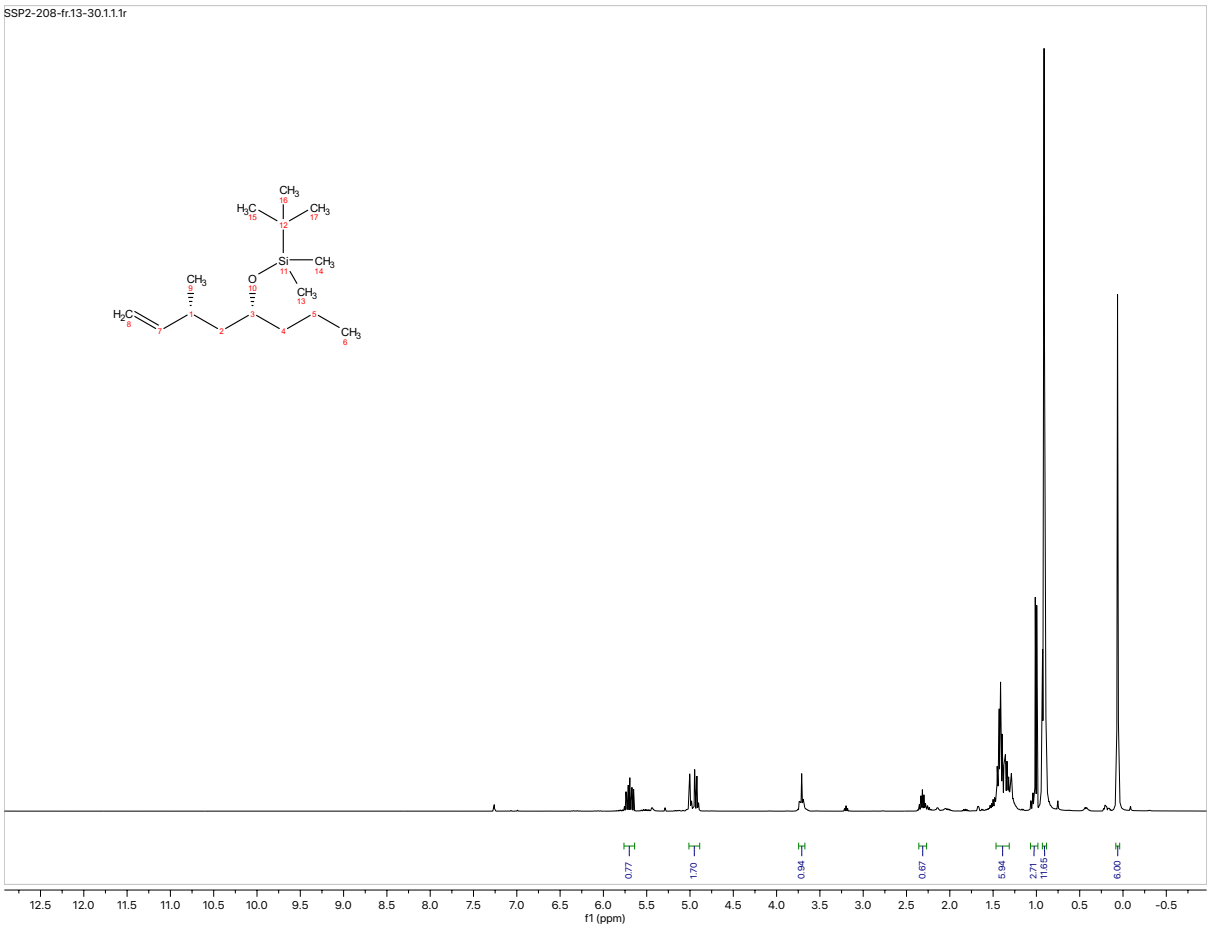
214 **215**

A flame dried RBF was charged with compound **214** (0.0493 g, 0.129 mmol, 1 eq.), anhydrous Et_2O (1.3 mL, 0.1M) followed by MS under an Ar atmosphere and cooled to -78 °C. Next, TMEDA (0.04 mL, 0.258 mmol, 2 eq.) followed by 1.6M nBuLi in hexanes (0.16 mL, 0.258 mmol, 2 eq.) was added dropwise. The reaction was stirred for 1 h at -78 °C, quenched with DI H_2O (1 eq. by volume), gradually brought to rt, and extracted with Et_2O (x3). The combined organic layers were dried over anhydrous Na_2SO_4 and concentrated under reduced pressure at rt. The crude compound was subjected to flash silica gel column chromatography (1:3 heptane: hexane or 100% hexane) to access **215** as a colorless oil (0.0303 g, 92% yield). ^{1}H NMR (400 MHz, $CDCl_3$) δ 5.74 – 5.64 (m, 1H), 5.01 – 4.89 (m, 2H), 3.71 (p, 1H), 2.31 (p, 1H), 1.46 – 1.28 (m, 6H), 1.00 (dd, J = 6.8 Hz, 3H), 0.94 – 0.88 (m, 12H), 0.06 (s, 6H).

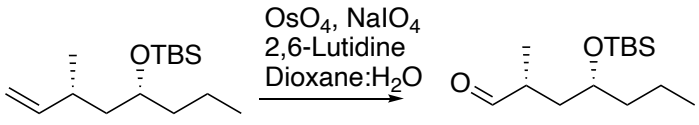
Notebook entries:

Procedure: SSP2-209

^{1}H NMR: SSP3-208


SSP2-208-fr.13-30.1.1.1r
0.77
1.70
0.94
0.67
5.94
2.71
11.65
6.00
f1 (ppm)

(2*R*,4*R*)-4-((*tert*-butyldimethylsilyl)oxy)-2-methylheptanal (216)



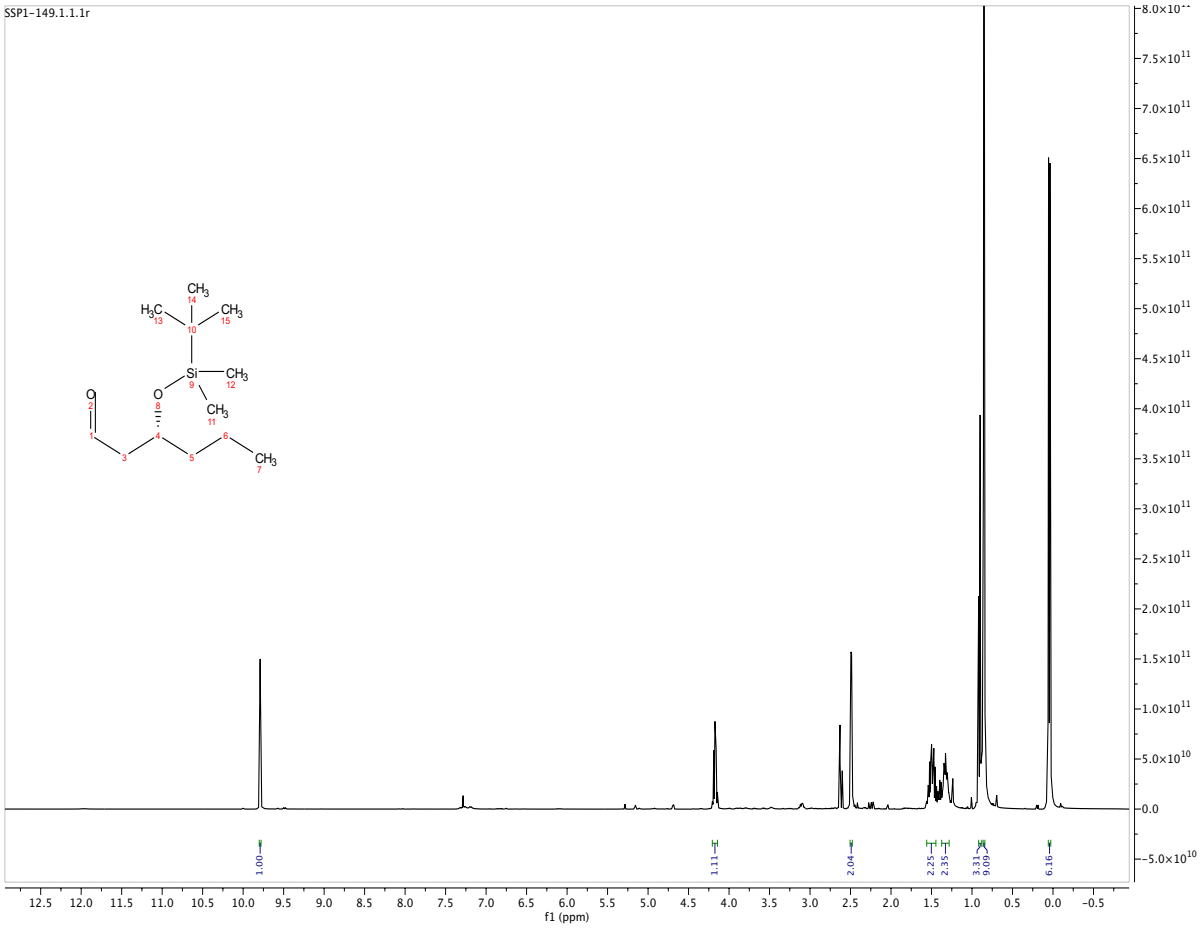
215 **216**

Alkene **215** (0.47 g, 1.83 mmol, 1 eq.) was dissolved in a 3:1 mixture of Dioxane: DI H_2O (0.13M, 14.1 mL). Next 2,6-lutidine (0.28 mL, 2.83 mmol, 1.3 eq.) followed by OsO_4 2.5wt.% in tert-butanol (3.7 mL, 0.366 mmol, 0.2 eq.) was added and stirred for 20 minutes (reaction turned black). Then $NaIO_4$ was added and stirred overnight. The reaction that has turned into an off-white slurry was quenched with a sat'd aqueous solution of $Na_2S_2O_3$, extracted with Et_2O (x3), the combined organic layers were dried over anhydrous Na_2SO_4 and concentrated under reduced pressure at rt. The crude material was carried forward to the next step without further purification. ^{1}H NMR (400 MHz, $CDCl_3$) δ 9.79 (t, *J* = 2.5 Hz, 1H), 4.17 (p, *J* = 5.9 Hz, 1H), 2.49 (dd, *J* = 5.7, 2.5 Hz, 2H), 1.56 – 1.45 (m, 2H), 1.32 (dddd, *J* = 13.9, 7.5, 6.1, 3.3 Hz, 2H), 0.90 (t, *J* = 7.3 Hz, 3H), 0.85 (s, 9H), 0.05 (s, 6H).

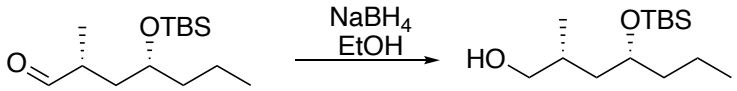
Notebook entries:

Procedure: SSP2-213

^{1}H NMR: SSP1-149


SSP1-149.1.1.1r
f1 (ppm)

(2*R*,4*R*)-4-((*tert*-butyldimethylsilyl)oxy)-2-methylheptan-1-ol (217)



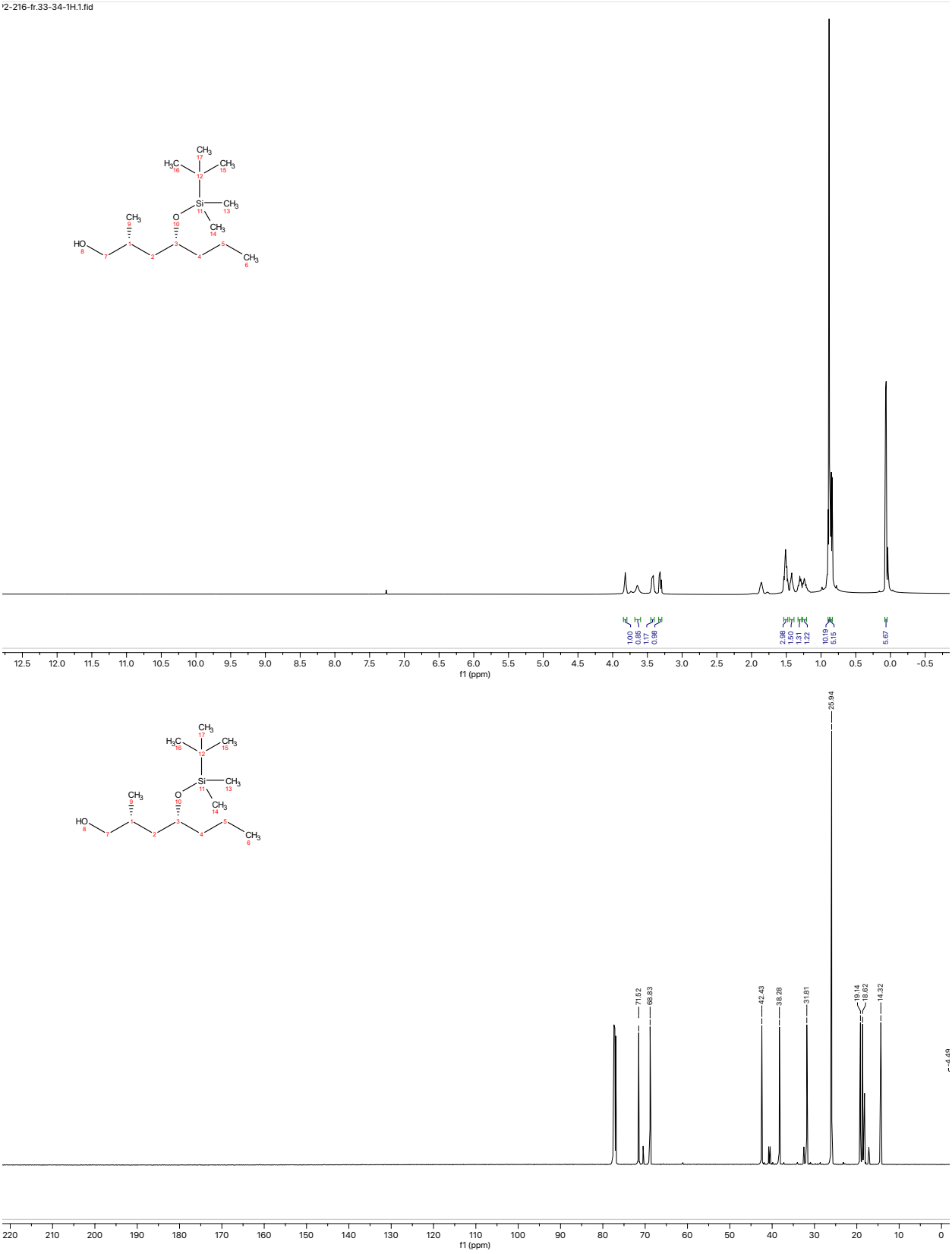
216 **217**

Aldehyde **216** (0.0786 g, 0.304 mmol, 1 eq.) was dissolved in anhydrous EtOH (dried over MS) (1.8 mL, 0.17M) under an Ar atmosphere and the RBF was cooled to 0 °C. Next, $NaBH_4$ (0.0284 g, 0.76 mmol, 2.5 eq.) was added portion wise and stirred the reaction for 2h at rt. The RBF was cooled to 0 °C, quenched with a sat'd $NH_4Cl_{(aq)}$ solution (addition was done dropwise), extracted with CH_2Cl_2 (x3), the combined organic layers were dried over anhydrous Na_2SO_4 and concentrated under reduced pressure at rt. The crude material was purified via flash silica column chromatography (1:9 EtOAc: hexane) to afford **217** as a colorless oil (0.0571g, 72% yield over two steps). ^{1}H NMR (600 MHz, $CDCl_3$) δ 3.82 (p, 1H), 3.65 (s, 1H), 3.43 (dd, *J* = 10.9, 4.4 Hz, 1H), 3.32 (dd, 1H), 1.54 – 1.48 (m, 3H), 1.42 (td, *J* = 9.2, 4.5 Hz, 2H), 1.34 – 1.28 (m, 1H), 1.26 – 1.21 (m, 1H), 0.89 (s, 10H), 0.85 (t, 5H), 0.07 (d, *J* = 2.1 Hz, 6H). ^{13}C NMR (151 MHz, $CDCl_3$) δ 71.52, 68.83, 42.43, 38.28, 31.81, 25.94, 19.14, 18.62, 14.32, -4.49, -4.53.

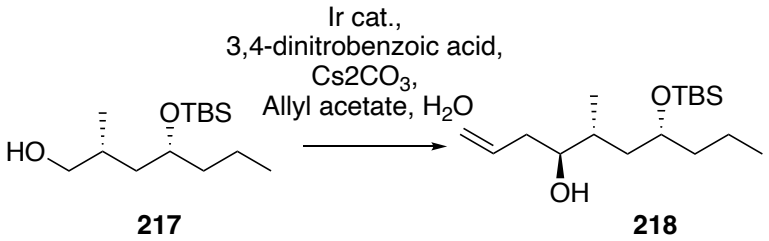
Notebook entries:

Procedure: SSP2- 038

^{1}H NMR and ^{13}C NMR: SSP2- 216


'2-216-fr.33-34-1H.1.fid
1.00
0.85
1.17
0.98
2.98
1.50
1.31
1.22
10.19
5.15
5.67
f1 (ppm)
25.94
71.52
68.83
42.43
38.28
31.81
19.14
18.62
14.32
f1 (ppm)

(4*S*,5*R*,7*R*)-7-((*tert*-butyldimethylsilyl)oxy)-5-methyldec-1-en-4-ol (218)



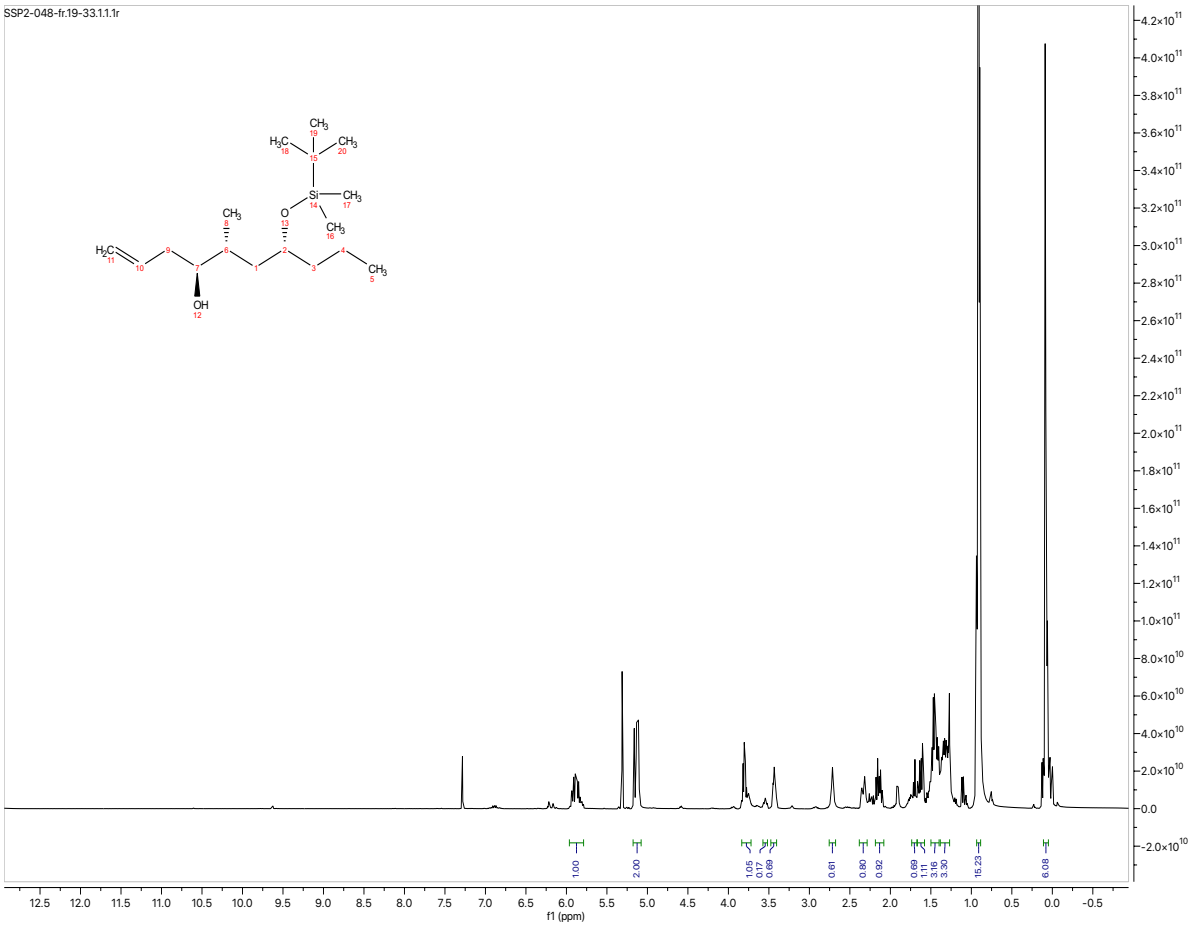
217 **218**

Alcohol **217** (0.2824 g, 1.08 mmol, 1 eq.) was dissolved in anhydrous THF (2.7 mL, 0.4M) and transferred to a pressure tube under an Ar atmosphere. Next, Iridium catalyst (0.12 g, 0.108 mmol, 0.1 eq.), 3,4 – dinitrobenzoic acid (0.023 g, 0.108 mmol, 0.1 eq.), $CsCO_3$ (0.14 g, 0.353 mmol, 1 eq.), allyl acetate (0.24 mL, 2.16 mmol, 2 eq.) and DI H_2O (~0.2 mL, 10.8 mmol, 10 eq.) was added respectively. Cap of the pressure tube was closed tightly and stirred the reaction at 100 °C overnight. The crude reaction mixture was subjected to flash silica gel column chromatography (1:9 EtOAc: hexane) to access **218** as a colorless oil (0.3239 g, quantitative yield). ^{1}H NMR (400 MHz, $CDCl_3$) δ 5.96 – 5.79 (m, 1H), 5.18 – 5.08 (m, 2H), 3.83 – 3.72 (m, 1H), 3.43 (ddd, *J* = 9.2, 6.2, 3.4 Hz, 1H), 2.71 (s, 1H), 2.34 (dddt, *J* = 14.2, 6.3, 3.2, 1.5 Hz, 1H), 2.14 (dt, *J* = 14.3, 8.1 Hz, 1H), 1.70 (dd, *J* = 12.9, 6.5 Hz, 1H), 1.67 – 1.58 (m, 1H), 1.50 – 1.40 (m, 3H), 1.38 – 1.27 (m, 3H), 0.93 – 0.89 (m, 15H), 0.08 (dd, *J* = 7.6, 3.1 Hz, 6H).

Notebook entries:

Procedure: SSP2- 225

^{1}H NMR: SSP2-048


SSP2-048-fr.19-33.1.1.1r
f1 (ppm)

***Tert*-butyl(((4*R*,6*R*,7*S*)-7-((4-methoxybenzyl)oxy)-6-methyldec-9-en-4-yl)oxy)dimethylsilane (219)**



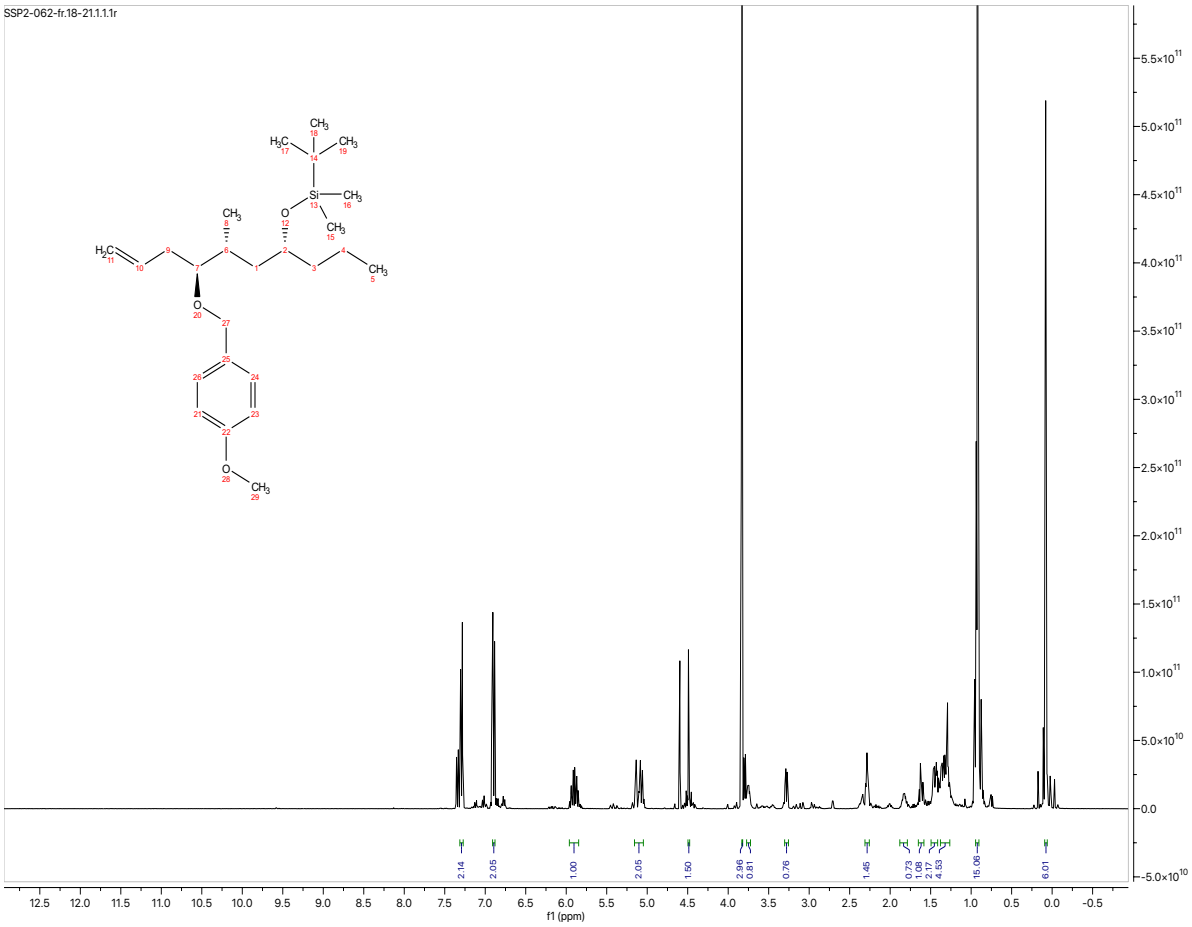
218 **219**

Alcohol **218** (0.0514 g, 0.171 mmol, 1 eq.) was dissolved in anhydrous THF (0.86 mL, 0.2M) in a flame dried RBF under an Ar atmosphere. Next, TBAI (0.0032 g, 0.0086 mmol, 0.05 eq.), 0.5M KHMDS solution in toluene (0.69 mL, 0.342 mmol, 2 eq.) followed by PMBCl (0.023 mL, 0.27 mmol, 1.6 eq.) was added and stirred overnight. The reaction was quenched with a sat'd $NH_4Cl_{(aq)}$ solution, extracted with CH_2Cl_2 (x3), the combined organic layers were dried over anhydrous Na_2SO_4 and concentrated under reduced pressure at rt. The crude compound was subjected to flash silica gel column chromatography (1:9 EtOAc: hexane) to afford the PMB ether **219** (0.0436 g, 61%). ^{1}H NMR (400 MHz, $CDCl_3$) δ 7.31 – 7.27 (m, 2H), 6.91 – 6.88 (m, 2H), 5.90 (ddt, *J* = 17.1, 10.1, 6.9 Hz, 1H), 5.16 – 5.05 (m, 2H), 4.49 (d, *J* = 2.8 Hz, 1H), 3.83 (s, 3H), 3.75 (dt, *J* = 8.0, 2.3 Hz, 1H), 3.28 (dt, *J* = 6.7, 5.1 Hz, 1H), 2.28 (ddq, *J* = 6.8, 5.1, 1.6 Hz, 1H), 1.88 – 1.79 (m, 1H), 1.65 – 1.58 (m, 1H), 1.49 – 1.41 (m, 2H), 1.38 – 1.26 (m, 5H), 0.94 – 0.90 (m, 15H), 0.08 (dd, *J* = 3.7, 1.7 Hz, 6H).

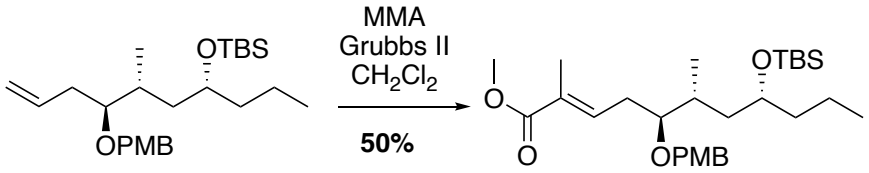
Notebook entries:

Procedure: SSP2-062

^{1}H NMR: SSP2- 062


SSP2-062-fr.18-21.1.1.1r
f1 (ppm)

Methyl(5*S*,6*R*,8*R*,*E*)-8-((*tert*-butyldimethylsilyl)oxy)-5-((4-methoxybenzyl)oxy)-2,6-dimethylundec-2-enoate (220)



219 **220**

Reaction was performed using standard protocol for cross metathesis except that 10 equivalents of the more substituted olefine, MMA was added. The crude material was subjected to flash column chromatography (1:9 EtOAc: hexane) to afford methyl ester **220** as a viscous oil in 50% yield.

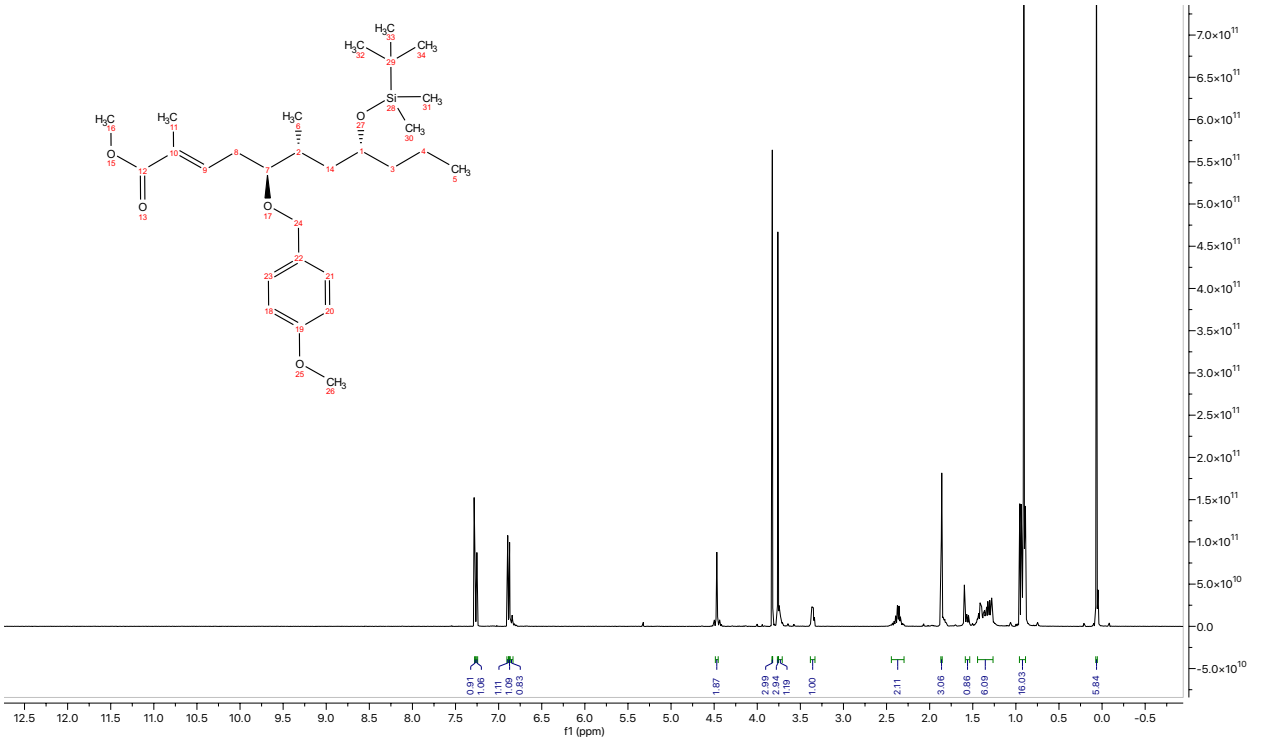
^{1}H NMR (400 MHz, $CDCl_3$) δ 7.27 (d, *J* = 2.1 Hz, 1H), 7.25 (d, *J* = 2.0 Hz, 1H), 6.89 (d, *J* = 2.1 Hz, 1H), 6.88 (d, *J* = 1.9 Hz, 1H), 6.85 (dq, *J* = 7.3, 1.4 Hz, 1H), 4.47 (d, *J* = 2.0 Hz, 2H), 3.83 (s, 3H), 3.76 (s, 3H), 3.75 – 3.71 (m, 1H), 3.36 (dt, *J* = 7.1, 4.7 Hz, 1H), 2.44 – 2.30 (m, 2H), 1.86 (d, *J* = 1.3 Hz, 3H), 1.59 – 1.54 (m, 1H), 1.44 – 1.26 (m, 6H), 0.96 – 0.89 (m, 16H), 0.06 (s, 6H).

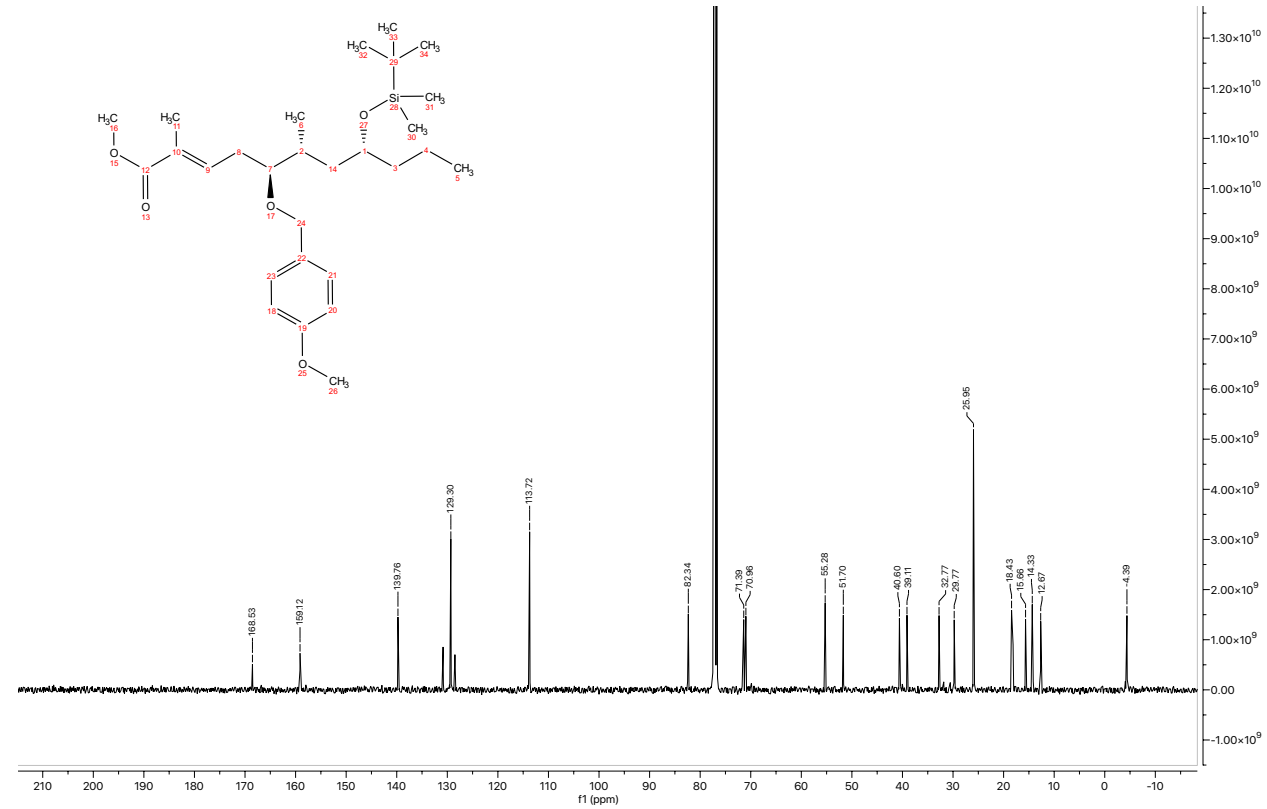
^{13}C NMR (101 MHz, $CDCl_3$) δ 168.53, 159.12, 139.76, 129.30, 113.72, 82.34, 76.72, 71.39, 70.96, 55.28, 51.70, 40.60, 39.11, 32.77, 29.77, 25.95, 18.43, 15.66, 14.33, 12.67, -4.39.

Notebook entries:

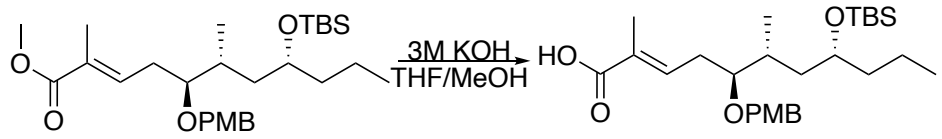
Procedure: SSP2-066

^{1}H NMR and ^{13}C NMR: SSP2-066


f1 (ppm)
0.91
1.06
1.10
1.04
0.83
1.87
2.99
2.84
1.19
1.00
2.11
3.06
0.86
6.09
16.03
5.84


f1 (ppm)
168.53
169.12
139.76
129.30
113.72
82.34
71.39
70.96
55.28
51.70
40.60
39.11
32.77
29.77
25.95
18.43
15.66
14.33
12.67
-4.39

(5S,6R,8R,E)-8-((tert-butyldimethylsilyl)oxy)-5-((4-methoxybenzyl)oxy)-2,6-dimethylundec-2-enoic acid (221)



220 **221**

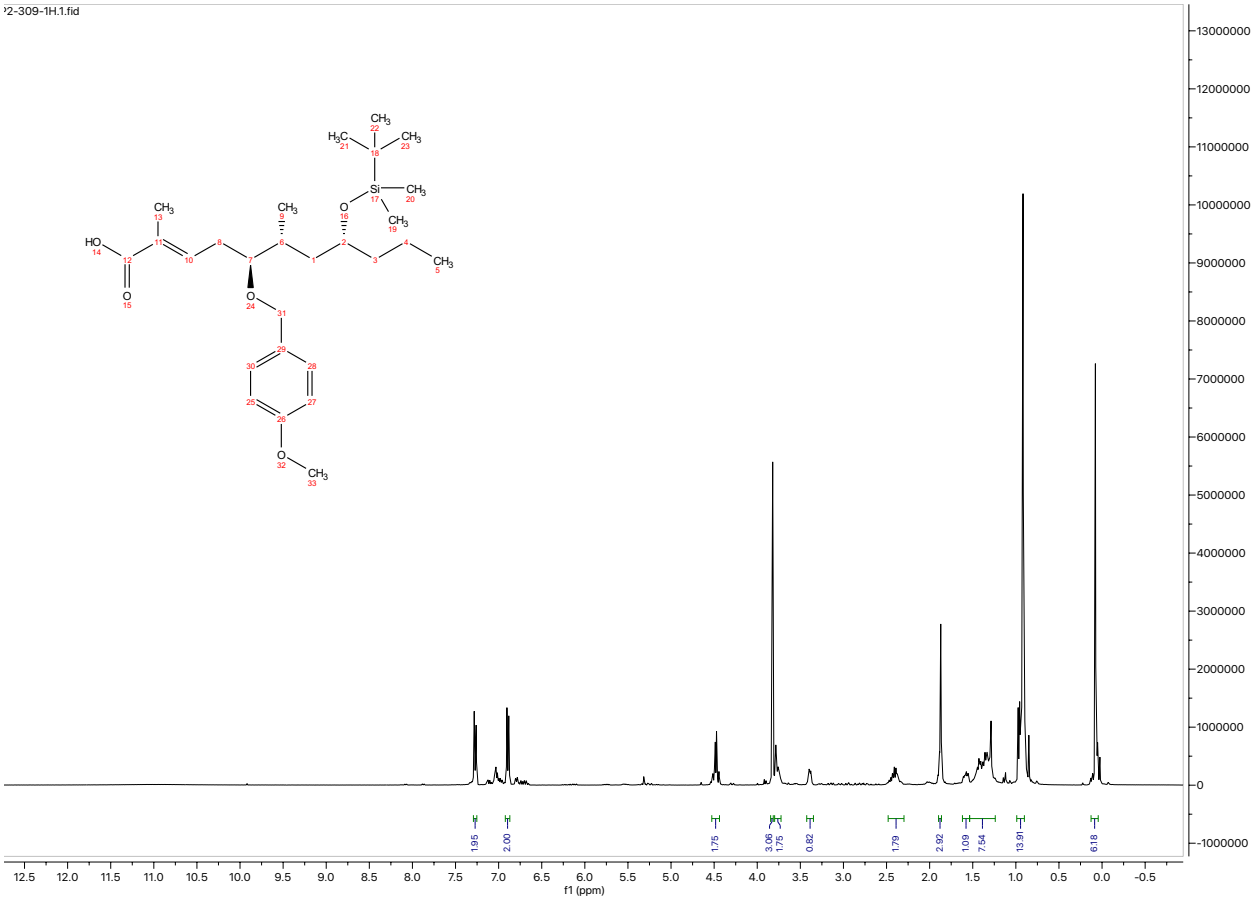
Methyl ester **220** (0.0644 g, 0.131 mmol, 1 eq) was dissolved in 1:1 mixture of THF:MeOH (1.3 mL, 0.1M). Next, a freshly prepared solution of aq. 3M KOH (~0.9 mL, 0.15M) was added and refluxed at boiling point of MeOH for 5 h. Reaction mixture was gradually brought to rt and quenched with a 1M HCl ($_{aq}$) solution until the reaction pH ~1. Resulting crude mixture was extracted with CH_2Cl_2 (x3), combined organic layers were dried over anhydrous Na_2SO_4 and concentrated under reduced pressure at rt to access carboxylic acid **221** as a white solid.

^{1}H NMR (400 MHz, $CDCl_3$) δ 7.27 (d, *J* = 8.9 Hz, 2H), 6.92 – 6.87 (m, 2H), 4.53 – 4.44 (m, 2H), 3.82 (s, 3H), 3.77 (dt, *J* = 13.5, 3.5 Hz, 2H), 3.39 (dt, *J* = 7.9, 4.4 Hz, 1H), 2.48 – 2.30 (m, 2H), 1.87 (s, 3H), 1.58 (ddt, *J* = 13.6, 7.5, 3.5 Hz, 1H), 1.54 – 1.24 (m, 8H), 0.99 – 0.90 (m, 14H), 0.07 (d, *J* = 5.0 Hz, 6H).

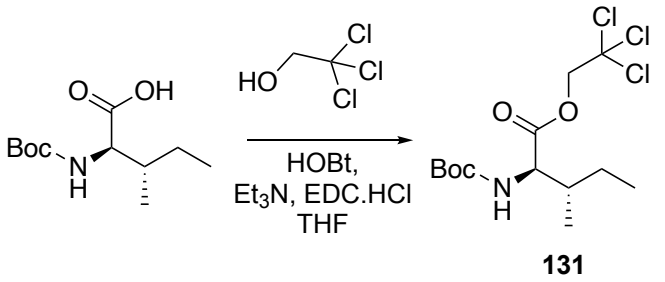
Notebook entries:

Procedure: SSP2- 309

^{1}H NMR and ^{13}C NMR: SSP2-309 (Crude)


2-309-1H.1.fid
f1 (ppm)
1.95
2.00
1.75
3.06
1.75
0.82
1.79
2.92
1.09
7.54
13.91
6.18

2,2,2-trichloroethyl (*tert*-butoxycarbonyl)-*D*-alloisoleucinate (131)



131

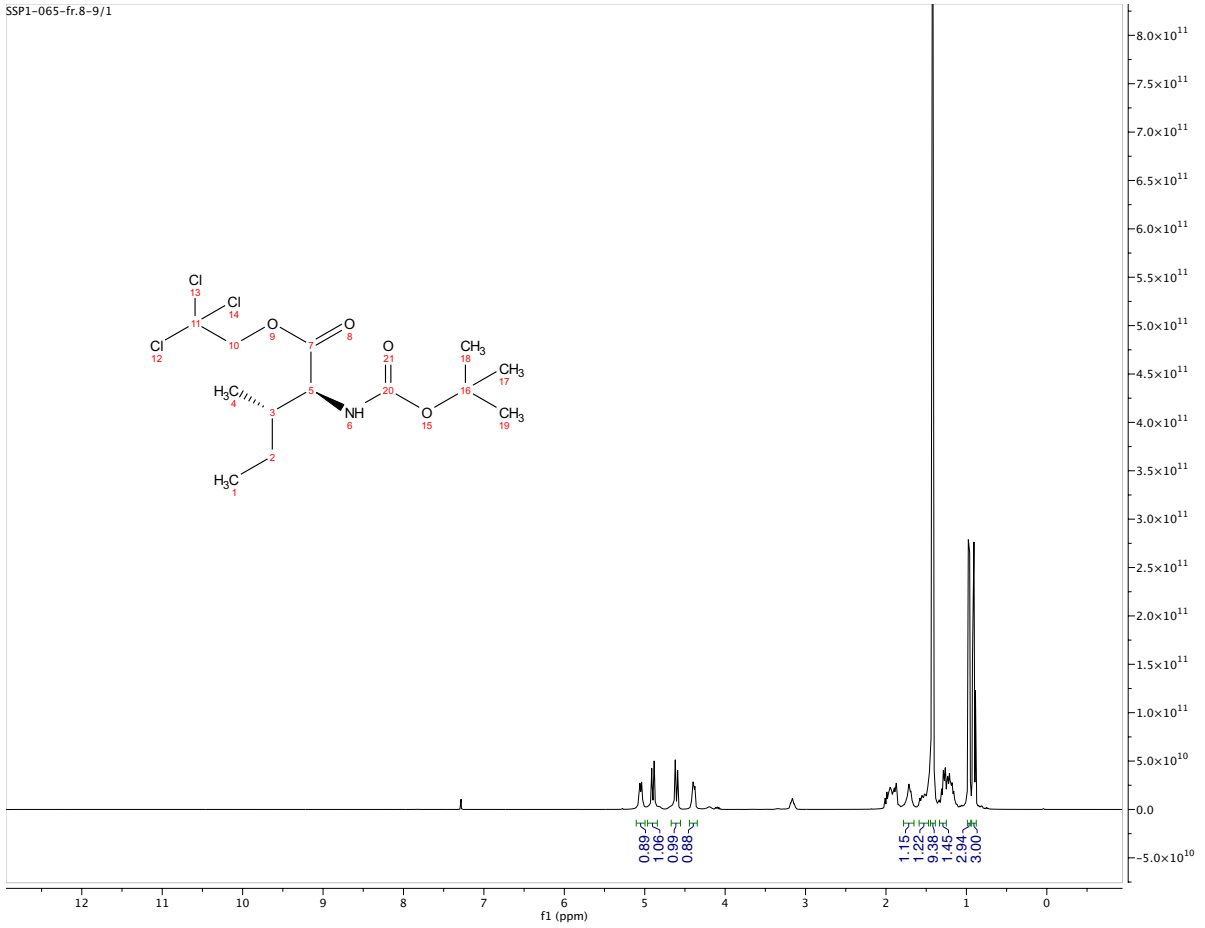
Reaction was performed using EDC·HCl mediated standard peptide coupling conditions to afford **131** in 95% yield after purification via flash column chromatography (1:9 EtOAc: hexane).

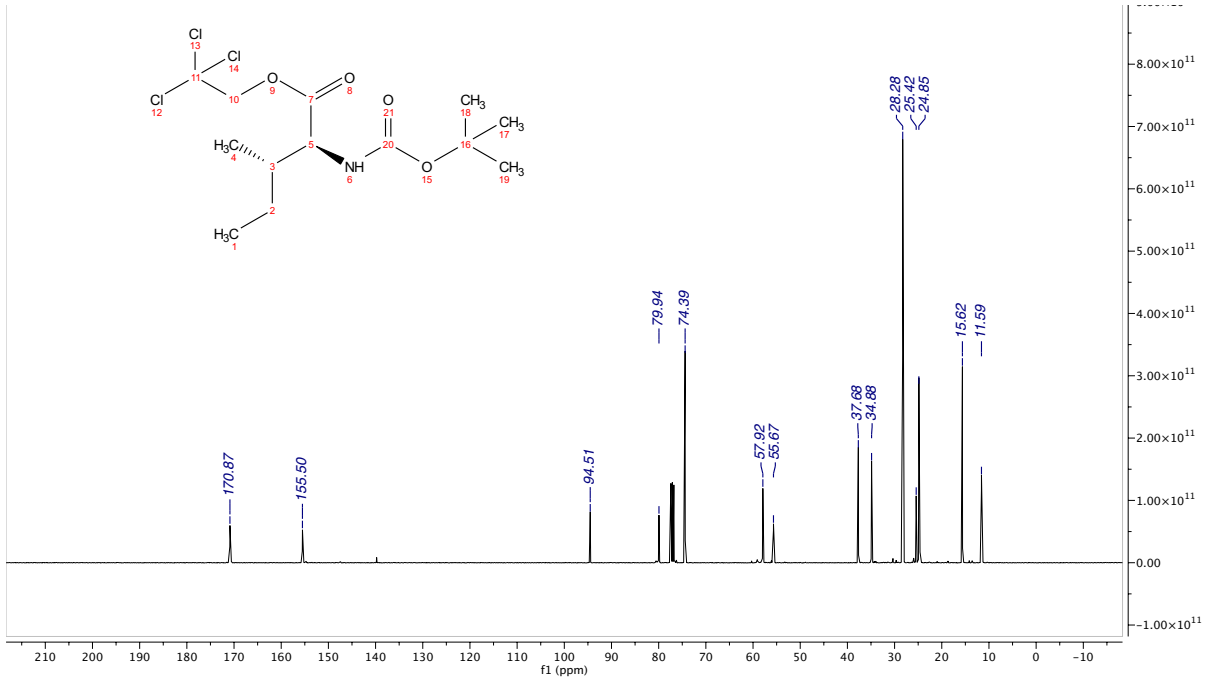
^{1}H NMR (400 MHz) δ 5.05 (d, *J* = 9.2 Hz), 4.90 (d, *J* = 12.0 Hz), 4.61 (d, *J* = 12.0 Hz), 4.39 (dd, *J* = 9.1, 4.5 Hz), 1.78 – 1.65 (m), 1.59 – 1.47 (m), 1.42 (d, *J* = 1.8 Hz), 1.33 – 1.25 (m), 0.97 (d, *J* = 6.9 Hz), 0.91 (t, *J* = 7.4 Hz). ^{13}C NMR (101 MHz,) δ 170.87, 155.50, 94.51, 79.94, 74.39, 57.92, 55.67, 37.68, 34.88, 28.28, 25.42, 24.85, 15.62, 11.59.

Notebook entries:

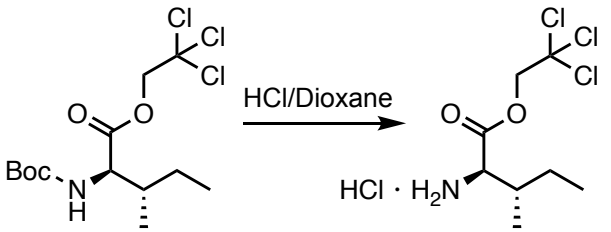
Procedure: SSP1-262

^{1}H NMR and ^{13}C NMR: SSP1-065 (Crude)


SSP1-065-fr.8-9/1
0.89
1.06
0.99
0.88
1.15
1.22
9.38
1.45
2.94
3.00
f1 (ppm)


170.87
155.50
94.51
79.94
74.39
57.92
55.67
37.68
34.88
28.28
25.42
24.85
15.62
11.59
f1 (ppm)

2,2,2-trichloroethyl *D*-alloisoleucinate hydrochloride (S4)



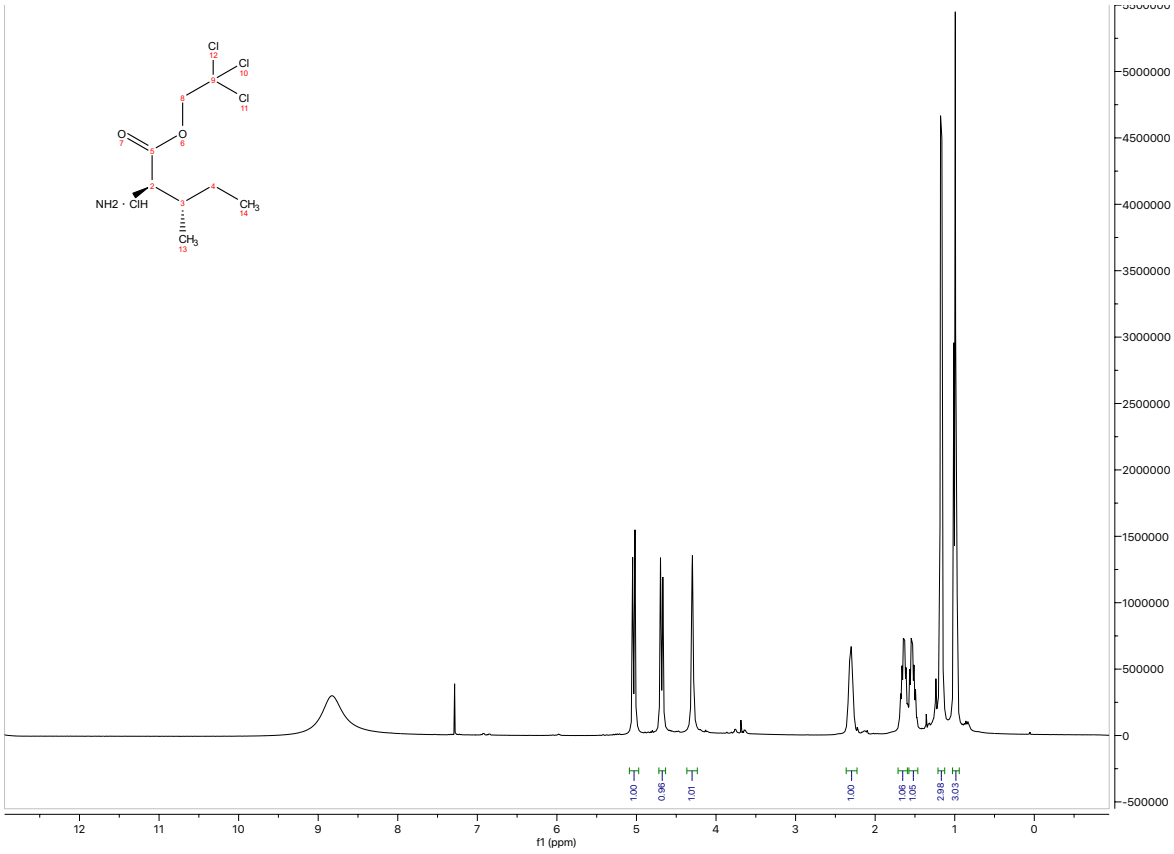
131 **S4**

Reaction was performed using standard Boc deprotection conditions to obtain the free amine **S4** in quantitative yield. ^{1}H NMR (400 MHz, $CDCl_3$) δ 5.03 (d, *J* = 11.7 Hz, 1H), 4.68 (d, *J* = 11.8 Hz, 1H), 4.37 – 4.24 (m, 1H), 2.31 (q, *J* = 7.3 Hz, 1H), 1.65 (dq, *J* = 13.6, 6.5 Hz, 1H), 1.58 – 1.46 (m, 1H), 1.17 (d, *J* = 6.7 Hz, 3H), 0.99 (t, *J* = 7.2 Hz, 3H).

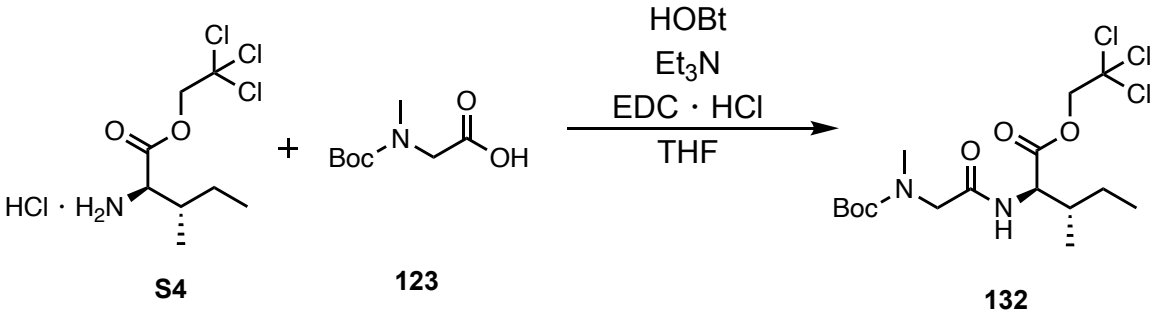
Notebook entries:

Procedure: SSP1-267

^{1}H NMR and ^{13}C NMR: SSP2- (Crude)


Cl
Cl
Cl
O
O
NH2 · ClH
CH3
CH3
1.00
0.96
1.01
1.00
1.06
1.05
2.98
3.03
f1 (ppm)

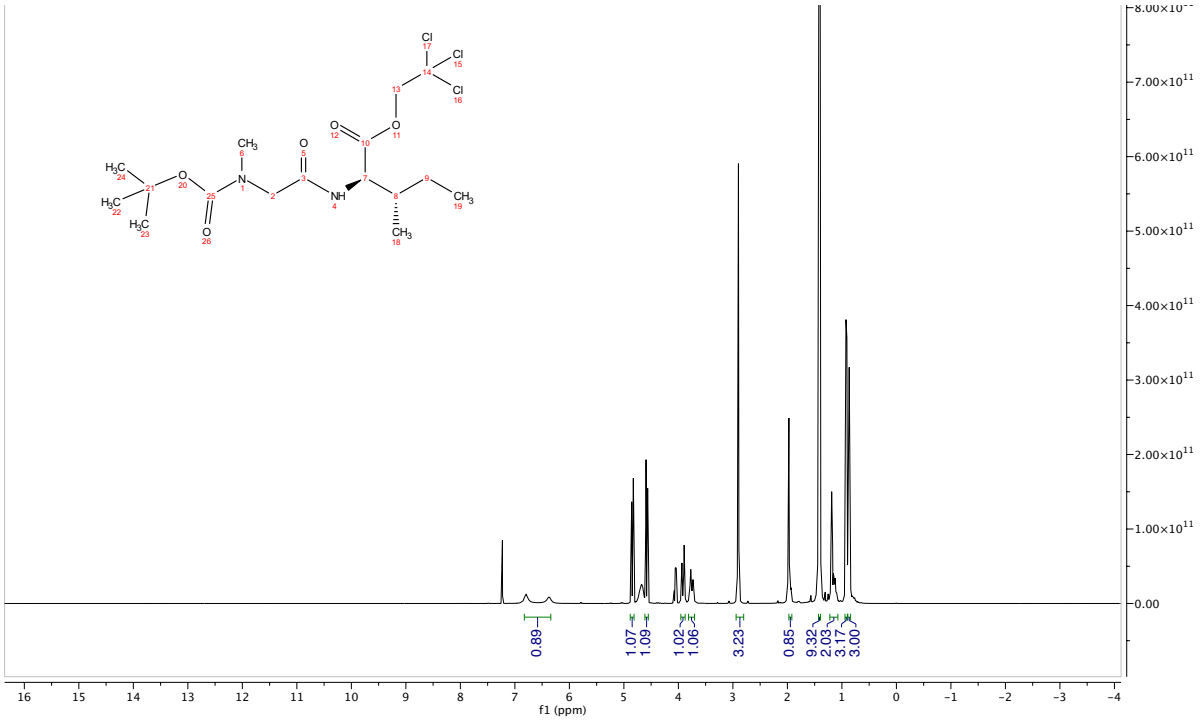
2,2,2-trichloroethyl *N*-(*tert*-butoxycarbonyl)-*N*-methylglycyl-*D*-alloisoleucinate (132)



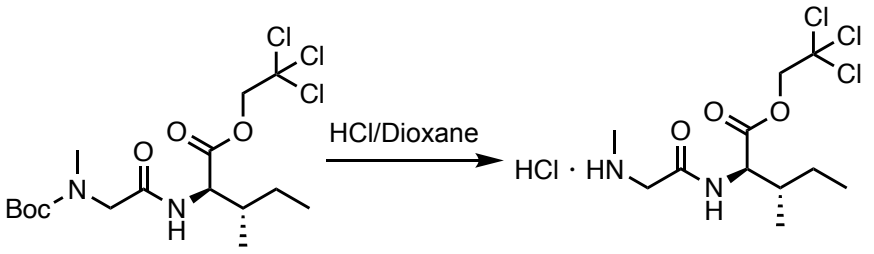
S4 **123** **132**

Reaction was performed using EDC·HCl mediated standard peptide coupling conditions to afford **132** in quantitative yield after purification via flash column chromatography (1:2 EtOAc: hexane). ^{1}H NMR (400 MHz,) δ 6.58 (d, *J* = 168.7 Hz), 4.84 (dd, *J* = 12.0, 1.5 Hz), 4.58 (dd, *J* = 12.0, 1.5 Hz), 3.92 (d, *J* = 16.3 Hz), 3.75 (d, *J* = 16.6 Hz), 2.90, 1.97 – 1.92 (m), 1.41 (d, *J* = 1.8 Hz), 1.22 – 1.07 (m), 0.92 (dd, *J* = 7.0, 1.6 Hz), 0.87 (t, *J* = 7.3 Hz).

Notebook entries: Procedure: SSP1-270; ^{1}H NMR: SSP1-070


f1 (ppm)
0.89
1.07
1.09
1.02
1.06
3.23
0.85
9.32
2.03
3.17
3.00

2,2,2-trichloroethyl methylglycyl-*D*-alloisoleucinate hydrochloride (S5)



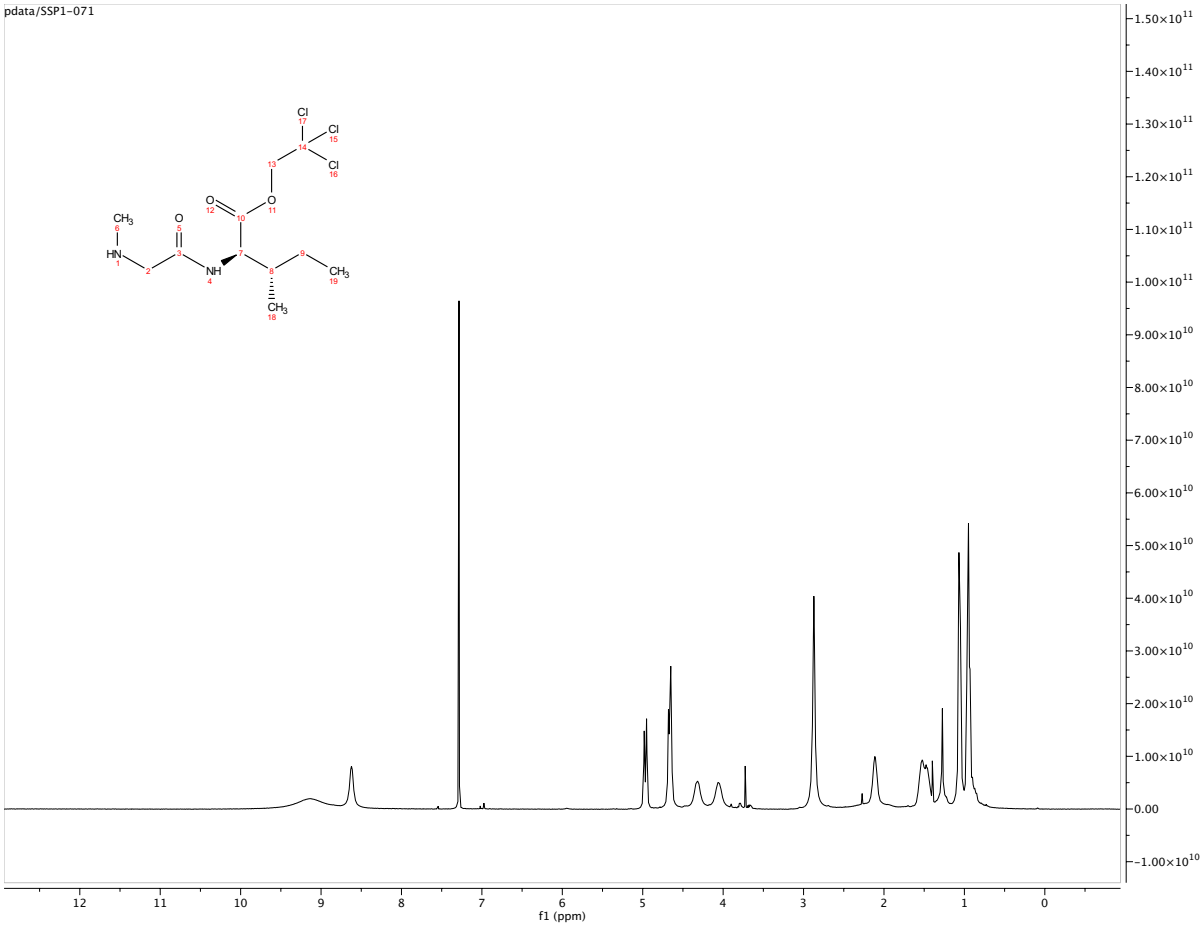
132 **S5**

Reaction was performed using standard Boc deprotection conditions to obtain the free amine **S5** in quantitative yield. Crude was carried forward to next step without further purification.

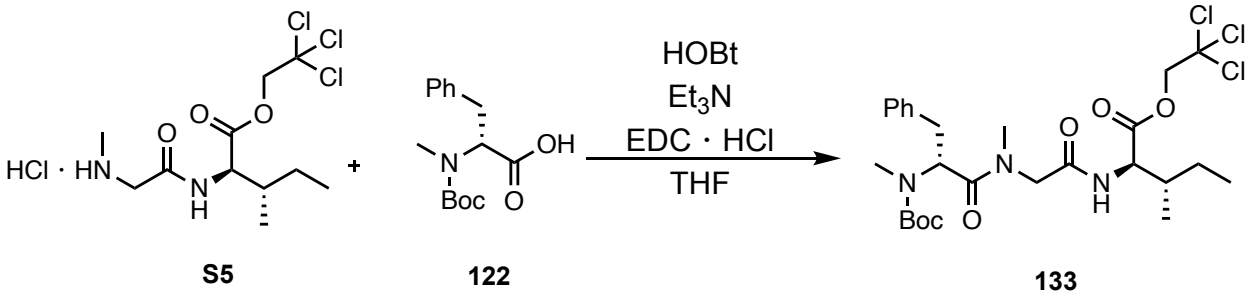
Notebook entries:

Procedure: SSP1-339

^{1}H NMR: SSP1- 071(Crude)


pdata/SSP1-071
Cl
17
Cl
15
Cl
16
13
14
O
12
O
11
10
CH3
6
O
5
HN
1
2
3
NH
4
7
8
9
CH3
19
CH3
18
1.50×10^11
1.40×10^11
1.30×10^11
1.20×10^11
1.10×10^11
1.00×10^11
9.00×10^10
8.00×10^10
7.00×10^10
6.00×10^10
5.00×10^10
4.00×10^10
3.00×10^10
2.00×10^10
1.00×10^10
0.00
-1.00×10^10
12
11
10
9
8
7
6
5
4
3
2
1
0
f1 (ppm)

2,2,2-trichloroethyl *N*-(*N*-(*tert*-butoxycarbonyl)-*N*-methyl-*D*-phenylalanyl)-*N*-methylglycyl-*D*-alloisoleucinate (133)



S5 **122** **133**

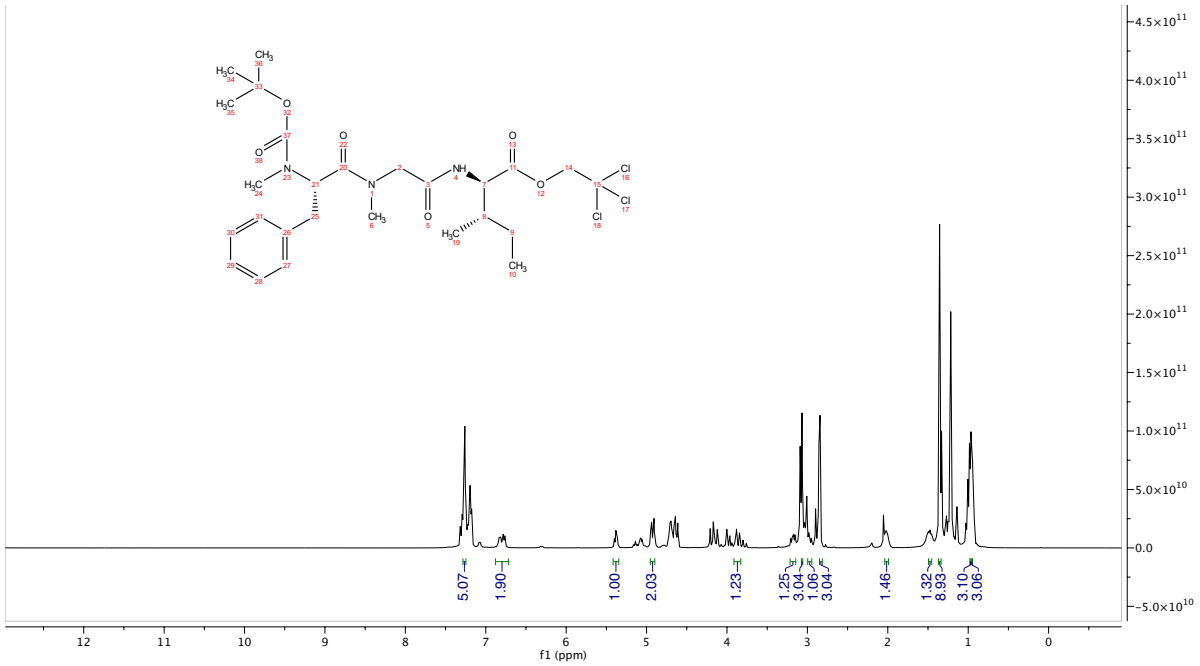
Reaction was performed using EDC·HCl mediated standard peptide coupling conditions to afford **133** in 79% yield after purification via flash column chromatography (1:2 EtOAc: hexane).

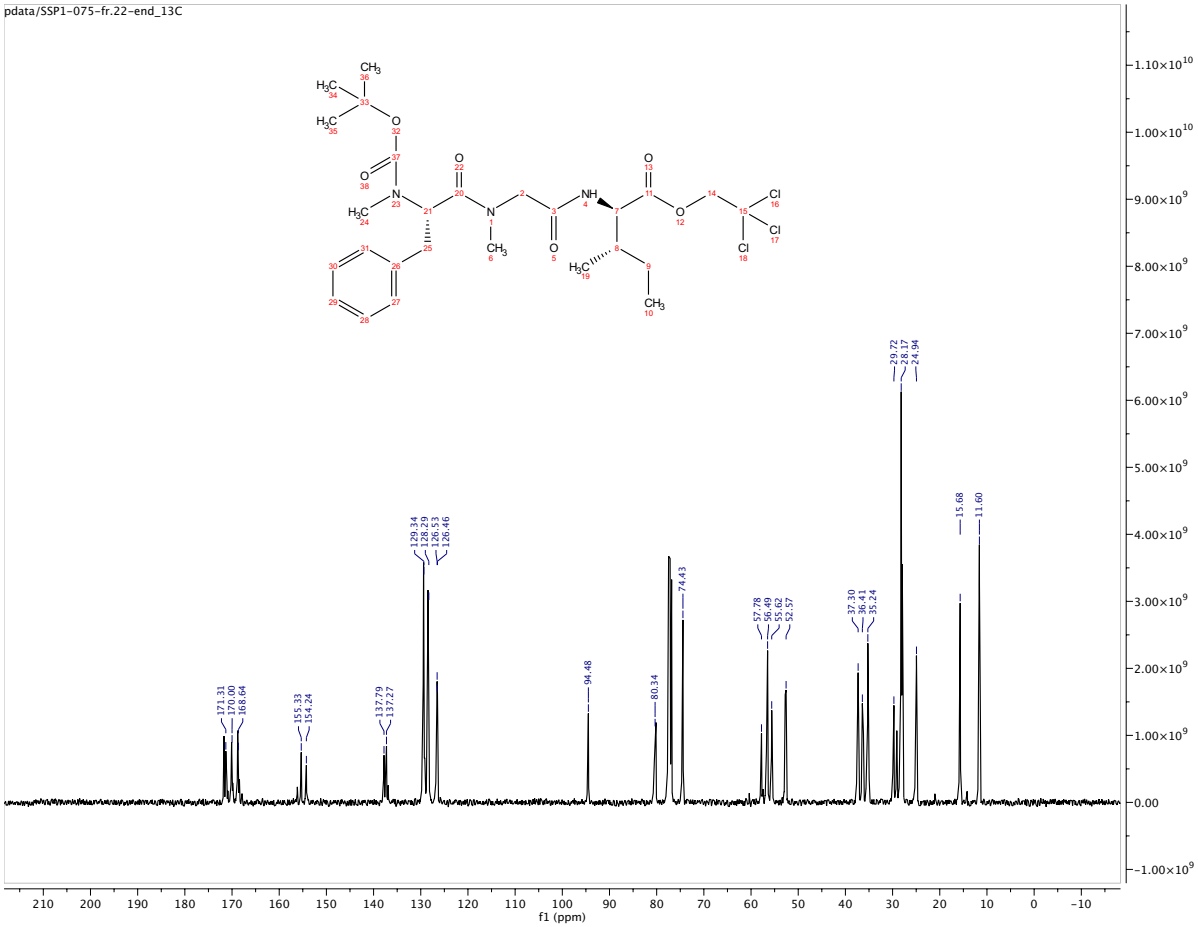
^{1}H NMR (400 MHz) δ 7.27 (d, *J* = 5.8 Hz), 6.80 (dd, *J* = 20.7, 8.6 Hz), 5.38 (t, *J* = 7.7 Hz), 4.93 (dd, *J* = 11.9, 4.7 Hz), 3.91 – 3.83 (m), 3.18 (dd, *J* = 14.0, 7.1 Hz), 3.07, 3.00 – 2.95 (m), 2.84, 2.04 – 1.99 (m), 1.49 – 1.45 (m), 1.36, 0.97, 0.95 (d, *J* = 3.6 Hz). ^{13}C NMR (101 MHz) δ 171.31, 170.00, 168.64, 155.33, 154.24, 137.79, 137.27, 129.34, 128.29, 126.53, 126.46, 94.48, 80.34, 74.43, 57.78, 56.49, 55.62, 52.57, 37.30, 36.41, 35.24, 29.72, 28.17, 24.94, 15.68, 11.60.

Notebook entries:

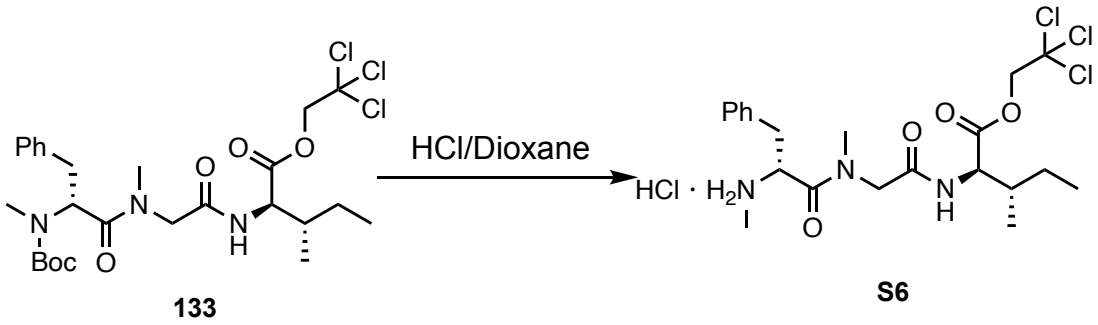
Procedure: SSP1-088

^{1}H NMR and ^{13}C NMR: SSP1-075


5.07
1.90
1.00
2.03
1.23
1.25
3.04
1.06
3.04
1.46
1.32
8.93
3.10
3.06
f1 (ppm)


pdata/SSP1-075-fr.22-end_13C
171.31
170.00
168.64
155.33
154.24
137.79
137.27
129.34
128.29
126.53
126.46
94.48
80.34
74.43
57.78
56.48
55.62
52.57
37.30
36.41
35.24
29.72
28.17
24.94
15.68
11.60
f1 (ppm)

2,2,2-trichloroethyl *N*-methyl-*N*-(methyl-*D*-phenylalanyl)glycyl-*D*-alloisoleucinate hydrochloride (S6)

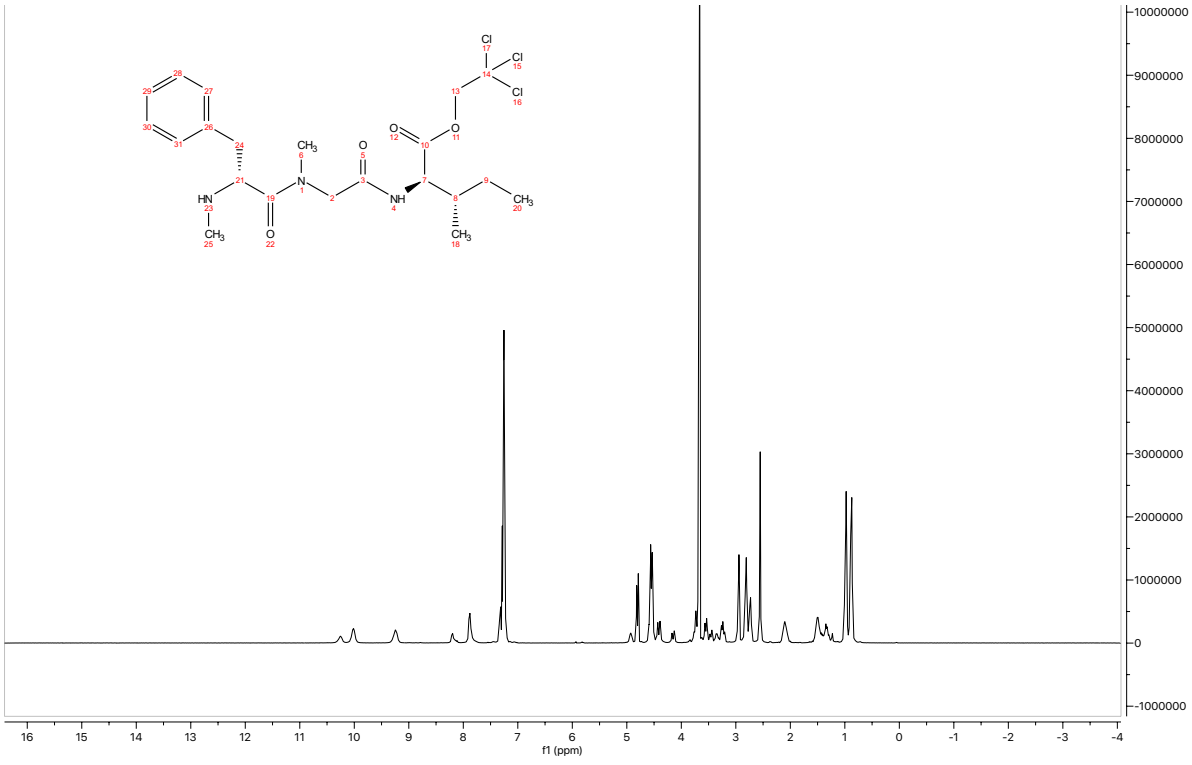


Reaction was performed using standard Boc deprotection conditions to obtain the free amine **S6** in quantitative yield. Crude was carried forward to next step.

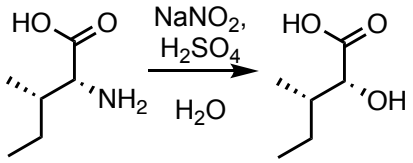
Notebook entries:

Procedure: SSP1-082

^{1}H NMR and: SSP1-082 (Crude)



(2*R*,3*S*)-2-hydroxy-3-methylpentanoic acid (124)



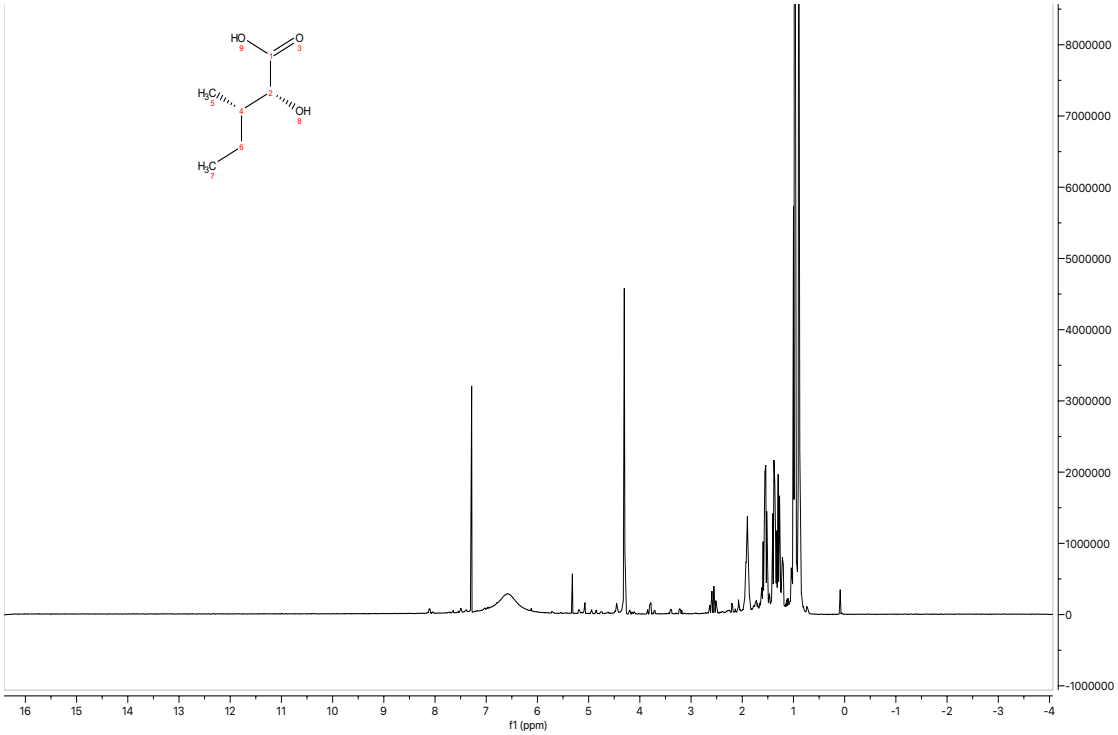
120 **124**

D-alloisoleucine (0.025 g, 0.191 mmol,1 eq.) was dissolved in 2N H_2SO_4 (~0.6 mL, 0.571 mmol, 3 eq.). Cooled the solution to 0˚C and a freshly prepared solution of sodium nitrite (0.132 g, 1.91 mmol, 10 eq.) in deionized water (0.6 mL) was added slowly over a period of 30 minutes. Ice bath was removed, and the reaction was stirred at rt for 40 hours. Saturated the reaction mixture with $NaCl_{(s)}$, extracted to EtOAc, the combined organic layers were washed with water (x2) followed by a sat'd brine solution (x2), dried over anhydrous sodium sulfate, and concentrated under vacuum to give (2*R*,3*S*)-2-hydroxy-3-methylpentanoic acid as a pale-yellow viscous liquid. (0.0822g, 99% yield). ^{1}H NMR (400 MHz) δ 4.28 (d, *J* = 2.8 Hz, 1H), 1.88 (dtt, *J* = 13.5, 8.9, 4.4 Hz, 1H), 1.52 (dq, *J* = 14.4, 7.2 Hz, 1H), 1.39 – 1.30 (m, 1H), 0.96 (t, *J* = 7.4 Hz, 3H), 0.87 (d, *J* = 6.9 Hz, 3H).

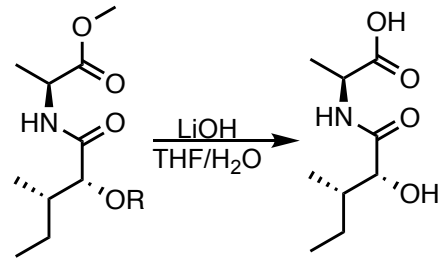
Notebook entries:

Procedure: SSP1-056

^{1}H NMR: SSP1-056 (Crude)


HO
9
O
3
1
2
H3C
5
4
OH
8
6
H3C
7
8000000
7000000
6000000
5000000
4000000
3000000
2000000
1000000
0
-1000000
16
15
14
13
12
11
10
9
8
7
6
5
4
3
2
1
0
-1
-2
-3
-4
f1 (ppm)

((2*R*,3*S*)-2-hydroxy-3-methylpentanoyl)-*L*-alanine (116)



R = OAc (**127'**)
R = H (**128**)

116

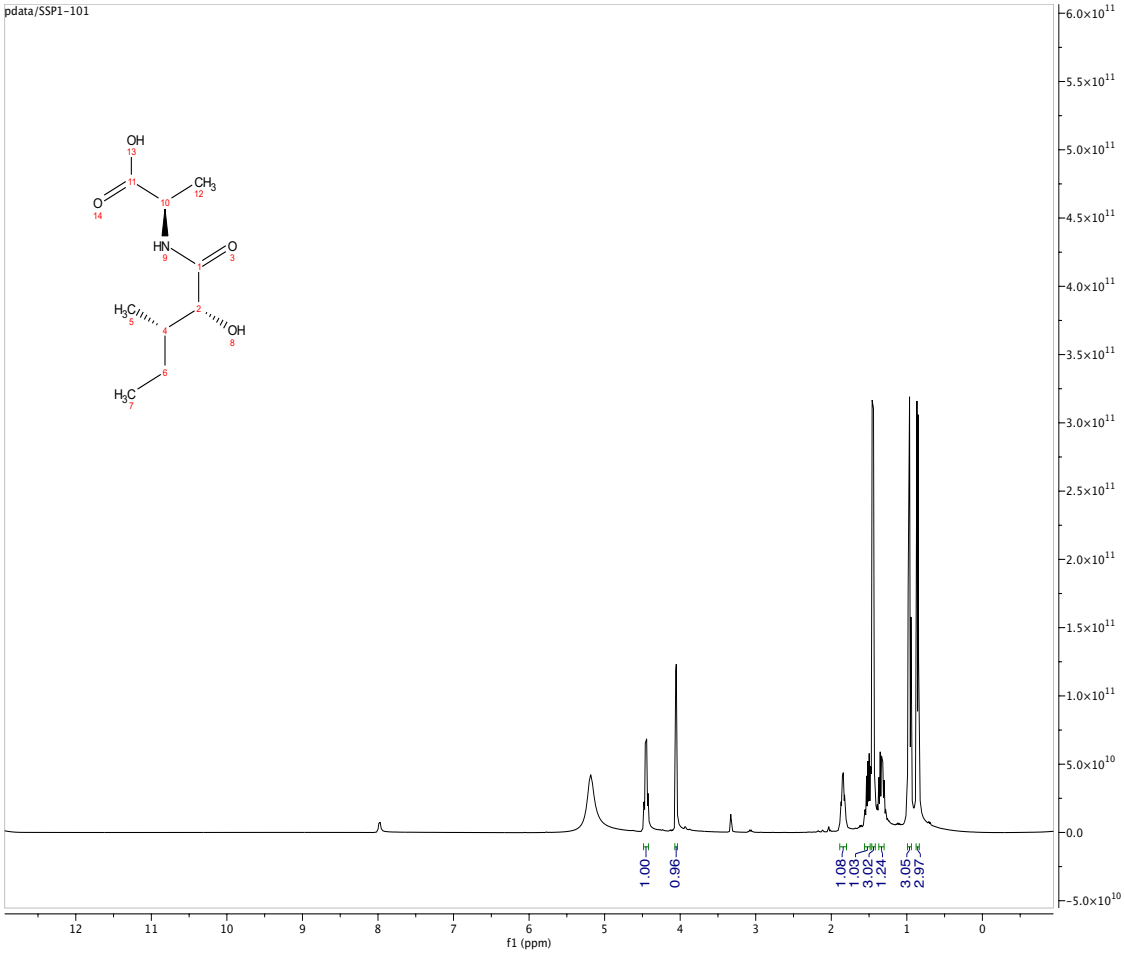
Reaction was performed using standard Boc deprotection conditions to obtain the carboxylic acid **116** in quantitative yield.

^{1}H NMR (400 MHz) δ 4.45 (q, *J* = 7.2 Hz), 4.06 (d, *J* = 2.9 Hz), 1.84 (pd, *J* = 7.0, 2.6 Hz), 1.52 (dd, *J* = 13.9, 7.1 Hz), 1.45 (d, *J* = 7.3 Hz), 1.37 – 1.30 (m), 0.96 (t, *J* = 7.5 Hz), 0.86 (d, *J* = 6.9 Hz).

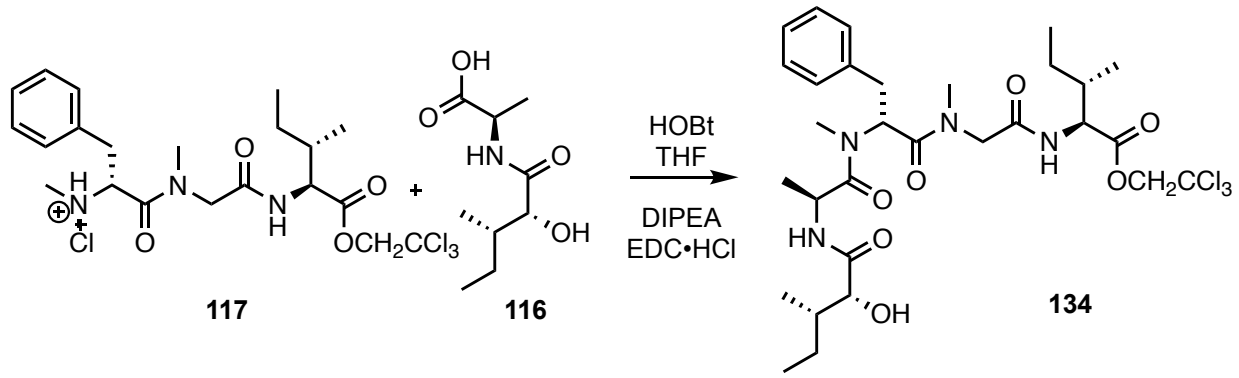
Notebook entries:

Procedure: SSP1- 285

^{1}H NMR: SSP1- 101 (Crude)


pdata/SSP1-101
OH
13
11
CH3
12
O
14
10
HN
9
1
O
3
H3C
5
2
OH
8
4
6
H3C
7
6.0x10^11
5.5x10^11
5.0x10^11
4.5x10^11
4.0x10^11
3.5x10^11
3.0x10^11
2.5x10^11
2.0x10^11
1.5x10^11
1.0x10^11
5.0x10^10
0.0
-5.0x10^10
1.00
0.96
1.08
1.03
3.02
1.24
3.05
2.97
12
11
10
9
8
7
6
5
4
3
2
1
0
f1 (ppm)

2,2,2-trichloroethyl *N*-(*N*-(((2*R*,3*S*)-2-hydroxy-3-methylpentanoyl)-*L*-alanyl)-*N*-methyl-*D*-phenylalanyl)-*N*-methylglycyl-*L*-isoleucinate (134)



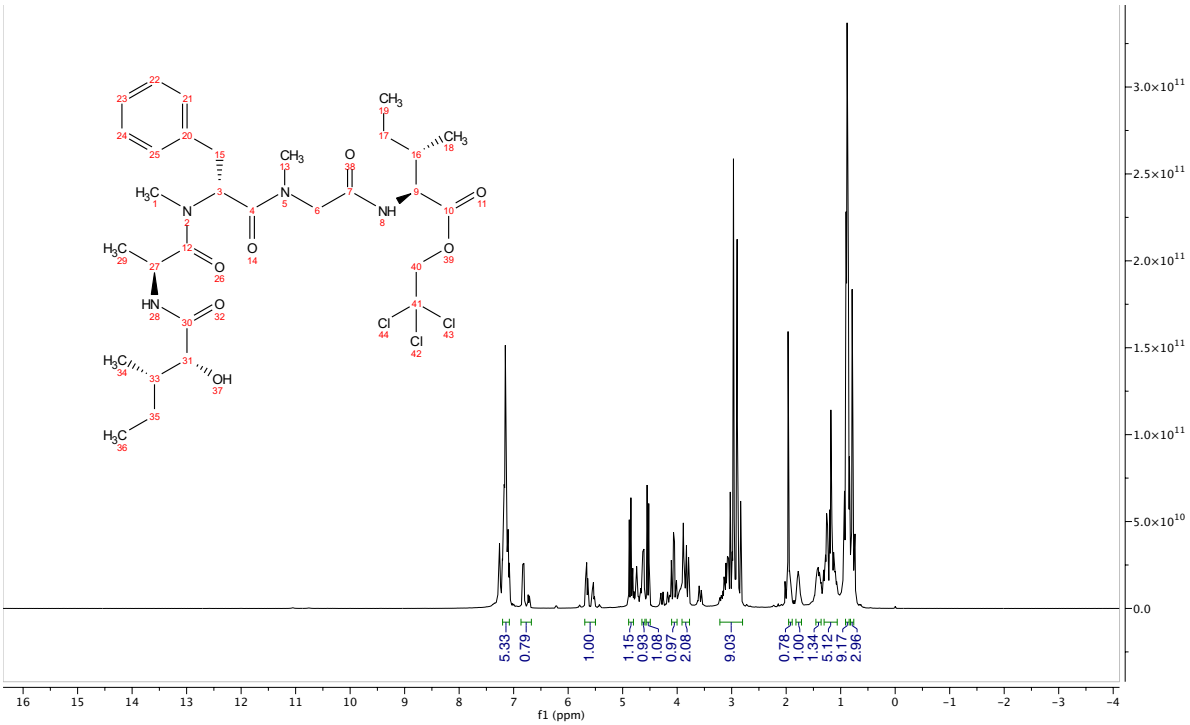
Standard peptide coupling protocol was used to access the pentapeptide **134** in 63% yield.

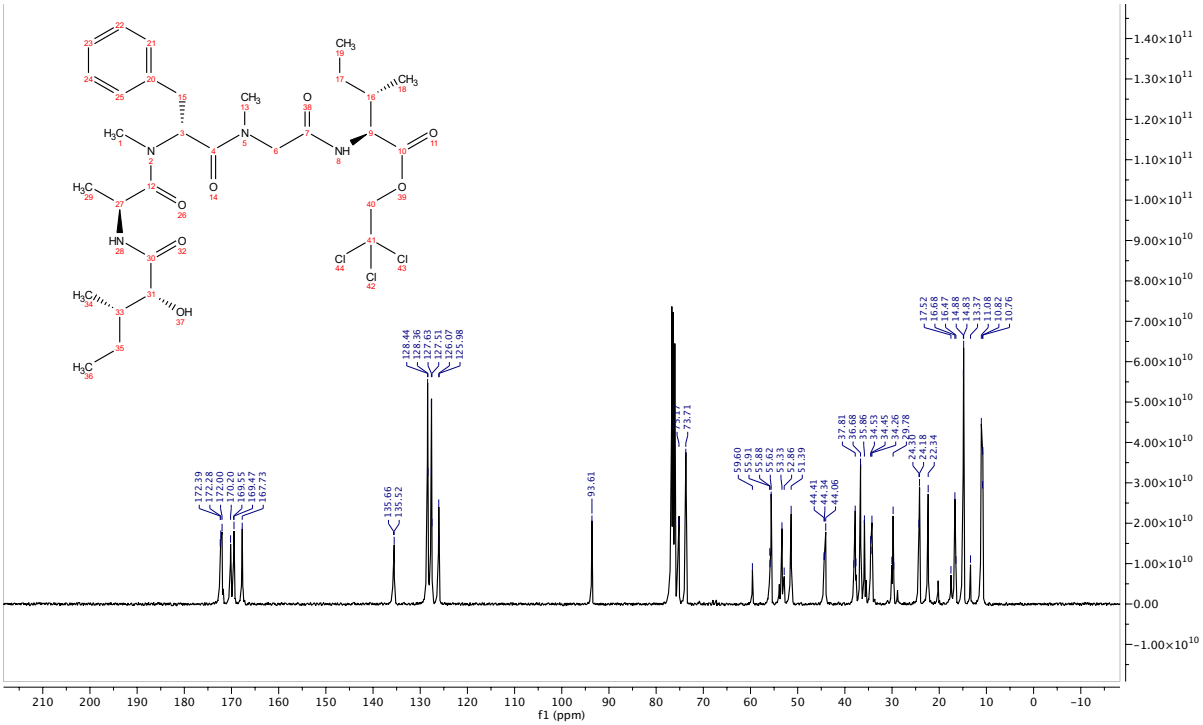
^{1}H NMR (400 MHz,) δ 7.20 – 7.08 (m), 6.77 (dd, *J* = 39.6, 8.6 Hz), 5.70 – 5.50 (m), 4.89 – 4.80 (m), 4.63 (dd, *J* = 8.6, 4.8 Hz), 4.53 (dd, *J* = 11.9, 2.7 Hz), 4.04 (dd, *J* = 14.5, 7.3 Hz), 3.91 – 3.77 (m), 3.22 – 2.80 (m), 1.93 (ddd, *J* = 11.5, 5.5, 3.3 Hz), 1.77 (tdt, *J* = 12.9, 9.7, 4.9 Hz), 1.41 (ddt, *J* = 17.0, 7.9, 3.2 Hz), 1.30 – 1.06 (m), 0.88 (ddd, *J* = 10.0, 7.0, 3.0 Hz), 0.79 (t, *J* = 7.5 Hz). ^{13}C NMR (101 MHz,) δ 172.39, 172.28, 172.00, 170.20, 169.55, 169.47, 167.73, 135.66, 135.52, 128.44, 128.36, 127.63, 127.51, 126.07, 125.98, 93.61, 75.17, 73.71, 59.60, 55.91, 55.88, 55.62, 53.33, 52.86, 51.39, 44.41, 44.34, 44.06, 38.11, 37.81, 37.65, 36.68, 35.86, 34.53, 34.45, 34.26, 30.04, 29.78, 29.64, 24.30, 24.18, 22.34, 17.52, 16.68, 16.47, 14.88, 14.83, 13.37, 11.08, 10.82, 10.76.

Notebook entries:

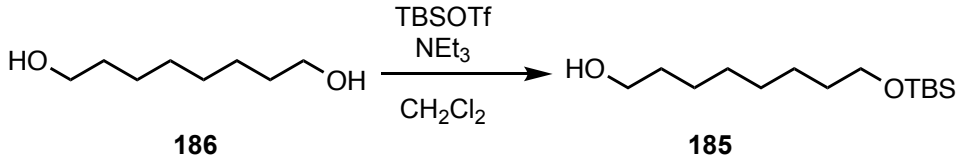
Procedure: SSP1- 083

^{1}H NMR: SSP1- 083


5.33
0.79
1.00
1.15
0.93
1.08
0.97
2.08
9.03
0.78
1.00
1.34
5.12
9.17
2.96
f1 (ppm)


172.39
172.28
172.00
170.00
169.55
169.47
167.73
135.66
135.52
128.44
128.36
128.03
127.51
126.07
125.98
93.61
73.71
59.60
55.91
55.88
55.62
53.33
52.86
51.39
44.41
44.34
44.06
37.81
36.68
35.86
34.51
34.45
34.26
30.78
24.30
24.18
22.34
17.52
16.68
16.47
14.88
13.37
11.08
10.82
10.76
f1 (ppm)

8-((*tert*-butyldimethylsilyl)oxy)octan-1-ol (185)



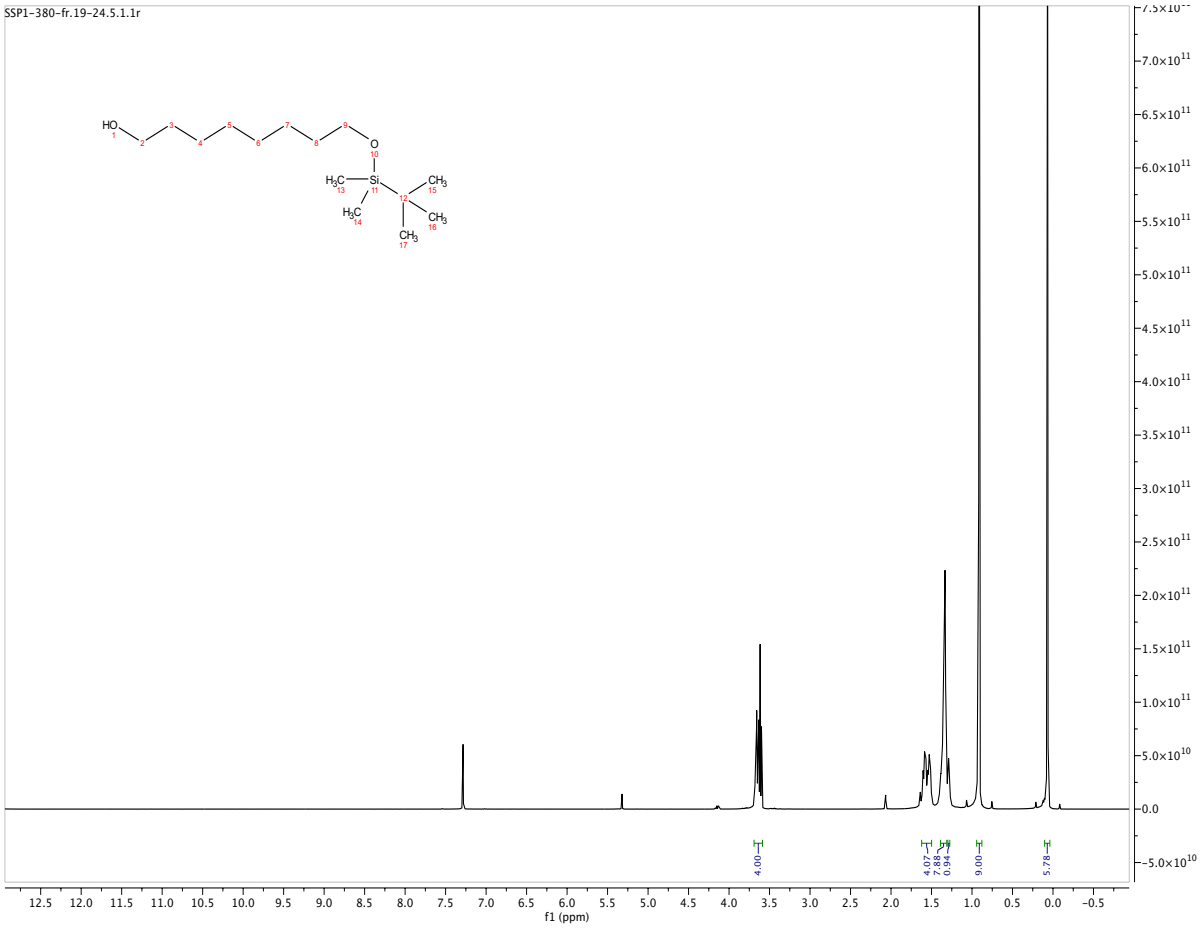
186 **185**

In a flame dried RBF, diol **186** (0.5 g, 3.42 mmol, 1eq.) was dissolved in anhydrous CH_2Cl_2 (4 mL, 0.9M). Few drops of DMF were added to increase solubility and cooled to 0˚C. NEt_3 (1 mL, 6.84 mmol, 2eq.) followed by TBSOTf (0.8 mL, 3.42 mmol, 1eq.) were added under Ar at 0˚C and reaction was stirred at rt overnight. The reaction was quenched with a sat'd $NH_4Cl_{(aq)}$ solution, extracted with CH_2Cl_2 (x3), the combined organic layers were dried over anhydrous Na_2SO_4 and concentrated under reduced pressure. The crude compound was subjected to flash silica gel column chromatography (1:3 EtOAc: hexane) to afford **185** as a colorless viscous oil (0.221 g, 25% yield). ^{1}H NMR (400 MHz, $CDCl_3$) δ 3.64 (dt, *J* = 16.9, 6.7 Hz, 4H), 1.62 – 1.50 (m, 4H), 1.39 – 1.31 (m, 8H), 1.28 (d, *J* = 4.0 Hz, 1H), 0.91 (s, 9H), 0.07 (s, 6H).

Notebook entries:

Procedure: SSP2-039

^{1}H NMR: SSP1-380


SSP1-380-fr.19-24.5.1.1r
HO
O
H3C
Si
CH3
H3C
CH3
CH3
4.00
4.07
7.88
0.94
9.00
5.78
f1 (ppm)

8-((*tert*-butyldimethylsilyl)oxy)octanoic acid (184)



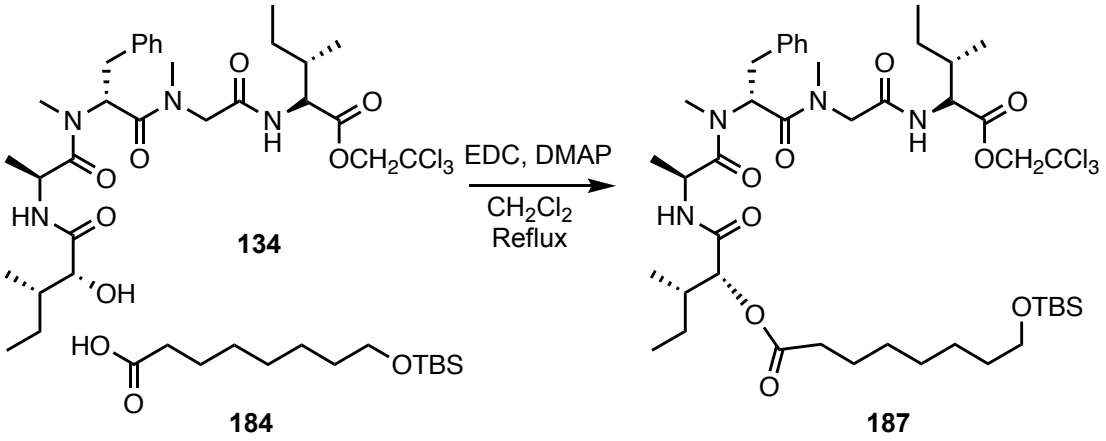
185 **184**

To a stirring mixture of **185** (0.171g, 0.656 mmol, 1eq.) in anhydrous DMF (2mL/g) was added a mixture of PDC (0.988 g, 2.63, 4 eq.) and celite (0.2 g) under an Ar atmosphere. The reaction was stirred at rt overnight, filtered via a fitted filter funnel under vacuum, collected filtrate was extracted with ether, dried over anhydrous Na_2SO_4, and concentrated under reduced pressure. The crude compound **184** was carried forward without further purification.

Notebook entries:

Procedure: SSP2-044

2,2,2-trichloroethyl (2*R*,8*R*,11*S*,14*R*,15*S*)-8-benzyl-2-((*S*)-*sec*-butyl)-14-((8-((*tert*-butyldimethylsilyl)oxy)octanoyl)oxy)-6,9,11,15-tetramethyl-4,7,10,13-tetraoxo-3,6,9,12-tetraazaheptadecanoate (187)



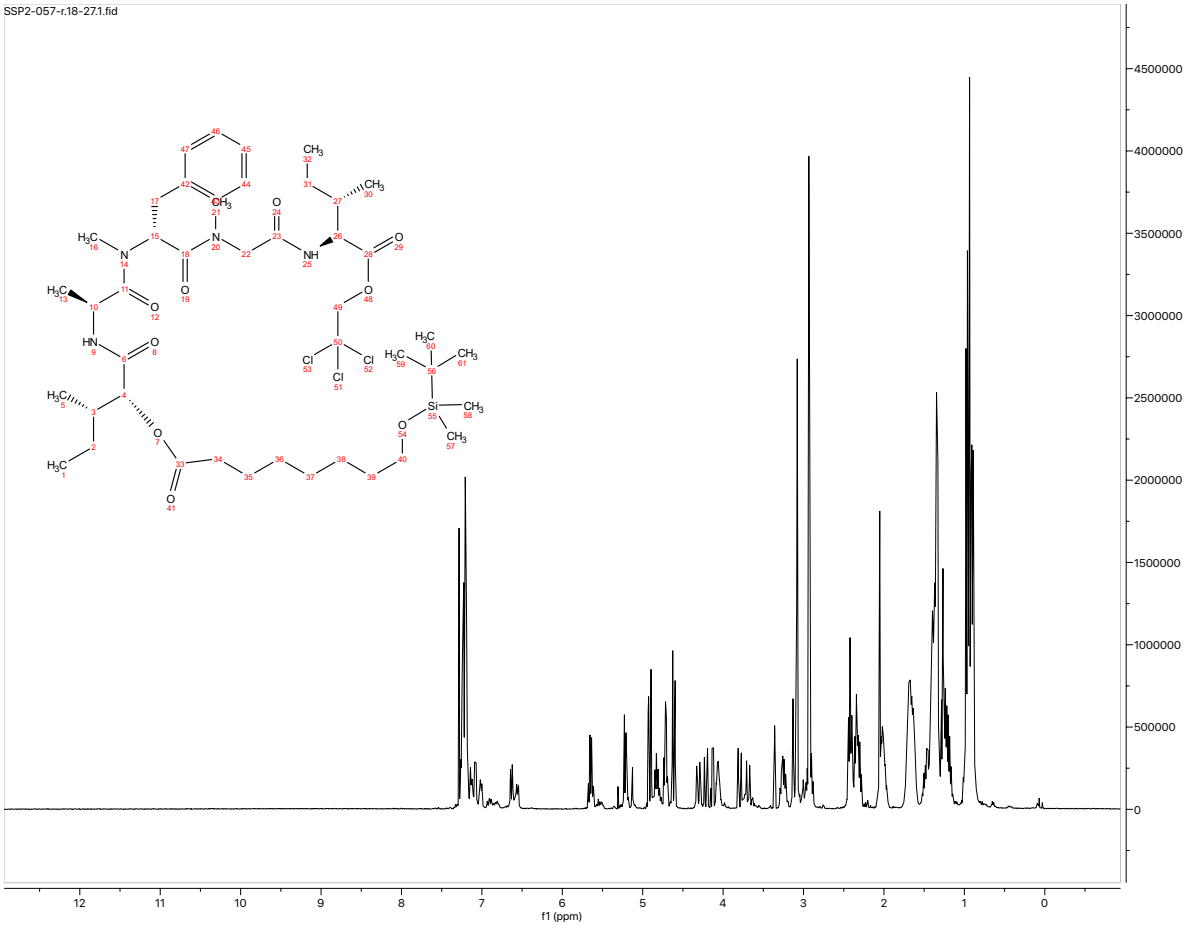
In a flame dried RBF, carboxyllic acid **184** (0.0262 g, 0.096 mmol, 1.3 eq.) was dissolved in anhydrous CH_2Cl_2 (0.48 mL, 0.2M) under an Ar atmosphere and cooled to 0 °C. Next, EDC (0.0282 g, 0.147 mmol, 2 eq.) followed by the free amine (0.050 g, 0.0735 mmol, 1 eq.) and DMAP (0.0045 g, 0.037 mmol, 0.5 eq.) that was dissolved in anhydrous CH_2Cl_2 (0.48 mL, 0.2M with respect to the free acid) in a separate flame dried RBF were added. The reaction was gradually brought to rt and refluxed under an Ar atmosphere. After two days, reaction was gradually brought to rt, quenched with 2 eq. of DI H_2O by volume and extracted with CH_2Cl_2 (x3), the combined organic layers were dried with anhydrous Na_2SO_4 and concentrated under reduced pressure. The crude compound was purified via flash column chromatography (gradient elution: 1:3 EtOAc: hexane, 1:1 EtOAc: hexane, 3:1 EtOAc: hexane, 100% EtOAc, 1:19 EtOAc:MeOH, 1:9 EtOAc:MeOH) to obtain **187** as a viscous oil (0.048 g, 70%). ^{1}H NMR (400 MHz, $CDCl_3$) δ 7.26 (d, *J* = 15.7 Hz, 1H), 7.26 – 7.18 (m, 3H), 7.19 (s, 1H), 7.17 – 6.98 (m, 1H), 6.67 – 6.52 (m, 1H), 5.65 (q, *J* = 8.0 Hz, 1H), 5.22 (dd, *J* = 10.9, 3.2 Hz, 1H), 4.91 (dd, *J* = 12.0, 2.3 Hz, 1H), 4.90 – 4.75 (m, 1H), 4.72 (dt, *J* = 8.6, 4.3 Hz, 1H), 4.61 (dd, *J* = 12.0, 1.5 Hz, 1H), 4.36 – 4.17 (m, 1H),

4.17 – 4.00 (m, 1H), 3.84 – 3.61 (m, 1H), 3.26 (ddd, *J* = 13.8, 8.6, 5.7 Hz, 1H), 3.18 – 3.04 (m, 3H), 3.02 – 2.86 (m, 4H), 2.42 (dd, *J* = 8.5, 6.7 Hz, 2H), 2.34 (s, 1H), 2.38 – 2.25 (m, 2H), 2.01 (dtt, *J* = 9.3, 6.9, 4.2 Hz, 1H), 1.74 – 1.64 (m, 4H), 1.64 (s, 2H), 1.64 – 1.58 (m, 0H), 1.54 – 1.45 (m, 1H), 1.48 – 1.33 (m, 3H), 1.34 (dd, *J* = 6.7, 1.6 Hz, 3H), 1.31 – 1.23 (m, 1H), 1.23 (dd, *J* = 6.9, 4.8 Hz, 1H), 1.23 – 1.12 (m, 1H), 1.06 – 0.83 (m, 14H).

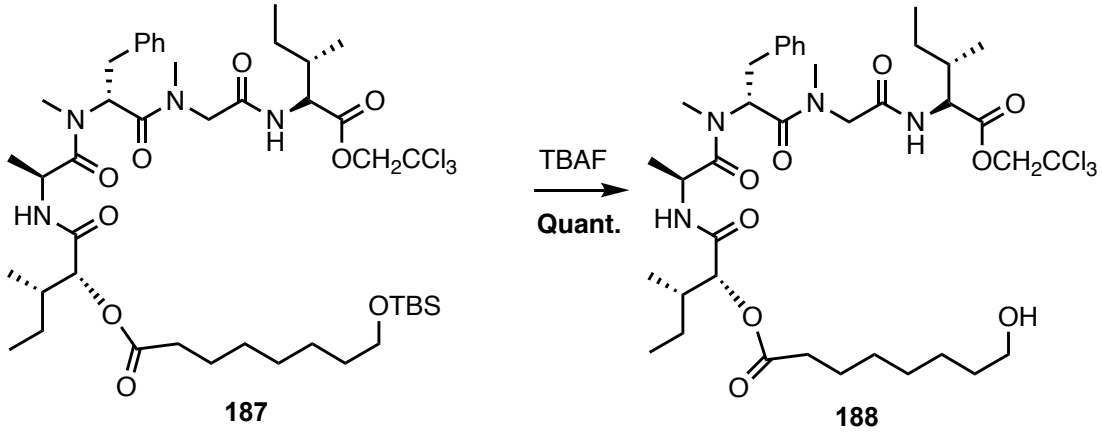
Notebook entries:

Procedure: SSP2-057

^{1}H NMR: SSP2-057


SSP2-057-r.18-27.1.fid
4500000
4000000
3500000
3000000
2500000
2000000
1500000
1000000
500000
0
12
11
10
9
8
7
6
5
4
3
2
1
0
f1 (ppm)

2,2,2-trichloroethyl (2*R*,8*R*,11*S*,14*R*,15*S*)-8-benzyl-2-((*S*)-*sec*-butyl)-14-((8-hydroxyoctanoyl)oxy)-6,9,11,15-tetramethyl-4,7,10,13-tetraoxo-3,6,9,12-tetraazaheptadecanoate (188)

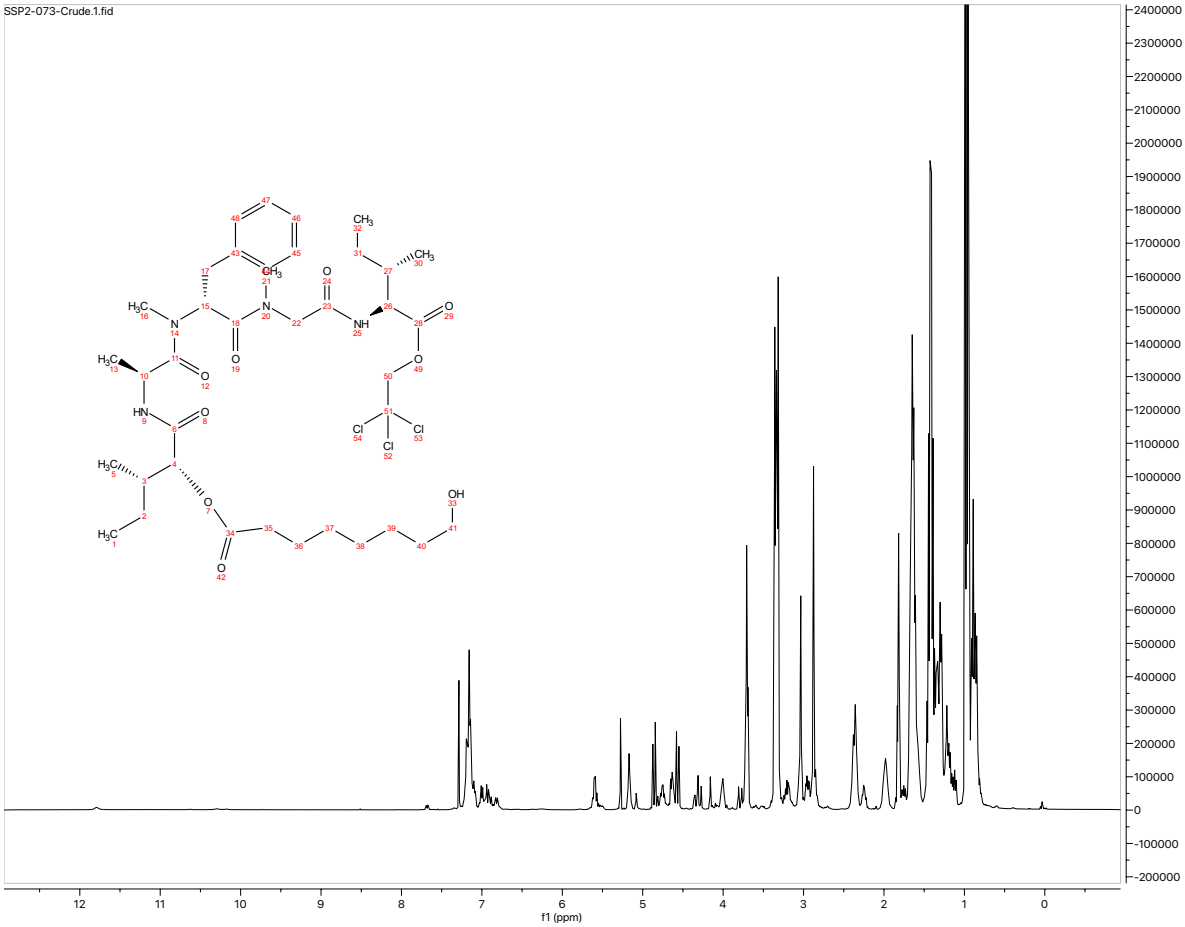


Standard protocol for silyl ether deprotection was followed to access the alcohol **188** in quantitative yield. ^{1}H NMR (400 MHz, $CDCl_3$) δ 7.24 – 7.14 (m, 1H), 7.18 – 7.06 (m, 1H), 5.20 – 5.12 (m, 0H), 4.68 – 4.53 (m, 1H), 3.79 – 3.67 (m, 2H), 3.38 – 3.29 (m, 7H), 3.19 (tt, *J* = 13.5, 6.9 Hz, 1H), 3.08 – 3.01 (m, 1H), 3.00 – 2.81 (m, 2H), 2.42 – 2.30 (m, 2H), 1.98 (s, 1H), 1.87 – 1.71 (m, 2H), 1.71 – 1.59 (m, 6H), 1.42 (h, *J* = 7.4 Hz, 7H), 1.32 (ddd, *J* = 17.4, 7.3, 2.7 Hz, 3H), 1.27 – 1.15 (m, 1H), 1.01 – 0.82 (m, 16H).

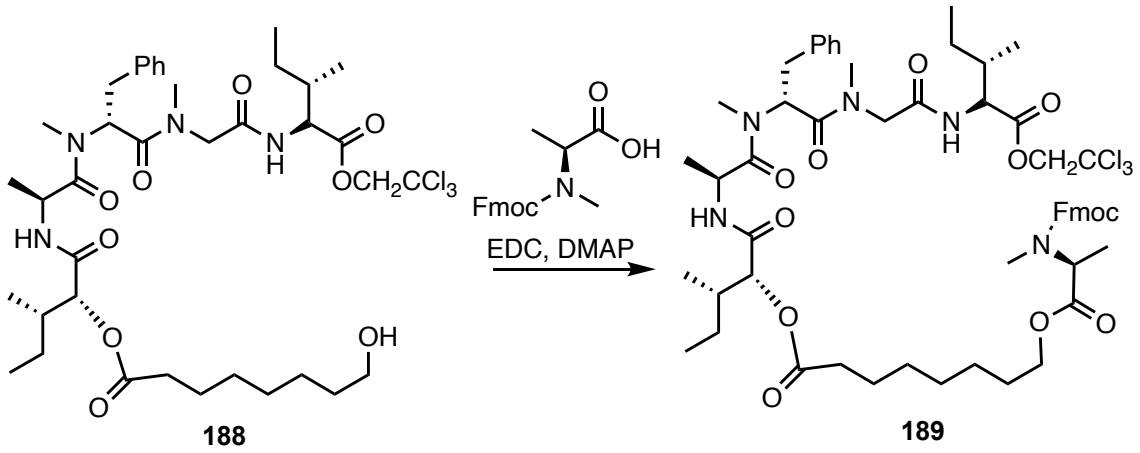
Notebook entries:

Procedure: SSP2- 073

^{1}H NMR: SSP2-073 (Crude)


SSP2-073-Crude.1.fid
f1 (ppm)

2,2,2-trichloroethyl (2*R*,8*R*,11*S*,14*R*,15*S*)-14-((8-((*N*-(((9*H*-fluoren-9-yl)methoxy)carbonyl)-*N*-methyl-*L*-alanyl)oxy)octanoyl)oxy)-8-benzyl-2-((*S*)-*sec*-butyl)-6,9,11,15-tetramethyl-4,7,10,13-tetraoxo-3,6,9,12-tetraazaheptadecanoate (189)



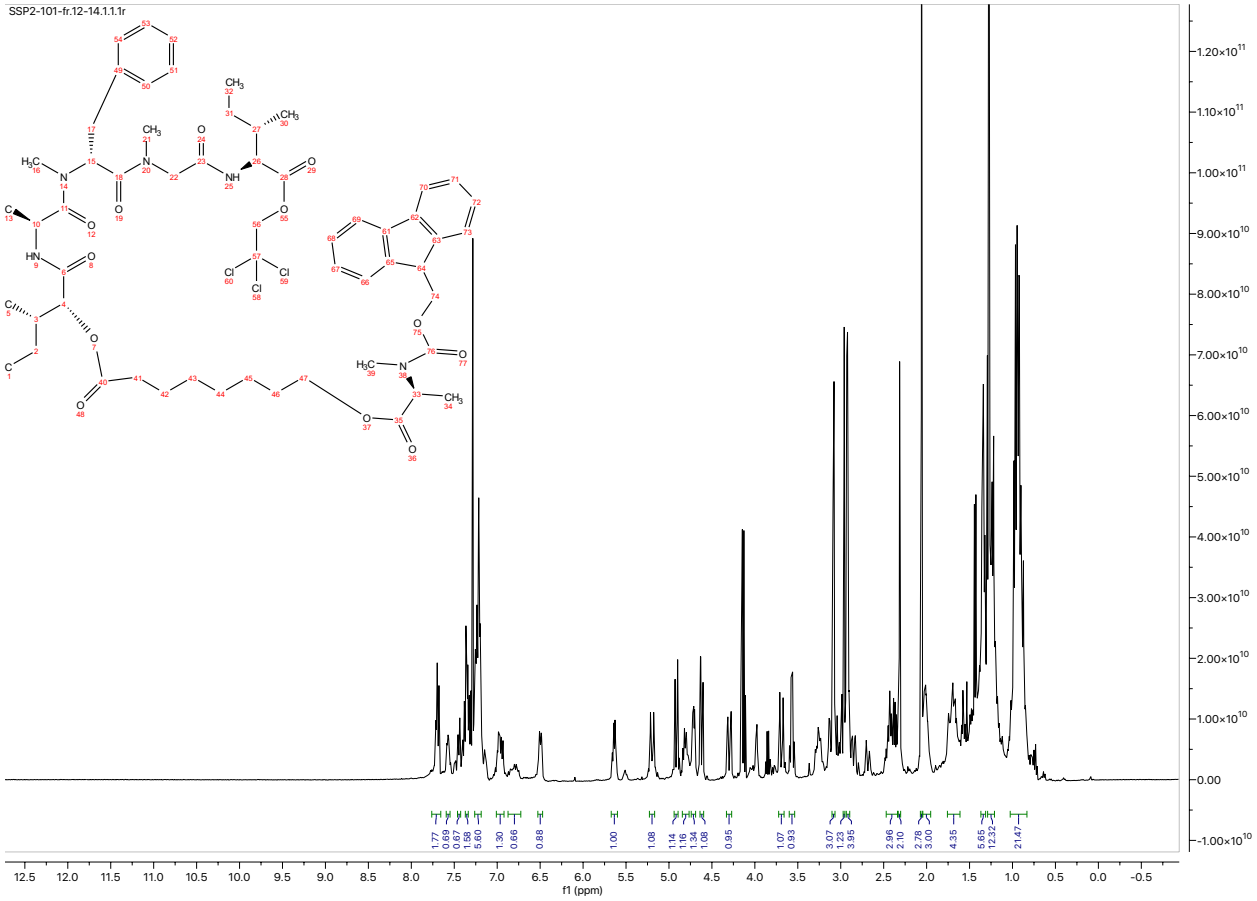
188 **189**

EDC mediated standard peptide coupling conditions were followed to access **189** in 16% yield. ^{1}H NMR (400 MHz, $CDCl_3$) δ 7.76 – 7.66 (m, 2H), 7.57 (dt, *J* = 8.3, 4.2 Hz, 1H), 7.45 (d, *J* = 7.6 Hz, 1H), 7.37 – 7.34 (m, 2H), 7.26 – 7.19 (m, 6H), 7.01 – 6.92 (m, 1H), 6.87 – 6.73 (m, 1H), 6.53 – 6.47 (m, 1H), 5.63 (td, *J* = 7.6, 4.9 Hz, 1H), 5.23 – 5.17 (m, 1H), 4.92 (dd, *J* = 12.0, 1.8 Hz, 1H), 4.84 – 4.77 (m, 1H), 4.72 (ddd, *J* = 8.8, 4.7, 1.6 Hz, 1H), 4.62 (dd, *J* = 12.0, 1.6 Hz, 1H), 4.30 (dd, *J* = 15.4, 2.8 Hz, 1H), 3.69 (d, *J* = 15.5 Hz, 1H), 3.57 (q, *J* = 7.2 Hz, 1H), 3.08 (d, *J* = 3.6 Hz, 3H), 2.96 (s, 1H), 2.92 (t, *J* = 4.0 Hz, 4H), 2.47 – 2.34 (m, 3H), 2.31 (s, 2H), 2.06 (s, 3H), 2.05 – 1.95 (m, 3H), 1.70 (ddd, *J* = 16.8, 12.6, 6.0 Hz, 4H), 1.34 (t, *J* = 7.0 Hz, 6H), 1.29 – 1.21 (m, 12H), 1.03 – 0.83 (m, 21H).

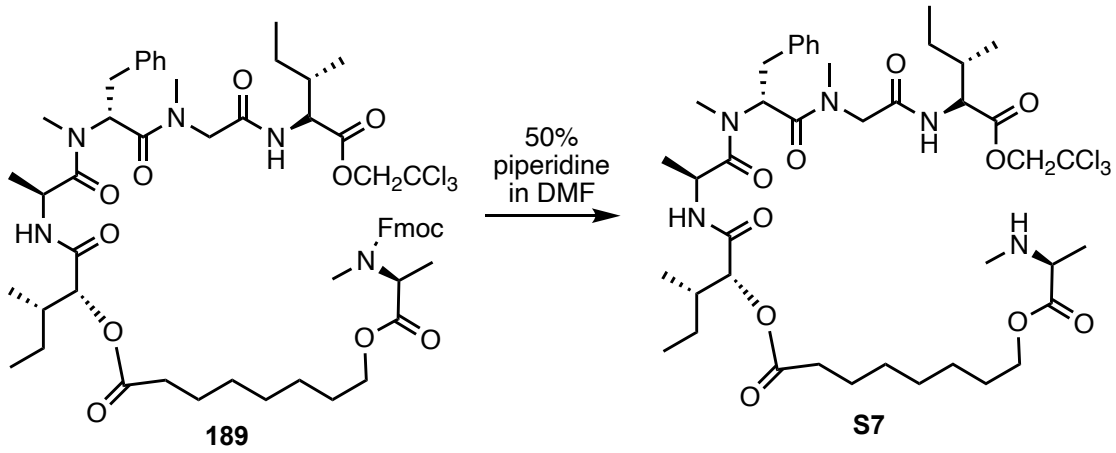
Notebook entries:

Procedure: SSP2-075

^{1}H NMR: SSP2-101


SSP2-101-fr.12-14.1.1.1r
1.77
0.69
0.67
1.58
5.60
1.30
0.66
0.88
1.00
1.08
1.14
1.16
1.34
1.08
0.95
1.07
0.93
3.07
1.23
3.95
2.96
2.10
2.78
3.00
4.35
5.65
12.32
21.47
f1 (ppm)

2,2,2-trichloroethyl (2*R*,8*R*,11*S*,14*R*,15*S*)-8-benzyl-2-((*S*)-*sec*-butyl)-6,9,11,15-tetramethyl-14-((8-((methyl-*L*-alanyl)oxy)octanoyl)oxy)-4,7,10,13-tetraoxo-3,6,9,12-tetraazaheptadecanoate (S7)



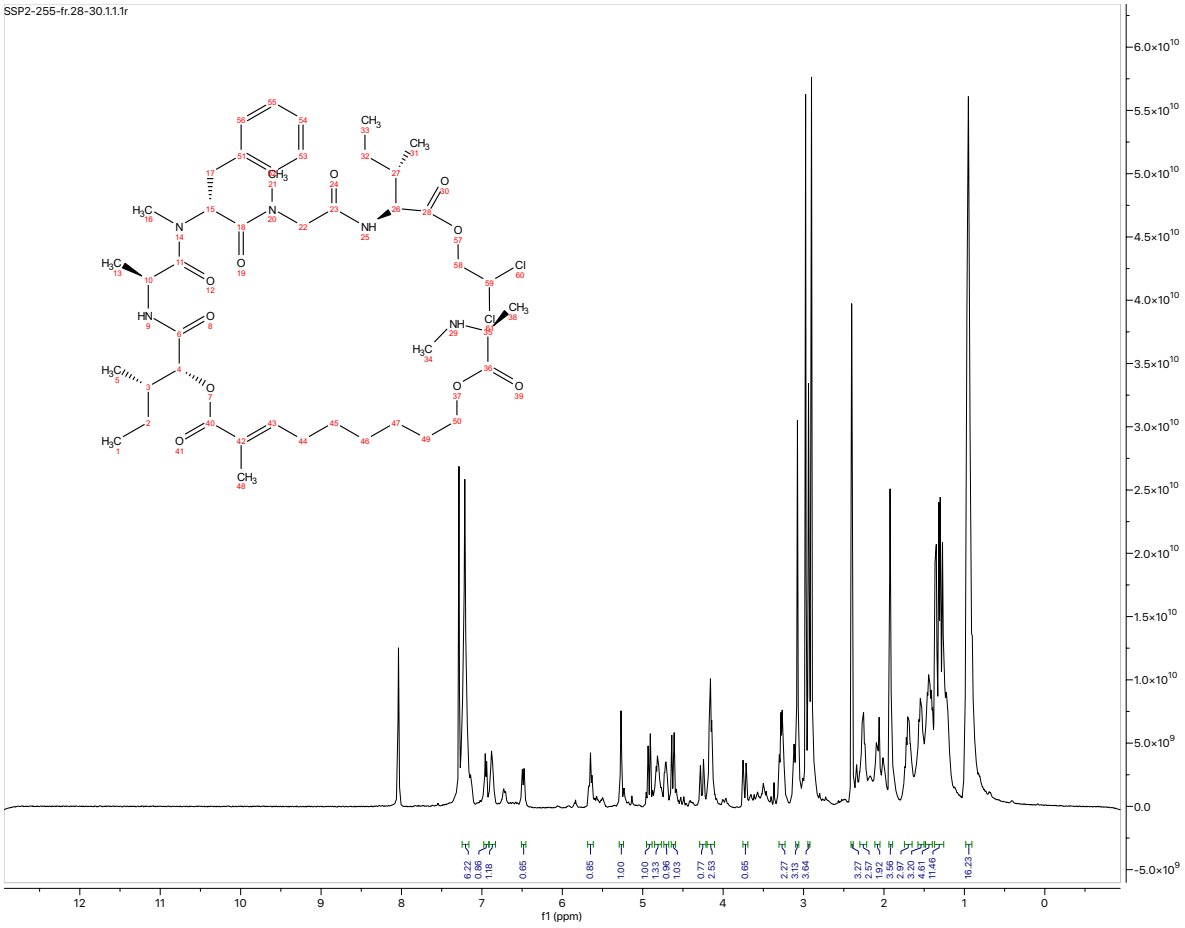
Standard Fmoc deprotection protocol was followed to access the free amine **S7** in 51% yield.

^{1}H NMR (400 MHz, $CDCl_3$) δ 7.20 (d, *J* = 7.9 Hz, 6H), 6.95 (d, *J* = 7.4 Hz, 1H), 6.89 (d, *J* = 9.9 Hz, 1H), 6.49 (d, *J* = 8.7 Hz, 1H), 5.65 (t, *J* = 7.6 Hz, 1H), 5.27 (t, *J* = 2.3 Hz, 1H), 4.95 – 4.88 (m, 1H), 4.81 (dd, *J* = 14.8, 7.8 Hz, 1H), 4.74 – 4.68 (m, 1H), 4.65 – 4.59 (m, 1H), 4.26 (d, *J* = 15.5 Hz, 1H), 4.16 (t, *J* = 7.0 Hz, 3H), 3.73 (d, *J* = 15.2 Hz, 1H), 3.27 (q, *J* = 7.4 Hz, 2H), 3.08 (s, 3H), 2.94 (s, 4H), 2.40 (d, *J* = 1.8 Hz, 3H), 2.26 (q, *J* = 7.2 Hz, 3H), 2.11 – 2.05 (m, 2H), 1.91 (d, *J* = 7.9 Hz, 4H), 1.70 (dt, *J* = 15.4, 7.7 Hz, 3H), 1.54 (q, *J* = 7.7 Hz, 3H), 1.44 (dd, *J* = 13.9, 6.9 Hz, 5H), 1.37 – 1.26 (m, 11H), 0.95 (dq, *J* = 11.6, 6.9, 6.4 Hz, 16H).

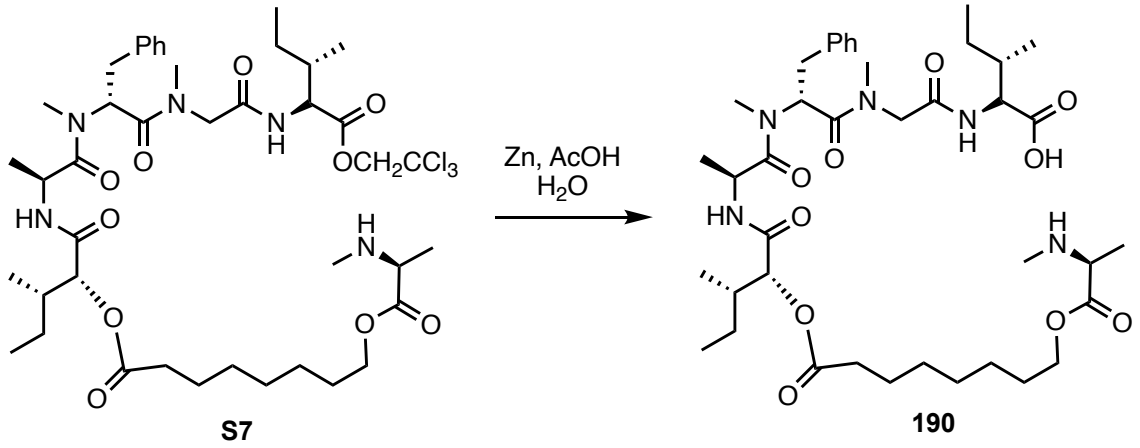
Notebook entries:

Procedure: SSP2-081

^{1}H NMR: SSP2-255


SSP2-255-fr.28-30.1.1.1r
f1 (ppm)

***N*-methyl-*N*-(*N*-methyl-*N*-(((2*R*,3*S*)-3-methyl-2-((8-((methyl-*L*-alanyl)oxy)octanoyl)oxy)pentanoyl)-*L*-alanyl)-*D*-phenylalanyl)glycyl-*D*-alloisoleucine (190)**

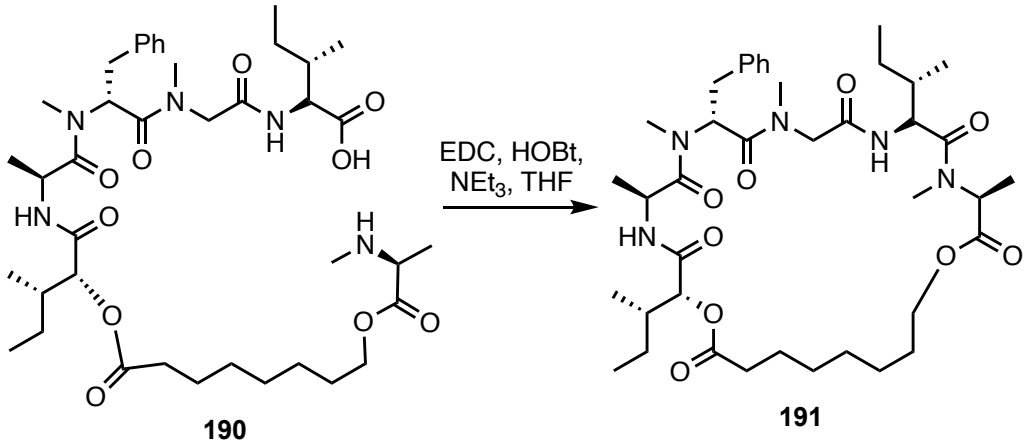


Standard trichloro ethanol deprotection conditions were used to access the free acid **190** in quantitative yield. The crude material was carried forward to the next step without further purification.

Notebook entries:

Procedure: SSP2-088

(3*S*,6*R*,12*R*,15*S*,18*R*)-12-benzyl-6,18-di((*S*)-*sec*-butyl)-3,4,10,13,15-pentamethyl-1,19-dioxa-4,7,10,13,16-pentaazacycloheptacosane-2,5,8,11,14,17,20-heptaone (191)



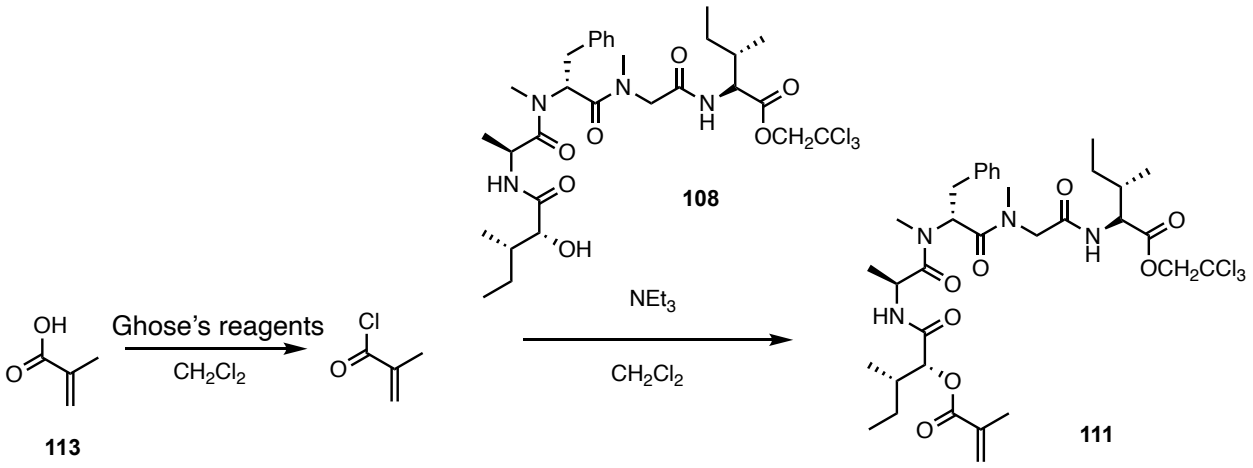
EDC mediated standard peptide coupling conditions at a dilute concentration of THF (0.0054M) were used to obtain the macrocycle **191** in 24% yield.

Notebook entries:

Procedure: SSP2-110

^{1}H NMR: SSP2-110

2,2,2-trichloroethyl *N*-(*N*-(((2*R*,3*S*)-2-(methacryloyloxy)-3-methylpentanoyl)-*L*-alanyl)-*N*-methyl-*D*-phenylalanyl)-*N*-methylglycyl-*D*-alloisoleucinate (111)

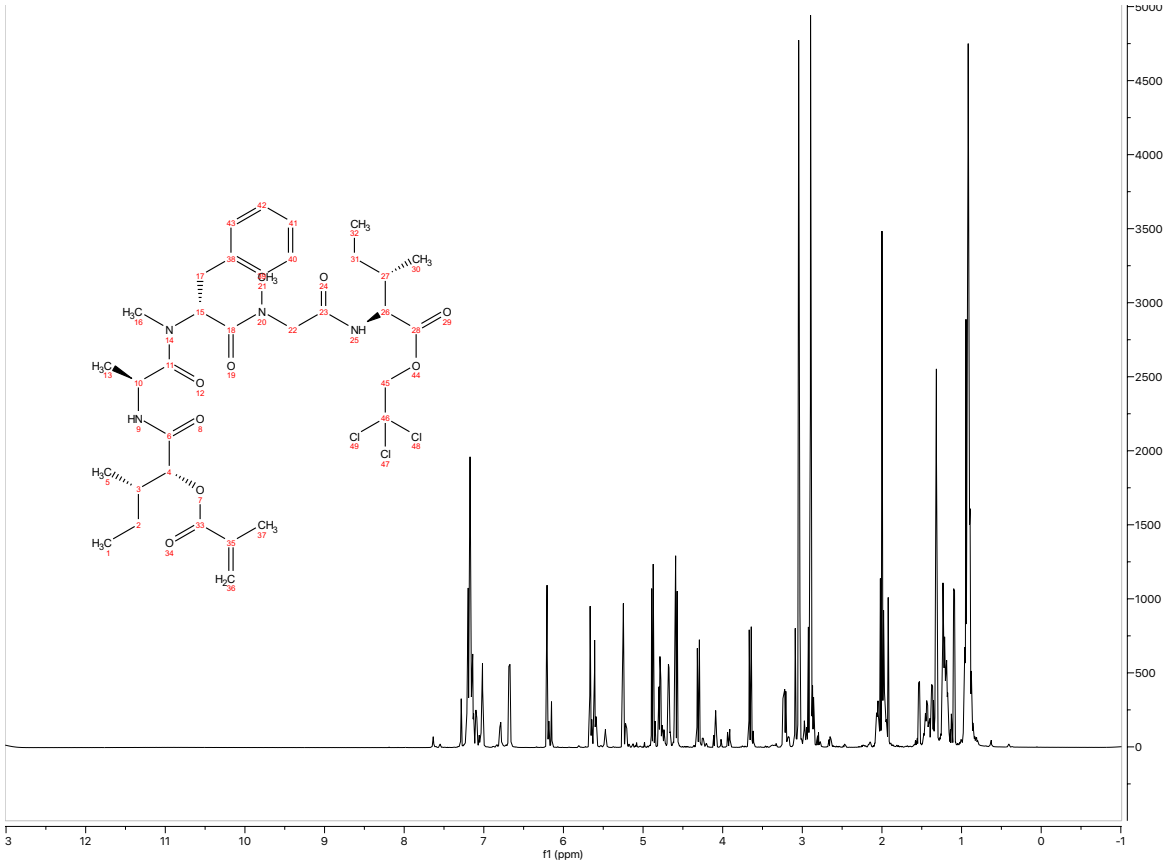


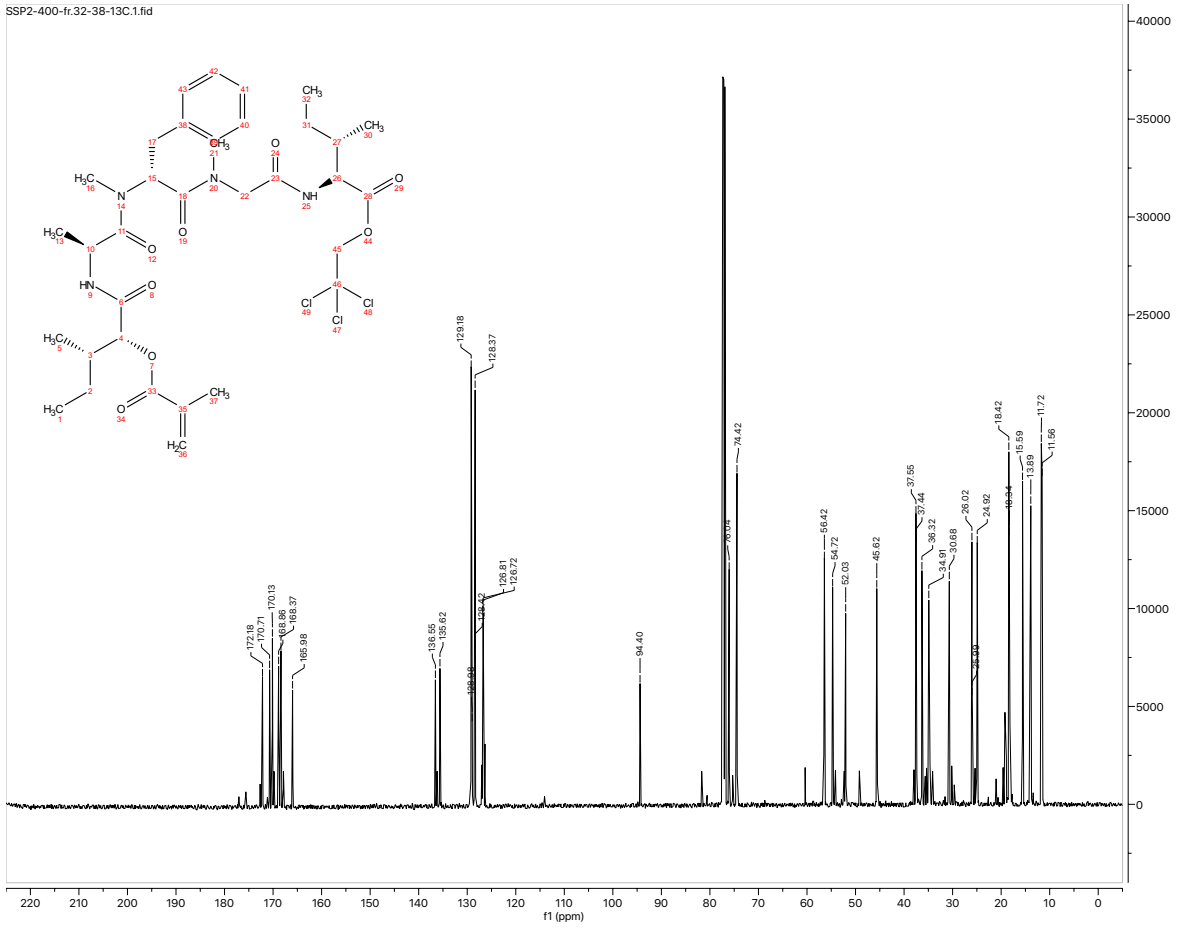
Reaction was performed using standard protocol for acid chloride mediated coupling conditions to access ester **111** in 93% yield after flash column chromatography (gradient elution; 1:3 EtOAc: hexane 1:1 EtOAc: hexane, 3:1 EtOAc: hexane, and 100% EtOAc). ^{1}H NMR (600 MHz, $CDCl_3$) δ 7.24 – 7.14 (m, 4H), 7.16 – 7.07 (m, 1H), 7.04 (dd, *J* = 17.1, 7.4 Hz, 1H), 6.68 (d, *J* = 8.7 Hz, 1H), 6.20 (d, *J* = 12.6 Hz, 1H), 5.65 (dt, *J* = 12.0, 1.7 Hz, 1H), 5.63 – 5.57 (m, 1H), 5.27 – 5.18 (m, 1H), 4.87 (t, *J* = 13.1 Hz, 1H), 4.77 (dp, *J* = 20.0, 6.9 Hz, 1H), 4.67 (dt, *J* = 9.3, 4.7 Hz, 1H), 4.59 (t, *J* = 11.6 Hz, 1H), 4.35 – 4.28 (m, 1H), 3.65 (d, *J* = 15.4 Hz, 1H), 3.26 – 3.15 (m, 1H), 3.09 (s, 0H), 3.04 (d, *J* = 9.7 Hz, 3H), 3.00 – 2.84 (m, 2H), 2.90 (s, 2H), 2.06 (ddq, *J* = 10.4, 6.8, 3.3 Hz, 1H), 2.04 – 1.96 (m, 3H), 1.99 – 1.90 (m, 1H), 1.44 (dtt, *J* = 15.0, 7.6, 3.9 Hz, 1H), 1.35 (dd, *J* = 28.8, 6.9 Hz, 3H), 1.26 – 1.14 (m, 3H), 1.20 (s, 1H), 1.15 – 1.06 (m, 1H), 0.99 – 0.83 (m, 13H). ^{13}C NMR (151 MHz, $CDCl_3$) δ 172.18, 170.71, 170.13, 168.86, 168.37, 165.98, 136.55, 135.62, 129.18, 128.98, 128.42, 128.37, 126.81, 126.72, 94.40, 76.04, 74.42, 56.42, 54.72, 52.03, 45.62, 37.55, 37.44, 36.32, 34.91, 30.68, 26.02, 25.99, 24.92, 18.42, 18.34, 15.59, 13.89, 11.72, 11.56.

Notebook entries:

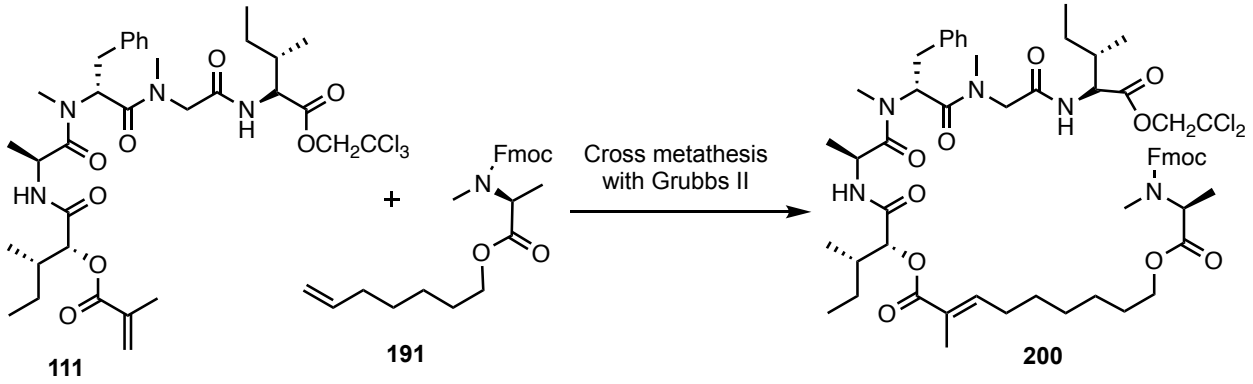
Procedure: SSP2-400

^{1}H NMR and ^{13}C NMR: SSP2-400




SSP2-400-fr.32-38-13C.1.fid
172.18
170.71
170.13
169.86
168.37
165.98
136.55
135.62
129.18
128.37
128.02
126.81
126.72
94.40
77.04
74.42
56.42
54.72
52.03
45.62
37.55
37.44
36.32
34.91
30.68
26.02
24.92
18.42
15.59
13.89
11.72
11.56
f1 (ppm)

2,2-dichloro-2λ^3-ethyl (2*R*,8*R*,11*S*,14*R*,15*S*)-14-(((*E*)-9-((*N*-(((9*H*-fluoren-9-yl)methoxy)carbonyl)-*N*-methyl-*L*-alanyl)oxy)-2-methylnon-2-enoyl)oxy)-8-benzyl-2-((*S*)-*sec*-butyl)-6,9,11,15-tetramethyl-4,7,10,13-tetraoxo-3,6,9,12-tetraazaheptadecanoate (200)



Standard protocol for olefine cross metathesis was followed to access **200** in 56% yield.

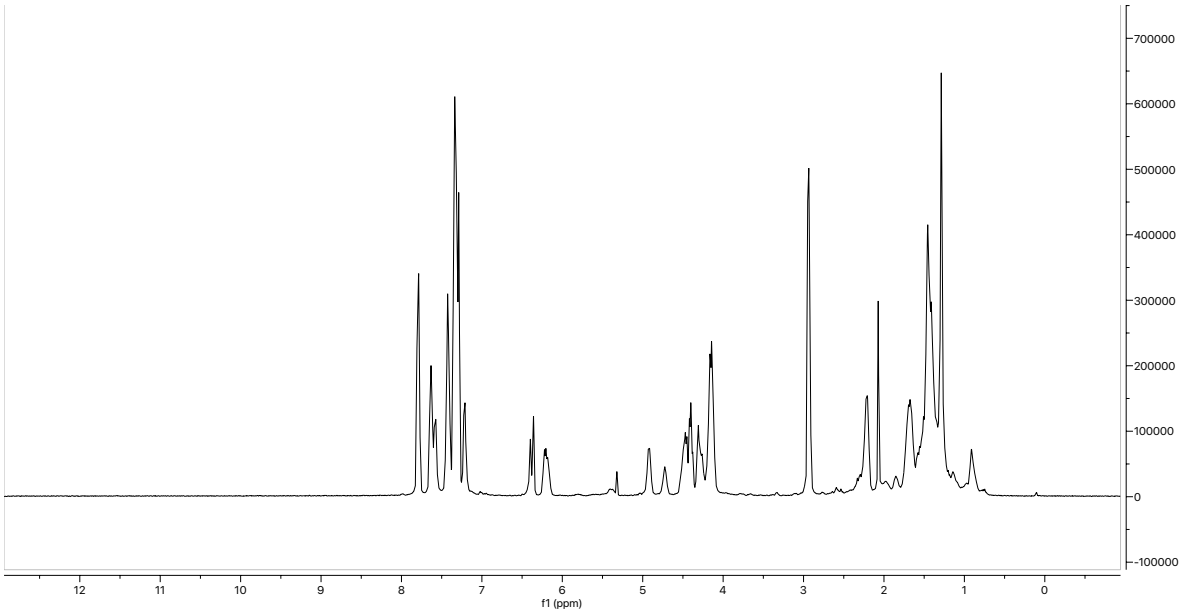
^{1}H NMR (400 MHz, $CDCl_3$) δ 7.79 (d, *J* = 7.5 Hz, 2H), 7.67 – 7.55 (m, 3H), 7.42 (d, *J* = 7.6 Hz, 3H), 7.38 – 7.26 (m, 5H), 7.21 (t, *J* = 7.4 Hz, 1H), 6.38 (d, *J* = 15.5 Hz, 1H), 6.20 (dt, *J* = 15.1, 7.3 Hz, 1H), 4.92 (q, *J* = 7.8 Hz, 1H), 4.72 (t, *J* = 7.1 Hz, 0H), 4.45 (dq, *J* = 29.4, 10.1, 8.9 Hz, 3H), 4.35 – 4.24 (m, 1H), 4.15 (qt, *J* = 13.6, 9.6, 7.5 Hz, 3H), 2.94 (d, *J* = 6.2 Hz, 3H), 2.23 (dq, *J* = 13.1, 7.1, 6.3 Hz, 2H), 2.07 (d, *J* = 2.5 Hz, 1H), 1.77 – 1.63 (m, 2H), 1.46 (d, *J* = 6.1 Hz, 2H), 1.42 (dd, *J* = 13.5, 6.7 Hz, 3H), 1.37 (s, 4H), 1.37 – 1.22 (m, 3H), 0.93 (dq, *J* = 20.5, 11.6 Hz, 1H).

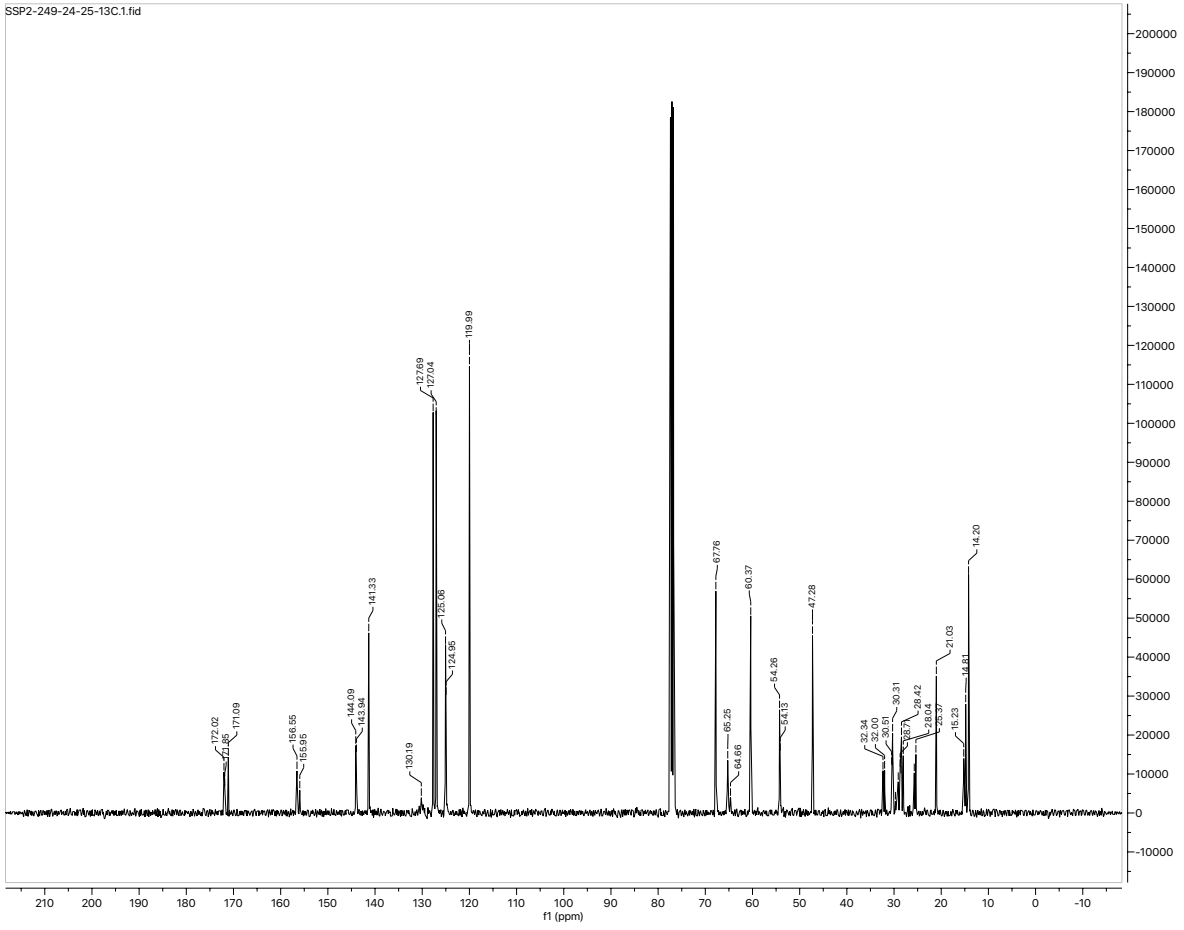
^{13}C NMR (101 MHz, $CDCl_3$) δ 172.02, 171.85, 171.09, 156.55, 155.95, 144.09, 143.94, 141.33, 130.19, 127.69, 127.04, 125.06, 124.95, 119.99, 67.76, 65.25, 64.66, 60.37, 54.26, 54.13, 47.28, 32.34, 32.00, 30.51, 30.31, 29.70, 29.11, 28.71, 28.54, 28.42, 28.17, 28.04, 25.72, 25.37, 21.03, 15.23, 14.81, 14.20.

Notebook entries:

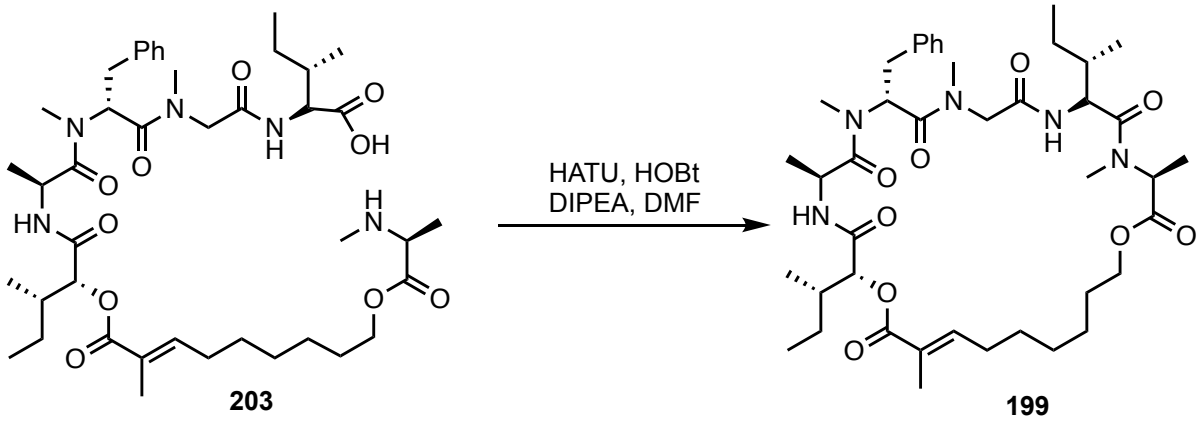
Procedure: SSP2-249

^{1}H NMR and ^{13}C NMR: SSP2-249


f1 (ppm)


SSP2-249-24-25-13C.1.fid
172.02
171.85
171.09
156.55
155.95
144.09
143.94
141.33
130.19
127.69
127.04
125.06
124.95
119.99
67.76
65.25
64.66
60.37
54.26
54.13
47.28
32.34
32.00
30.51
30.31
28.42
28.04
25.37
21.03
15.23
14.81
14.20
f1 (ppm)

(3*S*,6*R*,12*R*,15*S*,18*R*,*E*)-12-benzyl-6,18-di((*S*)-*sec*-butyl)-3,4,10,13,15,21-hexamethyl-1,19-dioxa-4,7,10,13,16-pentaazacyclooctacos-21-ene-2,5,8,11,14,17,20-heptaone (199)



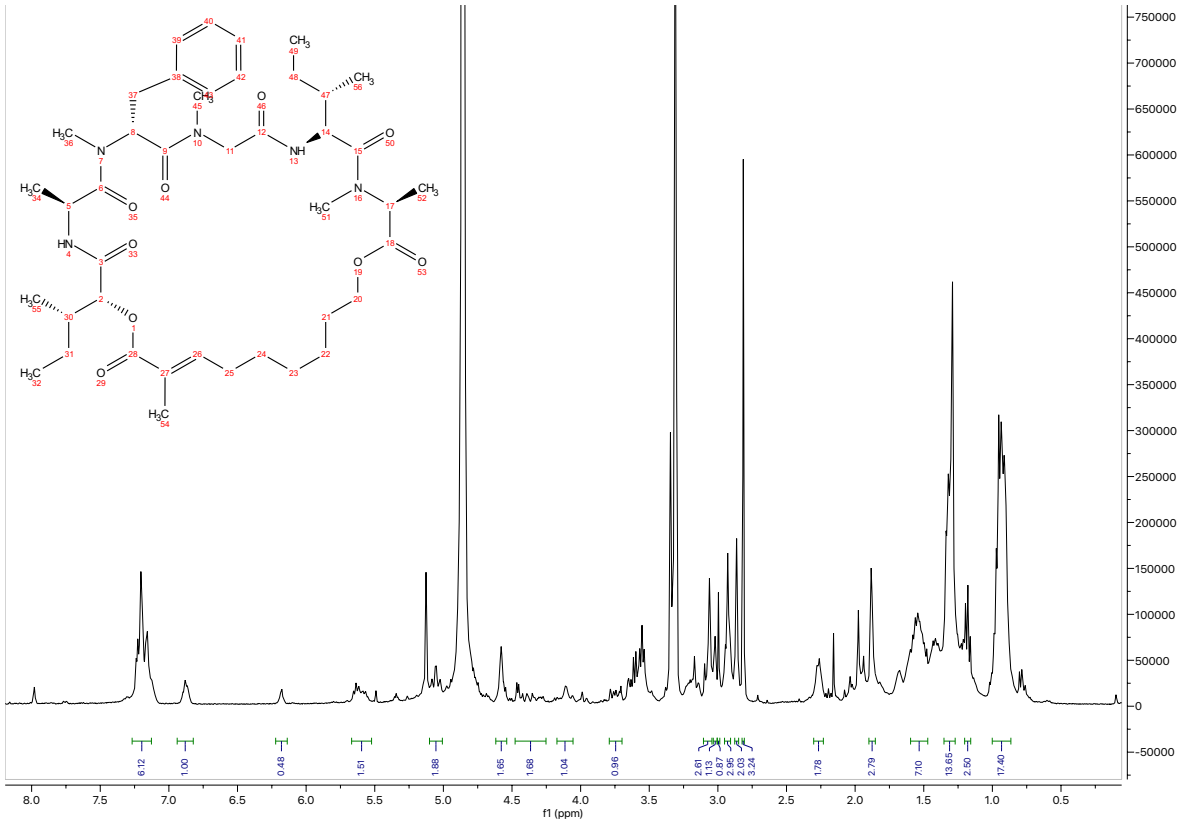
203 **199**

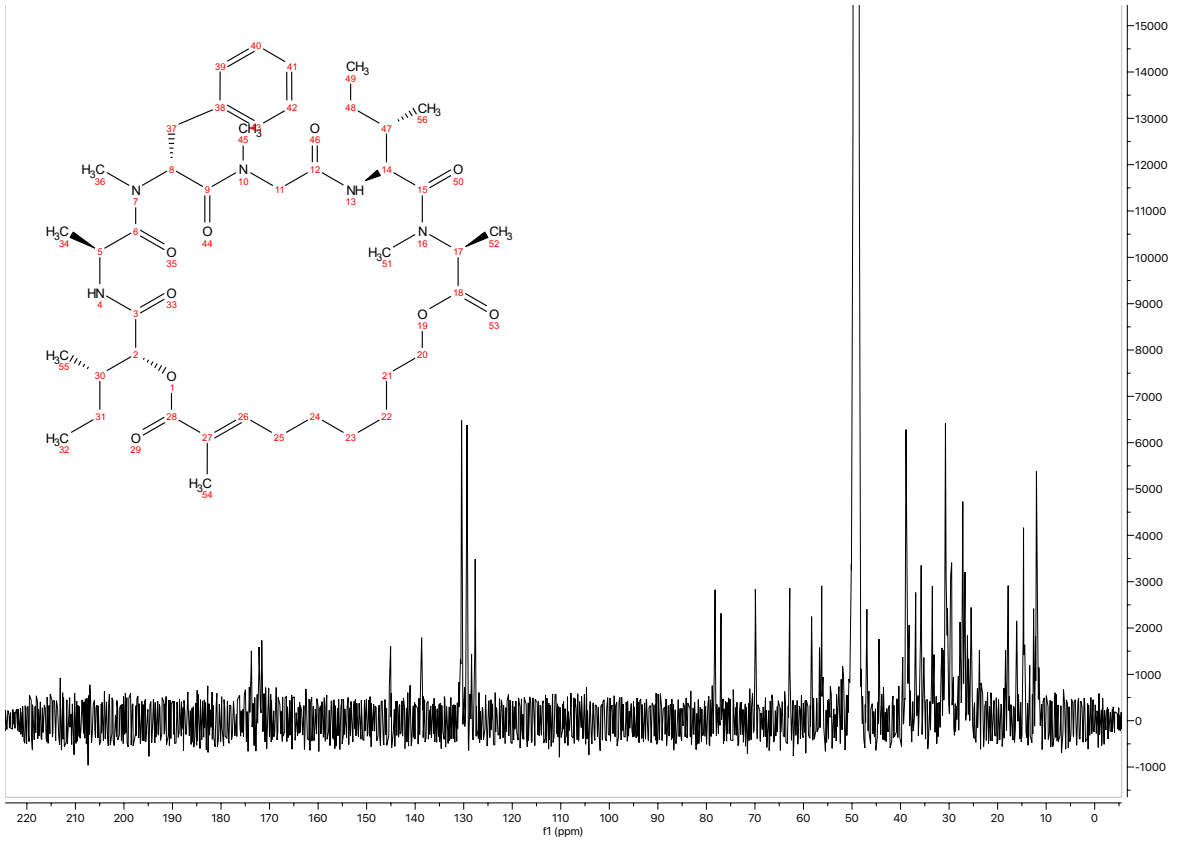
HATU mediated standard peptide coupling conditions were performed in a 0.001M anhydrous DMF solution for 7 days to access the macrocycle **199** in 44% yield after column chromatography.

Notebook entries:

Procedure: SSP2-262

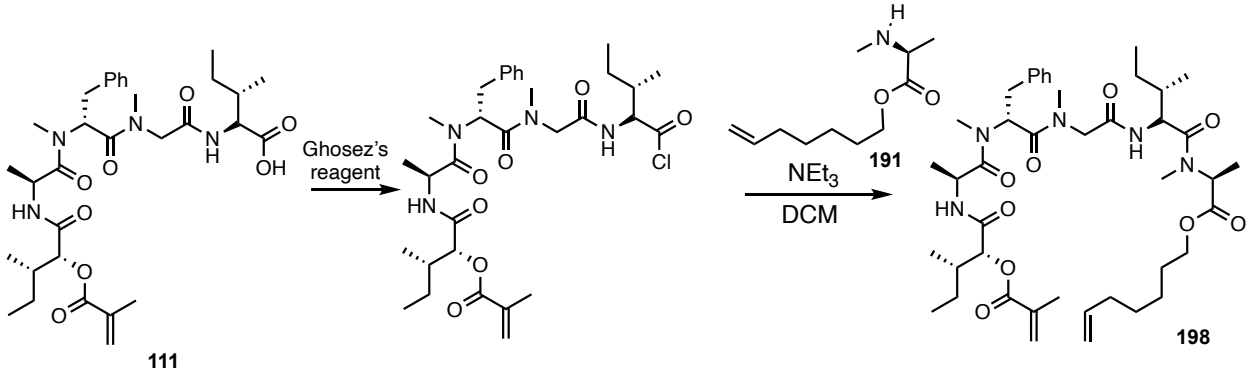
^{1}H NMR and ^{13}C NMR: SSP2-262


6.12
1.00
0.48
1.51
1.88
1.65
1.68
1.04
0.96
2.61
1.13
0.87
2.85
2.55
3.24
1.78
2.79
7.10
13.65
2.50
17.40
f1 (ppm)


f1 (ppm)

Synthesis of hept-6-en-1-yl (2*S*,5*R*,11*R*,14*S*,17*R*,18*S*)-11-benzyl-5-((*S*)-*sec*-butyl)-17-(methacryloyloxy)-2,3,9,12,14,18-hexamethyl-4,7,10,13,16-pentaoxo-3,6,9,12,15-pentaazaicosanoate (198)

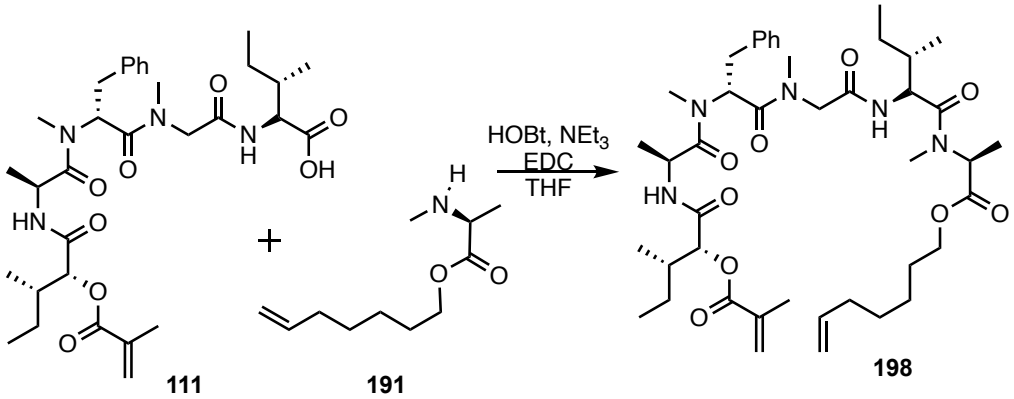
Method A - via acid chloride formation



Standard protocol for acid chloride mediated coupling was used to access diene **198** in 30% yield after flash column chromatography (gradient elution; 100% hexane 1:1 EtOAc: hexane, 3:1 EtOAc: hexane, and 100% EtOAc).

Notebook entries: Procedure: SSP2-304

Method B - via peptide coupling

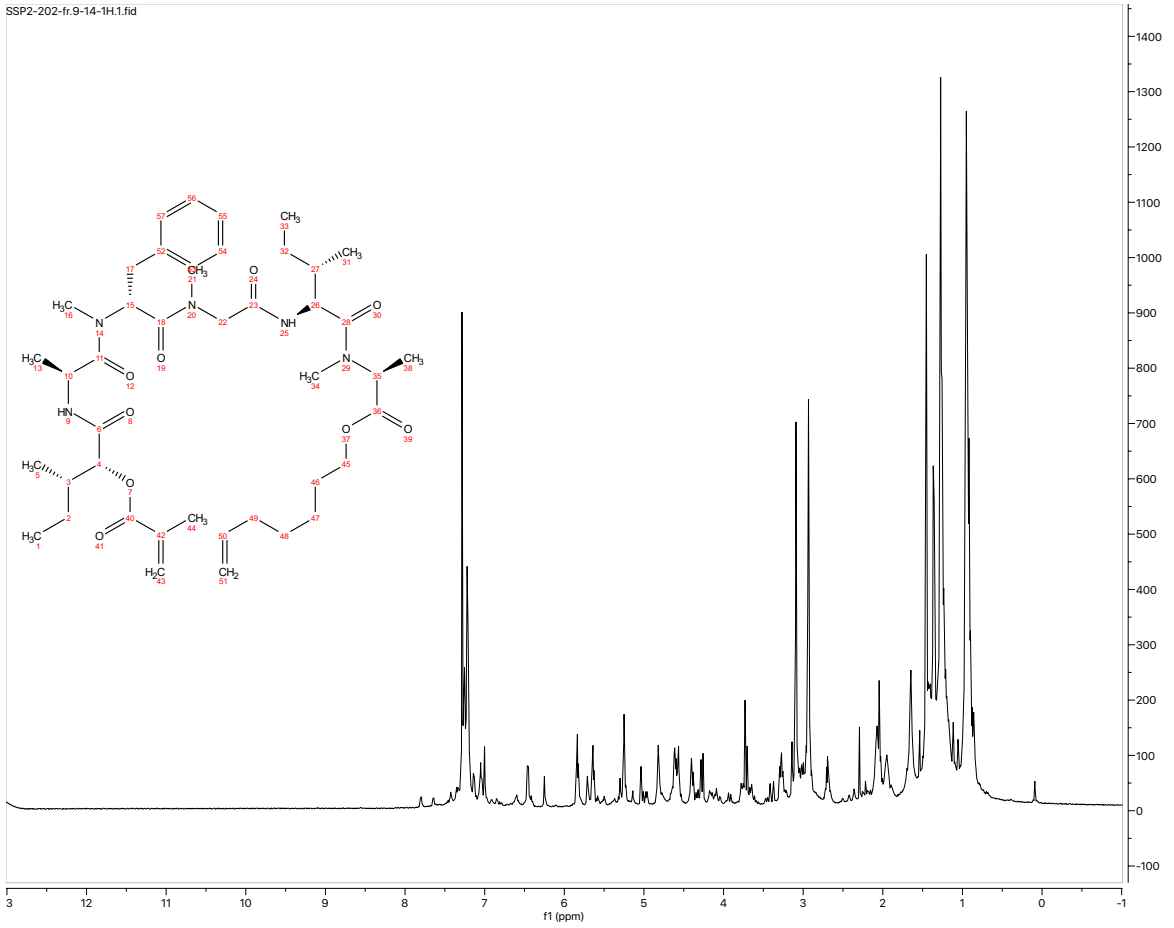


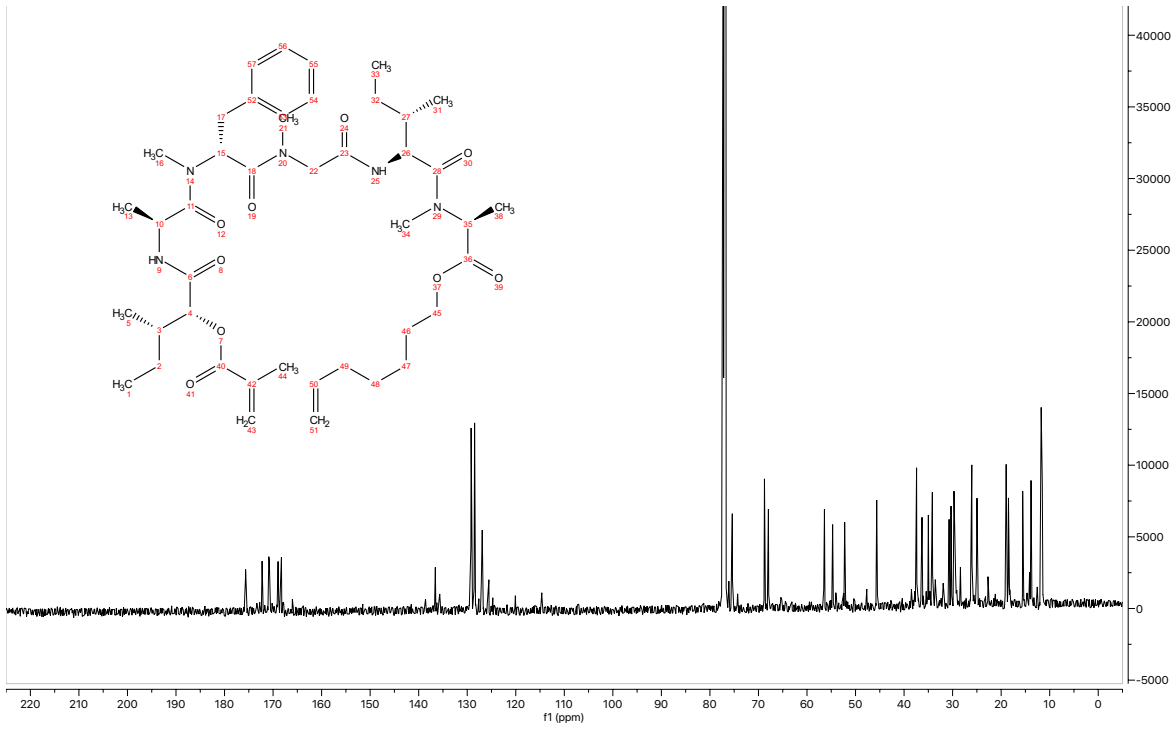
EDC mediated standard peptide coupling conditions were used to access the diene **198** in 28% yield.

Notebook entries:

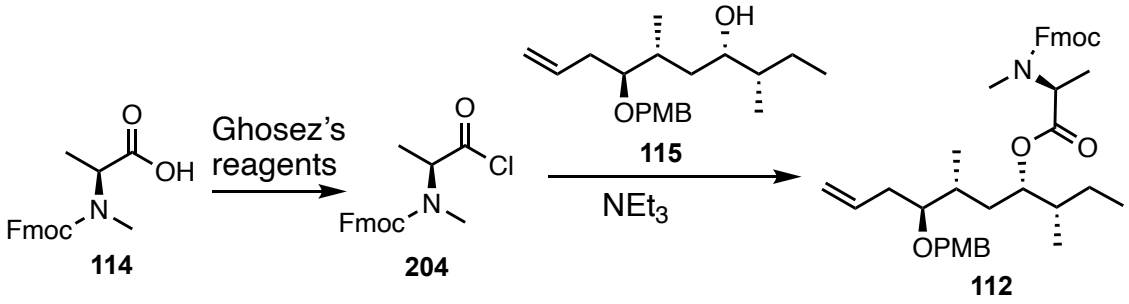
Procedure: SSP2-235

^{1}H NMR and ^{13}C NMR: SSP2-202


SSP2-202-fr.9-14-1H.1.fid
f1 (ppm)


f1 (ppm)

(3*S*,4*S*,6*R*,7*S*)-7-((4-methoxybenzyl)oxy)-3,6-dimethyldec-9-en-4-yl *N*-(((9*H*-fluoren-9-yl)methoxy)carbonyl)-*N*-methyl-*L*-alaninate (193)



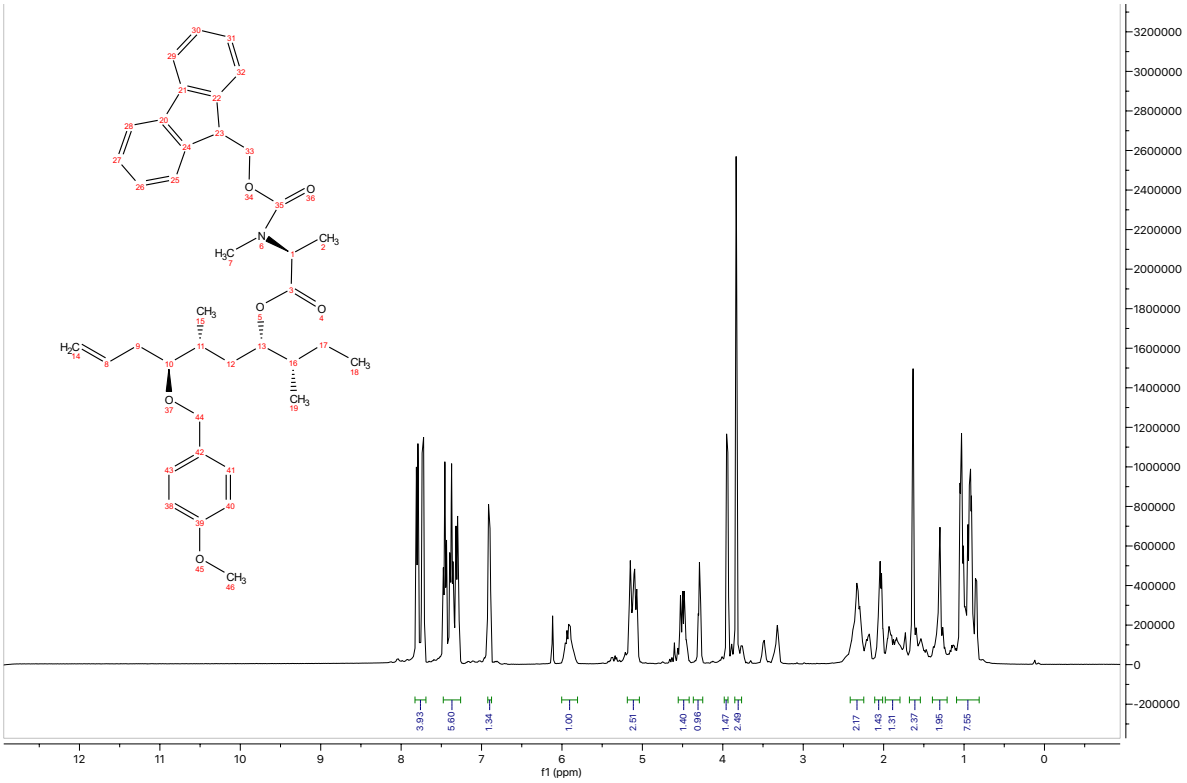
Standard protocol for acid chloride mediated coupling was followed to access the alkene **112** in 50% yield.

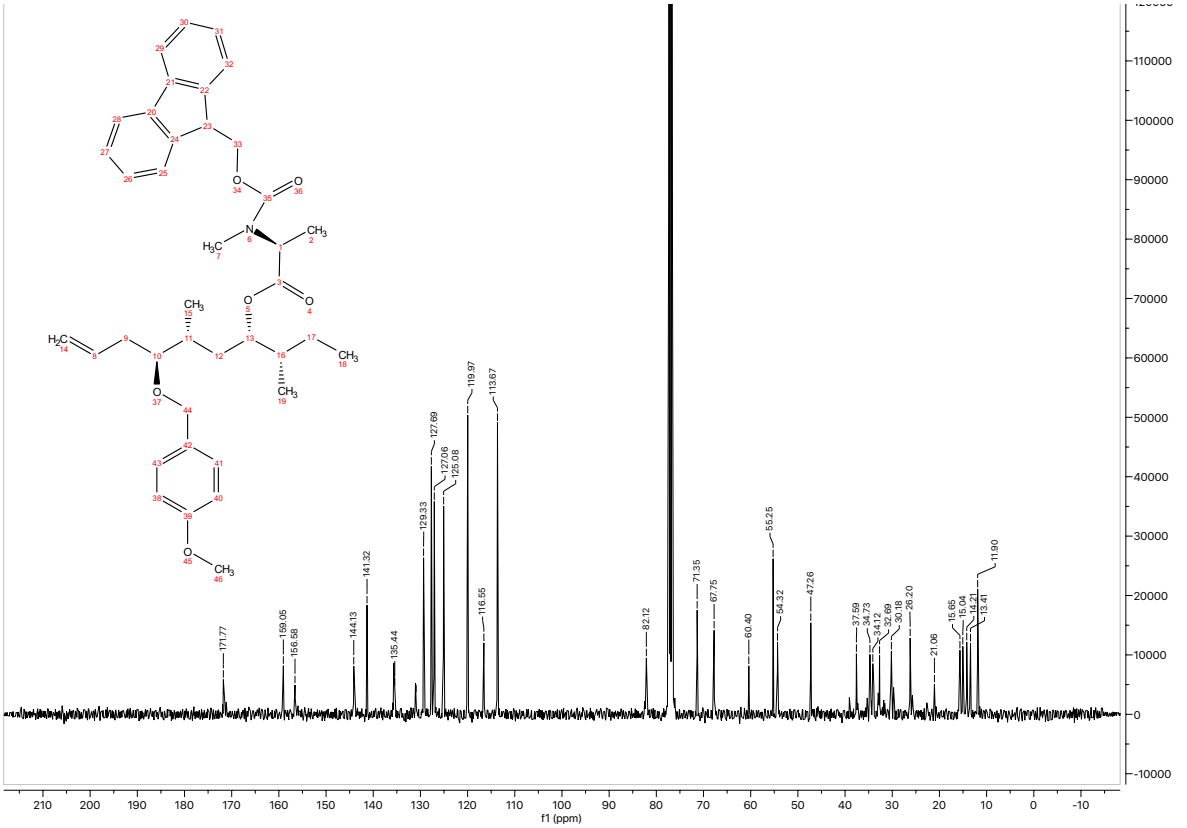
^{1}H NMR (400 MHz, $CDCl_3$) δ 7.83 – 7.69 (m, 4H), 7.48 – 7.26 (m, 6H), 6.92 – 6.88 (m, 1H), 5.91 (tq, *J* = 18.0, 7.9, 7.0 Hz, 1H), 5.11 (dd, *J* = 19.6, 13.1 Hz, 3H), 4.49 (ddd, *J* = 18.8, 10.6, 3.9 Hz, 1H), 4.29 (t, *J* = 6.8 Hz, 1H), 3.98 – 3.94 (m, 1H), 3.83 (d, *J* = 2.5 Hz, 2H), 2.34 (td, *J* = 16.0, 14.3, 7.4 Hz, 2H), 2.04 (t, *J* = 7.6 Hz, 1H), 1.98 – 1.80 (m, 1H), 1.65 (s, 2H), 1.39 – 1.21 (m, 2H), 1.09 – 0.81 (m, 8H). ^{13}C NMR (101 MHz, $CDCl_3$) δ 171.77, 159.05, 156.58, 144.13, 141.32, 135.44, 130.90, 129.33, 127.69, 127.06, 125.08, 119.97, 116.55, 113.67, 82.12, 71.35, 67.75, 60.40, 55.25, 54.32, 47.26, 37.59, 34.73, 34.12, 32.69, 30.18, 26.20, 21.06, 15.65, 15.04, 14.21, 13.41, 11.90.

Notebook entries:

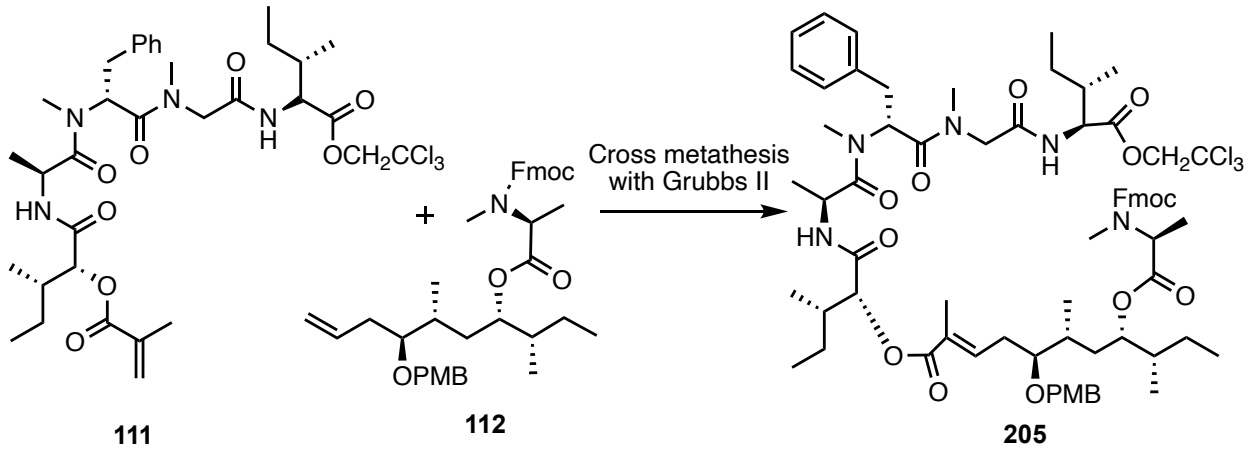
Procedure: SSP2-287

^{1}H NMR and ^{13}C NMR: SSP2-287


3.93
5.60
1.34
1.00
2.61
1.40
0.96
1.47
2.49
2.17
1.43
1.31
2.57
1.95
7.55
f1 (ppm)


171.77
159.05
156.58
144.13
141.32
135.44
129.33
127.69
127.06
125.08
119.97
116.55
113.67
82.12
71.35
67.75
60.40
55.25
54.32
47.26
37.59
34.73
34.12
32.89
30.18
26.20
21.06
15.65
15.04
13.41
11.90
f1 (ppm)

2,2,2-trichloroethyl(2*S*,8*R*,11*S*,14*R*,15*S*)-14-(((5*S*,6*R*,8*S*,9*S*,*E*)-8-((*N*-(((9*H*-fluoren-9-yl)methoxy)carbonyl)-*N*-methyl-*L*-alanyl)oxy)-5-((4-methoxybenzyl)oxy)-2,6,9-trimethylundec-2-enoyl)oxy)-8-benzyl-2-((*S*)-*sec*-butyl)-6,9,11,15-tetramethyl-4,7,10,13-tetraoxo-3,6,9,12-tetraazaheptadecanoate (205)



111 **112** **205**

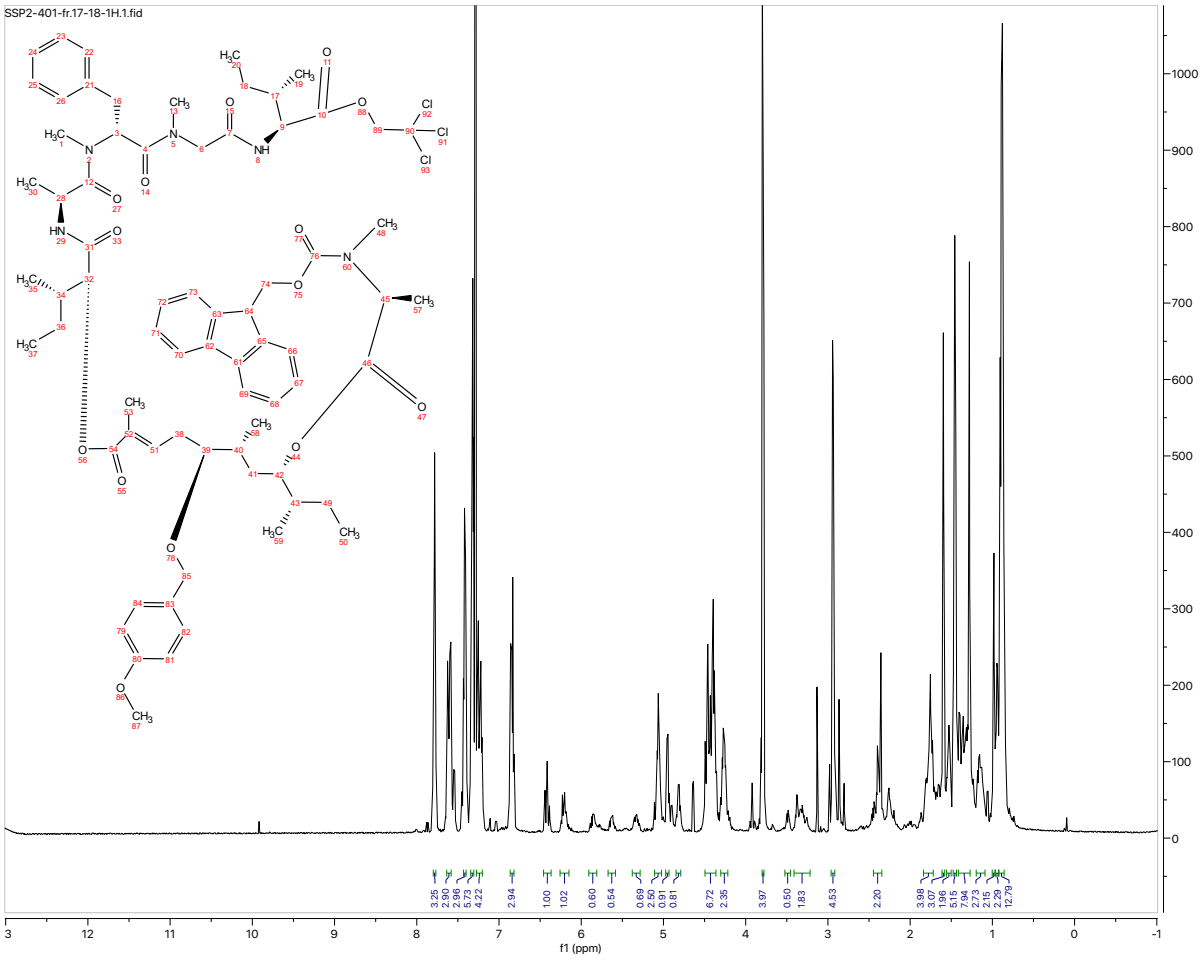
Standard protocol for olefine cross metathesis was followed to obtain **205** in 11% yield.

^{1}H NMR (600 MHz, $CDCl_3$) δ 7.78 (t, *J* = 7.1 Hz, 3H), 7.64 – 7.58 (m, 3H), 7.41 (d, *J* = 7.7 Hz, 3H), 7.32 (td, *J* = 7.1, 6.5, 3.3 Hz, 6H), 7.27 – 7.20 (m, 4H), 6.86 – 6.82 (m, 3H), 6.41 (t, *J* = 16.3 Hz, 1H), 6.21 (ddd, *J* = 17.7, 13.1, 7.1 Hz, 1H), 5.87 (td, *J* = 17.3, 7.2 Hz, 1H), 5.62 (td, *J* = 17.5, 16.4, 8.8 Hz, 1H), 5.33 (td, *J* = 18.3, 17.8, 9.4 Hz, 1H), 5.06 (dtd, *J* = 10.2, 7.0, 3.2 Hz, 3H), 4.96 (dd, *J* = 9.0, 5.7 Hz, 1H), 4.82 (dt, *J* = 14.4, 7.0 Hz, 1H), 4.50 – 4.36 (m, 7H), 4.27 (ddt, *J* = 16.5, 11.8, 7.2 Hz, 2H), 3.80 – 3.78 (m, 4H), 3.48 (dt, *J* = 14.9, 7.5 Hz, 1H), 3.41 – 3.22 (m, 2H), 2.96 – 2.92 (m, 5H), 2.45 – 2.34 (m, 2H), 1.76 (tq, *J* = 15.0, 8.7, 6.3 Hz, 4H), 1.56 – 1.50 (m, 2H), 1.46 (t, *J* = 7.9 Hz, 5H), 1.41 – 1.27 (m, 8H), 1.16 (dq, *J* = 15.6, 7.9 Hz, 3H), 0.99 (d, *J* = 6.8 Hz, 2H), 0.96 – 0.92 (m, 2H), 0.89 (dp, *J* = 10.3, 4.1, 3.6 Hz, 13H).

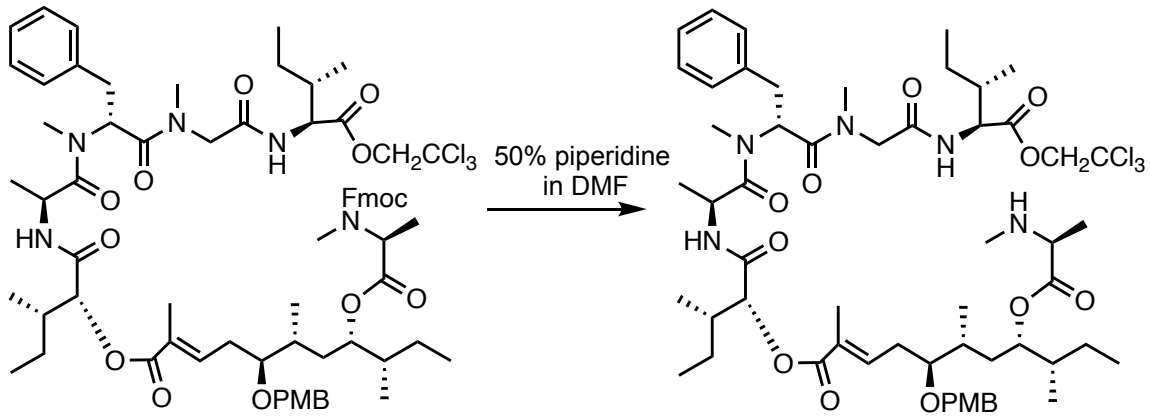
Notebook entries:

Procedure: SSP2-401

^{1}H NMR and ^{13}C NMR: SSP2-401


SSP2-401-fr.17-18-1H.1.fid
f1 (ppm)

2,2,2-trichloroethyl (2*S*,8*R*,11*S*,14*R*,15*S*)-8-benzyl-2-((*S*)-*sec*-butyl)-14-(((5*S*,6*R*,8*S*,9*S*,*E*)-5-((4-methoxybenzyl)oxy)-2,6,9-trimethyl-8-((methyl-*L*-alanyl)oxy)undec-2-enoyl)oxy)-6,9,11,15-tetramethyl-4,7,10,13-tetraoxo-3,6,9,12-tetraazaheptadecanoate (S8)



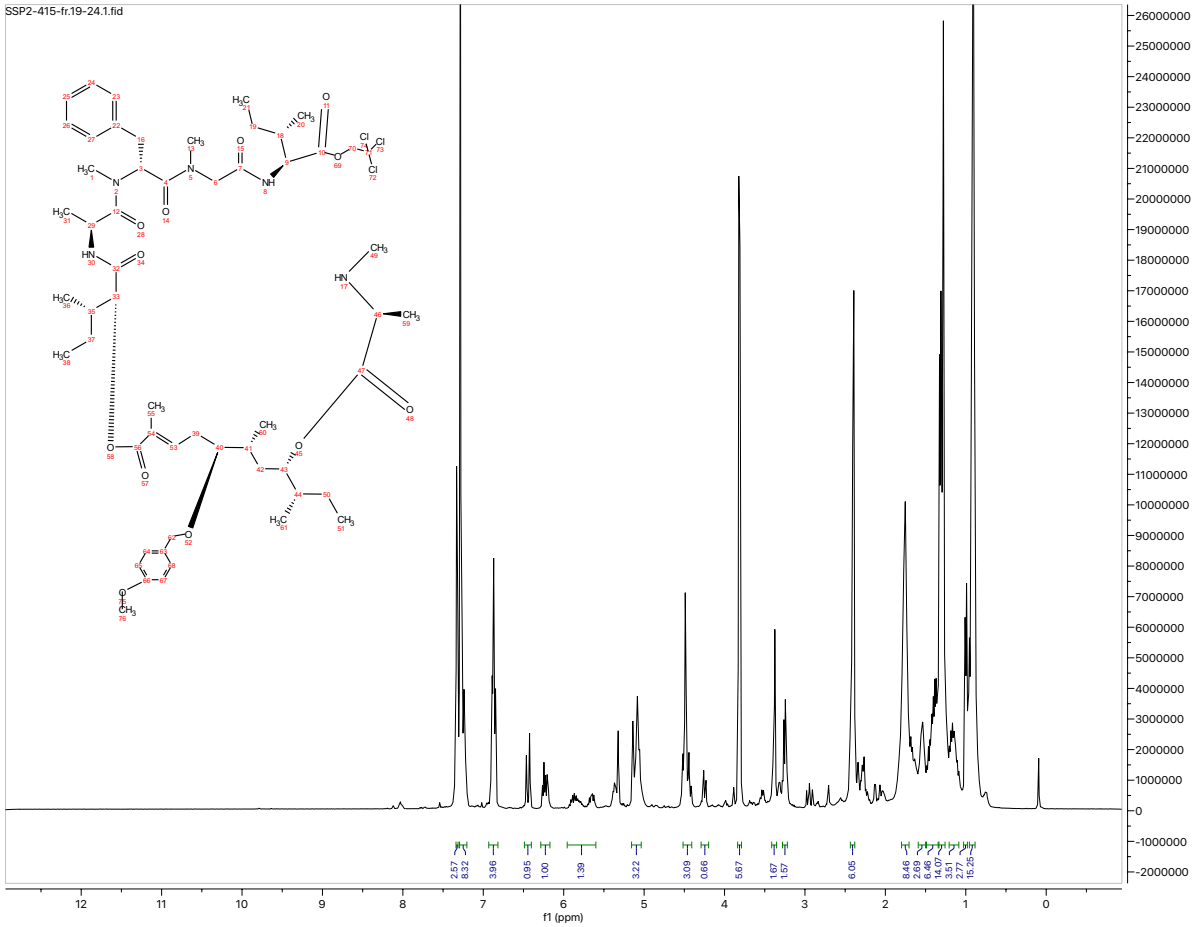
Standard protocol for Fmoc deprotection was followed to access the free amine **S8** in 14% yield after flash column chromatography (gradient elution; 100% hexane, 1:3 EtOAc: hexane, 1:1 EtOAc: hexane, 3:1 EtOAc: hexane, 100% EtOAc, 1:1 MeOH: EtOAc, and 100% MeOH).

^{1}H NMR (400 MHz, $CDCl_3$) δ 7.32 (d, *J* = 6.0 Hz, 3H), 7.25 (d, *J* = 10.0 Hz, 8H), 6.93 – 6.82 (m, 4H), 6.44 (d, *J* = 15.8 Hz, 1H), 6.23 (dt, *J* = 15.4, 7.2 Hz, 1H), 5.96 – 5.60 (m, 1H), 5.16 – 5.04 (m, 3H), 4.52 – 4.41 (m, 3H), 4.25 (dd, *J* = 11.5, 4.2 Hz, 1H), 3.82 (d, *J* = 5.6 Hz, 6H), 3.39 (d, *J* = 8.4 Hz, 2H), 3.25 (q, *J* = 6.9 Hz, 2H), 2.44 – 2.38 (m, 6H), 1.80 – 1.71 (m, 8H), 1.54 (q, *J* = 7.3 Hz, 3H), 1.42 (ddt, *J* = 26.6, 13.3, 7.0 Hz, 6H), 1.34 – 1.26 (m, 14H), 1.15 (tt, *J* = 16.8, 7.5 Hz, 4H), 1.00 (d, *J* = 6.6 Hz, 3H), 0.92 (q, *J* = 9.6, 7.3 Hz, 15H).

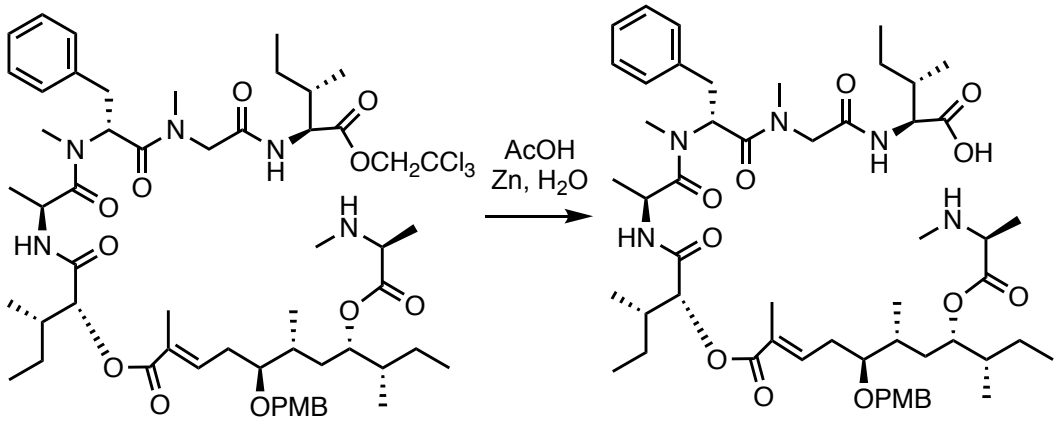
Notebook entries:

Procedure: SSP2-415

^{1}H NMR: SSP2-415


SSP2-415-fr.19-24.1.fid
f1 (ppm)

***N*-(*N*-(((2*R*,3*S*)-2-(((5*S*,6*R*,8*S*,9*S*,*E*)-5-((4-methoxybenzyl)oxy)-2,6,9-trimethyl-8-((methyl-*L*-alanyl)oxy)undec-2-enoyl)oxy)-3-methylpentanoyl)-*L*-alanyl)-*N*-methyl-*D*-phenylalanyl)-*N*-methylglycyl-*L*-isoleucine (107)**



S8 **107**

Standard protocol for trichloro ethanol deprotection was followed to access **107** as a pure white solid in quantitative yield. The crude material was carried forward to next step without further purification.

Notebook entries:

Procedure: SSP2-418

ADDENDUM

SHASHIKA S. PERERA

1852 Anderson Avenue Apt. 15, Manhattan, KS 66502 | 785 477 2919 | shashi2@ksu.edu

PROFESSIONAL SUMMARY

Highly motivated, innovative, and task-driven professional with expertise in synthetic organic chemistry, methodology development, and modern synthetic chemistry techniques. Strong communication skills in sharing research. Ability to collaborate and work as a team with fellow scientists. Skilled in critical thinking and problem solving with a record of academic publications in peer-reviewed journals. Strong drive to learn, improve, and give back to the local community.

EDUCATION

Ph.D. Chemistry, Kansas State University **2018 –** Present (Defense Scheduled: April 2024)
Dissertation Title (in progress): *Total Synthesis of Lagunamide C and Biological Evaluation, Synthesis of the Proposed Natural Product Lagunamide E, and Construction and Evaluation of Chemical Screening Libraries based on the Uvaretin Total Synthesis* (Cumulative GPA 3.95/4.00)

B.S. Chemistry, College of Chemical Sciences, Rajagiriya, Sri Lanka **2013 – 2016**
Dissertation Title**:** Development of a Pullulan Based Gene Delivery System (First Class Honors, GPA 3.66/4.00)

RESEARCH EXPERIENCE

Graduate Research Assistant, Kansas State University, Manhattan, KS **2018 – Present**

- Developed and optimized a scalable synthetic route to access polyketide moiety of lagunamide C, proposed lagunamide E, and final macrocyclization of lagunamide C
  - Investigation of crystallization and co-crystallization methods to confirm the stereochemistry of lagunamide C polyketide
  - Optimization of two different routes (macrolactamization and ring closing metathesis) to access lagunamide C
  - Synthesis of two analog macrocycles to study the mode of action of aurilide family of natural products
  - Optimized a scalable synthetic route to access polypeptide moiety of lagunamide family of natural products
- Developed a divergent synthetic route to access a chemical screening library based on intermediates of Uvaretin natural product
  - Accessed a hybrid enone/reduced enone chalcone with single digit μM cytotoxicity and strong synergistic properties with the known nucleotide mimic drug 6-thiopurine

Research Scientist, Sri Lanka Institute of Nano Technology (SLINTEC) **2017 – 2018**

- API synthesis – Levothyroxine, Beclomethasone Dipropionate
- Gene delivery – Pullulan was functionalized to undergoe click chemistry with a functionalized acid labile linker that was coupled to β-CD to result in a positively charged gene carrier vehicle in nanoscale
- GLP accreditation – Actively participated in establishing the first GLP accredited synthetic and medicinal organic chemistry laboratory in Sri Lanka

Intern, Sri Lanka Institute of Nano Technology (SLINTEC) **2015 – 2017**

- Development of a Pullulan based nano particle in gene delivery
- Extraction of Linamarin from Cassava plant

EXPERTISE & SKILLS

Chemistry
- Total synthesis of natural products
- Methodology development
- Polymer chemistry
- Structure Activity Relationship studies
- Chemical screening libraries
- API synthesis
- Reaction mechanisms

Technical
- NMR spectroscopy, FT-IR, UV-VIS
- HPLC, LC-MS, GC-MS
- Flow cytometry
- Thin layer & column chromatography
- Distillation under reduced pressure
- Laboratory equipment
- Mentoring
- *Mestrelab Mnova,* Chemdraw, MS office

Innovative
- Critical thinking and problem solving
- Effective communication
- Collaborative
- Resilient
- Flexibility, adaptability, risk management

PUBLICATIONS

- **Perera S.**, Fernando A., Dallman J., Weeramange C., Lansakara A., Nguyen T., Rafferty R. J., "Construction and Biological Evaluation of Small Libraries Based of the Intermediates within the Total Synthesis of Uvaretin", *ChemMedChem*, **2021**, *10*, 1631-1639
- **Perera S.**, Gunasekera D. S., Wanninayake U. K., Welideniya D. T., Jayathilaka A. S., Delpe Acharige A., Samanthi U., Kaleel S. S., Karunaratne V., Amaratunga G., "Updating Levothyroxine Synthesis for the Modern Age", *Curr Org Synth,* **2021**, *18*, 371-376
- Welideniya D.T., Jayathilaka A. S., Delpe Acharige A., Samanthi K.A.U., Wanninayake U.K., **Perera S.**, Rajapaksha W., Fernando C.C., Hewadikaram M., Buddhika J., Gunasekara P., Karunaratne V., Amaratunga G.A.J., Gunasekera D.S., "Practical and Scalable Synthesis of Beclomethasone Dipropionate", *Steroids*, **2021**, 177, 108948
- Samanthi K. A. U., Welideniya D.T., Delpe Acharige A., Samarakoon S. R., Rathnayaka R. K., DeSilva M., **Perera S.**, Pieris C., Wanninayake U. K., Jayathilaka A., Karunaratne V., Amaratunga G. A. J., Gunasekera D.S., "An Efficient and High-Yielding Method for Extraction and Purification of Linamarin from Cassava; *in vitro* Biological Evaluation", *Nat. Prod. Res.*, **2021**, *35*, 4169-4172

PRESENTATIONS

- **Perera S**., Fatino A., Wildeman K.R., Rafferty R**.,** "Final Structure Revision and Biological Evaluation Enroute to Total Synthesis of Lagunamide C", **American Chemical Society National Meeting, New Orleans, LA, March 2024** – oral presentation
- **Perera S.**, Fatino A., Rafferty R., "Lagunamide Family: Total Synthesis Efforts, Final Structural Determination, Biological Evaluation, and New Family Identification", **American Chemical Society Midwest Regional Meeting, Iowa City, IA, October 2022** – poster presentation
- **Perera S.**, Fatino A., Rafferty R., "Lagunamide Family to Combat Cancer", **K-State Cancer Research Week, Manhattan, KS, September 2022** – poster presentation
- **Perera S.**, Fatino A., Rafferty R., "Lagunamide Family: Total Synthesis Efforts, Final Structural Determination, Biological Evaluation, and New Family Identification", **Gordon Research Conference, Stereochemistry, Newport, RI, July 2022** – poster presentation
- **Perera S.**, Fatino A., Rafferty R., "Lagunamide Family: Total Synthesis Efforts, Final Structural Determination, Biological Evaluation, and New Family Identification", **Empowering Women in Organic Chemistry, Pfizer in Cambridge, MA, June 2022** – poster presentation

TEACHING EXPERIENCE

Graduate Teaching Assistant, Kansas State University, Manhattan, KS **2018 – Present**

- Classes taught – General Chemistry Labs (CHM 210 & CHM 230), Organic Labs (CHM 351, CHM 532), Recitation Leader for Organic I (CHM 531) and Organic II (CHM 550) Lectures

Graduate Research Assistant, Kansas State University, Manhattan, KS **2018 – Present**

- Mentored and supervised one graduate and four undergraduate students to excel in synthesis, data analysis, instrumentation, and perform research independently

AWARDS & PRIZES

- Ohno Award for Excellence in Research, Chemistry Department, Kansas State University **2023**
- James and Kathy Haymaker Cancer Research Award, Johnson Cancer Research Center, Kansas State Univ. **2022**
- Scott Fateley Travel Award, Chemistry Department, Kansas State University **2022**
- Graduate Classroom Award, Chemistry Department, Kansas State University **2020**

LEADERSHIP EXPERIENCE & COMMUNITY INVOLVEMENT

- Search Committee Member - Senior Research Scientist (NMR Director) Kansas State University **2022**
- Secretary of PLU, The National Chemistry Honor Society at Kansas State University **2020 – 2022**
- International Student Leader at Helping International Students (HIS), Manhattan, KS **2021 – 2022**
- Volunteer at fund raising events and cancer awareness programs organized by Johnson Cancer Research Center, Kansas State University **2022**
- Member of the Bandana Project at Kansas State University, a national campaign to spread suicide prevention and mental health awareness **2022 – Present**
- Member of Intervarsity campus ministry student chapter at Kansas State University **2022 – Present**
- Member of the Powercat Masters Toastmasters club at Kansas State University **2021 – 2023**
- Volunteer at Bridges international organization, Kansas State University **2018 – Present**
- Active member of the Rotaract District 3220 (Sri Lanka & Maldives) **2013 – 2017**

Check for updates

ChemMedChem

Full Papers
doi.org/10.1002/cmdc.202001010

Chemistry Europe
European Chemical Societies Publishing

Construction and Biological Evaluation of Small Libraries Based on the Intermediates within the Total Synthesis of Uvaretin

Shashika Perera,[a] Asantha Fernando,[a] Johnathan Dallman,[a] Chamitha Weeramange,[a] Ashabha Lansakara,[a] Thi Nguyen,[a] and Ryan J. Rafferty*[a]

Introduction

Natural products (NPs) have played a vital role in the treatment of diseases, and are the cornerstone for modern drug discovery, since 2600 B.C. in which oils from *Cupressus semperviren* and *Commiphora* were used in the treatment of coughs, colds, and inflammation.[1] From individual therapeutic agent discovery to inspiration for the construction of non-natural bioactive agents, their impact is immeasurable.[2] While NPs constituted the major pipeline for therapeutic agent discovery for decades, the introduction of high-throughput screening (HTS) in the late 1980s allowed for the discovery of drug lead scaffolds via chemical screening libraries (CSLs); initially solely populated by NPs, NP fragments, and NPs analogs.[3] To answer the call for the population of CSL in a rapid fashion the industry turned towards the use of sp^2–sp^2 metal catalyzed coupling reactions to gain access to tens to hundreds of thousands of small molecules for HTS, as means of identifying new drug lead scaffolds.[4] While numerous FDA approved drugs have been discovered in this fashion, these compounds tend to lack in the chemical diversity, complexity, and inherent biological activity of natural products.[4] To address the diversity of CSLs, multiple research programs have undertaken various approaches to construct new CSLs that either possess structural complexity, rapid small-molecule construction, biological activity-based design, and others.[5] All of these approaches, as expected, have their pros and cons associated with them. Noting the historical importance of NPs, the development of CSLs based upon NPs should deliver CSLs with not only biological activity, but chemical diversity in terms of structural complexity, biological modulating properties, and rich physicochemical properties.

Highlighting the importance of NPs, both in bioactivity and in chemical complexity, and acknowledging that each NP has been designed by nature to elicit a specific and discrete biological affect, our laboratory proposes that CSLs constructed from the intermediates of total synthesis campaigns will give access to new bioactive compounds with tunable chemical complexity. Previously, we have disclosed a new total synthesis route to the chalcone based uvaretin family of natural products.[6] To explore our concept of CSL construction from intermediates of a total synthesis campaign, this route served as the "proof-of-concept" to test feasibility. A chalcone based natural product was chosen for this given their well reported diverse biological activity. From this total synthesis route, and the intermediates within (**1** and **2**, shown for example), numerous small molecules (**3**–**5** and **6**–**7**, shown for example) were constructed and found to possess diverse and interesting biological activity (Figure 1). Furthermore, many of the various phenolic protected variants (MOM or methyl protected) were elaborated onto the carbon framework of uvaretin as analogs, in which the trimethylated **8** was shown to have moderate activity while its allyl protected *o*-hydroxybenzyl (**6**) precursor possessing single-digit micromolar cytotoxicity.

Over 45 compounds were synthesized through these efforts, which were then investigated for sole agent cytotoxicity and as possible small molecule potentiators. Intermediate **1** was used as a starting point for the construction of a 12-member library differing about the alkyl substitution of the phenol positions in ring A. Sole cytotoxicity of these compounds was variable, ranging from 2.2 ± 0.6 to >20 μM IC_{50} values. Interestingly, it was found that many of these varied alkyl substituted phenolic chalcones possessed mild to good potentiating properties with the clinical prescribed acute lymphocytic leukemia drug 6-thiopurine (6TP, Figure 1). 6TP is not commonly used in the treatment of other cancers, due to limited cytotoxicity. However, it was shown to be active in the pancreatic cancer cell line MIA PaCa-2 when used in combination with **4**. The specific alkylation patterns upon the phenolic positions in ring A did reveal interesting potentiation properties. However the alkyl substitutions explored were limited to methyl and methoxymethyl ethers. Elaboration of **1** onto its benzylated counterpart, ring C inclusion, revealed compounds with single digit μM cytotoxicity, but no potentiation properties were observed. Building above these findings, additional investigations into the role of each of the rings and the alkyl effects upon the phenolic central B-ring was explored and disclosed herein.

[a] *S. Perera, A. Fernando, J. Dallman, Dr. C. Weeramange, Dr. A. Lansakara, Dr. T. Nguyen, Prof. R. J. Rafferty*
Department of Chemistry
Kansas State University
1212 Mid-Campus Drive North
Manhattan, KS 66506 (USA)
E-mail: rjraff@ksu.edu

Supporting information for this article is available on the WWW under https://doi.org/10.1002/cmdc.202001010

© 2021 Wiley-VCH GmbH

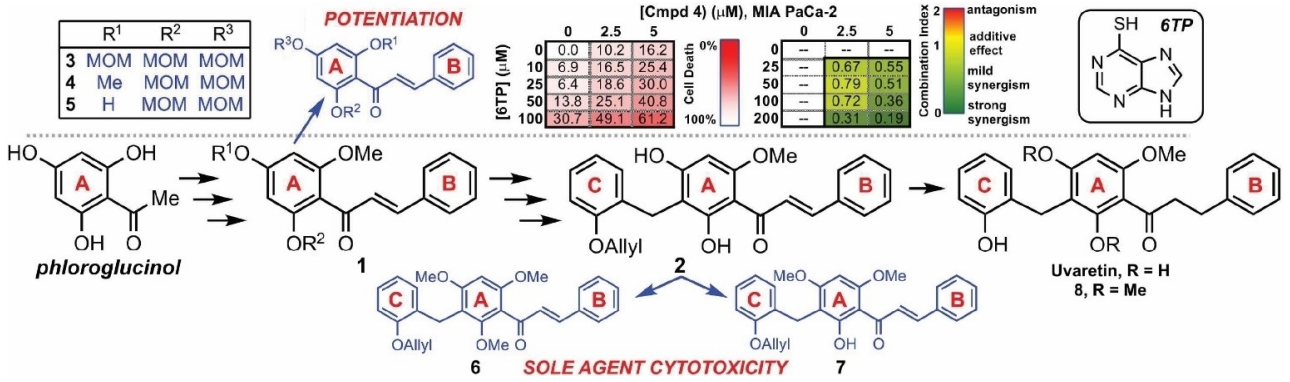
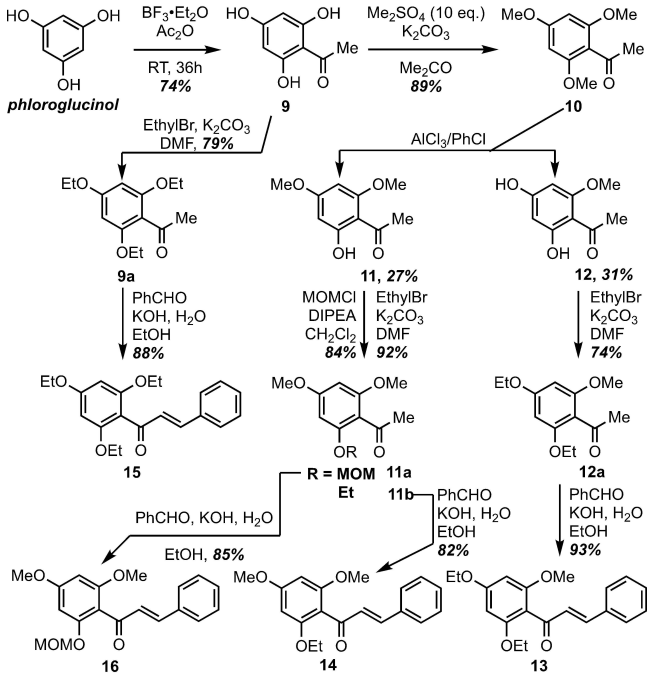


Figure 1. Previously disclosed total synthesis route to uvaretin and its unsaturated enone variant, token examples of small-molecule libraries constructed around intermediates **1** and **2**, and biological assessment.

Results and Discussion

Given the observed potentiation properties of **3**–**5**, and the moderately strong synergistic combination of **4** with 6TP, investigations into the substitution effects with the polyphenolic A ring of the chalcone small library were undertaken. No direct correlation between the number of MOM protected phenol groups was observed in the previously constructed small library. Furthermore, no correlation could be extrapolated on the overall effects of the MOM groups on the observed potentiation activity. In the effort to probe the substituent(s) effects upon this phenolic core, four new chalcones were constructed (Scheme 1). Acetylation of phloroglucinol with acetic anhydride and boron trifluoride etherate gave access to **9** in 74% yield,[7] which was then trimethylated with dimethyl sulfate in acetone affording **10** in 89% yield. Previously, no potentiation properties were observed with either 6TP or doxorubicin with the aldol condensation product of **10**. Demethylation was then performed with $AlCl_3$ in chlorobenzene to give access to demethylated **11** and monomethylated **12** in 27 and 31% yield, respectively. Introduction of diethyl group upon the free phenols of **12** followed by aldol condensation with benzaldehyde afforded chalcone **13** in 68% yield over two-steps.[6,8] In a similar fashion, the free phenol within **11** was ethylated and transformed into its corresponding chalcone **14** in 75% yield over two-steps. The triethylated phenol species was accessed from **9** through ethylation followed by aldol condensation to afford **15** in 70% yield over two-steps. A single MOM group was installed upon **11**, previously no single MOM protected chalcones were constructed and investigated for potentiation properties, in 84% yield and was transformed to its corresponding chalcone **16** in 85% yield.



Scheme 1. Construction of various ethyl, methyl, and MOM chalcones.

With these four analogs of the original chalcone small library set in hand, biological evaluation was then pursued in the same cancerous cell lines as our original study, in which cellular viability was assessed by Alamar Blue quantification:[9] cervical (HeLa), lymphoma (U937), lung (A549), and pancreatic (MIA PaCa-2). Our previously disclosed MOM-chalcone CSL possessed single to double digit μM IC_{50} activity in both HeLa and U937, but showed little to no active in both the A549 and MIA PaCa-2 cancerous cell lines. The diethylated/monomethylated chalcone **13**, possessing greater hydrophobic character than its corresponding di-MOM protected/monomethylated **4** counterpart previous disclosed, possessed 0.9–2.4 μM cytotoxicity in all cell lines screened. Cytotoxicity decreased for the monoethylated/dimethylated chalcone **14**, marginally within HeLa and U937 but drastically in A549 and MIA PaCa-2. The triethylated chalcone **15** had a drastic decrease in cytotoxicity, all values hovering at 20 μM. (Table 1). A common trend observed within the alkyl chalcone compounds **13, 14**, and **16** is that moderate increase in the hydrophobic character translates to decreased cytotoxicity, as observed with higher IC_{50} values in **15**, the triethylated chalcone, to the diethylated/monomethylated chalcone **13**. However, the monoethylated/dimethylated chalcone **14** was shown to possess weaker

© 2021 Wiley-VCH GmbH

18607187, 2021, 10, Downloaded from https://chemistry-europe.onlinelibrary.wiley.com/doi/10.1002/cmdc.202001010 by Kansas State University, Wiley Online Library on [28/06/2023]. See the Terms and Conditions (https://onlinelibrary.wiley.com/terms-and-conditions) on Wiley Online Library for rules of use; OA articles are governed by the applicable Creative Commons License

Table 1. Evaluation of chalcones **13**–**16** for cytotoxicity and potentiation properties.

Cmpd	Observed IC_{50} [μM][a]				C.I.[b]	
	HeLa	U937	A549	MIA PaCa-2	6TP	Dox
4	9.7 ± 1.3	5.9 ± 1.1	4.2 ± 1.9	2.2 ± 0.6	N.T.	N.T.
13	2.4 ± 0.8	0.9 ± 0.9	1.5 ± 1.0	1.1 ± 3.7	1.29	1.76
14	5.9 ± 2.1	8.2 ± 3.0	> 20	> 20	1.01	1.82
15	18.5 ± 3.2	15.3 ± 4.7	> 20	19.1 ± 2.3	1.84	1.99
16	8.3 ± 3.5	7.1 ± 1.4	16.8 ± 3.6	> 20	0.31	0.98

[a] Cytotoxicity was evaluated in 384-well plates over a 72 h treatment. Adherent cells were seeded at 1500 cells/well, whereas suspension cells at 2200 cells/well. Cellular viability was evaluated via Alamar Blue. Doxorubicin was used as the positive cell death control, and wells with only cells as the alive control. [b] Cytotoxicity evaluation for combinational index (C.I.) studies were the same as for sole agent cytotoxicity, and the C.I. was determined based on the Chou-Talalay protocol.[10] N.T.: not tested and n = three biological replicates.

cytotoxicity than **13**. This suggests that the tuning of the hydrophobic character of the phenolic A ring could alter and enhance the cytotoxic activity of the chalcone system. It was observed that with the inclusion of a single MOM group in the dimethylated chalcone, a general increase in cytotoxicity was observed with respect to the previous MOM-chalcone small library. In terms of small molecule potentiation with 6TP and doxorubicin, it was observed that the presence of at least one MOM group is essential for synergistic activity. Assessing the synergist properties of these compounds, and all other compounds disclosed herein, with either 6TP or doxorubicin was performed in a 3x5 matrix format. Two concentrations of the small molecule screened were used that would induce 10–20% cell death within a 72-h period. Concentrations of either 6TP or doxorubicin were chosen to result in 40–60% cell death within the same time period. Combinational effects of cell death verses concentration were then tabulated, and from these values the effects of potentiation were determined by their combination index (C.I.), a value calculated by employing the Chou-Talalay protocol.[10] C.I. values closer to 0 represent strong synergism, 0.5 mild synergism, 1 an additive effect, and values greater than 1 denote antagonism in this method. Synergy was shown with **16** and both 6TP and doxorubicin with C.I. of 0.31 and 0.98, respectively. Based upon these investigations a general trend of the effects of hydrophobicity of the phenolic core was observed; decreased synergy with increased hydrophobic character.

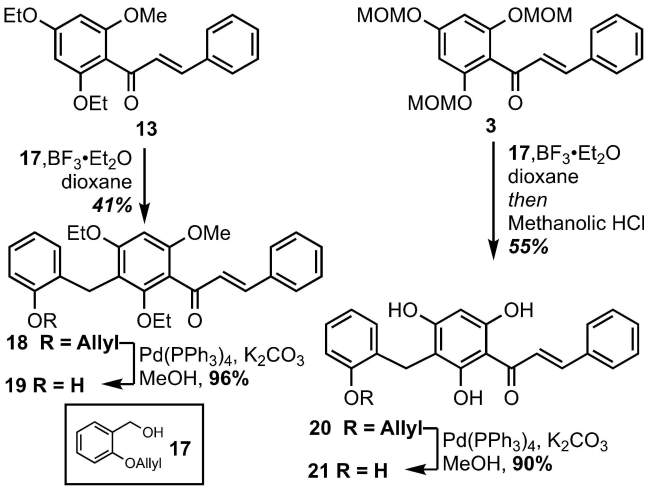
Incorporation of a *ortho*-hydroxybenzyl substituent upon the phenolic ring gives rise to the uvaretin family of natural products. We previously disclosed that **6** and **7** (Figure 1), the trimethylated phenol and allyl protected *o*-hydroxybenzyl group/allyl deprotected free phenol, possessed strong sole agent cytotoxicity (Table 2). From this, it was envisioned to incorporate **13**, the diethyl/monomethyl chalcone into this uvaretin carbon framework for cytotoxicity investigations. Subjecting **13** to our reported Friedel–Crafts alkylation conditions with **17** gave access to **18** in 41% yield, and treatment with $Pd(PPh_3)_4$ and potassium carbonate in methanol deprotected the allyl group to afford **19** in 96% yield (Scheme 2). In parallel, the free phenol analog was prepared from **3** by Friedel–Crafts alkylation with **17**, with subsequent MOM deprotection with methanolic HCl furnished **20** in 55%. Subsequent allyl deprotection with $Pd(PPh_3)_4$ and potassium carbonate in methanol gave access to **21** in 90% yield. Screening of **18**–**21** against the four cancerous cell line panel revealed interesting patterns. In both substitution patterns of the phenolic core, greater cytotoxicity was observed in allyl deprotected **19** and **21**. Overall, the more hydrophobic phenol core showed greater cytotoxicity. No potentiation properties with 6TP and **18**–**21** were observed.

Previously, *o*-allyloxy benzyl alcohol (**17**) was employed in our total synthesis of the natural product uvaretin, as well as in

Table 2. Evaluation of C-benzylated chalcones **18**–**21** for cytotoxicity properties.

Cmpd	Observed IC_{50} [μM][a]			
	HeLa	U937	A549	MIA PaCa-2
6	5.8 ± 0.5	7.5 ± 1.1	8.5 ± 0.6	9.4 ± 1.3
7	2.7 ± 0.6	4.2 ± 1.4	9.3 ± 1.1	4.1 ± 0.3
18	1.2 ± 0.9	0.8 ± 0.5	1.4 ± 1.2	9.7 ± 2.1
19	0.8 ± 0.7	0.9 ± 1.0	1.1 ± 0.7	4.1 ± 1.8
20	9.7 ± 1.1	11.7 ± 2.8	15.4 ± 3.5	> 20
21	2.7 ± 1.9	4.7 ± 1.8	3.1 ± 1.8	10.7 ± 4.3

[a] Cytotoxicity was evaluated in 384-well plates over 72 h of treatment. Adherent cells were seeded at 1500 cells/well, suspension cells at 2200 cells/well. Cellular viability was evaluated with Alamar Blue. Doxorubicin was used as the positive cell death control, and wells with only cells as the alive control (n = three biological replicates).



Scheme 2. Elaboration of chalcones **13** and **3** onto their C-benzylated variants.

© 2021 Wiley-VCH GmbH

18607187, 2021, 10, Downloaded from https://chemistry-europe.onlinelibrary.wiley.com/doi/10.1002/cmdc.202001010 by Kansas State University, Wiley Online Library on [28/06/2023]. See the Terms and Conditions (https://onlinelibrary.wiley.com/terms-and-conditions) on Wiley Online Library for rules of use; OA articles are governed by the applicable Creative Commons License

the uvaretin framework of chalcone analogs disclosed herein. Keeping in mind the overarching goals of this project, construction of new small chemical screening libraries, efforts were placed towards modifications upon the benzyl (left ring) of the trimethylated chalcone uvaretin system to explore what effects, if any, they had upon cytotoxicity. Initially, *para*-allyloxy benzyl alcohol was attached onto **22** via our Friedel–Crafts alkylation protocol for the construction of its corresponding uvaretin carbon core **23** in 67% yield, which was subsequently transformed into the free phenol under our standard allyl deprotection condition to access **24** in 33% yield (Figure 2). The Friedel–Crafts alkylation worked well for both the *ortho* and *para* substituted allyloxy benzyl alcohols, however, the *meta* system, **25**, failed to give any desired product. Lower yields were obtained with the Friedel–Crafts alkylations of the *ortho* (**26**) and *para* (**27**) chloro benzyl alcohols, 28 and 25% yields, respectively. Treating **22** with 2,3-methylenedioxy benzyl alcohol afforded **28** in 29% yield, further supporting carbocation stabilization. No product was observed when benzyl alcohol (**29**) or 2-(hydroxymethyl)benzaldehyde (**30**) were attempted. Based on these results, it can be concluded that electron donating groups are required in the *ortho* and *para* positions to stabilize the induced carbocation from the boron trifluoride complexation with the benzyl alcohol. Screening of **26** and **27** showed $>20\,\mu M$ cytotoxicity, and no potentiation properties with either 6TP or doxorubicin. Unexpectedly, both the allyl (**23**) and free phenol (**24**) uvaretin carbon core analogs showed cytotoxicity low double digit μM cytotoxicity, with no potentiating properties observed. Limited cytotoxicity was observed from **28**, IC_{50} of $18.5\pm3.8\,\mu M$ in U937, but had strong synergism with doxorubicin possessing a combination index of 0.33. From this, it can be speculated that the substitution pattern upon the left benzyl ring plays a critical role in the cytotoxicity of uvaretin based small libraries.

Previously, we disclosed that the trimethylated chalcone **22** was shown to have 4.3–6.7 μM activity in HeLa, U937, and A549 cancerous cells lines, with no activity observed in MIA PaCa-2.[6] Varying the groups upon the phenolic oxygens with a mixture of MOM, ethyl, and methyl groups gave rise to different small-molecule potentiators with varying micromolar cytotoxicity. Based on this, it could be concluded that the enone functionality is not only responsible for cytotoxicity, but also potentiation. To explore this further, the enone in **22** was reduced to **31** in 99% yield (Scheme 3). Noting the single digit μM cytotoxicity observed with **22**, the complete loss of activity for **31** was unexpected. Uvaretin, the parent natural product that spurred these investigations, is a 2.0–3.7 μM cytotoxic compound that possesses no enone functional group. Given that uvaretin does not possess an enone group, we speculate that the *o*-hydroxyl benzyl group along with the phenolic central ring is responsible for its cytotoxicity. To probe the effects of the reduced enone portion of the chalcone, noting that no sole cytotoxicity was observed, potentiating studies were undertaken. A mild synergism, combinational index of 0.72, was observed with **31** and 6TP in MIA PaCa-2 suggesting that the reduced enone portion could be responsible for potentiation character or transport.

To exploit the possibility that the enone and *o*-hydroxy benzyl group are responsible for cytotoxicity and the reduced enone responsible for potentiation and transport properties, our focus shifted towards the construction of a hybrid trimethylated uvaretin analog possessing all of these attributes. Diacetylation of phloroglucinol was accomplished with acetic anhydride and boron trifluoride etherate accessing **32** in 52% yield, which was subsequently trimethylated with dimethyl sulfate in acetone to afford **33** in quantitative yield (Scheme 4). Aldol condensation upon **33** with excess equivalences of benzylaldehyde and potassium hydroxide furnished chalcone **34** in 82% yield. Subjecting **34** to Friedel–Crafts alkylation conditions with **17** furnished the dienone/*o*-allyloxybenzyl chalcone **35** in 46% yield, followed by allyl deprotection with $Pd(PPh_3)_4$ and potassium carbonate in methanol to afford **36** in 90% yield. Full reduction of the enones within **34** gave access to **37** in quantitative yield, subjection to Friedel–Crafts alkylation conditions with **17** afforded **38** in 29% yield. Allyl deprotection upon **38** was troublesome, as such, reduction of the enones in **36** was accomplished to give access to **39**. Biological assessment of these compounds, discussed below, lead to the construction of a hybrid chalcone possessing both an enone and reduced enone. Accessing the enone/reduced enone system was undertaken by treating **33** to Aldol Condensation with benzaldehyde (0.9 equiv.) to access **40** in 69% yield. Reduction of the enone was accomplished with palladium on carbon in 71% yield followed by Aldol Condensation to afford **41** in 45% yield. Unfortunately, all attempts to include the *o*-allyloxy benzyl alcohol upon **41** failed.

Screening **34**–**41** for sole agent cytotoxicity against the four panel cancerous cell lines used in this work was then undertaken (Table 3). The di-enone chalone (**34**) possessed similar IC_{50} values in comparison to its mono-enone chalcone counterpart **22**, suggesting that the presence of a second enone does not

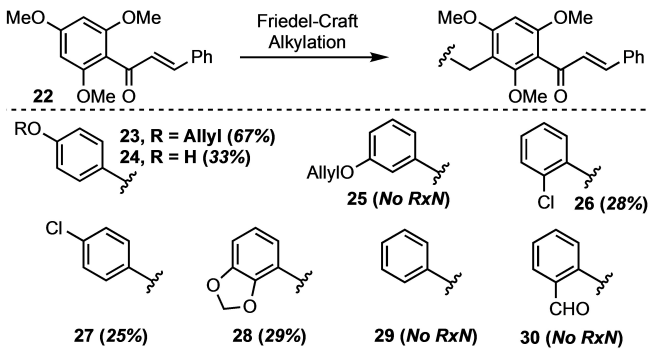
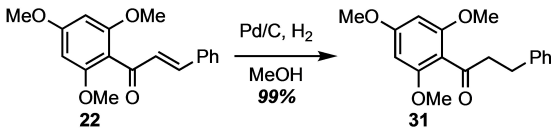


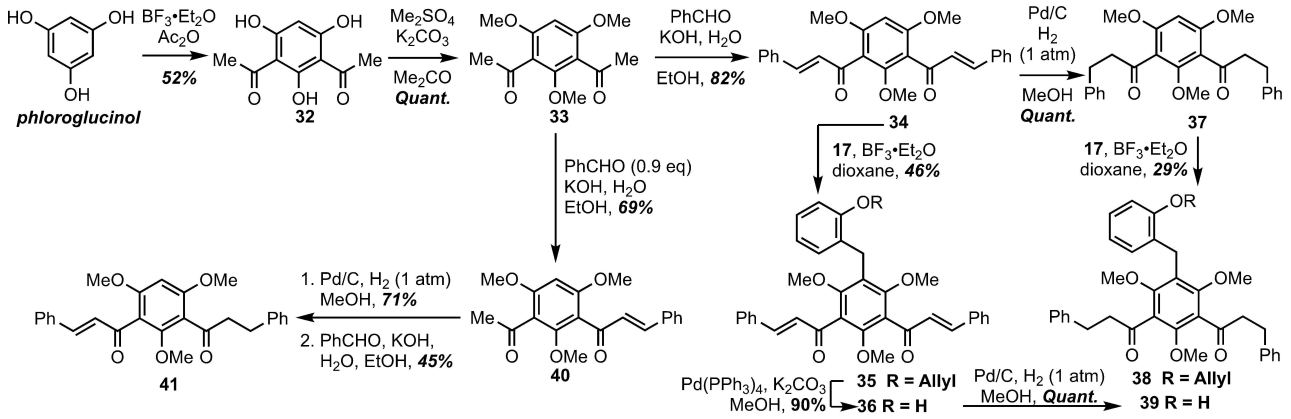
Figure 2. Friedel–Crafts alkylation attempts upon **22** with varied substituted benzyl alcohol systems.



Scheme 3. Enone reduction for potentiation and cytotoxicity comparisons.

© 2021 Wiley-VCH GmbH

18607187, 2021, 10, Downloaded from https://chemistry-europe.onlinelibrary.wiley.com/doi/10.1002/cmdc.202001010 by Kansas State University, Wiley Online Library on [28/06/2023]. See the Terms and Conditions (https://onlinelibrary.wiley.com/terms-and-conditions) on Wiley Online Library for rules of use; OA articles are governed by the applicable Creative Commons License



Scheme 4. Construction of hybrid chalcone and reduced enone chalcones.

Table 3. Evaluation of chalcones **34**–**41** for cytotoxicity and potentiation properties.

Cmpd	Observed IC_{50} [μM][a]				C.I.[b]
	HeLa	U937	A549	MIA PaCa-2	**6TP**
22	5.2 ± 1.4	6.7 ± 0.8	4.3 ± 0.9	> 20	N.T.
34	4.7 ± 2.4	5.4 ± 0.7	3.7 ± 1.1	18.4 ± 5.8	1.51
35	1.1 ± 0.5	1.7 ± 1.2	0.8 ± 0.9	12.4 ± 8.2	1.78
36	1.0 ± 0.9	2.0 ± 0.8	1.5 ± 1.5	13.5 ± 4.7	1.67
37	19.7 ± 5.1	> 20	18.0 ± 2.4	> 20	N.T.
38	13.4 ± 5.0	16.7 ± 6.2	11.8 ± 1.9	13.9 ± 2.5	1.18
39	11.8 ± 2.1	15.8 ± 4.8	12.0 ± 3.7	15.0 ± 3.2	1.04
41	4.7 ± 2.0	4.8 ± 3.1	3.7 ± 2.9	19.2 ± 7.3	0.42

[a] Cytotoxicity was evaluated in 384-well plates over a 72 h treatment. Adherent cells were seeded at 1500 cells/well, whereas suspension cells at 2200 cells/well. Cellular viability was evaluated via Alamar Blue. Doxorubicin was used as the positive cell death control, and wells with only cells as the alive control. [b] Cytotoxicity evaluation for combinational index (C.I.) studies were the same as for sole agent cytotoxicity, and the C.I. was determined based on the Chou-Talalay protocol.[10] N.T.: not tested and n = three biological replicates.

increase the cytotoxic character of the chalcone. Incorporation of the *o*-allyloxy benzyl group did translate into an across-the-board increase in cytotoxicity. However, deprotection of the allyl group did not significantly affect cytotoxic properties. A near complete loss of cytotoxicity was observed in the reduced di-enone **37**, *o*-allyloxy benzyl incorporation (**38**) did show a marginal increase in cytotoxicity relative to **37**. Like with **35** and **36**, de-allylated **39** showed non-significant changes in cytotoxicity relative to allylated **38**. Investigating possible potentiating properties of **34**–**39** with 6TP in MIA PaCa-2 were concluded to investigate, and elucidate, the possible role of the enone and reduced enone. All enone containing compounds (**34**–**36**) were found to possess antagonism, non-synergist relationships. In contrast, the reduced enones (**38** and **39**) were shown to possess borderline mild synergism. These biological investigations led support to our initial theory that both the enone and *o*-allyloxy and hydroxy benzyl groups tend to be responsible for sole agent cytotoxicity and the reduced enone supports potentiation properties. Evaluation of the enone/reduced enone hybrid **41** for sole agent cytotoxicity revealed cytotoxicity similar to **34** and **22**. Most excitingly, potentiation of **34** with 6TP in MIA Paca-2 was shown to have mild to strong synergism, while also possessing sole cytotoxic properties.

Conclusion

The construction of new small-molecule chemical libraries based upon the intermediates of our total synthesis route towards the uvaretin class of natural products is disclosed. Building from our previous efforts, further structure–activity relationship (SAR) studies were performed upon the sole chalcone core, possessing no benzylated system. Previously, we found interesting potentiation properties for the MOM protected chalcone system **3**–**5**, of which **4** was shown to have good synergistic properties towards 6TP in the pancreatic cell line MIA PaCa-2; 6TP has no reported activity in this cell line. In the efforts to optimize the potentiation properties of these chalcones, we constructed **13**–**16** possessing various states of methyl, ethyl, and single MOM group inclusion upon the triphenol ring. It was found that increasing the hydrophobic character upon the triphenol ring led to an overall decrease in cytotoxicity. Unexpectedly, the dimethylated mono-MOM protected **16**, while showing moderating cytotoxicity, was found to possess strong synergistic properties with both 6TP and doxorubicin in comparison to its more hydrophobic counterparts **13**–**15**. Through our previous efforts, and the ones disclosed herein, the role of the benzyl group was explored. The triethylated chalcone (**15**) was observed to have little to no cytotoxicity, however when incorporation of the *o*-hydroxybenzyl to form **18**/**19** gave access to cytotoxic activity. Thus, suggesting that the *o*-hydroxybenzyl group possess cytotoxicity in its own right, thus helping to explain the cytotoxic activity of uvaretin. Through these efforts, the identification of the enone as the bioactive portion of the chalcone was further confirmed, and through the libraries constructed and evaluated it was observed that the reduced enone systems, while possessing marginal cytotoxicity, possess potentiation properties. In the efforts to merge these two characteristics, we set forth to construct our final library set of eight compounds, **34**–**41**. Sole

© 2021 Wiley-VCH GmbH

18607187, 2021, 10, Downloaded from https://chemistry-europe.onlinelibrary.wiley.com/doi/10.1002/cmdc.202001010 by Kansas State University, Wiley Online Library on [28/06/2023]. See the Terms and Conditions (https://onlinelibrary.wiley.com/terms-and-conditions) on Wiley Online Library for rules of use; OA articles are governed by the applicable Creative Commons License

18607187, 2021, 10, Downloaded from https://chemistry-europe.onlinelibrary.wiley.com/doi/10.1002/cmdc.202001010 by Kansas State University, Wiley Online Library on [28/06/2023]. See the Terms and Conditions (https://onlinelibrary.wiley.com/terms-and-conditions) on Wiley Online Library for rules of use; OA articles are governed by the applicable Creative Commons License

agent cytotoxicity was observed with dienones **34**–**37**, and potentiation properties with the dual reduced enones **37**–**39**. Construction of the hybrid enone/reduced enone **41** was accomplished and was shown to possess single digit μM cytotoxicity in all cell lines screened, except MIA PaCa-2, and retained strong synergistic properties with 6TP in MIA PaCa-2. We can conclude that small chemical library construction, as well as SAR studies upon said libraries, has led to the identification of new and interesting small molecules with diverse biological activities.

Experimental Section

Chemistry and general methods

All reagents were commercially available and used without purification unless otherwise stated. NMR spectra were recorded with a Varian and Bruker 400 MHz instrument. The chemical shifts are given in parts per million (ppm) relative to residual $CHCl_3$ at δ 7.26 ppm or DMSO at δ 2.50 ppm for proton spectra and relative to $CDCl_3$ at δ 77.23 ppm or DMSO at δ 39.52 ppm for carbon spectra, unless otherwise noted. Low-resolution mass spectra were obtained using a Waters Xevo-TQD via direct injection; samples were dissolved in methanol, filtered, and the supernatant injected. Flash column chromatography was performed with silica gel grade 60 (230–400 mesh). Dichloromethane (CH_2Cl_2), and methanol (CH_3OH) were all degassed with argon and passed through a solvent purification system containing alumina or molecular sieves. All commercially available reagents were used as received. All procedures including anhydrous solvents were performed with rigorously dried glassware under inert atmosphere.

General procedures

Aldol condensation. To a round bottom flask (RBF) was added the acetophenone species (1.0 equiv.), benzaldehyde (1.0 equiv., unless otherwise noted), and EtOH (20 mL) and brought to 0 °C. Once at temperature, a solution of KOH (17 equiv.) in water (25 mM final concentration) was added dropwise, after which the mixture was brought to 25 °C and left to stir for 14 h. The reaction was diluted with EtOAc, washed with water, acidified with 1 M HCl, and extracted with EtOAc (×2). The organic layers were combined, washed with brine, dried over sodium sulfate and concentrated to afford the crude material. Specific purification protocols are given with each specific reaction.

Friedel–Crafts alkylation. To a flamed dried RBF under an argon atmosphere was added chalcone (1.0 equiv.) and dry dioxane (final concentration of 46 mM) and stirred at RT. In a second flamed dried RBF was added **17**[6] (1.2 equiv.) in dry dioxane (final concentration of 0.22 M), which after stirring for 5 min at RT was added to the chalcone mixture. To a separate flamed dried RBF under an argon atmosphere was added $BF_3 \cdot Et_2O$ (3.05 equiv.) and dioxane (final concentration of 0.56 M), this solution was added to the previously prepared RBF in four portions 10 min apart. The reaction was then brought to 60 °C and stirred for 3 h. The reaction was cooled, diluted with EtOAc, washed with water (×2), and extracted with EtOAc (×2). The combined organic layers were combined, washed with brine, dried over sodium sulfate, and concentrated under reduced pressure. Specific purification protocols are given with each specific reaction.

Allyl deprotection. To a flamed dried RBF under an argon atmosphere was added chalcone species (1.0 equiv.), K_2CO_3 (6 equiv.), and $Pd(PPh_3)_4$ (0.02 equiv.) in MeOH (final concentration relative to chalcone 16 mM) and allowed to stir at reflux for 2 h. The reaction mixture was filtered through a short silica plug, rinsed with MeOH (1 vol. equiv. to initial MeOH), and concentrated to afford the desired product.

Enone reduction. To a flamed dried RBF under an argon atmosphere was added the enone material (1.0 equiv.) and 10% palladium over carbon in MeOH (2.3 M final concentration relative to the enone). A hydrogen balloon was introduced and the mixture was left to stir at 25 °C for 2 h, filtered through Celite, and rinsed with MeOH or $CHCl_3$. The filtrate was concentration to afford the ketone species.

Compound synthesis

*2,4,6-Trihydroxyacetophenone (**9**):*[11] $BF_3 \cdot OEt_2$ (7.5 mL, 59.4 mmol) and acetic anhydride (1.9 mL, 19.8 mmol) followed by phloroglucinol (2.5 g, 19.8 mmol) was added to a RBF under argon, and the mixture was stirred at room temperature (RT). After 15 h, the reaction mixture was poured onto a 10% NaOAc solution (70 mL) and left to stir overnight (o/n) under ambient atmosphere. The precipitate was filtered off and washed with water to obtain **9** (2.9 g) in 88% yield. ^{1}H NMR (400 MHz, CD_3OD) δ 5.79 (s, 2H), 2.59 (m, 3H). ^{13}C NMR (101 MHz, CD_3OD) δ 204.56, 166.32, 165.90, 105.60, 95.59, 32.71.

*2,4,6-Trimethyoxyacetophenone (**10**):*[12] Compound **9** (0.5 g, 2.98 mmol), K_2CO_3 (2.0 g, 14.9 mmol), and anhydrous acetone (10 mL) were added to a flamed RBF under argon. The reaction mixture was stirred at 25 °C for 15 h, and then brought to reflux for an additional 4 h. The reaction was quenched by the addition of saturated ammonium chloride, and the mixture was extracted with EtOAc (×3). The organic layers were combined, washed with brine, dried over sodium sulfate and concentrated under reduced pressure. The crude material was purified by flash silica gel chromatograph (Hex/EtOAc 1:1) to afford the **10** (556 mg) in 89% yield. ^{1}H NMR ($CDCl_3$, 400 MHz) δ (ppm): 6.10 (s, 2H), 3.82 (s, 3H), 3.79 (s, 6H), 2.46 (s, 3H). ^{13}C NMR ($CDCl_3$, 101 MHz) δ (ppm): 202.1, 162.5, 158.6, 113.8, 90.7, 56.0, 55.7, 32.8.

*2,4-Dimethoxy-6-hydroxy-acetephone (**11**) and 2-Methoxy-4,6-dihydroxy-acetophenone (**12**):* To a flamed-dried RBF was added **10** (0.5 g, 2.38 mmol) and PhCl (24 mL) followed by $AlCl_3$ (0.64 g, 4.8 mmol), and the mixture was left to stir o/n at RT. The mixture was then brought to 70 °C and stirred for an additional 24 h. The reaction was quenched with saturated Rochelle Salt, and the mixture was stirred for 30 min, then extracted with EtOAc (×3). The organic layers were combined, dried over sodium sulfate, and concentrated under reduced pressure. The crude material was purified by flash silica gel chromatography (Hex/EtOAc 7:3) to afford **11** (126 mg) in 27% yield and **12** (134 mg) in 31% yield. Compound **8**: ^{1}H NMR ($CDCl_3$, 400 MHz) δ (ppm): 5.90 (1H, d, J = 2.1 Hz), 3.84 (3H, s), 3.80 (3H, s), 2.60 (3H, s). ^{13}C NMR ($CDCl_3$, 101 MHz) δ (ppm): 203.97, 166.83, 166.41, 162.85, 105.60, 92.14, 32.98. Compound **9**: ^{1}H NMR ($CDCl_3$, 400 MHz) δ (ppm): 8.30 (s, 1H), 6.03 (d, J = 2.0 Hz, 1H), 5.99 (d, J = 2.0 Hz, 1H), 3.91 (s, 3H), 2.59 (s, 3H). ^{13}C NMR ($CDCl_3$, 101 MHz) δ (ppm): 204.0, 166.7, 165.2, 164.6, 106.5, 96.8, 92.0, 56.0, 33.0.

*(E)-1-(2,4-Diethoxy-6-methoxyphenyl)-3-phenylprop-2-en-1-one (**13**):* The general procedure for aldol condensation was followed using **12a** (0.3 g, 1.26 mmol). The crude material was purified by flash silica gel chromatography (Hex/EtOAc 7:3) to give **13** (382 mg, pale-white solid) in 93% yield. ^{1}H NMR ($CDCl_3$, 400 MHz) δ (ppm): 7.67–7.58 (m, 3H), 7.55–7.44 (m, 3H), 7.30 (d, J = 15.0 Hz, 1H), 6.56 (dd, J = 15.6, 2.0 Hz, 2H), 4.39 (q, J = 5.9 Hz, 2H), 4.06 (q, J = 5.9 Hz, 2H), 3.91 (s, 3H), 1.65 (t, J = 5.9 Hz, 3H), 1.34 (t, J = 5.9 Hz, 3H). ^{13}C NMR ($CDCl_3$, 101 MHz) δ (ppm): 192.6, 162.4, 162.1, 161.9, 142.9,

© 2021 Wiley-VCH GmbH

135.5, 129.8, 129.0, 128.6, 126.1, 112.1, 95.4, 92.8, 65.2, 63.9, 56.0, 14.7, 14.2. LRMS (ESI): *m/z* calcd for $C_{20}H_{23}O_4^+$: $[M+H]^+$ 327.15, found 327.16.

*(E)-1-(2-Ethoxy-4,6-dimethoxyphenyl)-3-phenylprop-2-en-1-one (**14**):* The general procedure for aldol condensation was followed using **11a** (0.37 g, 1.65 mmol). The crude material was purified by flash silica gel chromatography (Hex/EtOAc 7:3) to give **14** (423 mg, white solid) in 82% yield. ^{1}H NMR ($CDCl_3$, 400 MHz) δ (ppm): 7.67–7.60 (m, 3H), 7.54–7.43 (m, 6H), 7.29 (d, J=15.1 Hz, 1H), 6.50 (s, 2H), 4.39 (q, J=5.9 Hz, 2H), 3.91 (s, 3H), 3.80 (s, 3H), 1.65 (t, J=5.9 Hz, 3H). ^{13}C NMR ($CDCl_3$, 101 MHz) δ (ppm): 192.6, 165.4, 162.6, 162.0, 142.9, 135.5, 129.8, 129.0, 128.6, 126.1, 111.2, 95.9, 93.8, 65.2, 56.0, 14.2. LRMS (ESI): *m/z* calcd for $C_{20}H_{21}O_4^+$: $[M+H]^+$ 313.14, found 313.14.

(E)-3-Phenyl-1-(2,4,6-triethoxyphenyl)prop-2-en-1-one (): The general procedure for aldol condensation was followed using **9a** (0.28 g, 1.11 mmol). The crude material was purified by flash silica gel chromatography (Hex/EtOAc 7:3) to give **15** (332 mg, white solid) in 88% yield. ^{1}H NMR ($CDCl_3$, 400 MHz) δ (ppm): 7.68–7.59 (m, 3H), 7.56–7.42 (m, 3H), 7.30 (d, J=15.1 Hz, 1H), 6.57 (s, 2H), 4.39 (q, J=5.9 Hz, 4H), 4.06 (q, J=5.9 Hz, 2H), 1.65 (t, J=5.9 Hz, 6H), 1.34 (t, J=5.9 Hz, 3H). ^{13}C NMR ($CDCl_3$, 101 MHz) δ (ppm): 192.7, 162.5, 162.0, 142.9, 135.5, 129.8, 129.0, 128.6, 126.1, 113.9, 95.2, 65.2, 63.9, 14.6, 14.2. LRMS (ESI): *m/z* calcd for $C_{21}H_{24}O_4^+$: $[M+H]^+$ 340.17, found 340.17.

*(E)-1-(2,4-Dimethoxy-6-(methoxymethoxy)phenyl)-3-phenylprop-2-en-1-one (**16**):* The general procedure for aldol condensation was followed using **11b** (0.3 g, 1.25 mmol). The crude material was purified by flash silica gel chromatography (Hex/EtOAc 7:3) to give **16** (348 mg, white solid) in 85% yield. ^{1}H NMR ($CDCl_3$, 400 MHz) δ (ppm): 7.65–7.59 (m, 3H), 7.54–7.44 (m, 3H), 7.31 (d, J=15.1 Hz, 1H), 6.52 (d, J=2.0 Hz, 1H), 6.51 (d, J=1.8 Hz, 1H), 6.02 (s, 2H), 3.91 (s, 3H), 3.80 (s, 3H), 3.24 (s, 3H). ^{13}C NMR ($CDCl_3$, 101 MHz) δ (ppm): 192.6, 165.3, 161.4, 142.9, 135.5, 129.8, 129.0, 128.6, 126.1, 110.8, 96.0, 95.2, 94.4, 56.4. LRMS (ESI): *m/z* calcd for $C_{19}H_{21}O_5^+$: $[M+H]^+$ 329.14, found 329.14.

*(E)-1-(3-(2-(Allyloxy)benzyl)-2,4-diethoxy-6-methoxyphenyl)-3-phenylprop-2-en-1-one (**18**):* The general procedure for Friedel–Crafts alkylation was followed using **13** (0.2 g, 0.61 mmol). The crude material was purified by flash silica gel chromatography (Hex/EtOAc 7:3) to give **18** (118 mg, white solid) in 41% yield. ^{1}H NMR ($CDCl_3$, 400 MHz) δ (ppm): 7.65–7.60 (m, 3H), 7.53–7.44 (m, 3H), 7.26 (d, J=15.1 Hz, 1H), 7.22 (ddt, J=7.4, 2.0, 1.0 Hz, 1H), 7.00 (td, J=7.5, 2.0 Hz, 1H), 6.90 (td, J=7.4, 2.1 Hz, 1H), 6.81 (dd, J=7.4, 2.0 Hz, 1H), 6.77 (s, 1H), 6.05 (ddt, J=16.3, 10.1, 6.2 Hz, 1H), 5.58 (ddt, J=13.9, 10.1, 1.1 Hz, 1H), 5.33 (ddt, J=16.7, 13.7, 0.9 Hz, 1H), 4.57 (dt, J=6.2, 1.1 Hz, 2H), 4.34 (q, J=8.0 Hz, 2H), 4.08 (q, J=8.0 Hz, 2H), 3.91 (s, 3H), 3.90 (d, J=1.1 Hz, 2H), 1.64–1.58 (m, 3H), 1.43 (t, J=8.0 Hz, 3H). ^{13}C NMR ($CDCl_3$, 101 MHz) δ (ppm): 192.1, 162.1, 161.5, 160.3, 156.2, 142.1, 135.5, 133.0, 131.0, 129.8, 129.3, 129.0, 128.6, 128.2, 16.0, 121.6, 117.8, 114.0, 113.8, 113.6, 97.4, 69.2, 68.5, 65.0, 56.2, 23.0, 15.0, 14.5. LRMS (ESI): *m/z* calcd for $C_{30}H_{33}O_5^+$: $[M+H]^+$ 473.23, found 473.22.

*(E)-1-(2,4-Diethoxy-3-(2-hydroxybenzyl)-6-methoxyphenyl)-3-phenylprop-2-en-1-one (**19**):* The general procedure for allyl deprotection was followed using **18** (93 mg, 0.19 mmol) to give **19** (82 mg, pale yellow oil) in 96% yield. ^{1}H NMR ($CDCl_3$, 400 MHz) δ (ppm): 7.68–7.63 (m, 3H), 7.54–7.44 (m, 3H), 7.35 (d, J=15.1 Hz, 1H), 7.28 (ddt, J=7.4, 2.0, 1.0 Hz, 1H), 7.14 (td, J=7.5, 2.0 Hz, 1H), 6.93 (td, J=7.5, 2.0 Hz, 1H), 6.85 (dd, J=7.5, 2.0 Hz, 1H), 6.71 (s, 1H), 4.34 (q, J=5.9 Hz, 2H), 4.08 (q, J=5.9 Hz, 2H), 3.91 (s, 3H), 3.90 (d, J=1.1 Hz, 2H), 1.61 (t, J=5.9 Hz, 3H), 1.43 (t, J=5.9 Hz, 3H). ^{13}C NMR ($CDCl_3$, 101 MHz) δ (ppm): 192.1, 162.1, 161.5, 160.3, 154.2, 142.1, 135.5, 130.2, 129.8, 129.0, 128.6, 128.3, 126.9, 126.0, 120.9, 115.8, 97.4, 68.5, 65.0, 56.2, 22.9, 15.0, 14.5. LRMS (ESI): *m/z* calcd for $C_{27}H_{29}O_5^+$: $[M+H]^+$ 433.12, found 433.12.

*(E)-1-(3-(2-(Allyloxy)benzyl)-2,4,6-trihydroxyphenyl)-3-phenylprop-2-en-1-one (**20**)*: The general procedure for Friedel–Crafts alkylation was followed using **3** (0.3 g, 0.77 mmol). The crude material was purified by flash silica gel chromatography (Hex/EtOAc 7:3) to give **20** (171 mg, white solid) in 55% yield. ^{1}H NMR ($CDCl_3$, 400 MHz) δ (ppm): 7.70–7.65 (m, 3H), 7.63 (dt, J=15.0, 0.9 Hz, 1H), 7.54–7.35 (m, 5H), 7.00 (td, J=7.5, 2.1 Hz, 1H), 6.95 (td, J=7.4, 2.2 Hz, 1H), 6.83 (dd, J=7.4, 2.2 Hz, 1H), 6.27 (s, 1H), 6.05 (ddt, J=16.3, 10.1, 6.2 Hz, 1H), 5.58 (ddt, J=13.9, 10.1, 1.1 Hz, 1H), 5.33 (ddt, J=16.7, 13.7, 0.9 Hz, 1H), 4.57 (dt, J=6.2, 1.1 Hz, 2H), 3.90 (d, J=1.1 Hz, 2H). ^{13}C NMR ($CDCl_3$, 101 MHz) δ (ppm): 193.5, 164.1, 162.4, 160.6, 156.2, 142.1, 135.5, 133.0, 131.0, 129.8, 129.3, 129.0, 128.6, 128.2, 126.0, 121.6, 117.8, 114.0, 107.1, 105.3, 98.2, 69.2, 23.1. LRMS (ESI): *m/z* calcd for $C_{25}H_{23}O_5^+$: $[M+H]^+$ 403.15, found 403.14.

*(E)-3-Phenyl-1-(2,4,6-trihydroxy-3-(2-hydroxybenzyl)phenyl)prop-2-en-1-one (**21**):* The general procedure for allyl deprotection was followed using **20** (88 mg, 0.22 mmol) to give **21** (71 mg, pale oil) in 90% yield. ^{1}H NMR ($CDCl_3$, 400 MHz) δ (ppm): 7.67–7.43 (m, 7H), 7.20 (ddt, J=7.5, 2.1, 1.1 Hz, 1H), 7.12 (td, J=7.4, 2.0 Hz, 1H), 6.91 (td, J=7.5, 2.0 Hz, 1H), 6.78 (dd, J=7.4, 2.0 Hz, 1H), 6.22 (s, 1H), 3.90 (d, J=1.1 Hz, 2H). ^{13}C NMR ($CDCl_3$, 101 MHz) δ (ppm): 193.5, 164.1, 162.4, 160.6, 154.2, 142.1, 135.5, 130.2, 129.8, 129.0, 128.6, 128.3, 126.8, 126.0, 120.9, 115.8, 107.1, 105.3, 98.2, 22.8. LRMS (ESI): *m/z* calcd for $C_{22}H_{19}O_5^+$: $[M+H]^+$ 363.12, found 363.13.

*1,1′-(2,4,6-Trihydroxy-1,3-phenylene)bis(ethan-1-one) (**32**):* To a flame dried RBF under an argon atmosphere was added $BF_3{\cdot}OEt_2$ (0.44 mL, 3.56 mmol) and acetic anhydride (0.12 mL, 1.19 mmol) under argon and left to stir for 30 min at RT. The solution was added dropwise over 10 min to a flame dried RBF charged with phloroglucinol (0.1 g, 0.59 mmol) under argon and left to stir at RT overnight. The reaction was quenched with a 10% sodium acetate (2.8 mL) solution and left to stir overnight. The mixture was filtered, rinsed with water and air dried to obtain **32** (64 mg, white solid) in 52% yield. ^{1}H NMR ($CDCl_3$, 400 MHz) δ (ppm): 5.82 (s, 1H), 2.73 (s, 8H). LRMS (ESI): *m/z* calcd for $C_{10}H_{10}O_5Na^+$: $[M+Na]^+$ 233.04, found 233.03.

*1,1′-(2,4,6-Trimethoxy-1,3-phenylene)bis(ethan-1-one) (**33**):* To a flamed dried RBF under argon was added acetone (3.2 mL), **32** (0.2 g, 0.95 mmol) and potassium carbonate (0.66 g, 4.76 mmol) followed by dimethyl sulfate (0.9 mL, 9.52 mmol) and left to stir at RT for 12 h and then brought to reflux for 4 h. The mixture was allowed to cool to RT and then was quenched with $NH_4Cl_{(satd)}$ and extracted with EtOAc (x2). The organic layers were combined, dried over sodium sulfate, and concentrated under reduced pressure. The crude material was purified by flash silica gel chromatography (Hex/EtOAc 3:1) to afford **33** (239 mg, white solid)in quantitative yield. ^{1}H NMR ($CDCl_3$, 400 MHz) δ (ppm): 6.19 (s, 1H), 3.78 (s, 6H), 3.64 (s, 3H), 2.41 (s, 6H). LRMS (ESI): *m/z* calcd for $C_{13}H_{17}O_5^+$: $[M+H]^+$ 253.10, found 253.10.

*(2E,2′E)-1,1′-(2,4,6-Trimethoxy-1,3-phenylene)bis(3-phenylprop-2-en-1-one) (**34**):* To a RBF was added **33** (0.20 g, 0.79 mmol), benzylaldehyde (0.16 mL, 1.58 mmol), and ethanol (10.5 mL). The mixture was cooled to 0 °C to which a solution of KOH (1.51 g, 2.55 mmol) in water (3.16 mL) was added dropwise and left to stir overnight while warming to RT. The reaction mixture was quenched by acidification with 1 M HCl and extracted with EtOAc (x3). The organic layers were combined, dried over sodium sulfate, and concentrated under reduced pressure. The crude material was purified by flash silica gel chromatography (Hex/EtOAc 3:1) to afford **34** (277 mg, yellow solid) in 82% yield. ^{1}H NMR ($CDCl_3$, 400 MHz) δ (ppm): 7.61–7.53 (m,

© 2021 Wiley-VCH GmbH

18607187, 2021, 10, Downloaded from https://chemistry-europe.onlinelibrary.wiley.com/doi/10.1002/cmdc.202001010 by Kansas State University, Wiley Online Library on [28/06/2023]. See the Terms and Conditions (https://onlinelibrary.wiley.com/terms-and-conditions) on Wiley Online Library for rules of use; OA articles are governed by the applicable Creative Commons License

4H), 7.50–7.38 (m, 7H), 7.05 (d, $J=16.1$ Hz, 2H), 6.37 (s, 2H), 3.89 (s, 6H), 3.71 (s, 3H). ^{13}C NMR ($CDCl_3$, 101 MHz) δ (ppm): 193.6, 159.6, 159.5, 157.1, 145.2, 134.6, 130.6, 128.9, 128.6, 128.5, 116.2, 91.1, 63.4, 56.1. LRMS (ESI): *m/z* calcd for $C_{27}H_{25}O_5^+$: $[M+H]^+$ 429.17, found 429.18.

*(2E,2′E)-1,1′-(5-(2-Hydroxybenzyl)-2,4,6-trimethoxy-1,3-phenylene)bis (3-phenylprop-2-en-1-one) (**35**):* The general procedure for Friedel–Crafts alkylation was followed using **34** (0.1 g, 0.23 mmol). The crude material was purified by flash silica gel chromatography (gradient Hex/EtOAc: 100:0, 9:1, 5:1, to 7:3) to afford **35** (60 mg, white solid) in 46% yield. ^{1}H NMR ($CDCl_3$, 400 MHz) δ (ppm): 7.47–7.42 (m, 6H), 7.33 (d, $J=16.1$ Hz, 2H), 7.30–7.26 (m, 4H), 6.96 (d, $J=16.0$ Hz, 1H), 6.83–6.62 (m, 3H), 6.07–5.97 (m, 1H), 5.40 (dq, $J=17.3$, 1.7 Hz, 1H), 5.20 (dt, $J=10.6$, 1.6 Hz, 1H), 4.53 (dt, $J=5.0$, 1.7 Hz, 2H), 3.94 (s, 2H), 3.76 (s, 3H), 3.72 (s, 3H), 3.44 (s, 3H). ^{13}C NMR ($CDCl_3$, 101 MHz) δ (ppm): 194.6, 160.6, 158.0, 157.1, 156.3, 144.7, 134.9, 133.8, 133.0, 130.3, 129.8, 129.6, 128.89, 128.84, 127.8, 126.5, 120.9, 120.4, 117.7, 116.8, 116.5, 116.4, 114.2, 114.2, 111.5, 111.2, 91.5, 68.8, 68.7, 62.9, 62.2, 56.0, 55.8, 22.8. LRMS (ESI): *m/z* calcd for $C_{37}H_{35}O_6^+$: $[M+H]^+$ 575.24, found 575.24.

*(2E,2′E)-1,1′-(5-(2-Hydroxybenzyl)-2,4,6-trimethoxy-1,3-phenylene)bis (3-phenylprop-2-en-1-one) (**36**):* The general procedure for allyl deprotection was followed using **35** (26 mg, 0.05 mmol) to afford **36** (60 mg, white solid) in 46% yield. ^{1}H NMR ($CDCl_3$, 400 MHz) δ (ppm): 7.72–7.63 (m, 3H), 7.59–7.42 (m, 6H), 7.41–7.30 (m, 6H), 7.08 (td, $J=7.7$, 1.8 Hz, 2H), 6.99 (d, $J=16.1$ Hz, 2H), 6.86–6.75 (m, 2H), 3.91 (s, 3H), 3.79 (s, 3H), 3.77 (s, 3H). ^{13}C NMR ($CDCl_3$, 101 MHz) δ (ppm): 194.1, 159.6, 157.3, 157.2, 155.8, 154.9, 145.5, 134.7, 13.0, 132.0, 131.98, 131.96, 131.6, 130.5, 128.9, 128.5, 128.33, 128.29, 127.8, 125.7, 119.7, 116.3, 116.10, 116.08, 114.02, 114.00, 92.1, 63.6, 56.1, 55.9, 29.7, 24.4. LRMS (ESI): *m/z* calcd for $C_{34}H_{30}O_6Na^+$: $[M+Na]^+$ 557.19, found 557.19.

*1,1′-(2,4,6-Trimethoxy-1,3-phenylene)bis(3-phenylpropan-1-one) (**37**):* The general procedure enone reduction was followed using **34** (25 mg, 0.058 mmol) to give afford **37** (25 mg, white solid) in quantitative yield. ^{1}H NMR ($CDCl_3$, 400 MHz) δ (ppm): 7.25–7.04 (m, 10H), 6.12 (s, 1H), 3.71 (s, 6H), 3.46 (s, 3H), 3.01 (ddd, $J=8.4$, 6.9, 1.7 Hz, 4H), 2.93 (ddd, $J=8.6$, 6.8, 1.7 Hz, 4H). ^{13}C NMR ($CDCl_3$, 101 MHz) δ (ppm): 202.7, 158.70, 158.67, 155.8, 141.2, 128.50, 128.45, 128.37, 128.32, 128.2, 126.0, 118.29, 118.28, 91.1, 64.4, 55.9, 46.4, 29.8. LRMS (ESI): *m/z* calcd for $C_{27}H_{29}O_5^+$: $[M+H]^+$ 433.20, found 433.20.

*1,1′-(5-(2-(Allyloxy)benzyl)-2,4,6-trimethoxy-1,3-phenylene)bis(3-phenylpropan-1-one) (**38**):* The general procedure for Friedel–Crafts alkylation was followed using **37** (83 mg, 0.19 mmol). The crude material was purified by flash silica gel chromatography (gradient Hex/EtOAc: 100:0, 9:1, 5:1, 7:3, to 1:1) to afford **38** (32 mg, white solid) in 29% yield. ^{1}H NMR ($CDCl_3$, 400 MHz) δ (ppm): 7.24–6.94 (m, 8H), 6.92–6.57 (m, 4H), 6.11–5.90 (m, 3H), 5.41–5.33 (m, 1H), 5.26–5.10 (m, 1H), 4.64 (s, 2H), 4.52 (ddt, $J=5.3$, 3.4, 1.6 Hz, 4H), 3.88 (s, 2H), 3.72 (d, $J=2.0$ Hz, 3H), 3.67 (s, 3H), 3.37 (s, 3H), 3.09–3.01 (m, 2H), 2.97–2.90 (m, 2H). ^{13}C NMR ($CDCl_3$, 101 MHz) δ (ppm): 204.0, 160.5, 157.3, 156.5, 154.5, 141.5, 134.0, 133.5, 133.0, 132.6, 131.2, 129.7, 129.4, 129.0, 128.5, 127.4, 127.0, 120.9, 120.6, 118.3, 117.7, 116.9, 114.3, 111.7, 111.5, 111.4, 91.4, 68.9, 63.2, 55.8, 46.4, 35.1, 30.0. LRMS (ESI): *m/z* calcd for $C_{37}H_{39}O_6^+$: $[M+H]^+$ 579.27, found 579.27.

*1,1′-(5-(2-Hydroxybenzyl)-2,4,6-trimethoxy-1,3-phenylene)bis(3-phenylpropan-1-one) (**39**):* The general procedure for enone reduction was followed using **36** (8 mg, 0.015 mmol) to afford **39** (7 mg, white solid) in quantitative yield. ^{1}H NMR ($CDCl_3$, 400 MHz) δ (ppm): 7.86–7.76 (m, 1H), 7.75–7.65 (m, 2H), 7.63–7.52 (m, 2H), 7.49–7.31 (m, 2H), 7.25–7.02 (m, 4H), 7.29–6.98 (m, 4H), 6.88–6.74 (m, 4H), 3.92 (s, 3H), 3.81 (s, 2H), 3.78 (s, 3H), 3.77 (s, 3H), 3.11 (t, $J=8.2$ Hz, 2H), 3.02 (t, $J=7.6$ Hz, 2H). LRMS (ESI): *m/z* calcd for $C_{34}H_{34}O_6Na^+$: $[M+Na]^+$ 561.23, found 561.23.

*(E)-3-Phenyl-1-(2,4,6-trimethoxy-3-(3-phenylpropanoyl)phenyl)prop-2-en-1-one (**41**):* The general procedure for enone reduction was followed using **40** (70 mg, 0.21 mmol) to give afford the reduced enone in 71% yield. The general procedure for aldol condensation was followed using the formed reduced enone (50 mg, 0.19 mmol). The crude material was purified by flash silica gel chromatography (gradient Hex/EtOAc: 100:0, 5:1, 7:3, 3:2, to 1:1) to give **38** in 45% yield. ^{1}H NMR ($CDCl_3$, 400 MHz) δ (ppm): 7.50–7.44 (m, 2H), 7.33–7.29 (m, 4H), 7.23–7.14 (m, 3H), 7.14–7.06 (m, 2H), 6.92 (d, $J=16.0$ Hz, 1H), 6.20 (s, 1H), 3.76 (s, 3H), 3.74 (s, 3H), 3.55 (s, 3H), 3.09–3.01 (m, 2H), 3.00–2.92 (m, 2H). ^{13}C NMR ($CDCl_3$, 101 MHz) δ (ppm): 202.8, 193.4, 159.4, 158.8, 156.5, 145.2, 141.2, 134.6, 130.6, 129.6, 128.9, 128.6, 128.50, 128.46, 128.4, 128.3, 126.0, 118.2, 116.3, 91.1, 63.8, 56.1, 56.0, 46.4, 29.8. LRMS (ESI): *m/z* calcd for $C_{27}H_{27}O_5^+$: $[M+H]^+$ 431.18, found 431.18.

Biological

Cell culture information. The cancerous cell lines used in these investigations were purchased directly from the American Type Culture Collection. Cell were grown in media supplemented with fetal bovine serum (FBS) and antibiotics (100 μg/mL penicillin and 100 U/mL streptomycin). Specifically, experiments were performed using the following cell lines and media compositions: HeLa, U937, Reh (RPMI-1640 + 10% FBS), Mia PaCa-2 (DMEM + 10% FBS), A549 (F-12K + 10% FBS), and HCT-116 (McCoy 5A + 10% FBS). Cells were incubated at 37 °C in a 5% CO_2, 95% humidity atmosphere for all experiments.

IC_{50} value determination for adherent cells using Alamar Blue. Adherent cells were added to 384-well plated (1500 cells/well) in 10 μL of media and were allowed to adhere to 2–3 h. Compounds were solubilized in DMSO (10 μM stock solutions), added to a 96-well plate over a range of concentrations (31.6 nM to 200 μM) with media, 40 μL was added to the 384-well plate in triplicate for each concentration of compound. After 69 h of continuous exposure, 5 μL of Alamar blue was added to each well and the cells were allowed to incubate for an additional 3 h. The plates were then read for fluorescence intensity with an excitation of 560 nm and emission of 590 nm on a BioTek Synergy H1 plate reader. Doxorubicin and etoposide were both used as positive death controls and wells with no compounds added as negative death controls. IC_{50} values were determined from three or more independent experiments using GraphPad Prism 7.0. (LaJolla California)

IC_{50} value determination for non-adherent cells using Alamar Blue. The same procedure for adherent cells was used, with the following modifications. Cells (2200 cell/well) in media (10 μL) were added after 40 μL of compound in medium were added to the 384-well plate. No time was given to allow cells to adhere.

Combination studies: All combinational cell death experiments were performed in 96-well plates with a total volume of 100 μL. To each well was added 49 μL of cell media, either 2.5 or 5 μM of 6TP (from a DMSO stock solution), and compounds independently. To each well on the plate was added two different concentration of each compound and five concentrations of 6TP or doxorubicin (both prepared from 10 mM stock solutions in DMSO), cell media (adjusted to reach 50 μL volume) and 0.5 μL of DMSO to achieve a 1% DMSO concentration. To each well was then added 50 μL of a suspension of cells to obtain a final cell density of 4000 cells/well (adherent cells) and 7000 cells/well (suspension cells). Doxorubicin and etoposide were both used as positive death controls, and wells

© 2021 Wiley-VCH GmbH

18607187, 2021, 10, Downloaded from https://chemistry-europe.onlinelibrary.wiley.com/doi/10.1002/cmdc.202001010 by Kansas State University, Wiley Online Library on [28/06/2023]. See the Terms and Conditions (https://onlinelibrary.wiley.com/terms-and-conditions) on Wiley Online Library for rules of use; OA articles are governed by the applicable Creative Commons License

with no compounds added as negative death controls. Plates were incubated at 37 °C with 5% CO_2 for 72 h, at which time they were assessed by Alamar Blue. IC_{50} values were determined from three or more independent experiments using GraphPad Prism 7.0.

Acknowledgements

This work could not have been undertaken without the gracious financial support from the Johnson Cancer Research Center of Kansas State University, Startup Capital from Kansas State University, and NSF (CHE-1848186). Funding for this research was also provided by the NSF REU program under grant number MPS-1852182 and CHE-1460898. J. Dallman was supported by the NSF-REU program.

Conflict of Interest

The authors declare that they have no known competing financial interests or personal relationships that could have appeared to influence the work reported in this paper.

Keywords: library construction · medicinal chemistry · natural products · small-molecule potentiating agents

[1] a) D. A. Dias, S. Urban, U. Roessner, *Metabolites* **2012**, *2*, 303–336; b) G. M. Cragg, D. J. Newman, *Pure Appl. Chem.* **2005**, *77*, 7–24.
[2] a) G. M. Cragg, P. G. Grothaus, D. J. Newman, *Chem. Rev.* **2009**, *109*, 3012–3043; b) A. Ganesan, *Curr. Opin. Chem. Biol.* **2008**, *12*, 306–317; c) S. Dev, **2010**.Reference 2c should read: N.E. Thomford, D. A. Senthebane, A. Rowe, D. Munro, P. Seele, A. Maroy, K. Dzobo, *Int. J. Mol. Sci.* **2018**, *19*, 1578-1606
[3] a) D. C. Swinney, J. Anthony, *Nat. Rev. Drug Discovery* **2011**, *10*, 507–519; b) J. T. Heeres, P. J. Hergenrother, *Chem. Soc. Rev.* **2011**, *40*, 4398–4410; c) E. Perola, *J. Med. Chem.* **2010**, *53*, 2986–2997; d) J. R. Broach, J. Thorner, *Nature* **1996**, *384*, 14–16; e) A. Carnero, *Clin. Transl. Oncol.* **2006**, *8*, 482–490.
[4] a) S. Dandapani, L. A. Marcaurelle, *Nat. Chem. Biol.* **2010**, *6*, 861–863; b) W. P. Walters, J. Green, J. R. Weiss, M. A. Murcko, *J. Med. Chem.* **2011**, *54*, 6405–6416; c) P. D. Leeson, S. A. St-Gallay, *Nat. Rev. Drug Discovery* **2011**, *10*, 749–765.
[5] a) R. W. Huigens III, K. C. Morrison, R. W. Hicklin, T. A. Flood Jr, M. F. Richter, P. J. Hergenrother, *Nat. Chem.* **2013**, *5*, 195; b) W. R. Galloway, A. Isidro-Llobet, D. R. Spring, *Nat. Commun.* **2010**, *1*, 1–13; c) E. Comer, H. Liu, A. Joliton, A. Clabaut, C. Johnson, L. B. Akella, L. A. Marcaurelle, *Proc. Natl. Acad. Sci. USA* **2011**, *108*, 6751–6756; d) S. Wetzel, R. S. Bon, K. Kumar, H. Waldmann, *Angew. Chem.* **2011**, *123*, 10990–11018; *Angew. Chem. Int. Ed.* **2011**, *50*, 10800–10826; e) B. C. Goess, R. N. Hannoush, L. K. Chan, T. Kirchhausen, M. D. Shair, *J. Am. Chem. Soc.* **2006**, *128*, 5391–5403; f) H. E. Pelish, N. J. Westwood, Y. Feng, T. Kirchhausen, M. D. Shair, *J. Am. Chem. Soc.* **2001**, *123*, 6740–6741; g) B. R. Balthaser, M. C. Maloney, A. B. Beeler, J. A. Porco, J. K. Snyder, *Nat. Chem.* **2011**, *3*, 969–973; h) C. Aquino, M. Sarkar, M. J. Chalmers, K. Mendes, T. Kodadek, G. C. Micalizio, *Nat. Chem.* **2012**, *4*, 99–104; i) H. Lachance, S. Wetzel, K. Kumar, H. Waldmann, *J. Med. Chem.* **2012**, *55*, 5989–6001.
[6] J. Dallman, A. Lansakara, T. Nguyen, C. Weeramange, W. Hulangamuwa, R. J. Rafferty, *MedChemComm* **2019**, *10*, 1420–1431.
[7] T. Liu, Y. Hu, *Synth. Commun.* **2004**, *34*, 3209–3218.
[8] Y. K. Rao, S.-H. Fang, Y.-M. Tzeng, *Bioorg. Med. Chem.* **2004**, *12*, 2679–2686.
[9] a) A. X. T. Hernandez, C. J. Weeramange, P. Desman, A. Fatino, O. Haney, R. J. Rafferty, *MedChemComm* **2019**, *10*, 169–179; b) V. L. Hoang, Y. Zhang, R. J. Rafferty, *Tetrahedron Lett.* **2017**, *58*, 4432–4435; c) A. Fatino, G. Baca, C. Weeramange, R. J. Rafferty, *J. Nat. Prod.* **2017**, *80*, 3234–3240.
[10] T.-C. Chou, P. Talalay, *Adv. Enzyme Regul.* **1984**, *22*, 27–55.
[11] G. Wei, B. Yu, *Eur. J. Org. Chem.* **2008**, *2008*, 3156–3163.
[12] a) R. S. Khupse, P. W. Erhardt, *J. Nat. Prod.* **2007**, *70*, 1507–1509; b) S. Vogel, S. Ohmayer, G. Brunner, J. Heilmann, *Bioorg. Med. Chem.* **2008**, *16*, 4286–4293.

Manuscript received: December 30, 2020
Accepted manuscript online: January 25, 2021
Version of record online: April 15, 2021

© 2021 Wiley-VCH GmbH

18607187, 2021, 10, Downloaded from https://chemistry-europe.onlinelibrary.wiley.com/doi/10.1002/cmdc.202001010 by Kansas State University, Wiley Online Library on [28/06/2023]. See the Terms and Conditions (https://onlinelibrary.wiley.com/terms-and-conditions) on Wiley Online Library for rules of use; OA articles are governed by the applicable Creative Commons License

Synthesis of Spirooxepinisoxazoline Synthetic Scaffold and Convergent Total Synthesis of Psammaplysin A-D, and H towards Drug Discovery

Research Prepositional Oral Examination

Shashika Perera

Advisor: Prof. Ryan J. Rafferty

Department of Chemistry

Kansas State University

10/04/2021

Project overview and specific aims

Cancer is a widely spread disease that affect many human lives and scientists are still in search of a better treatment for it. HIV is another disease that medicinal chemists doesn't have a promising treatment yet. Then is malaria that has become a huge burden mainly in African countries. Due to the emergence of new drug resistant strains of malaria, the therapeutic efficacy of existing antimalarial drugs is being lost. Hence, it is important to find treatments for these diseases in order to save thousands of innocent lives. The psammaplysin family of natural products is reported to exhibit a wide range of therapeutic properties including anti HIV, anti-malarial, and most importantly cytotoxicity against many cancer cell lines making it a good therapeutic candidate for above mentioned diseases. Psammaplysin A and B were initially isolated in 1982 by Kashman and coworkers from the marine Verongiid sponge *Psammapfysilla purpureu* found in red sea, and to date a total of 26 members have been isolated (psammaplysin A – Z). Among all 26 different compounds, psammaplysin A-D, and H are therapeutically significant. Psammaplysin A, B, and C are reported to exhibit cytotoxicity towards the human colon tumor cell-line HCT116 with IC_{50} values in single digit μg levels. Psammaplysin D shows anti HIV activity while psammaplysin H is reported to exhibit the most potent and selective antimalarial activity. Hence, this report focus on following specific aims to access a group of novel therapeutic agents to treat HIV, malaria, and cancer.

Specific aim 1: Synthesis of spirooxepinisoxazoline core and total synthesis of psammaplysin A-D, and H.

This project proposal discuss a novel, cost effective, and efficient synthetic route to access the challenging spirooxepinisoxazoline core of psammaplysins and thereby convergent total synthesis of pharmaceutically important psammaplysin A-D, and H.

Specific aim 2: Investigation of mode of action of psammaplysin A-D, H and structure activity relationship studies (SAR) – In collaboration with a fellow research group.

A library of analogues will be accessed using the synthesized or isolated natural products to enhance the existing biological activity and also to explore new therapeutic effects. This library will be tested on a range of cell lines for their cytotoxicity, anti HIV, anti-malarial, anti-bacterial, and anti-fouling properties.

Table of contents

1. Introduction 4

2. Psammaplysin group of natural products 6

2.1. Discovery and structure determination of psammaplysins 6

2.2. Biological activity of psammaplysins 7

2.3. Proposed biosynthesis pathway 8

2.4. Previous synthetic efforts 9

3. Synthesis of the spirooxepinisoxazoline core 10

3.1. Retro synthetic analysis for the psammaplysin scaffold 10

3.2. Synthesis of psammaplysin scaffold 10

4. Convergent total synthesis of psammaplysin A, B, C, D, and H 12

4.1. Total synthesis of psammaplysin A 12

4.2. Total synthesis of psammaplysin B and C 13

4.3. Total synthesis of psammaplysin D 14

4.4. Total synthesis of psammaplysin H 15

4.5. Structural determination of synthesized psammaplysin A-D, and H 16

4.6. Biological assays of synthesized psammaplysin A-D, and H 16

5. Investigation of mode of action of psammaplysin A-D, and H 16

6. Structure activity relationship studies of psammaplysin A-D, and H 18

7. Supporting Information 20

1. Introduction

Cancer is a globally burdened disease that is a leading cause of deaths worldwide. It ranks very top when it comes to the cause of deaths before age of 70 years.[1] Number of new cancer cases continue to increase worldwide and medicinal chemists need to improve the existing methods/ explore novel therapeutics to identify and treat cancer. According to the International Agency for Research on Cancer (IARC) 19.3 million new cases of cancer and almost 10 million deaths from cancer were reported worldwide in 2020.[2] Malaria is another disease that burden most countries in the world specially the African region. According to the latest world malaria report, there were 229 million cases of malaria in 2019 worldwide.[3] Quinine, artemisinin, and their derivatives have been widely used to treat this deadly, yet preventive and curable disease. However, due to the development and spread of new drug resistant strains of malaria, the therapeutic efficacy of these existing antimalarial drugs is being greatly reduced. Therefore, the development of a new class of antimalarial drugs is urgently needed.[4]

In discovering treatments to many life threatening diseases, including the above mentioned diseases, natural sources like plants, herbs, and marine organisms have become very useful. Secondary metabolites present in the natural products plays a vital role in the drug discovery process.[5] These secondary metabolites possess a diverse range of biological activities and promising therapeutic activities. The ocean covers approximately 70% of the earth, in which marine organisms are a source of innumerous amounts of secondary metabolites, which have become a main attraction of many medicinal chemists. It's been only 60 years since the start of investigating marine biota and there are number of marine derived drugs in commercial use and/or under clinical trials. Trabectedin (Yondelis),[6] isolated from Ecteinascidia turbinata, which is used for the treatment of advanced soft tissue sarcoma,[7] and the peptide ω-conotoxin (Ziconitide) isolated from Conus catus, used for the treatment of chronic and neuropathic pain are examples of marine drugs.[5] Examples of marine-derived drugs include eribulin (Halaven), a synthetic truncated derivative of halichondrin B that was approved by the FDA for the treatment of refractory metastatic breast cancer,[8] and panobinostat (Farydak),[9] derived from the lead compound psammaplin A, which has recently been approved for the treatment of multiple myeloma (Figure 1).[10] Among all the marine derived secondary metabolites reported to date,

~26% are been isolated from marine sponges and hence they have become a main attraction of isolation and synthetic chemists.[11]

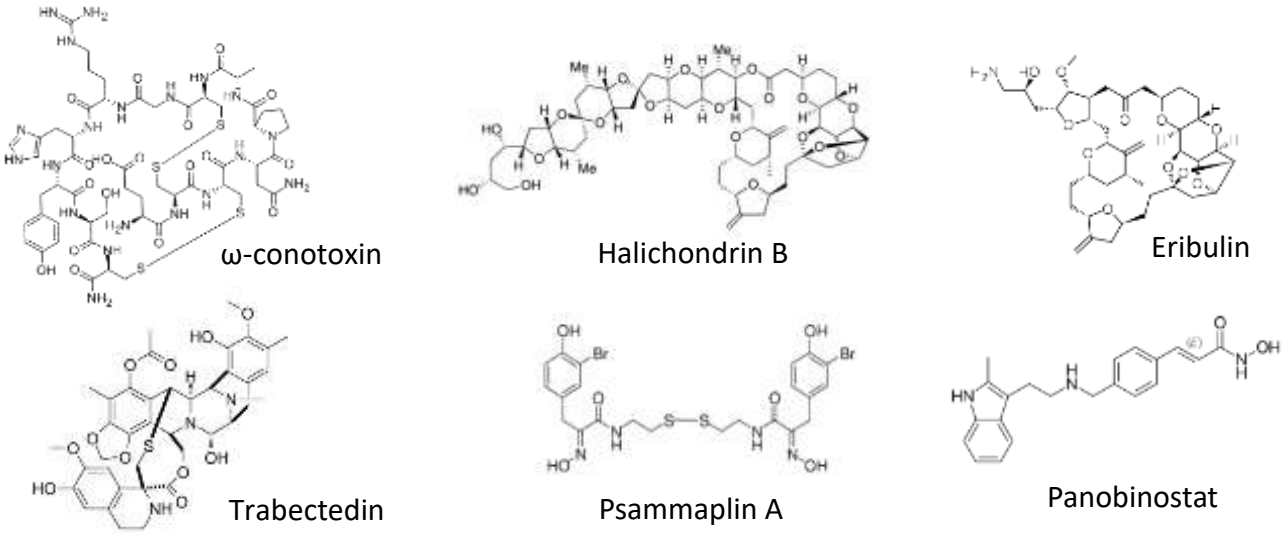


Figure 1- Marine derived dugs

These secondary metabolites from marine sponges possess complex and challenging core structures which make them difficult to access and analyse. Bromotyrosine-derived alkaloids that are present abundantly in sponges belonging to the order Verongiida are an example. Bromotyrosine-derived alkaloids can be categorized into six groups depending on their core structure; simple bromotyrosine derivatives, spirocyclohexadienylisoxazolines, spirooxepinisoxazolines, oximes, bastadins, and other bromotyrosine-derived alkaloid structural classes (Figure 2).[12,13] Bromotyrosine alkaloids containing the exclusive spirooxepinisoxazoline core are considered the most interesting among all both architecturally and biologically.

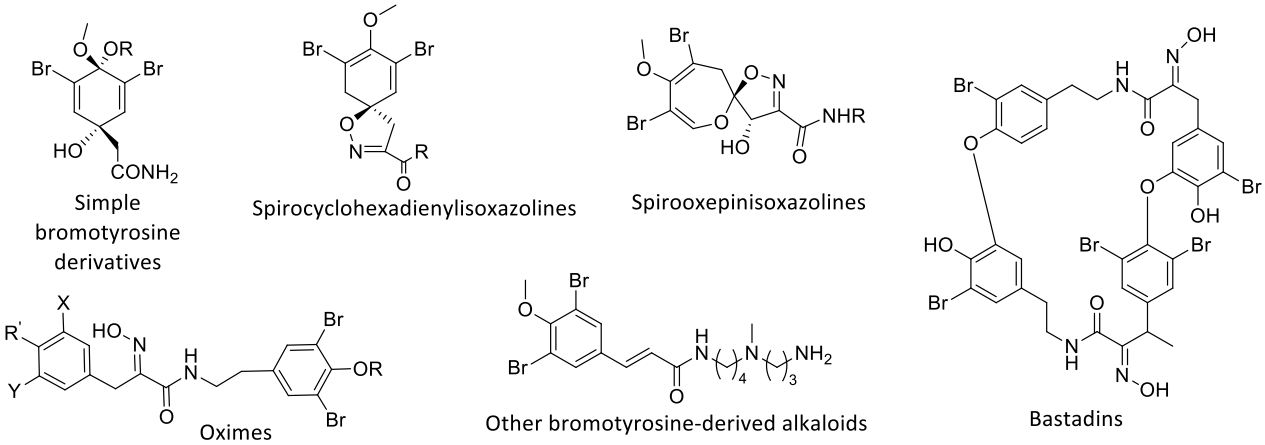
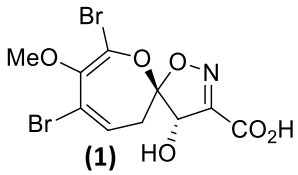


Figure 2- Bromotyrosine-derived alkaloid classes

By 2021, more than 33 metabolites possessing this unique and rare core structure like psammaplysins A–Z **(S1-S25)** and ceratinamides A **(S26a)** and B **(S26b)** have been isolated from various sponges (Figure S1).[14] It is being reported that they exhibit a wide range of therapeutic properties including anti HIV, anti-malarial, anti-bacterial, anti-fouling, and most importantly cytotoxicity against many cancer cell lines.[14–21]

Extraction and isolation of a specific secondary metabolite from any natural product source is always time consuming, contain difficult procedures and results in only a small amount of the pure compound. Hence, development of synthetic routes towards these identified secondary metabolites is important. Currently, apart from a semisyntheses, up-to-date total synthesis of the spirooxepinisoxazoline moiety containing metabolites has not been reported (Figure 3). Therefore, this report proposes a synthetic route to access the spirooxepinisoxazoline core to be used for the total synthesis of therapeutically significant psammaplysin A-D, and H.



(1)

Figure 3 - Synthetically challenging spirooxepinisoxazoline moiety

2. Psammaplysin group of natural products

2.1. Discovery and structure determination of psammaplysins

Psammaplysins are a group of secondary metabolites isolated from the marine Verongiid sponge *Psammapfysilla purpureu* found in the Red Sea. Psammaplysin A and B were the first to be discovered and they were isolated and characterised by Kashman and coworkers in 1982 (Figure 4A).[22] Later in 1985 Clardy and coworkers reisolated psammaplysin A and B and proved that the spiro[4.5]oxazadecane (spiro[cyclohexadieneoxazoline]) structure proposed by Kashman should be corrected as a spiro[4.6]dioxazundecane (spirooxepinisoxazoline) (Figure 4B).[23] The absolute stereochemistry at C6 and C7 of psammaplysin A was unambiguous until Garson and coworkers confirmed it to be 6R,7R by analysis of α-methoxyphenylacetic acid (MPA) esters prepared from the acetamide derivative of psammaplysin A via experimental and calculated electronic circular

dichroism (ECD) data and NMR in 2015.[24] Since 1982 a total of 26 psammaplysins have been isolated, characterised and evaluated for biological activities.

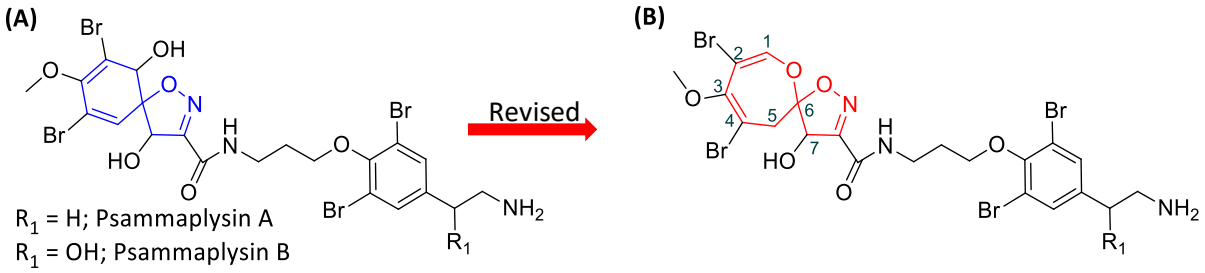


Figure 4 - (A) Structure of psammaplysin by Kashman; (B) Revised structure of psammaplysin by Clardy

2.2. Biological activity of psammaplysins

Psammaplysin family shares the common structural spirooxepinisoxazoline motif and every member of the family differ from each other only by the functionality of the bromotyrosine side chain. Psammaplysins exhibit a wide range of therapeutic properties including anti HIV, anti-malarial, anti-bacterial, anti-fouling, and most importantly cytotoxicity against many cancer cell lines (Table S1).[14–21] Based on the biological assays performed by Lee and coworkers the spirooxepinisoxazoline core is a requirement for the cytotoxic activities of psammaplysins. Psammaplysin A-C exhibits cytotoxicity towards the human colon tumor cell-line HCT116 with IC_{50} values of 6, 6, and 3 µg/mL, respectively.[25] Psammaplysin D shows low cytotoxic activity due to its highly lipophilic side chain but high anti-HIV activity against the Haitian RF strain of HIV-I with a 51% inhibition at 0.1 mg/mL.[26] Psammaplysin E is cytotoxic to LoVo (human colon adenocarcinoma) and KB (epidermal carcinoma) cell lines at 5.0 µg/mL and exhibits moderate immunosuppressive activity.[15] It also act as a potent antimigratory agent against HeLa (human cervical adenocarcinoma) and MDA-MB-231 (human breast adenocarcinoma) cells with IC_{50} values of 2.19 and 0.31 µM, respectively.[27] Psammaplysin F exhibits antiplasmodial activity against 3D7 (most dangerous) and Dd2 strains of the common malarial parasite *P. falciparum* with IC_{50} values of 0.87 and 1.4 µM[17], respectively, and inhibits 80% of four bacterial strains at 50 µM.[28] When tested against the drug-resistant (K1) and drug-sensitive (FCR3) strains of P. falciparum, psammaplysin F is active with IC_{50} values of 3.77 and 2.45 µg/mL, respectively.[4] Recently, psammaplysin F was found to regulate the synthesis of stress granules, leading to increase the efficacy of bortezomib and sorafenib.[29] psammaplysin G inhibits 98% of the Dd2 cell strain of P. falciparum at 40 µM.[17] Among all the psammaplysins that exhibit antimalarial activity,

psammaplysin H is reported to be the most potent and selective. It possess potent antiplasmodial activity against the 3D7 strain with an IC_{50} value of 0.41 µM and selective towards the 3D7 strain with a selectivity index (SI) of >97%.[30] Terminal N-methyl group of psammaplysins appears to be important and critical for antimalarial activity. Due to the stability issues, psammaplysin I and J were not tested for their biological activity. Psammaplysins X and Y shows potent cytotoxicity towards six cancer cell lines with a GI_{50} value up to 0.8 µM.[26] (Table S1)

2.3. Proposed biosynthesis pathway

Considering the biosynthetic pathways of bromotyrosine natural products proposed by Rogers,[31] Roll,[23] and Lindel[32] the following pathway has been proposed for the biogenesis of spirooxepinisoxazoline core of psammaplysins. Dibromotyrosine intermediate **(3)** can be obtained via bromination of tyrosine **(2)** catalysed by bromoperoxidase, a vanadium-dependent haloperoxidase.[33] Dibromo tyrosin **(3)** then undergoes an oxidation to give an arene epoxide **(5)** through an oxime **(4)**. It is suggested that arene epoxidation is achieved by a monooxygenase (possibly a cytochrome P450).[33,34] The obtained arene epoxide **(5)** will undergo an oxide-oxepin pathway generating the carbocation intermediate **6**,[35,36] which will undergo a nucleophilic attack by the hydroxyl group of oxime leading to the spirooxepinisoxazoline ring moiety (Figure 5).[37]

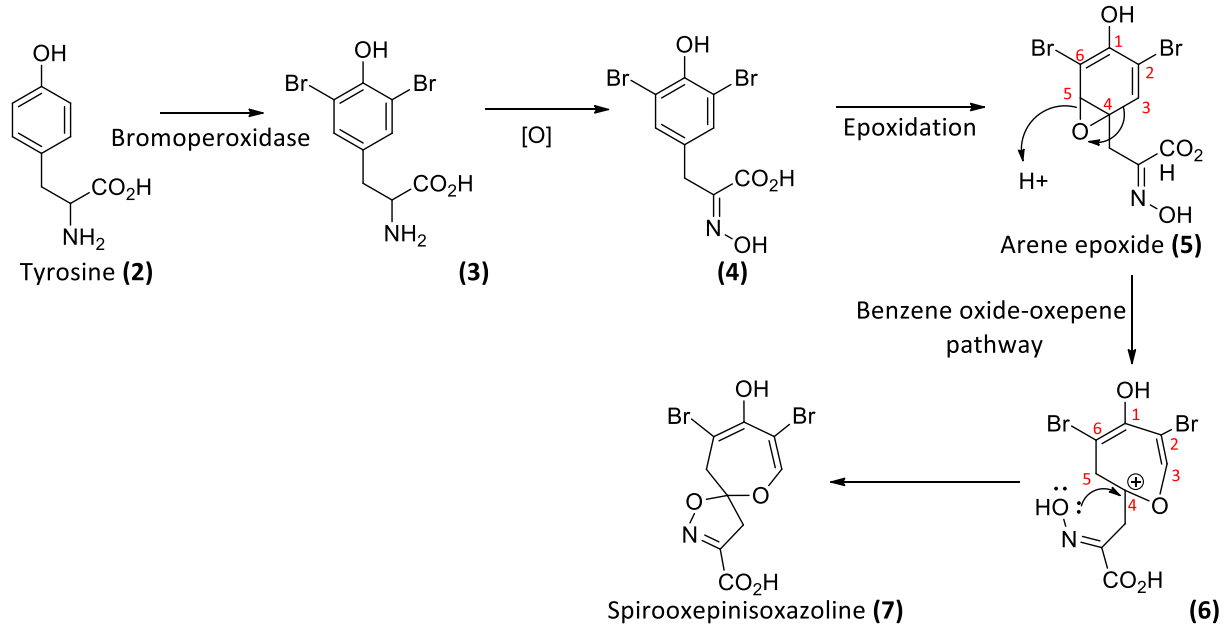


Figure 5- Proposed biosynthetic pathway of spirooxepinisoxazoline core of psammaplysins

2.4. Previous synthetic efforts

Previous research on psammaplysin family suggests that the spirooxepinisoxazoline ring core is a requirement for its cytotoxicity.[26] Hence, this scaffold can serve as an important building block in designing potential anticancer agents.[14] To date, no research group has attempted total synthesis of any of the psammaplysins, which might be due to its challenging architecture. Mioskowski and co-workers reported a model study to access spiroisoxazolines of different ring sizes by condensation of hydroxylamine onto a tricarbonyl derivative for spontaneous spiro cyclization. Here they report only one example of a low functionalised spiro[4;6]-ring system with a low yield (Figure 6A).[32,38] Considering the biosynthetic pathway of psammaplysins, Joseph Carlson from University of California Irvine suggested the following synthetic route to access the psammaplysin core in his PhD thesis (Figure 6B).[39] He envisioned to access spirooxepinisoxazoline ring via formation of a donor-acceptor cyclopropane ring and its expansion to access the spirocycle. Unfortunately, formation of the cyclopropane ring was not successful. Having considered prior efforts to access this spirooxepinisoxazoline ring core, a novel and synthetically efficient synthetic pathway to access this unique framework will be proposed in this report and thereby a convergent synthetic route to access psammaplysins A-D, and F.

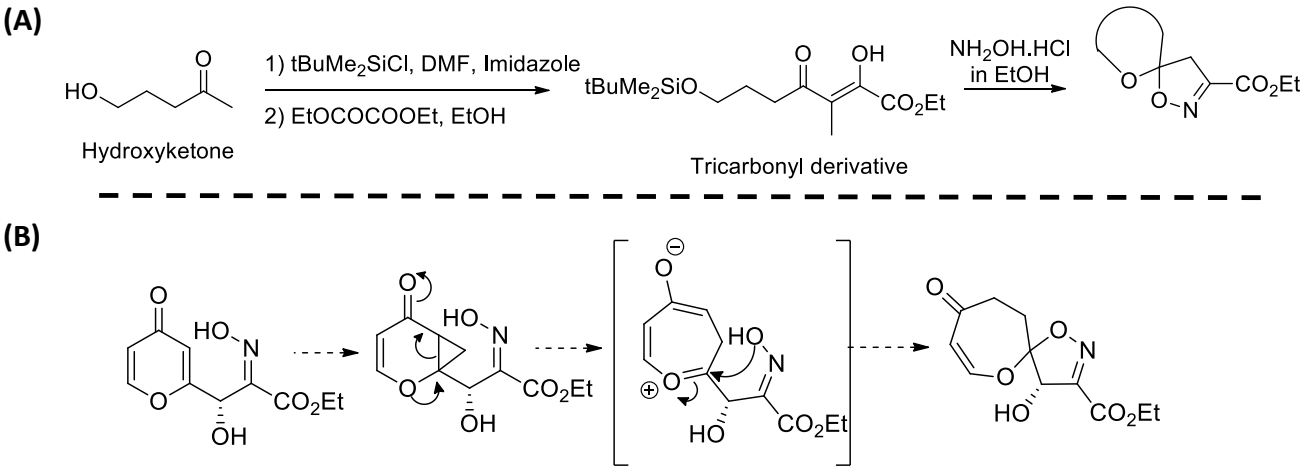
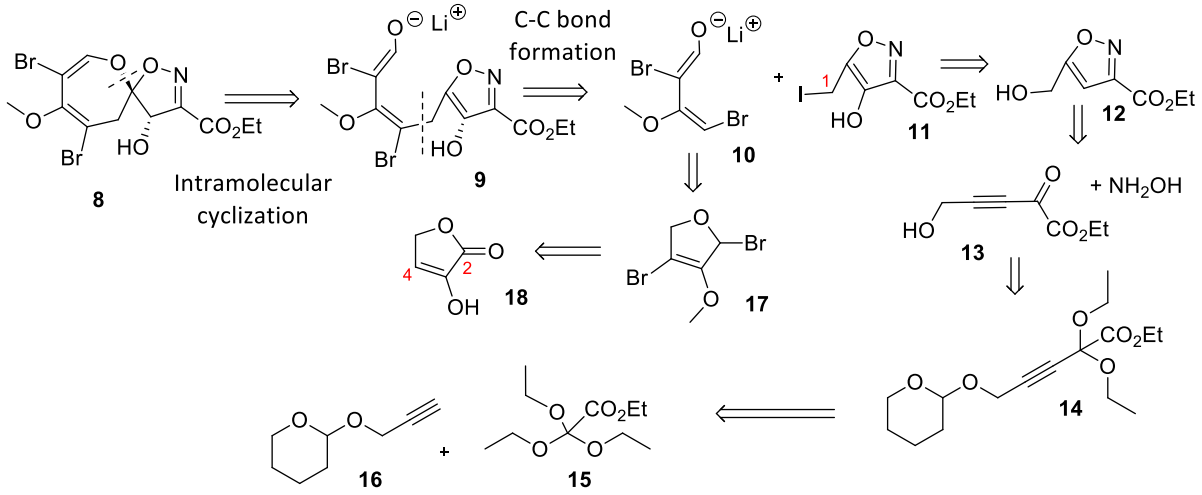


Figure 6 - (A) Mioskowski and co-workers model study; (B) PhD work of Joseph Carlson

3. Synthesis of the spirooxepinisoxazoline core

3.1. Retro synthetic analysis for the psammaplysin scaffold

It is envisioned that spirooxepin-isoxazoline **(8)** can be accessed via an intramolecular cyclization of the ring opened intermediate **9**. The enolate diene **(9)** will be accessed via a conjugate S_N2' like cascade reaction beteween **10** and **11.** Substituted diene is expected to access by an allylic deprotonation leading to a rapid ring opening of the substituted furan ring **17**. Performance of Williamson ether synthesis on furanone **18** and bromination at 2 and 4 positions will give access to furan **17**. The substituted isoxazole **(11)** will be accessed by reacting hydroxylamine with α,β-acetylenic carbonyl compound **13** which would result from the reaction between tetrahydro-2-(2-propynyloxy)-2H-pyran **(16)** and ethyl 2,2,2-triethoxyacetate **(15)** (Scheme 1).

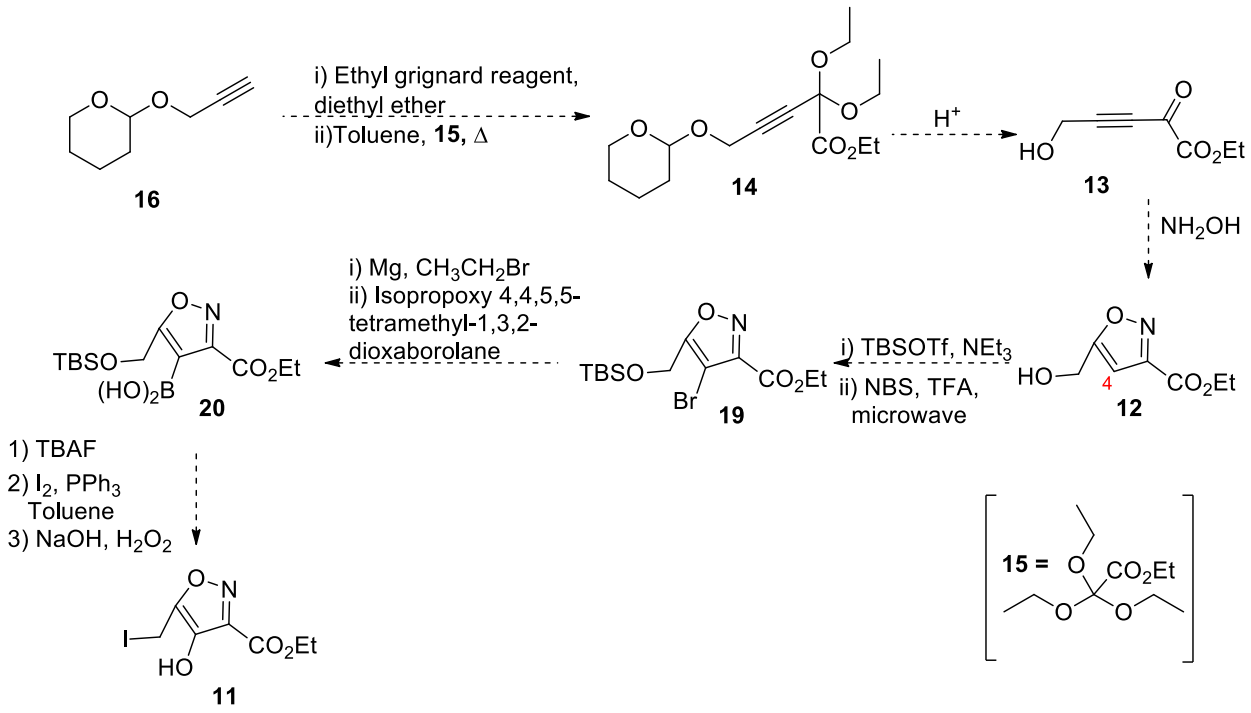


Scheme 1- Proposed retrosynthetic route for psammaplysin scaffold

3.2. Synthesis of psammaplysin scaffold

Ethyl 2,2-diethoxy-5-((tetrahydro-2H-pyran-2-yl)oxy)pent-3-ynoate **(14)** will be accessed by reacting tetrahydro-2-(2-propynyloxy)-2H-pyran **(16)** and ethyl 2,2,2-triethoxyacetate **(15)** under the conditions reported in patent no. JP2009073776 invented by Daisuke Takaoka.[40] Compound **14** will then be subjected to an acidic hydrolysis with para toluene sulfonic acid (pTSA) to perform an universal deprotection of both the THP and acetal groups yielding the α,β-acetylenic carbonyl compound **13.** The substituted isoxazole **12** will be obtained by subjecting **13** to oxime chemistry reported by Ricca and coworkers. [41] Primary alcohol of **12** will be protected using a silyl protecting agent under standard conditions and the resulting isoxazole will be brominated at C4 utilizing the conditions reported by Li and coworkers to access compound **19.**[42] With **19** in hand it will be

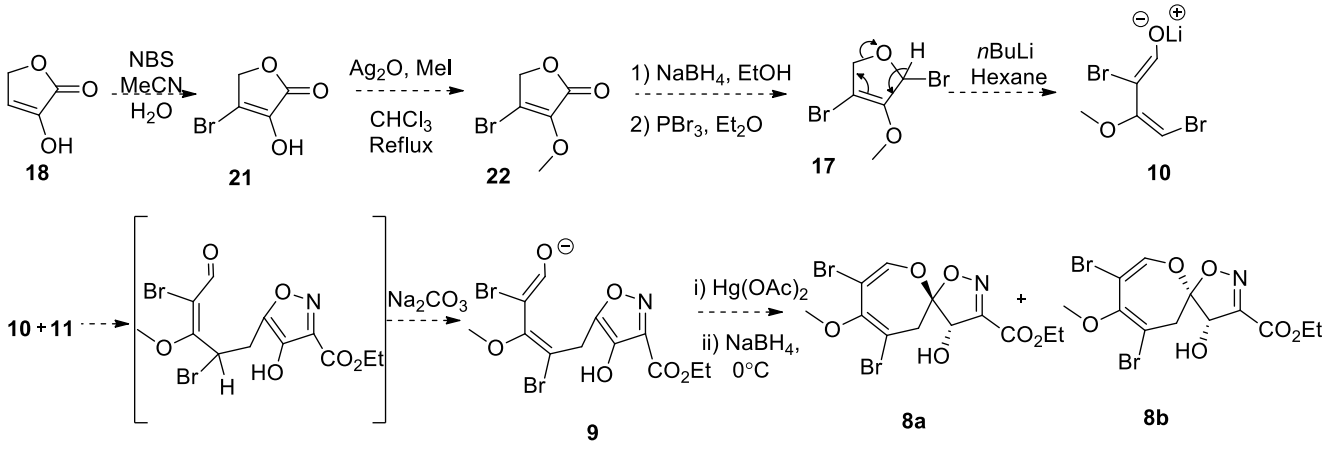
subjected to hydroboration via a Grignard reaction using reaction conditions reported by Cogoli and coworkers.[43] Compound **20** will be TBS deprotected under standard conditions and the free alcohol obtained will be converted to an iodide utilizing the iodination conditions reported by Tan and coworkers in the synthesis of Acortatarins A and B.[44] Isoxazole will then be subjected to oxidation conditions with NaOH and hydrogen peroxide to access the key intermediate **11** (Scheme 2).



Scheme 2 - Proposed synthetic route to access the isoxazole **(11)**

It is expected to access the substituted diene **10** starting from commercially available 3-hydroxyfuran-2(5H)-one **(18)**.[45] Reaction conditions from E. Lopušanskaja and coworkers will be utilized to brominate C4 of compound **18** to access compound **21**.[46] Compound **22** will be synthesized by performing a Williamson ether synthesis on **21** using the conditions reported by E. Lopušanskaja and coworkers.[46] The carbonyl group on **22** will be reduced to an alcohol using an ethanolic solution of a milder reducing agent followed by bromination utilizing Yang and coworkers conditions in synthesis of dibenzylbutyrolactone lignans.[47] The substituted furan **17** will be subjected to an allylic deprotonation followed by a subsequent ring opening to yield the expected key intermediate **10** using the reaction conditions reported by Sebastian and coworkers in the synthesis of 7-Lithio-2,3,4,5-tetrahydrooxepin.[48] Inspired by the Linchpin approach

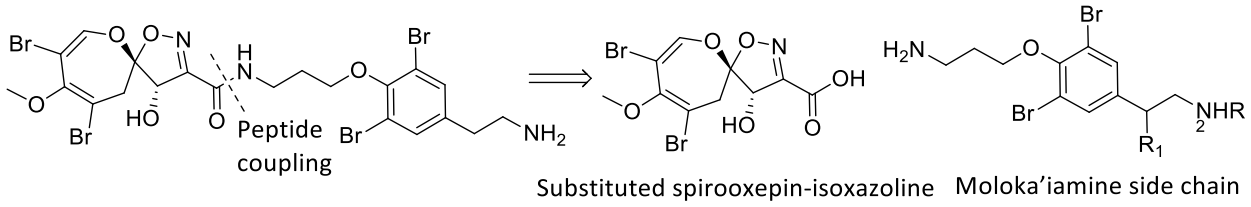
followed by Ziegler in the synthesis of minovine in 1970, it is expected for the dienol and the isoxazole to undergo a similar type of reaction to yield compound **9**.[49] Intramolecular cyclization of compound **9** to access the targeted psammaplysin scaffold **8a** is envisioned to achieve by utilizing Tan and coworkers rection conditions for oxidative cyclization in synthesis of acortatarin A.[44] It is expected to obtain a minor quantity of the diastereomer **8b** (Scheme 3).



Scheme 3- Proposed synthetic route for psammaplysin core

4. Convergent total synthesis of psammaplysin A, B, C, D, and H

Upon accessing the core it is envisioned to access the psammaplysin A and other members of the group of natural products by coupling the core with the respective substituted Moloka'iamine side chain (Scheme 4). Suggested total synthesis route to psammaplysin A-D, and H are discussed below.

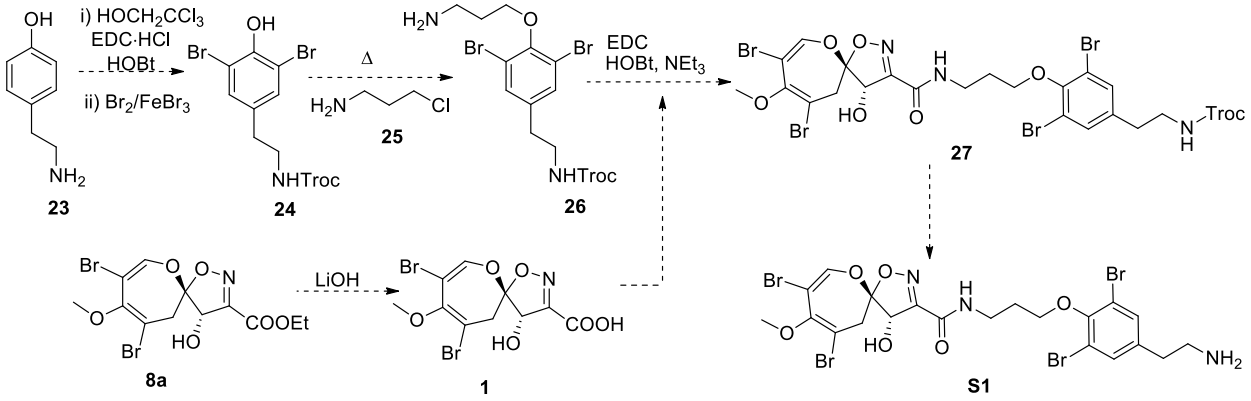


Scheme 4 - Convergent total synthesis of psammaplysin A, B, C, D, and H

4.1. Total synthesis of psammaplysin A

The free amine of the commercially available amino acid tyramine **(23)** will be troc protected via standard conditions followed by bromination of both ortho positions with standard electrophilic

aromatic substitution to give compound **24.** The resulting phenol **24** will then be reacted with commercially available 3-chloropropy amine **(25)** to yield the expected dibromo substituted side chain of psammaplysin A **(26)** (Scheme 5). Psammaplysin core **8a** will then be saponified utilizing LiOH to result in the free carboxylic end that will then be subjected to peptide coupling conditions with EDC to achieve the troc protected psammaplysin A structure **(27)**. Compound **27** will be exposed to troc deprotection with trimethyltin hydroxide in DCE[50] to successfully achieve the first total synthesis of psammaplysin A **(S1)** (Scheme 5).

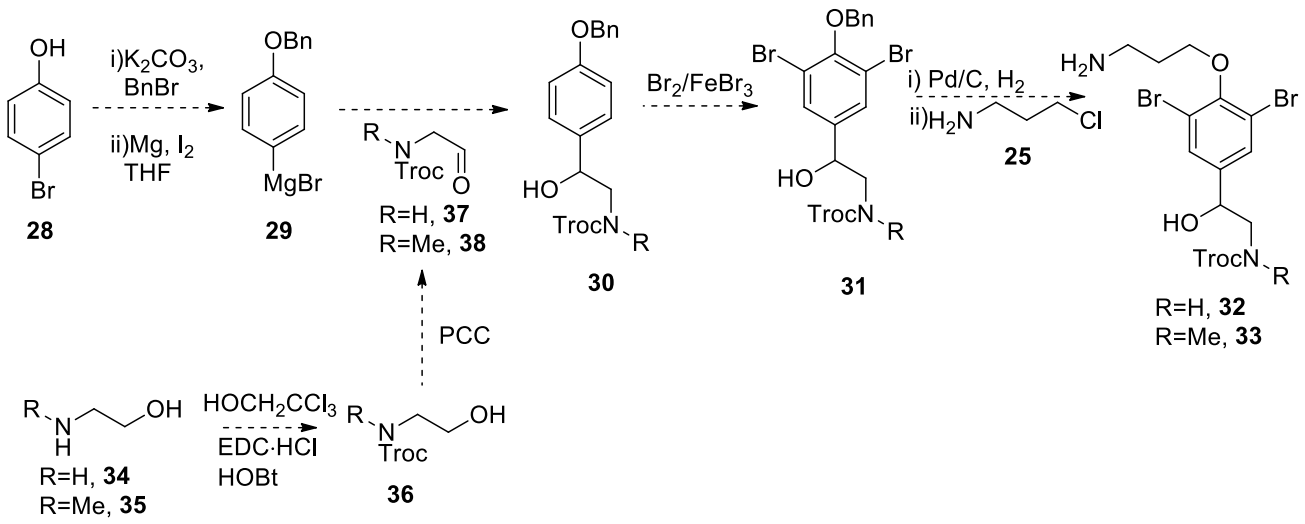


Scheme 5 - Total synthesis of psammaplysin A

4.2. Total synthesis of psammaplysin B and C

The phenol of commercially available 4-Bromophenol **(28)** will be protected by a benzyl group with benzyl bromide and then exposed to the conditions reported by Pingyan and coworkers in the synthesis of pyrrolotriazine derivatives to access the Grignard reagent **29**. Compound **29** will be added on to N-boc-2-aminoacetaldehyde **(37)** utilizing the reaction conditions reported by Fisher and coworkers.[51] N-troc-2-aminoacetaldehyde **(37)**/ N-troc-(methylamino)acetaldehyde **(38)** will be accessed by subjecting 2-aminoethanol **(34)** /2-(methylamino)ethanol **(35)** to troc protection followed by a PCC oxidation under standard conditions. Aromatic intermediate **30** will be brominated via a standard aromatic substitution reaction to yield compound **31**. It will then undergo benzyl deprotection in the presence of Pd/C and H_2 followed by reaction of the phenolic alcohol with 3-chloropropyl amine **(25)** as discussed above in scheme 3 to yield the expected dibromo side chain of psammaplysin B (R=H, **32**) and psammaplysin C (R=Me, **33**) respectively. Obtained side chains **32** and **33** will be reacted with saponified product of compound **8a** as

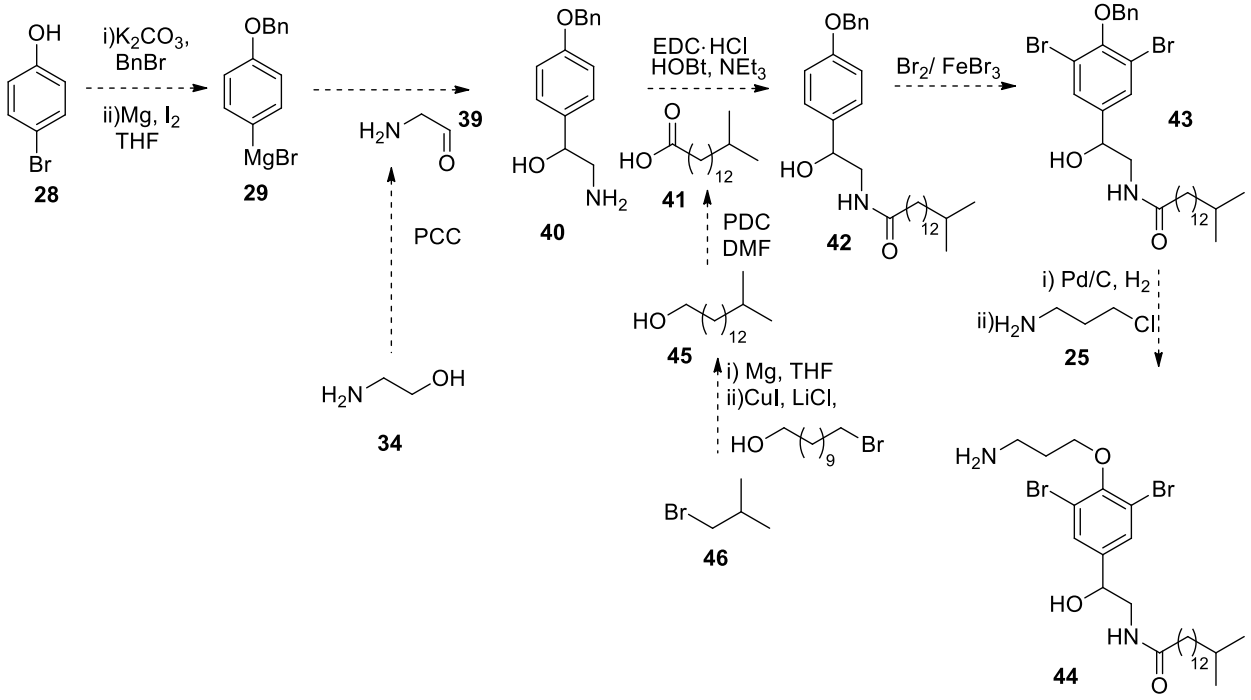
explained in scheme 5 above to achieve the first total synthesis of psammaplysin B **(S2)** and C **(S3)**, respectively (Scheme 6).



Scheme 6 - Synthesis of substituted side chains of psammaplysin B (R=H) and C (R=Me)

4.3. Total synthesis of psammaplysin D

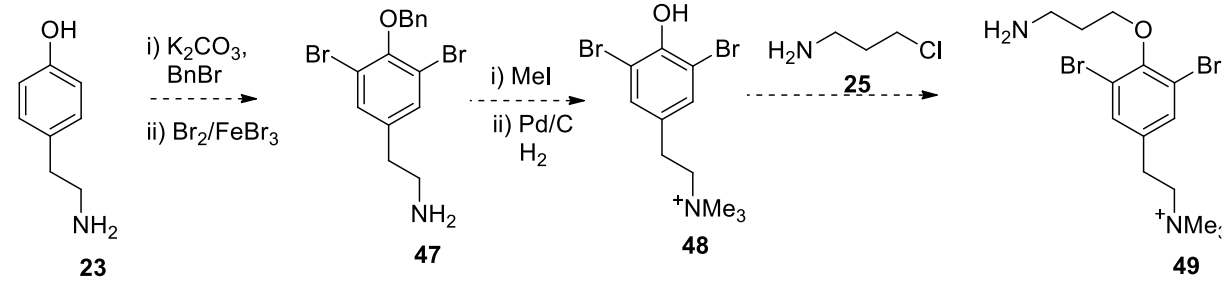
As discussed in section 4.2 above, commercially available **28** will be benzyl protected and the Grignard reagent **29** will be accessed under standard conditions. Compound **29** will then undergo a Grignard reaction with the aldehyde **39**, obtained by PCC oxidation of 2-aminoethanol **(34)**, to yield compound **40**. Compound **40** and 14-methylpentadecanoic acid **(41)** will undergo a peptide coupling reaction with EDC·HCl resulting compound **42**. Aromatic ring of **42** will be brominated at both ortho positions via an electrophilic aromatic substitution reaction followed by the reaction of phenol of benzyl deprotected **43** with commercially available 3-chloropropy amine **(25)** as discussed above in scheme 5 to yield the expected dibromo side chain of psammaplysin D **(44)** (Scheme 7). The dibromo side chain **44** and the carboxylic acid **1** will undergo a peptide coupling reaction with EDC to achieve the first total synthesis of psammaplysin D **(S4)**.



Scheme 7 - Synthesis of substituted side chain of psammaplysin D

4.4. Total synthesis of psammaplysin H

The phenol of tyramine **(23)** will be protected with benzyl bromide and bromination of both ortho positions will be performed with a standard electrophilic aromatic substitution resulting compound **47**. Compound **47** will then be subjected to N-methylation under standard conditions with methyl iodide followed by benzyl deprotection with Pd/C and H_2 to access the phenolic intermediate **48**, which will then be reacted with 3-chloropropy amine as discussed above in scheme 3 to yield the expected dibro side chain of psammaplysin H **(49)** (Scheme 8). The dibromo side chain **49** and carboxylic acid **1** will undergo a peptide coupling reaction with EDC to achieve the first total synthesis of psammaplysin H (**S18**).



Scheme 8 - Synthesis of substituted side chain of psammaplysin H

4.5. Structural determination of synthesized psammaplysin A-D, and H

Extensive and careful analysis of 1D (^{1}H, ^{13}C, and DEPT) and 2D (^{1}H -^{1}H COSY, HMBC, HSQC, and ROESY) NMR data together with HRMS data will be done to confirm the structure of synthesized compounds. Optical rotations of the compounds will be compared with reported values in literature to confirm the absolute stereochemistry. It is anticipated to support the structures determined using above data with XRD data.

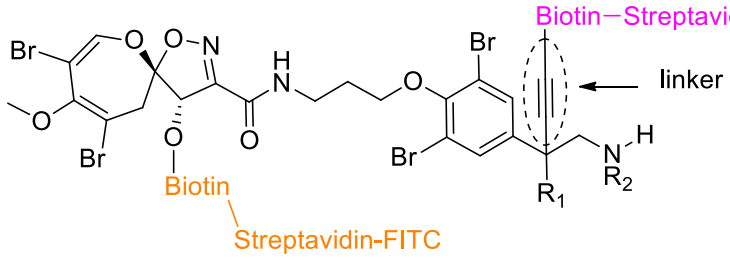
4.6. Biological assays of synthesized psammaplysin A-D, and H

Psammaplysin A-C will be tested in vitro against the human colon tumor cell-line HCT116 and the obtained IC_{50} values will be compared with the values reported by isolation chemists. Psammaplysin D will be tested for its anti HIV activity in vitro against HIV-1 (IIIB) obtained from the culture supernatants of HIV-1 infected MT-4 cell lines and the values obtained will be compared with the literature. Psammaplysin H will be tested in vitro against the 3D7 line of Plasmodium falciparum and mammalian cell lines (HEK293 and HepG2) for its antimalarial activity and the obtained values will be compared with the reported data. These studies will be carried out in collaboration with a fellow research group.

5. Investigation of mode of action of psammaplysin A-D, and H

Understanding the mode of action of a drug and its target proteins inside a cell is essential in drug discovery to design effective therapeutics.[52] Hence this report propose an experimental design that will be done in collaboration with a fellow research group to investigate the mode of action of psammaplysin A-D, and H. Spirooxepinisoxazoline ring portion of psammaplysins will be conjugated to biotin at the secondary alcohol (Figure 10) and biological assays will be carried out separately with each cell line (human colon tumor cell-line HCT116 for psammaplysin A-C; HIV-1 infected MT-4 cell line for psammaplysin D; 3D7 line of plasmodium falciparum and mammalian cell lines (HEK293 and HepG2) for psammaplysin H) again to test if activity remains after biotin is conjugated to the molecule. If there is a change in values then that particular concentration will be taken to carry out the incubation with the respective cells lines. After incubation with psammaplysin conjugated to biotin, the cells will be treated with streptavidin conjugated to FITC using standard protocols.[53,54] Similarly, the dibromo side chain of psammaplysins will be conjugated to biotin via a linker (Figure 10) and biological assays will be carried out separately with each cell line to test if activity remains after biotin is conjugated to the molecule. If there is

a change in values then that particular concentrations will be taken to carry out the incubation with the respective cells. After incubation with psammaplysin conjugated to biotin, the cells will be treated with streptavidin conjugated to APC using standard protocols. An antibody titration will be performed before conjugating to obtain the optimum antibody concentration and stain index. Thereafter, flow cytometric analysis will be carried out using 488 nm laser as excitation wavelength and 520/20 bandpass channel to detect its emission (emission of FITC). An isotype control will be done to account for background fluorescence to get the actual fluorescence with streptavidin conjugated to FITC.[55]



R_1 = R_2 = H = Psammamplysin A
R_1 = OH, R_2 = H = Psammamplysin B
R_1 = OH, R_2 = Me = Psammamplysin C
R_1 = H, R_2 = $CO(CH_2)_{12}CH(CH_3)_2$ = Psammamplysin D
R_1 = H, R_2 = Me_3 = Psammamplysin H

Figure 7 - Fluorescence tagged psammaplysin A-D, and H

Finally, cells will be sorted under purity mode for cells detected with FITC. The sorted cells will be lysed, purified, and further analyzed using gel electrophoresis. The two fluorophores FITC and APC will be utilized to observe the gel electrophoresis under 488 nm (FITC emission wavelength) and 633 nm (APC emission wavelength) light, respectively.[56]

Following are the 3 possible results;

1) If there are proteins that give fluorescence only under 633 nm, then the dibromo substituted side chain has been released from the whole molecule and bound to proteins.

2) If there are proteins that give fluorescence only under 488 nm, then the Spirooxepinisoxazoline ring moiety has been released from the whole molecule and bound to proteins.

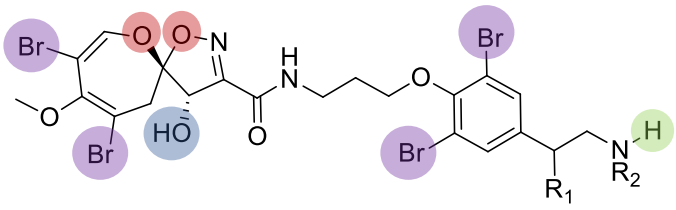
3) If there are proteins that give fluorescence under both wavelengths 488 nm and 633 nm, then the psammaplysin molecule as itself is bound to proteins.

Depending on the results that will be observed as explained above it will be possible to understand if a specific moiety is released/or if it is necessary to be released to give the therapeutic effect. Furthermore, isolation and analysis of the proteins that give fluorescence

under 488 nm and 633 nm in gel electrophoresis would assist to identify interaction of psammaplysins with its target proteins, so that its structure activity data could be gathered to design effective analogues.

6. Structure activity relationship studies of psammaplysin A-D, and H

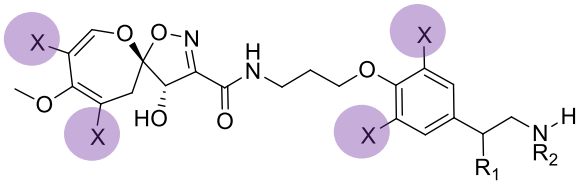
Psammaplysin A-D, and H can be functionalised at the substitution sites highlighted in red below in Figure 8 to access a library of analogues that can exhibit novel therapeutic properties with a probability of being potential drugs to treat many diseases. Moreover, it is expected to enhance the existing biological activity of psammaplysin A-D, and H through this library of compounds. If the attempts in total synthesis of psammaplysin A-D, and H were not successful, following chemical library will be accessed utilizing respective isolated psammaplysins and/or other synthetic methodologies especially in the synthesis of analogues **60** - **64** and **70** - **79**.



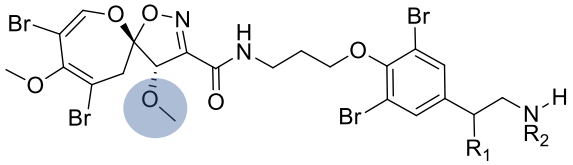
$R_1 = R_2 = H$ = Psammamplysin A
$R_1 = OH$, $R_2 = H$ = Psammamplysin B
$R_1 = OH$, $R_2 = Me$ = Psammamplysin C
$R_1 = OH$, $R_2 = CO(CH_2)_{12}CH(CH_3)_2$ = Psammamplysin D
$R_1 = H$, $R_2 = Me_3$ = Psammamplysin H

Figure 8 – Possible substitution sites in psammaplysin A-D, and H

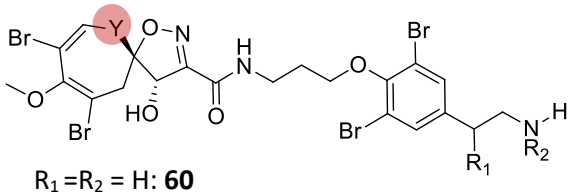
It is reported that spirooxepinisoxazoline ring moiety act as a pharmacaphore in the psammaplysins to exhibit cytotoxicity against human colon tumor cells. Hence, it is envisioned to explore the potential of its cytotoxicity by replacing the oxygen atoms in the spirooxepinisoxazoline ring by carbon, sulphur, and nitrogen. Furthermore, secondary alcohol in the isoxazoline ring can be substituted by an ether, amine, or a thiol group and observe the efficacy of its biological activity. Moreover, substituting the R_2 group on the amine by michael acceptor moieties is also expected to exhibit potential therapeutic effects (Figure 9). All the analogues synthesized will be screened in a wide range of cell lines for cytotoxicity, anti HIV, anti-malarial, anti-bacterial, and anti-fouling properties in collaboration with a fellow research group.



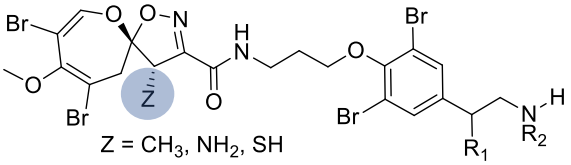
R_1 =R_2 = H: **50**
R_1 = OH, R_2 = H: **51**
R_1 = OH, R_2 = Me: **52**
R_1 = H, R_2 = $CO(CH_2)_{12}CH(CH_3)_2$: **53**
R_1 = H, R_2 = Me_3: **54**



R_1 =R_2 = H: **55**
R_1 = OH, R_2 = H: **56**
R_1 = OH, R_2 = Me: **57**
R_1 = H, R_2 = $CO(CH_2)_{12}CH(CH_3)_2$: **58**
R_1 = H, R_2 = Me_3: **59**

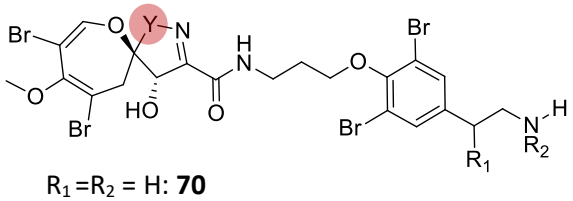


R_1 =R_2 = H: **60**
R_1 = OH, R_2 = H: **61**
R_1 = OH, R_2 = Me: **62**
R_1 = H, R_2 = $CO(CH_2)_{12}CH(CH_3)_2$: **63**
R_1 = H, R_2 = Me_3: **64**

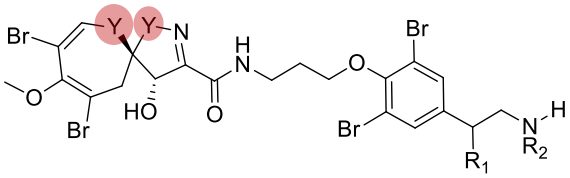


Z = CH_3, NH_2, SH

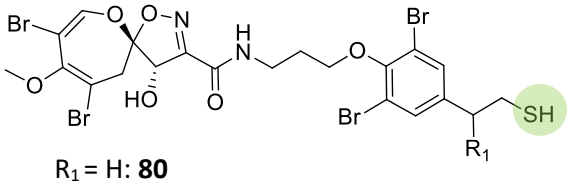
R_1 =R_2 = H: **65**
R_1 = OH, R_2 = H: **66**
R_1 = OH, R_2 = Me: **67**
R_1 = H, R_2 = $CO(CH_2)_{12}CH(CH_3)_2$: **68**
R_1 = H, R_2 = Me_3: **69**



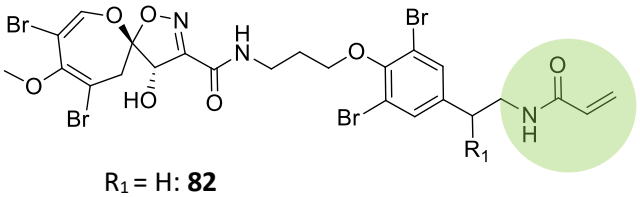
R_1 =R_2 = H: **70**
R_1 = OH, R_2 = H: **71**
R_1 = OH, R_2 = Me: **72**
R_1 = H, R_2 = $CO(CH_2)_{12}CH(CH_3)_2$: **73**
R_1 = H, R_2 = Me_3: **74**



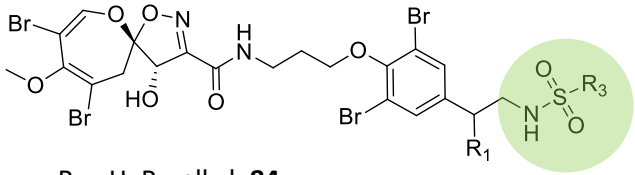
R_1 =R_2 = H: **75**
R_1 = OH, R_2 = H: **76**
R_1 = OH, R_2 = Me: **77**
R_1 = H, R_2 = $CO(CH_2)_{12}CH(CH_3)_2$: **78**
R_1 = H, R_2 = Me_3: **79**



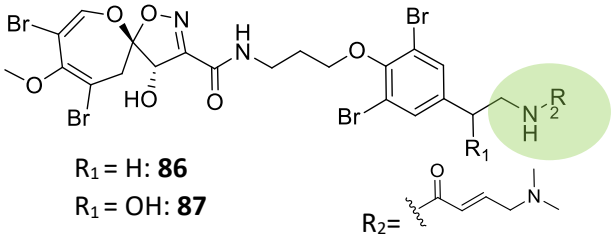
R_1 = H: **80**
R_1 = OH: **81**



R_1 = H: **82**
R_1 = OH: **83**



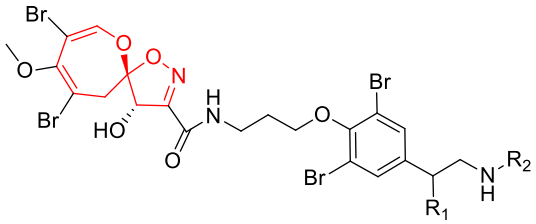
R_1 = H, R_3=alkyl: **84**
R_1 = OH, R_3=alkyl: **85**

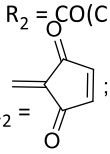


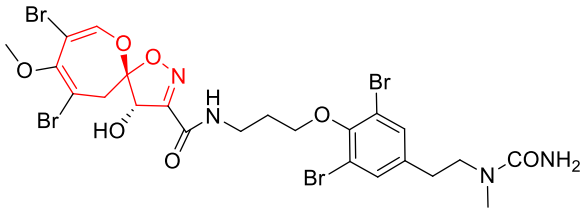
R_1 = H: **86**
R_1 = OH: **87**

Figure 9 - Proposed analogues of psammaplysin A-D, and H (X= Cl or F; Y= C, S or N)

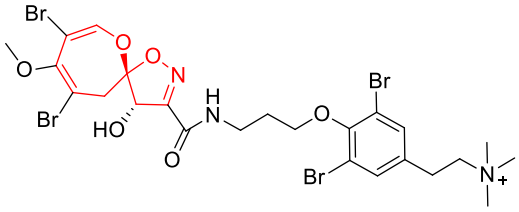
7. Supporting Information



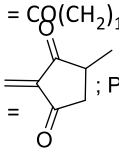
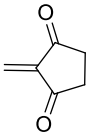
$R_1 = R_2 = H$; Psammaplysin A (**S1**)
R1 = OH, R2 = H; Psammaplysin B (**S2**)
$R_1 = OH$, $R_2 = Me$; Psammaplysin C (**S3**)
$R_1 = OH$, $R_2 = CO(CH_2)_{11}CHMe_2$; Psammaplysin D (**S4**)
$R_1 = H$, $R_2 =$  ; Psammaplysin E (**S5**)

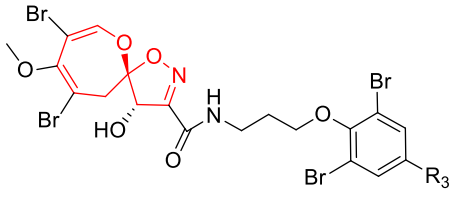


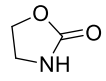
Psammaplysin G (**S17**)



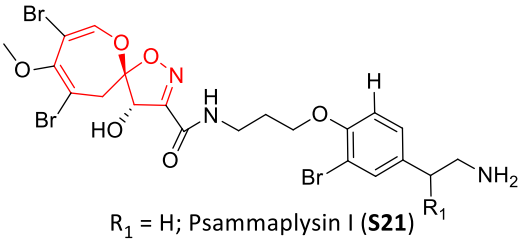
Psammaplysin H (**S18**)

$R_1 = H$, $R_2 = Me$; Psammaplysin F (**S6**)
$R_1 = OH$, $R_2 = COCH_2OH$ Psammaplysin M (**S7**)
$R_1 = H$, $R_2 = CO(CH_2)_{12}CHMe_2$; Psammaplysin N (**S8**)
$R_1 = H$, $R_2 = CO(CH_2)_{14}CH_3$; Psammaplysin O (**S9**)
$R_1 = H$, $R_2 = CO(CH_2)_{16}CH_3$; Psammaplysin P (**S10**)
$R_1 = H$, $R_2 = CO(CH_2)_{12}CH_3$; Psammaplysin Q (**S311**)
$R_1 = H$, $R_2 =$  ; Psammaplysin X (**S12**)
$R_1 = H$, $R_2 =$  ; Psammaplysin Y (**S13**)

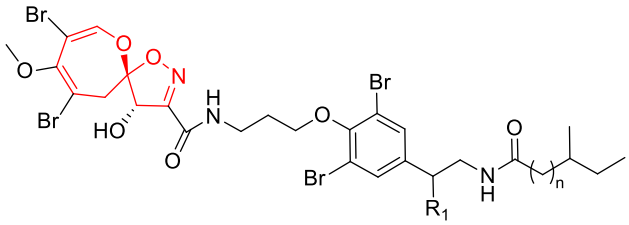


$R_3 = CHO$; Psammaplysin K (**S19**)
$R_3 =$  ; Psammaplysin L (**S20**)

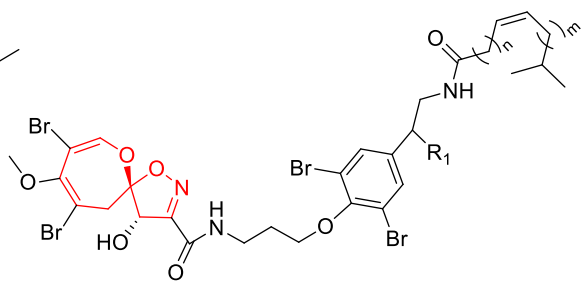
$R_1 = H$, $R_2 = CONH_2$ Psammaplysin Z (**S14**)
$R_1 = H$, $R_2 = CHO$; Ceratinamide A (**S26a**)
$R_1 = H$, $R_2 = CO(CH_2)_{11}CHMe_2$; Ceratinamide B (**S26b**)



$R_1 = H$; Psammaplysin I (**S21**)
$R_1 = OH$; Psammaplysin J (**S22**)



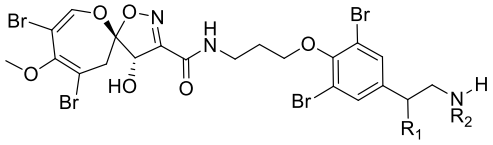
$R_1 = H$, n = 11; Psammaplysin R (**S15**)
$R_1 = H$, n = 12; Psammaplysin S (**S16**)
$R_1 = H$, n = 14; Psammaplysin T (**S17**)

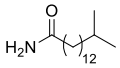
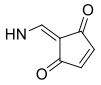


$R_1 = H$, n = 8, m = 3; Psammaplysin U (**S23**)
$R_1 = H$, n = 8, m = 4; Psammaplysin V (**S24**)
$R_1 = OH$, n = 11, m = 4; Psammaplysin W (**S25**)

Figure S 1 - Structures of psammaplysin A-Y and ceratinamides A and B

Table S1- Biological activity of Psammaplysins



Psammaplysin	Biological activity
A R1=R2=H	cytotoxicity against the human colon tumor cell-line HCT116,[25] Inhibition of mycothiol-S-conjugate amidase,[57] antifouling Activity, antibacterial against *Flavobacterium marinotypicum*.[18]
B R1=OH, R2=H	cytotoxicity against the human colon tumor cell-line HCT116.[25] Inhibition of mycothiol-S-conjugate amidase.[57]
C R1=OH, R2=Me	cytotoxicity against the human colon tumor cell-line HCT116.[25]
D R1=OH, R2= 	Anti-HIV activity against the Haitian RF strain of HIV-I.[15]
E R1=H R2= 	cytotoxicity against KB (human oral, epidermoid carcinoma) and L_0V_0 (human colon, adenocarcinoma), modest immunosuppressive activity (a potency of 40, IC50 8.32E-01 for mixed lymphocyte reaction assay),[15] cytotoxicity against P388 murine leukemia cells.[18]
F R1=H, R2=Me	Anti-bacterial activity,[28] Anti-malarial properties.[17] Regulation of stress granule formation.
G R1=H, R2=$MeCONH_2$	Anti-malarial properties ((IC50 1.38 uM and 40 uM, respectively).[17]
H R1=H, R2=Me_3	most potent and selective (>97-fold) antimalarial activity.[30]
I and J 14-desbromo-psammaplysin A and B	Not carried out.[58]
K(C19 aldehyde),	Anti-malarial activity.[59]

L, M, N, O, P, Q, R, S, T, U, V, and W	Anti-malarial activity.[59]
X	Anti-cancer properties.[60]
Y	Anti-cancer properties.[60]
Z	Moderate cytotoxic activity against MBA-MB-231 and HeLa cell lines.[61]

References

(1) Howlader N, Noone AM, Krapcho M, Neyman N, Aminou R, Waldron W, Altekruse SF, Kosary CL, Ruhl J, Tatalovich Z, Cho H, Mariotto A, Eisner MP, Lewis DR, Chen HS, Feuer EJ, Cronin KA, E. B. (Eds). SEER Cancer Statistics Review 1975-2008 National Cancer Institute SEER Cancer Statistics Review 1975-2008 National Cancer Institute. *Cancer* **2011**, 1975–2008.

(2) Wild CP, Weiderpass E, S. B. *World Cancer Report 2020*; 2020.

(3) 2020, W. *World Malaria Report 2020*; 1997; Vol. 73.

(4) Kurimoto, S. I.; Ohno, T.; Hokari, R.; Ishiyama, A.; Iwatsuki, M.; Ōmura, S.; Kobayashi, J.; Kubota, T. Ceratinadins E and F, New Bromotyrosine Alkaloids from an Okinawan Marine Sponge Pseudoceratina Sp. *Mar. Drugs* **2018**, *16* (12), 2–8.

(5) Jiménez, C. Marine Natural Products in Medicinal Chemistry. *ACS Med. Chem. Lett.* **2018**, *9* (10), 959–961.

(6) Le, V. H.; Inai, M.; Williams, R. M.; Kan, T. Ecteinascidins. A Review of the Chemistry, Biology and Clinical Utility of Potent Tetrahydroisoquinoline Antitumor Antibiotics. *Nat. Prod. Rep.* **2015**, *32* (2), 328–347.

(7) Mayer, A. M. S.; Rodríguez, A. D.; Taglialatela-Scafati, O.; Fusetani, N. Marine Pharmacology in 2009-2011: Marine Compounds with Antibacterial, Antidiabetic, Antifungal, Anti-Inflammatory, Antiprotozoal, Antituberculosis, and Antiviral Activities; Affecting the Immune and Nervous Systems, and Other Miscellaneous Mechanisms Of . *Mar. Drugs* **2013**, *11* (7), 2510–2573.

(8) Kil, Y. S.; Risinger, A. L.; Petersen, C. L.; Liang, H.; Grkovic, T.; O'Keefe, B. R.; Mooberry, S. L.; Cichewicz, R. H. Using the Cancer Dependency Map to Identify the Mechanism of Action of a Cytotoxic Alkenyl Derivative from the Fruit of Choerospondias Axillaris. *J. Nat. Prod.* **2020**, *83* (3), 584–592.

(9) Flick, A. C.; Ding, H. X.; Leverett, C. A.; Kyne, R. E.; Liu, K. K. C.; Fink, S. J.; O'Donnell, C. J. Synthetic Approaches to the New Drugs Approved during 2015. *J. Med. Chem.* **2017**, *60* (15), 6480–6515.

(10) Raedler, B. L. a; Writer, M. Monoclonal Antibody Approved for Patients with Relapsed Multiple Myeloma. *Am. Heal. Drug Benefits* **2016**, *9* (March), 84–89.

(11) Kumar, R.; Bidgood, C. L.; Levrier, C.; Gunter, J. H.; Nelson, C. C.; Sadowski, M. C.; Davis, R. A. Synthesis of a Unique Psammaplysin F Library and Functional Evaluation in Prostate Cancer Cells by Multiparametric Quantitative Single Cell Imaging. *J. Nat. Prod.* **2020**, *83* (8), 2357–2366.

(12) Yongfeng Tao, Keighley Reisenauer, Joseph H. Taube, and D. R. Total Synthesis and Anticancer Activity of (+)-Hypercalin C and Congeners. *Angew Chem Int Ed Engl.* **2019**, *58* (9), 2734–2738.

(13) Richards et al.Jiangnan Peng, Jing Li, and M. T. H. The Marine Bromotyrosine Derivatives.

Alkaloids Chem Biol. **2005**, *61*, 59–262.

(14) Jaisamut, S.; Prabpai, S.; Tancharoen, C.; Yuenyongsawad, S.; Hannongbua, S.; Kongsaeree, P.; Plubrukarn, A. Bridged Tricyclic Sesquiterpenes from the Tubercle Nudibranch Phyllidia Coelestis Bergh. *J. Nat. Prod.* **2013**, *76* (11), 2158–2161.

(15) Ichiba, T.; Scheuer, P. J.; Kelly-Borges, M. Three Bromotyrosine Derivatives, One Terminating in an Unprecedented Diketocyclopentenylidene Enamine. *J. Org. Chem.* **1993**, *58* (15), 4149–4150.

(16) Liu, S.; Fu, X.; Schmitz, F. J.; Kelly-Borges, M. Psammaplysin F, a New Bromotyrosine Derivative from a Sponge, Aplysinella Sp. *J. Nat. Prod.* **1997**, *60* (6), 614–615.

(17) Yang, X.; Davis, R. A.; Buchanan, M. S.; Duffy, S.; Avery, V. M.; Camp, D.; Quinn, R. J. Antimalarial Bromotyrosine Derivatives from the Australian Marine Sponge Hyattella Sp. *J. Nat. Prod.* **2010**, *73* (5), 985–987.

(18) Tsukamoto, S.; Kato, H.; Hirota, H.; Fusetani, N. Ceratinamides A and B: New Antifouling Dibromotyrosine Derivatives from the Marine Sponge Pseudoceratina Purpurea. *Tetrahedron* **1996**, *52* (24), 8181–8186.

(19) Sirimangkalakitti, N.; Yokoya, M.; Chamni, S.; Chanvorachote, P.; Plubrukrn, A.; Saito, N.; Suwanborirux, K. Synthesis and Absolute Configuration of Acanthodendrilline, a New Cytotoxic Bromotyrosine Alkaloid from the Thai Marine Sponge Acanthodendrilla Sp. *Chem. Pharm. Bull.* **2016**, *64* (3), 258–262.

(20) Shaala, L. A.; Youssef, D. T. A.; Badr, J. M.; Sulaiman, M.; Khedr, A. Bioactive Secondary Metabolites from the Red Sea Marine Verongid Sponge Suberea Species. *Mar. Drugs* **2015**, *13* (4), 1621–1631.

(21) Rotem, M.; Carmely, S.; Kashman, Y.; Loya, Y. Two New Antibiotics from the Red Sea Sponge Psammaplysilla Purpurea. *Tetrahedron* **1983**, *39* (4), 667–676.

(22) Rotem, M.; Carmely, S.; Kashman, Y.; Loya, Y. Two New Antibiotics from the Red Sea Sponge Psammaplysilla Purpurea. Total 13C-NMR Line Assignment of Psammaplysins A and B and Aerothionin. *Tetrahedron* **1983**, *39* (4), 667–676.

(23) Roll, D. M.; Chang, C. W. J.; Scheuer, P. J.; Gray, G. A.; Shoolery, J. N.; Matsumoto, G. K.; Duyne, G. D. Van; Clardy, J. Structure of the Psammaplysins1. *J. Am. Chem. Soc.* **1985**, *107*, 2916–2920.

(24) Mándi, A.; Mudianta, I. W.; Kurtán, T.; Garson, M. J. Absolute Configuration and Conformational Study of Psammaplysins A and B from the Balinese Marine Sponge Aplysinella Strongylata. *J. Nat. Prod.* **2015**, *78* (8), 2051–2056.

(25) Copp, B. R.; Ireland, C. M.; Barrows, L. R. Psammaplysin C: A New Cytotoxic Dibromotyrosine-Derived Metabolite from the Marine Sponge Druinella (psammaplysilla) Purpurea. *J. Nat. Prod.* **1992**, *55* (6), 822–823.

(26) Lee, Y. J.; Han, S.; Lee, H. S.; Kang, J. S.; Yun, J.; Sim, C. J.; Shin, H. J.; Lee, J. S. Cytotoxic Psammaplysin Analogues from a Suberea Sp. Marine Sponge and the Role of the

Spirooxepinisoxazoline in Their Activity. *J. Nat. Prod.* **2013**, *76* (9), 1731–1736.

(27) Shaala, L. A.; Youssef, D. T. A.; Badr, J. M.; Sulaiman, M.; Khedr, A.; El Sayed, K. A. Bioactive Alkaloids from the Red Sea Marine Verongid Sponge Pseudoceratina Arabica. *Tetrahedron* **2015**, *71* (41), 7837–7841.

(28) Ramsey, D. M.; Amirul Islam, M.; Turnbull, L.; Davis, R. A.; Whitchurch, C. B.; McAlpine, S. R. Psammaplysin F: A Unique Inhibitor of Bacterial Chromosomal Partitioning. *Bioorganic Med. Chem. Lett.* **2013**, *23* (17), 4862–4866.

(29) Christen, K. E.; Davis, R. A.; Kennedy, D. Psammaplysin F Increases the Efficacy of Bortezomib and Sorafenib through Regulation of Stress Granule Formation. *Int. J. Biochem. Cell Biol.* **2019**, *112* (November 2018), 24–38.

(30) Xu, M.; Andrews, K. T.; Birrell, G. W.; Tran, T. L.; Camp, D.; Davis, R. A.; Quinn, R. J. Psammaplysin H, a New Antimalarial Bromotyrosine Alkaloid from a Marine Sponge of the Genus Pseudoceratina. *Bioorganic Med. Chem. Lett.* **2011**, *21* (2), 846–848.

(31) Rogers, E. W.; Molinski, T. F. Highly Polar Spiroisoxazolines from the Sponge Aplysina Fulva. *J. Nat. Prod.* **2007**, *70* (7), 1191–1194.

(32) Hentschel, F.; Lindel, T. Synthesis of Oximinotyrosine-Derived Marine Natural Products. *Synthesis (Stuttg).* **2010**, No. 2, 181–204.

(33) Aximilians, D. E. R. L. U.; Ünchen, N. M. Studies toward the Total Synthesis of Psammaplysin A and Acid-Catalyzed Cycloisomerization of Neopentylic Epoxides. **2020**.

(34) Stok, J. E.; Chow, S.; Krenske, E. H.; Farfan Soto, C.; Matyas, C.; Poirier, R. A.; Williams, C. M.; De Voss, J. J. Direct Observation of an Oxepin from a Bacterial Cytochrome P450-Catalyzed Oxidation. *Chem. - A Eur. J.* **2016**, *22* (13), 4408–4412.

(35) Neuss, N.; Nagarajan, R.; Molloy, B. B.; Huckstep, L. L. Aranotin and Related Metabolites. II. Isolation, Characterization, and Structures of Two New Metabolites. *Tetrahedron Lett.* **1968**, *9* (42), 4467–4471.

(36) Vogel, E.; Gunther, H. Benzene Oxide-Oxepin Tautomerisation. *1967*, *6* (5), 385–401.

(37) Ahmad, S.; Khan, F. A. *Marine Brominated Alkaloids: Isolation, Biosynthesis, Biological Activity and Synthesis*; 2015.

(38) Smietana, M.; Gouverneur, V.; Mioskowski, C. A New Access to Spiro-Isoxazolines Derivatives. *Tetrahedron Lett.* **1999**, *40* (7), 1291–1294.

(39) Carlson, J. S. General Approach to the Synthesis of the Chlorosulfolipids Danicalipin A, Mytilipin A, and Malhamensilipin A in Enantioenriched Form and Progress towards the Synthesis of the Psammaplysin Family of Natural Products, University of California, Irvine, 2015.

(40) Takaoka, D. 4-Hydroxy-2-Butynal Synthesis Ref.Pdf. 73776A, 2009.

(41) Wakefield, B. J. Product Class 9: Isoxazoles. *Sci. Synth.* **2002**, 229–288.

(42) Li, G.; Kakarla, R.; Gerritz, S. W. A Fast and Efficient Bromination of Isoxazoles and Pyrazoles

by Microwave Irradiation. *Tetrahedron Lett.* **2007**, *48* (26), 4595–4599.

(43) Amsterdam, P. C. Synthesis of 4-Isoxazoleboronic Acids: A New Route to 4-Isoxazolones. *J. Organometal. Chem.* **1967**, *9*, 19–22.

(44) Wurst, J. M.; Verano, A. L.; Tan, D. S. Stereoselective Synthesis of Acortatarins A and B. *Org. Lett.* **2012**, *14* (17), 4442–4445.

(45) Zhang Yan, Li Shu-shu. A Study on the Green Synthetic Technology of γ-hydroxy-2-(5H)-furanone. **2013**, *21* (12), 12–15.

(46) Lopušanskaja, E.; Paju, A.; Järving, I.; Lopp, M. Synthesis of Cyclic 3-Aryl-Substituted 1,2-Dicarbonyl Compounds via Suzuki Cross-Coupling Reactions. *Synth.* **2018**, *50* (9), 1883–1890.

(47) Li-Ming yang, Shwu-Jiuan Lin, Tsang-Hsiung yang, and K.-H. L. Synthesis and Anti-HIV Activity of Dibenzylbutyrolactone Lignans. *Bioorg. Med. Chem. Lett.* **1996**, *6* (8), 941–944.

(48) Oakes, F. T.; Yang, F.; Sebastian, J. F. Allylic vs. Vinylic Deprotonation Reactions of Cyclic Vinyl Ethers. 7-Lithio-2,3,4,5-Tetrahydrooxepin: Synthesis and Carbon-13 Nuclear Magnetic Resonance Spectrum. *J. Org. Chem.* **1982**, *47* (16), 3094–3097.

(49) Hart, D. J.; Krakower, J. M. The Biogenetically Modeled Total Synthesis of (±)-Minovine. *J. Am. Chem. Soc.* **1970**, *92* (11), 3492–3494.

(50) Trost, B. M.; Kalnmals, C. A.; Tracy, J. S.; Bai, W. J. Highly Chemoselective Deprotection of the 2,2,2-Trichloroethoxycarbonyl (Troc) Protecting Group. *Org. Lett.* **2018**, *20* (24), 8043–8046.

(51) Fisher, K. M.; Bolshan, Y. Brønsted Acid-Catalyzed Reactions of Trifluoroborate Salts with Benzhydryl Alcohols. *J. Org. Chem.* **2015**, *80* (24), 12676–12685.

(52) Hughes, J. P.; Rees, S. S.; Kalindjian, S. B.; Philpott, K. L. Principles of Early Drug Discovery. *Br. J. Pharmacol.* **2011**, *162* (6), 1239–1249.

(53) Tamura, T.; Hamachi, I. Chemistry for Covalent Modification of Endogenous/Native Proteins: From Test Tubes to Complex Biological Systems. *J. Am. Chem. Soc.* **2019**.

(54) Zhang, Y.; Park, K. Y.; Suazo, K. F.; Distefano, M. D. Recent Progress in Enzymatic Protein Labelling Techniques and Their Applications. *Chem. Soc. Rev.* **2018**, *47* (24), 9106–9136.

(55) Maciorowski, Z.; Chattopadhyay, P. K.; Jain, P. Basic Multicolor Flow Cytometry. *Curr. Protoc. Immunol.* **2017**, *2017*, 5.4.1-5.4.38.

(56) Michael, B. Y. By Michael. *Blood* **1987**, *70* (05), 1316–1324.

(57) Nicholas, G. M.; Eckman, L. L.; Ray, S.; Hughes, R. O.; Pfefferkorn, J. A.; Barluenga, S.; Nicolaou, K. C.; Bewley, C. A. Bromotyrosine-Derived Natural and Synthetic Products as Inhibitors of Mycothiol-S-Conjugate Amidase. *Bioorganic Med. Chem. Lett.* **2002**, *12* (17), 2487–2490.

(58) Wright, A. D.; Schupp, P. J.; Schrör, J. P.; Engemann, A.; Rohde, S.; Kelman, D.; De Voogd,

N.; Carroll, A.; Motti, C. A. Twilight Zone Sponges from Guam Yield Theonellin Isocyanate and Psammaplysins i and J. *J. Nat. Prod.* **2012**, *75* (3), 502–506.

(59) Mudianta, I. W.; Skinner-Adams, T.; Andrews, K. T.; Davis, R. A.; Hadi, T. A.; Hayes, P. Y.; Garson, M. J. Psammaplysin Derivatives from the Balinese Marine Sponge Aplysinella Strongylata. *J. Nat. Prod.* **2012**, *75* (12), 2132–2143.

(60) Kim, J. J.; Lim, S. G.; Lee, G. S.; Kim, D. H.; Yoo, J. H.; Lee, B. M. 10-2015–0051599, 2015.

(61) Lamiaa A. Shaala and Diaa T. A. Youssef. Cytotoxic Psammaplysin Analogues from the Verongid Red Sea Sponge Aplysinella Species. *Biomolecules* **2019**, *9* (841), 1–10.